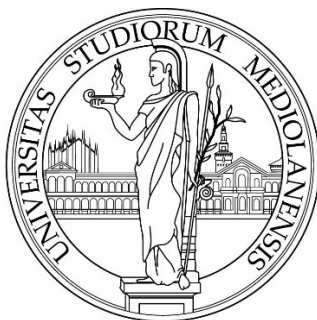


**UNIVERSITÀ DEGLI STUDI DI MILANO**

**FACOLTÀ DI SCIENZE E TECNOLOGIE**

Doctorate School in Industrial Chemistry – XXXV Cycle



**SUSTAINABLE PRODUCTION AND  
PHYSICO-CHEMICAL CHARACTERIZATION OF  
BIOSURFACTANTS FROM RENEWABLE RESOURCES**

**Sara SANGIORGIO**

R12512

*Tutor:* Prof. Giovanna SPERANZA

*Co-tutor:* Prof. Giuseppe CAPPELLETTI

Prof. Daniela UBIALI

Academic Year: 2021/2022

*... Il chimico trova il composto che cerca  
(quando c'è: a volte, se è poco esperto, anche quando non c'è),  
ma per trovare quello che non cerca deve essere estremamente abile  
o sfacciatamente fortunato....*

*Primo Levi, Saggi, 1985*

---

# Contents

<b>1   INTRODUCTION</b>	<b>1</b>
<b>1.1 Sustainable Chemistry</b>	<b>2</b>
1.1.1 Origins of Sustainable Chemistry	2
1.1.2 The 12 Principles of Green Chemistry	4
<b>1.2 Surfactants</b>	<b>7</b>
1.2.1 Stabilization of emulsions	7
1.2.2 Surfactants market and environmental awareness	9
<b>1.3 Natural surfactants</b>	<b>12</b>
1.3.1 Definition and categories of natural surfactants	12
1.3.2 Sugar fatty acid esters	16
<b>1.4 Chemical vs enzymatic synthesis of SFAEs</b>	<b>18</b>
1.4.1 Lipases as biocatalysts	20
1.4.2 SFAEs synthetic strategies	23
<b>1.5 Exploitation of renewable raw materials</b>	<b>25</b>
1.5.1 Oils and fats as renewable raw materials	25
1.5.2 Cheese whey valorization	27
<b>2   AIM OF THE WORK</b>	<b>31</b>
<b>3   RESULTS AND DISCUSSION</b>	<b>33</b>
<b>3.1 Green credentials of Sugar Fatty Acid Esters</b>	<b>34</b>
<b>3.2 Lactose monoesters</b>	<b>36</b>
3.2.1 Sustainable vs chemical synthesis	36
3.2.2 Solubility measurements and Hydrophilic-Lipophilic Balance (HLB)	39
<b>3.3 Glucose monoesters</b>	<b>41</b>
3.3.1 Green credentials of glucose-based fatty acid esters	41
3.3.2 Preliminary experiments	43
3.3.3 Optimization of experimental conditions by Design of Experiment (DoE) approach	47
3.3.4 Influence of solvents	51
3.3.5 Optimized synthesis	53
3.3.6 Physico-chemical characterization	55
<b>3.4 6-O-palmitoyl-1,2-O-isopropylidene-<math>\alpha</math>-D-glucofuranose</b>	<b>57</b>
3.4.1 Acetalization strategy	57

3.4.2 Well-known vs alternative synthesis	59
3.4.3 Partial hydrolysis	62
3.4.4 Enzymatic esterification	64
3.4.5 Physico-chemical characterization	67
<b>3.5 Alkyl D-glucosides</b>	<b>70</b>
3.5.1 Fischer glycosylation strategy	70
3.5.2 Synthesis	72
3.5.3 MS and NMR characterization	74
<b>3.6 1-Butyl 6-O-acyl-D-glucosides</b>	<b>77</b>
3.6.1 Enzymatic esterification with different fatty acids	77
3.6.2 Physico-chemical characterization	80
3.6.3 Emulsifying properties and stability over time	83
3.6.4 Confocal microscopy images of W/O emulsions	87
<b>3.7 Alkyl 6-O-palmitoyl-D-glucosides</b>	<b>90</b>
3.7.1 Enzymatic esterification	90
3.7.2 Physico-chemical characterization: pyranosides vs furanosides	92
3.7.3 Physico-chemical characterization: pyranosides vs isomeric mixtures	96
3.7.4 Preliminary molecular dynamic simulations	99
<b>3.8 Alkyl 6-O-palmitoyl-D-galactosides</b>	<b>102</b>
3.8.1 Fischer glycosylation	102
3.8.2 MS and NMR characterization	104
3.8.3 Enzymatic esterification	107
3.8.4 Physico-chemical characterization: D-galactosides vs D-glucosides	109
3.8.5 Emulsifying properties and stability over time	112
<b>3.9 Preliminary study on the valorization of cheese whey permeate</b>	<b>114</b>
3.9.1 Enzymatic hydrolysis of cheese whey permeate	114
3.9.2 Fischer glycosylation	116
3.9.3 Solvent-free enzymatic esterification	119
3.9.4 Preliminary results of the physico-chemical characterization	121
<b>4   CONCLUSIONS AND FUTURE PERSPECTIVES</b>	<b>123</b>
<b>5   EXPERIMENTAL SECTION</b>	<b>125</b>
<b>5.1 Materials and methods</b>	<b>126</b>
<b>5.2 Synthesis of lactose monoesters</b>	<b>128</b>
5.2.1 Enzymatic synthesis of lactose monoesters	128
5.2.2 Chemical synthesis of 6- and 6'-O-palmitoyl-D-lactose (3)	130
<b>5.3 6-O-lauroyl-, 6-O-palmitoyl-, 6-O-stearoyl-D-glucose</b>	<b>132</b>
5.3.1 Optimized enzymatic synthesis of glucose monoesters	132
5.3.2 Characterization of 6-O-lauroyl-D-glucose (13)	133
5.3.3 Characterization of 6-O-palmitoyl-D-glucose (14)	134

5.3.4 Characterization of 6- <i>O</i> -stearoyl- <i>D</i> -glucose (15)	135
<b>5.4 1,2:5,6-Di-<i>O</i>-isopropylidene-<math>\alpha</math>-<i>D</i>-glucofuranose</b>	<b>136</b>
5.4.1 Chemical synthesis of 1,2:5,6-di- <i>O</i> -isopropylidene- $\alpha$ - <i>D</i> -glucofuranose (16)	136
5.4.2 Alternative synthesis of 1,2:5,6-di- <i>O</i> -isopropylidene- $\alpha$ - <i>D</i> -glucofuranose (16)	137
5.4.3 Characterization of 1,2:5,6-di- <i>O</i> -isopropylidene- $\alpha$ - <i>D</i> -glucofuranose (16)	138
<b>5.5 1,2-<i>O</i>-Isopropylidene-<math>\alpha</math>-<i>D</i>-glucofuranose</b>	<b>139</b>
<b>5.6 6-<i>O</i>-Palmitoyl-1,2-<i>O</i>-isopropylidene-<math>\alpha</math>-<i>D</i>-glucofuranose</b>	<b>140</b>
5.6.1 Enzymatic synthesis of 6- <i>O</i> -palmitoyl-1,2- <i>O</i> -isopropylidene- $\alpha$ - <i>D</i> -glucofuranose (18) with methyl palmitate as acyl donor	140
5.6.2 Enzymatic synthesis of 6- <i>O</i> -palmitoyl-1,2- <i>O</i> -isopropylidene- $\alpha$ - <i>D</i> -glucofuranose (18) with palmitic acid as acyl donor	141
5.6.3 Characterization of 6- <i>O</i> -palmitoyl-1,2- <i>O</i> -isopropylidene- $\alpha$ - <i>D</i> -glucofuranose (18)	142
<b>5.7 Alkyl <i>D</i>-glucoside isomeric mixtures</b>	<b>143</b>
5.7.1 Sustainable synthesis of alkyl <i>D</i> -glucosides (20ad-27ad)	143
5.7.2 Characterization of ethyl <i>D</i> -glucoside isomeric mixture (20ad)	145
5.7.3 Characterization of 1-propyl <i>D</i> -glucoside isomeric mixture (21ad)	146
5.7.4 Characterization of 2-propyl <i>D</i> -glucoside isomeric mixture (22ad)	147
5.7.5 Characterization of 1-butyl <i>D</i> -glucoside isomeric mixture (23ad)	148
5.7.6 Characterization of 2-butyl <i>D</i> -glucoside isomeric mixture (24ad)	149
5.7.7 Characterization of 2-methyl-1-butyl <i>D</i> -glucoside isomeric mixture (25ad)	151
5.7.8 Characterization of 3-methyl-1-butyl <i>D</i> -glucoside isomeric mixture (26ad)	153
5.7.9 Characterization of 1-hexyl <i>D</i> -glucoside isomeric mixture (27ad)	154
<b>5.8 Alkyl 6-<i>O</i>-acyl-<i>D</i>-glucoside isomeric mixtures</b>	<b>155</b>
5.8.1 Enzymatic synthesis of 1-butyl 6- <i>O</i> -lauroyl-, 6- <i>O</i> -palmitoyl-, 6- <i>O</i> -stearoyl- <i>D</i> -glucosides (36ad-38ad)	155
5.8.2 Characterization of 1-butyl 6- <i>O</i> -lauroyl- <i>D</i> -glucopyranosides (36ab)	157
5.8.3 Characterization of 1-butyl 6- <i>O</i> -lauroyl- <i>D</i> -glucofuranosides (36cd)	158
5.8.4 Characterization of 1-butyl 6- <i>O</i> -palmitoyl- <i>D</i> -glucopyranosides (37ab)	159
5.8.5 Characterization of 1-butyl 6- <i>O</i> -palmitoyl- <i>D</i> -glucofuranosides (37cd)	160
5.8.6 Characterization of 1-butyl 6- <i>O</i> -stearoyl- <i>D</i> -glucopyranosides (38ab)	161
5.8.7 Characterization of 1-butyl 6- <i>O</i> -stearoyl- <i>D</i> -glucofuranosides (38cd)	162
5.8.8 Enzymatic synthesis of alkyl 6- <i>O</i> -palmitoyl- <i>D</i> -glucoside isomeric mixtures (37ad,39ad-45ad)	163
5.8.9 Characterization of ethyl 6- <i>O</i> -palmitoyl- <i>D</i> -glucopyranosides (39ab)	165
5.8.10 Characterization of ethyl 6- <i>O</i> -palmitoyl- <i>D</i> -glucofuranosides (39cd)	166
5.8.11 Characterization of 1-propyl 6- <i>O</i> -palmitoyl- <i>D</i> -glucopyranosides (40ab)	167
5.8.12 Characterization of 1-propyl 6- <i>O</i> -palmitoyl- <i>D</i> -glucofuranosides (40cd)	168
5.8.13 Characterization of 2-propyl 6- <i>O</i> -palmitoyl- <i>D</i> -glucopyranosides (41ab)	169
5.8.14 Characterization of 2-propyl 6- <i>O</i> -palmitoyl- <i>D</i> -glucofuranosides (41cd)	170
5.8.15 Characterization of 2-butyl 6- <i>O</i> -palmitoyl- <i>D</i> -glucopyranosides (42ab)	171
5.8.16 Characterization of 2-butyl 6- <i>O</i> -palmitoyl- <i>D</i> -glucofuranosides (42cd)	172
5.8.17 Characterization of 2-methyl-1-butyl 6- <i>O</i> -palmitoyl- <i>D</i> -glucopyranosides (43ab)	173

5.8.18	Characterization of 2-methyl-1-butyl 6-O-palmitoyl-D-glucofuranosides (43cd)	174
5.8.19	Characterization of 3-methyl-1-butyl 6-O-palmitoyl-D-glucopyranosides (44ab)	175
5.8.20	Characterization of 3-methyl-1-butyl 6-O-palmitoyl-D-glucofuranosides (44cd)	176
5.8.21	Characterization of 1-hexyl 6-O-palmitoyl-D-glucopyranosides (45ab)	177
5.8.22	Characterization of 1-hexyl 6-O-palmitoyl-D-glucofuranosides (45cd)	178
<b>5.9</b>	<b>Alkyl D-galactoside isomeric mixtures</b>	<b>179</b>
5.9.1	Sustainable synthesis of alkyl D-galactosides (47ad-54ad)	179
5.9.2	Characterization of ethyl D-galactoside isomeric mixture (47ad)	181
5.9.3	Characterization of 1-propyl D-galactoside isomeric mixture (48ad)	182
5.9.4	Characterization of 2-propyl D-galactoside isomeric mixture (49ad)	183
5.9.5	Characterization of 1-butyl D-galactoside isomeric mixture (50ad)	184
5.9.6	Characterization of 2-butyl D-galactoside isomeric mixture (51ad)	185
5.9.7	Characterization of 2-methyl-1-butyl D-galactoside isomeric mixture (52ad)	187
5.9.8	Characterization of 3-methyl-1-butyl D-galactoside isomeric mixture (53ad)	189
5.9.9	Characterization of 1-hexyl D-galactoside isomeric mixture (54ad)	190
<b>5.10</b>	<b>Alkyl 6-O-acyl-D-galactoside isomeric mixtures</b>	<b>191</b>
5.10.1	Enzymatic synthesis of alkyl 6-O-palmitoyl-D-galactoside isomeric mixtures (55ad-62ad)	191
5.10.2	Characterization of ethyl 6-O-palmitoyl-D-galactopyranosides (55ab)	193
5.10.3	Characterization of ethyl 6-O-palmitoyl-D-galactofuranosides (55cd)	194
5.10.4	Characterization of 1-propyl 6-O-palmitoyl-D-galactopyranosides (56ab)	195
5.10.5	Characterization of 1-propyl 6-O-palmitoyl-D-galactofuranosides (56cd)	196
5.10.6	Characterization of 2-propyl 6-O-palmitoyl-D-galactopyranosides (57ab)	197
5.10.7	Characterization of 2-propyl 6-O-palmitoyl-D-galactofuranosides (57cd)	198
5.10.8	Characterization of 1-butyl 6-O-palmitoyl-D-galactopyranosides (58ab)	199
5.10.9	Characterization of 1-butyl 6-O-palmitoyl-D-galactofuranosides (58cd)	200
5.10.10	Characterization of 2-butyl 6-O-palmitoyl-D-galactopyranosides (59ab)	201
5.10.11	Characterization of 2-butyl 6-O-palmitoyl-D-galactofuranosides (59cd)	202
5.10.12	Characterization of 2-methyl-1-butyl 6-O-palmitoyl-D-galactopyranosides (60ab)	203
5.10.13	Characterization of 2-methyl-1-butyl 6-O-palmitoyl-D-galactofuranosides (60cd)	204
5.10.14	Characterization of 3-methyl-1-butyl 6-O-palmitoyl-D-galactopyranosides (61ab)	205
5.10.15	Characterization of 3-methyl-1-butyl 6-O-palmitoyl-D-galactofuranosides (61cd)	206
5.10.16	Characterization of 1-hexyl 6-O-palmitoyl-D-galactopyranosides (62ab)	207
5.10.17	Characterization of 1-hexyl 6-O-palmitoyl-D-galactofuranosides (62cd)	208
<b>5.11</b>	<b>Synthesis of 1-butyl 6-O-palmitoyl-D-glycosides from cheese whey permeate</b>	<b>209</b>
5.11.1	Enzymatic hydrolysis of D-lactose found in cheese whey permeate	209
5.11.2	Fischer glycosylation of D-glucose and D-galactose mixture	210
5.11.3	Enzymatic esterification of 1-butyl D-glycosides	211
<b>5.12</b>	<b>Quantitative TLC and image analysis</b>	<b>212</b>

<b>5.13 Fatty acid composition of commercial sunflower oil</b>	<b>214</b>
<b>5.14 Preliminary physico-chemical characterization</b>	<b>215</b>
5.14.1 Solubility measurements	215
5.14.2 Hydrophilic-lipophilic balance (HLB) calculation	215
5.14.3 Contact angle measurement	215
<b>5.15 Surfactant properties study</b>	<b>216</b>
5.15.1 Interfacial tension measurements	216
5.15.2 Emulsifying properties	216
<b>6   REFERENCES</b>	<b>218</b>
<b>A   APPENDIX A</b>	<b>233</b>
<b>A.1 Biocatalytic methods for the hydrolysed vegetable proteins from renewable resources</b>	<b>234</b>

---

# Abbreviations

The following abbreviations have been used in the text.

2,2-DMP	2,2-Dimethoxypropane
2M2B	2-Methyl-2-butanol
$\alpha$ -Fu	$\alpha$ -Furanoside
$\alpha$ -Py	$\alpha$ -Pyranoside
$\beta$ -Fu	$\beta$ -Furanoside
$\beta$ -Py	$\beta$ -Pyranoside
APT	Attached proton test
CALB	Lipase B from <i>Candida antartica</i>
Ce(SO <sub>4</sub> ) <sub>2</sub>	Cerium(IV) sulfate
COSY	<sup>1</sup> H- <sup>1</sup> H Correlation spectroscopy
(NH <sub>4</sub> ) <sub>6</sub> Mo <sub>7</sub> O <sub>24</sub> ×4H <sub>2</sub> O	Ammonium molybdate tetrahydrate
D <sub>2</sub> O	Deuterium oxide
DCM	Dichloromethane
DMF	<i>N,N</i> -Dimethylformamide
DMSO	Dimethyl sulfoxide
DMSO- <i>d</i> <sub>6</sub>	Deuterated dimethyl sulfoxide
DoE	Design of experiments
EtOAc	Ethyl acetate
HLB	Hydrophilic-lipophilic balance
HMBC	Heteronuclear multiple bond correlation spectroscopy
HSQC	Heteronuclear multiple quantum correlation spectroscopy
MeOD	Deuterated methanol
MeOH	Methanol
Na <sub>2</sub> SO <sub>4</sub>	Sodium sulfate
NaHCO <sub>3</sub>	Sodium bicarbonate
NaOH	Sodium hydroxide
OVAT	One-Variable-At-a-Time
PTSA	<i>p</i> -Toluenesulfonic acid
R <sub>f</sub>	Retention factor
<i>t</i> -BuOH	<i>tert</i> -Butanol
THF	Tetrahydrofuran
TLC	Thin Layer Chromatography
TMS	Tetramethylsilane



# 1 | Introduction

## 1.1 Sustainable Chemistry

Designing chemical processes and products able to eliminate or reduce the generation and the use of hazardous substances represents the main goal of the Sustainable or Green Chemistry. According to the US Environmental Protection Agency (EPA), this definition can be applied through the overall life cycle of a chemical product, *i.e.*, its design, manufacture, use, and ultimate disposal (EPA United States Environmental Protection Agency, 2023).

### 1.1.1 Origins of Sustainable Chemistry

After the World War II, the huge economic development due to the rapid growth of industrial activities, especially in the chemical sector, contributed to the improvement of the living standards in industrialized countries at the expenses of the environment (Tobiszewski et al., 2009).

The environmental damages on local ecosystems resulted by the indiscriminate use of hazardous chemicals, *i.e.*, the hazardousness of dichlorodiphenyltrichloroethane (DDT), was highlighted only in 1962 by Rachel Carson, a marine biologist. Her book *Silent Spring* (Carson, 1962) served as a wake-up call for scientists and global government policies, moreover, provoking the creation of environmental movements.

Few years later, in 1970, the federal regulatory agency dedicated to the protection of human health and the environment, US Environmental Protection Agency (EPA), was established. The huge impact of Rachel Carson's book influenced the EPA's first main decision of banning the use of DDT and other chemical pesticides (ACS Chemistry for Life, 2019).

However, despite the global awareness of the human impact on the environment, many years were necessary to introduce the concept of sustainable development. According to the *Brundtland Report*, it is a development that meets the needs of the current generation without compromising the future generation, thus combining formally for the first time environmental and social issues (de Marco et al., 2019).

Therefore, the need of reducing the amount of pollution by directly preventing the waste generation became evident to industries, governments and public. The US *Pollution Prevention Act*, adopted at the beginning of the '90s, encouraged the abandoning of end-of-pipe solutions on waste or pollution remediation in favour of cost-effective changes in operating procedures and raw materials selection. Indeed, the economic competitiveness of an industrial process can be strengthened by a more efficient use of raw materials and a minimization of waste at the source, concomitantly reducing their treatment cost. Substantially, these fundamental changes have planted the seeds for the introduction of the term "Green Chemistry" (Sheldon, 2016).

In 1996, the first publication of Anastas and Williamson, "*Green Chemistry: An Overview*" in *Green Chemistry: Designing Chemistry for the Environment*" firstly approached the philosophy of Green or Sustainable Chemistry, which is still followed nowadays (Linthorst, 2010).

The application of chemical knowledge and skills in order to decrease or eliminate the production and the use of hazardous substances during the planning, manufacturing and application of chemicals, thus minimizing health and environmental risks represent the scope of Green Chemistry (Anastas, 1999).

Thus, Green Chemistry is not a separate scientific discipline, but it can be considered as an interdisciplinary field which promotes innovative research able to find and maintain a balance between the exploitation of natural sources, the economic growth and the environmental conservation, being aware of having chemical, ecological and social responsibility (Ivanković, 2017).

### 1.1.2 The 12 Principles of Green Chemistry

“*Green Chemistry: Theory and Practice*”, published by Paul Anastas and John C. Warner in 1998 (Anastas & Warner, 1998), is considered the herald of the Green Chemistry philosophy and it resembles the Hippocrates’s code “*Primum non nocere*” (“*First, do no harm*”), applied both to humans and the environment. Within this manual, the fundamental concepts of the Sustainable Chemistry are depicted as 12 Principles, see **Figure 1.1**.

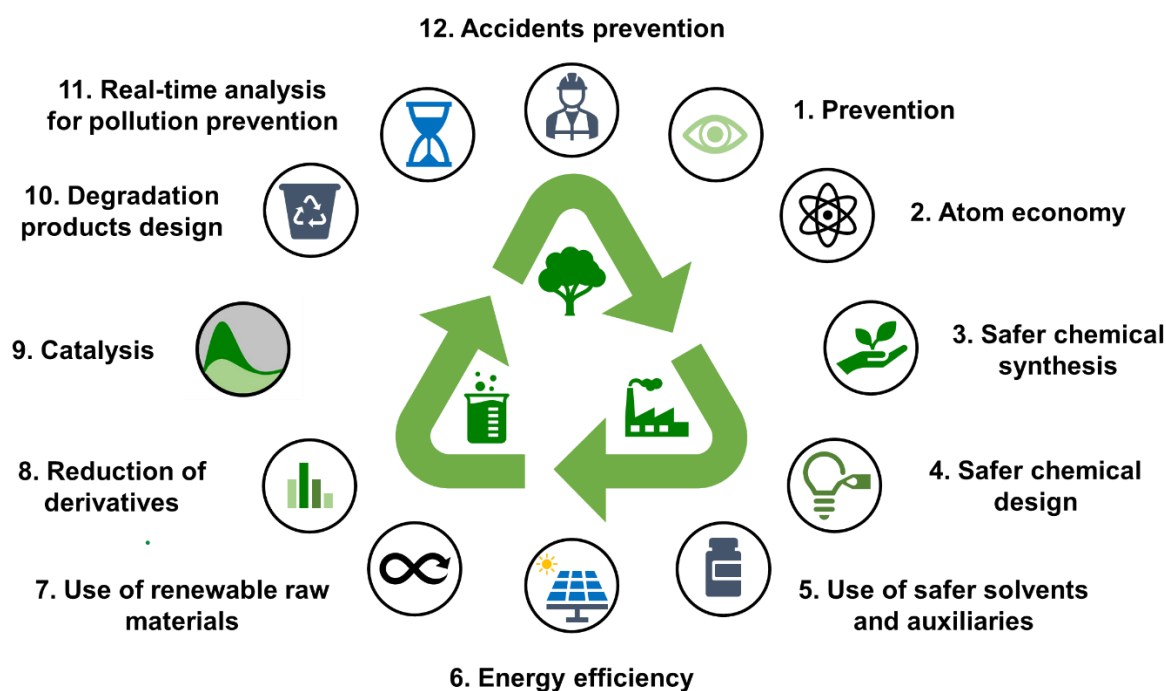


**Figure 1.1.** Overview of the 12 Principles of Green Chemistry.

The 12 Principles of Green Chemistry, see **Table 1.1**, can guide academic and industrial scientists in the designing products with an environmentally friendly life cycle, thus minimizing both their occupational risks inherent to industrial activities and their environmental burden, by preventing the formation of waste (Tobiszewski et al., 2009).

**Table 1.1.** Description of the 12 Principles of Green Chemistry proposed by Anastas and Warner.

<b>Number</b>	<b>Principle</b>	<b>Description</b>
1	Prevention	It is better to prevent waste than to treat or clean up waste after it is formed.
2	Atom Economy	Synthetic methods should be designed to maximize the incorporation of all materials used in the process into the final product.
3	Safer Chemical Synthesis	Wherever practicable, synthetic methodologies should be designed to use and generate substances that possess little or no toxicity to human health and the environment.
4	Safer Chemical Design	Chemical products should be designed to preserve efficacy of function while reducing toxicity.
5	Use of Safer Solvents and Auxiliaries	The use of auxiliary substances (e.g., solvents, separation agents, etc.) should be made unnecessary wherever possible and, innocuous then used.
6	Energy Efficiency	Energy requirements should be recognized for their environmental and economic impacts and should be minimized. Synthetic methods should be conducted at ambient temperature and pressure.
7	Use of Renewable Raw Materials	A raw material or feedstock should be renewable rather than depleting, whenever technically and economically practicable.
8	Reduction of Derivatives	Unnecessary derivatization (blocking group, protection/deprotection, temporary modification of physical/chemical processes) should be avoided whenever possible.
9	Catalysis	Catalytic reagents (as selective as possible) are superior to stoichiometric reagents.
10	Degradation Products Design	Chemical products should be designed so that at the end of their function they do not persist in the environment and break down into innocuous degradation products.
11	Real-Time Analysis for Pollution Prevention	Analytical methodologies need to be further developed to allow for a real-time, in-process monitoring and control prior to the formation of hazardous substances.
12	Accidents Prevention	Substances and the form of a substance used in a chemical process should be chosen so as to minimize the potential for chemical accidents, including releases, explosions, and fires.

In industrial chemical processes, the atom economy, the exploitation of safe and renewable raw materials, as well as the limitation of the use of toxic solvents take priority. Moreover, the energy savings and the reduction of waste produced can be also achieved by passing from the stoichiometric reagents to catalyst-mediated syntheses, which usually led to lower by-products formation and can be performed in milder reaction conditions. Indeed, the chemical production of substances must be carried out reducing potential accidents, both personnel and environmental. Finally, considering the overall life cycle of products, it is mandatory to consciously develop chemicals able to decompose in degradation products harmless to the environment, thus avoiding bioaccumulation (de Marco et al., 2019).

Aiming at adopting more sustainable processes to face environmental issues, companies have to upgrade their conventional production and product development habits, by improving chemical research and ecological engineering (de Marco et al., 2019).

The 12 Principles of Green Chemistry should not be considered as a list of compulsory requirements to be met, but they represent guidelines for the chemical industry to be followed in order to achieve the greenest possible result (Ivanković, 2017).

## 1.2 Surfactants

Amphiphilic compounds bear hydrophobic and hydrophilic moieties, thus, their energetically most favourable orientation is at surfaces or interfaces. These molecules, which are spontaneously adsorbed at interfaces, are termed surface-active agents or surfactants (Sarney & Vulfson, 1995).

They constitute a unique class of chemical compounds with the ability to radically alter surface and interfacial properties. Such properties provide the means to apply surfactants in several industrially relevant processes, *i.e.*, detergency, wettability modification, displacement of liquid phases through porous media, stabilization and destabilization of dispersed systems (Schramm, 2005).

Among the other surfactant features, the stabilization of emulsions is one of the most investigated.

### 1.2.1 Stabilization of emulsions

An emulsion is a colloidal dispersion in which a liquid is finely dispersed in a continuous liquid phase of different composition (Schramm, 2005).

Emulsions are thermodynamically unstable systems, if compared to the separated states of the phases they are constituted of (usually water and oil), because of the unfavourable interactions between the oil and water molecules at the interface. (McClements & Jafari, 2018).

Considering only the molecules of one liquid phase, they equally feel the attractive van der Waals forces between each other, except those in the interfacial region. This imbalance pulls the latter molecules towards the interior part of the liquid phase. The contracting force at the interface is known as the interfacial tension (IFT), which is often relatively high at an oil-water interface.

Indeed, if no stabilizing agent is present, an emulsion, will tend to adopt the configuration that minimizes the interfacial free energy, thus undergoing emulsion breaking processes. Contrarily, the adsorption of a surfactant at an interface provides an expanding force acting against the normal IFT. Thus, surfactants tend

to lower interfacial tension and, if the IFT reaches a sufficiently low value, emulsification can take place (Schramm, 2005). These molecules able to induce a huge variation of the IFT and to stabilize emulsions are usually labelled as emulsifying agents.

In emulsions, surfactants acting as emulsifiers tend to arrange themselves so that each part of the molecules can reside in the environment towards which it has the greatest affinity. Thus, “polar heads” will be directed towards the water phase, on the contrary, the fatty alkyl “tails” to the oil one, see **Figure 1.2**.

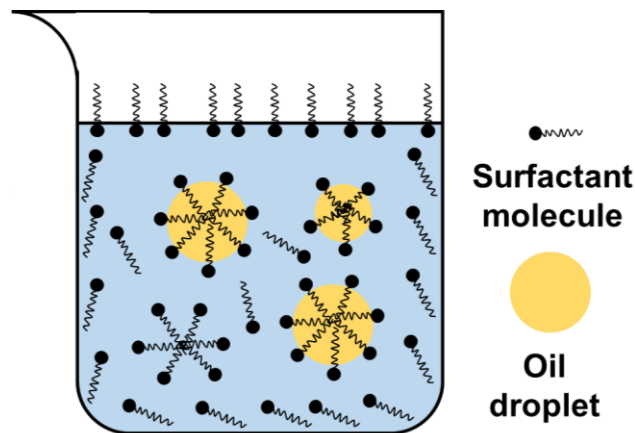


**Figure 1.2.** Surfactant distribution in an oil-in-water (O/W) emulsion. The size of the surfactant molecules compared to the oil droplets has been exaggerated for the purposes of illustration.

Two main types of emulsions can be generated, depending on the nature of the dispersed phase: oil-in-water (O/W) or water-in-oil (W/O).

According to the oriented-wedge theory, a simple and practical rule of thumb, if an emulsifying agent is preferentially soluble by one of the phases, then more of that agent can be accommodated at the interface, if that interface is convex towards that phase – *i.e.*, if that phase is the continuous phase. Therefore, more hydrophilic surfactants will tend to stabilize O/W emulsions, on the other hand, W/O emulsions are more easily stabilized by lipophilic emulsifying agents.

The hydrophilic-lipophilic balance (HLB) represents an empirical predictive approach to investigate the surfactant positioning at the interface. For non-ionic surfactants, it is a dimensionless scale ranges from 0–20. A low HLB (<9) refers to a lipophilic or oil soluble tenside, on the other hand, a high HLB (>11) to a hydrophilic-water soluble one (Schramm, 2005).



## 1.2.2 Surfactants market and environmental awareness

The global surfactants market was recently valued at USD 42.1 billion because of the widespread use of surfactants in several sectors of the modern industry (Markets and Markets, 2023). Their application ranges from household detergents and personal care products to industrial & institutional (I&I) cleaners, food processing, oilfield and agricultural chemicals, textiles, plastics, paints & coatings, adhesives, etc. (Begum et al., 2020)

Moreover, the global surfactant market is estimated to register an annual growth rate of 4.5% from 2020 to 2025, reaching USD 52.4 billion by 2025 (Markets and Markets, 2023). This market growth is triggered by the growing population and the increasing urbanization. The latter is usually strictly related to consumer lifestyle changes and incremented personal income.

In particular, the rising customer consciousness towards hygiene represents the driving factor for the increasing demand towards household detergents and personal care products in developed and developing economies. These two sectors shared more than a half of the surfactants market in 2016 (**Figure 1.3**) and they will support its expansion in the next years (GVR Grand View Research, 2023).

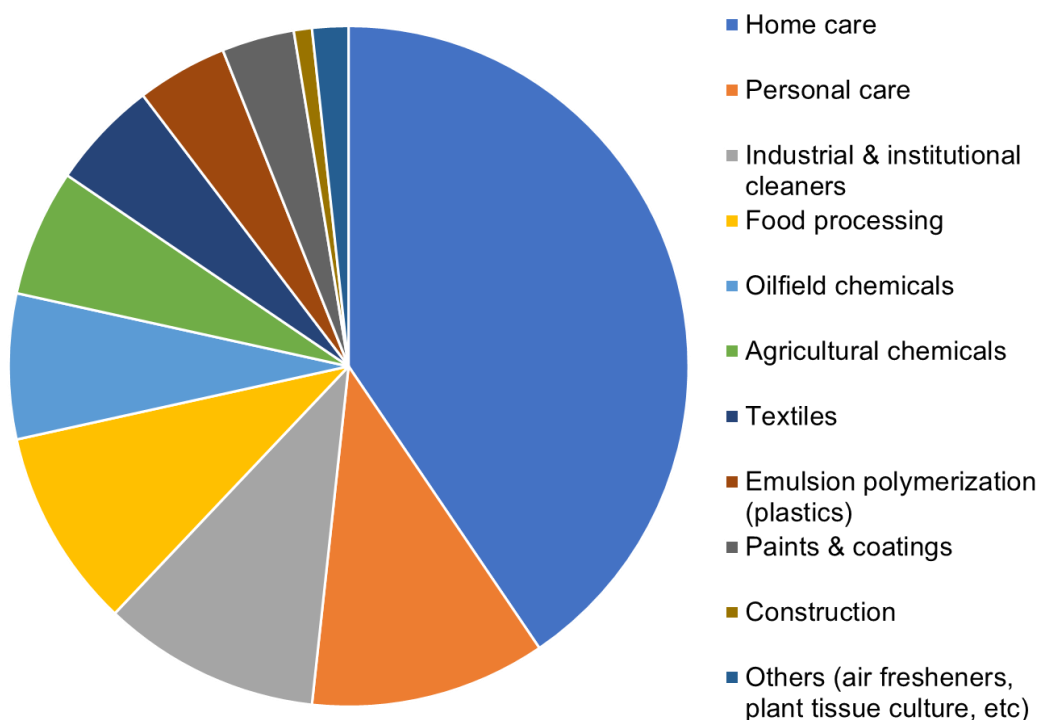


**Figure 1.3.** Global surfactants market by applications in 2016.

Chemically synthesized surfactants are usually classified according to the nature of their “polar head” groups. They can be divided in anionic, cationic, amphoteric and non-ionic.

Anionic surfactants (bearing a negative charge) dominate the market due to their excellent detergency and foaming properties, low cost and ease availability. Linear alkylbenzene sulfonates (LAS), alkyl ethoxy sulphates (AESs) are the mostly produced surfactants, which usually find application as dishwashing and laundry detergents and soaps, as well as industrial cleaners and shampoos (Mungray & Kumar, 2009).

Cationic surfactants, *i.e.*, quaternary ammonium compounds, have a positive charge that makes them useful in anti-static products as fabric softeners and conditioners. It also serves as an antimicrobial agent, having major use in disinfectants (FBI Fortune Business Insights, 2023).

Amphoteric or zwitterionic tensides possess dual charges permanent or pH dependent on the hydrophilic end. They have huge potential and are usually applied as additives in shampoos and cosmetic products due to their mildness to the skin, eyes and mucous membranes. However, they account for just 5% of the overall surfactant market because of their higher manufacturing cost with respect to the other type of surfactants (Sarkan et al., 2021).

Finally, non-ionic surfactants are available in a wide variety of different chemical structures by combining uncharged head and hydrophobic groups. Their non-charged nature makes them effective in several applications, *i.e.*, wetting, spreading, low-foaming and emulsifier agents. Moreover, they represent a major ingredient of several industrial formulation due to their attractive characteristics, such as low cost, low toxicity and minimal skin and eye irritation effects, as well as biodegradability. Alcohol polyethoxylates (AEOs) are the most synthesized and widespread used non-ionic surfactants (Xiang et al., 2019; Zhao & Wan, 2007).

The extensive use and high worldwide consumption volumes of surfactants-based products, especially household detergents, is becoming an environmental burden. Surfactant residues continuously discharged into treated and untreated wastewaters tend to bioaccumulate, causing environmental toxicity, in several

compartments, *i.e.*, surface and marine waters, sediments and sludge-amended soils, *etc.* (Traverso-Soto et al., 2013).

Environmental and human health concerns related to the extensive use of petroleum-based surfactants are driving the search and the market towards new natural or bio-based surfactants to be employed as valid alternatives to existing products.

Recently, customers' inclination towards green and sustainable products, motivated by a sense of environmental or social responsibility or by the supposition that such products are better, safer and healthier, is supporting the growth of the biosurfactants market.

Concomitantly, the increased environmental awareness among the chemical community and the tightening regulations are favouring the research of safer and more eco-friendly processes and products.

Moreover, producers can earn from the economic benefits generated by the application of the Green Chemistry Principles, *i.e.*, lower investments in effluent storage and waste treatment and in the payment of indemnities for ecological damages, as well as energy saving, due to milder reaction conditions and fewer chemical steps for the product synthesis (Prado, 2003).

Only green technology or discovery demonstrated to be economically advantageous can impact the market. On the other hand, the market cannot ignore environmental needs and human involvement to prosper (Tundo et al., 2000).

## 1.3 Natural surfactants

The designing of safer chemical products, showing reduced toxicity, while maintaining their efficacy of function represents the key topic of the fourth Principle of Green Chemistry (Anastas & Warner, 1998).

Balancing safety and efficiency of chemical products or processes is a challenge task. It is mandatory to find the proper equilibrium between optimal performances and toxicity and hazardous minimization, both for humans and the environment. Aiming at achieving this goal, interdisciplinary knowledges are compulsory, *i.e.*, chemistry, principles of toxicology and environmental science. (Ivanković, 2017).

Thus, with the purpose to satisfy the ever-growing demands of the Green Chemistry, the research efforts on the production of non-toxic and biodegradable natural surfactants as functionally and economically valuable alternatives to chemical surfactants have grown exponentially in the last two decades.

### 1.3.1 Definition and categories of natural surfactants

Strictly speaking, only molecules obtained directly from a natural source, either of plant or animal origin, by separation procedures, *i.e.*, extraction, precipitation or distillation, completely avoiding organic synthetic steps, not even as an after-treatment, can be labelled as “natural surfactant”.

Very few commercially available tensides in use nowadays can meet these requirements, *i.e.*, lecithin extracted from soybean or egg yolk.

The industrial production of truly natural surfactants is often limited by the costs related to their purification procedures. Despite the availability of the natural sources from which they can be obtained, these products are usually found in small amounts and the work-up tends to be tedious. In most cases, the costs related to their separation / isolation exceeds by far the manufacturing costs of synthetic chemical surfactants equivalent in terms of performance.

However, the term “natural surfactant” is often used in a broader sense. Indeed, surfactants obtained through biocatalysis or fermentation, in which either the

hydrophobic or the hydrophilic part is derived from natural raw materials, are usually referred to as natural or bio-based surfactants (Holmberg et al., 2001).

Thus, considering this definition, several compounds can be labelled as “natural surfactant”, which can be divided into three main categories.

- **Surfactants produced through fermentation**

These natural surfactants are obtained by fermentation processes of yeasts and bacteria optimized to produce tensides, thus representing promising products for the modern biotechnology. Sophorolipids and rhamnolipids (**Figure 1.4.a** and **1.4.b**), are considered prominent examples of this category of bio-based surfactants. They are glycolipids, namely compounds in which sugars are bonded to hydroxy fatty acids *via* a glycosidic bond. Moreover, they are generated by the yeasts of the genus *Candida* and by the bacterium *Pseudomonas aeruginosa*, respectively (Marchant & Banat, 2012). Surfactin® (**Figure 1.4.c**) is another deeply investigated compound within this field. It is a cyclic lipopeptide, comprised of a carboxylic acid linked by a lactone ring to a heptapeptide. It is produced by various strains of *Bacillus subtilis* and it is known for its excellent surfactancy and biodegradability (Sen & Swaminathan, 1997).

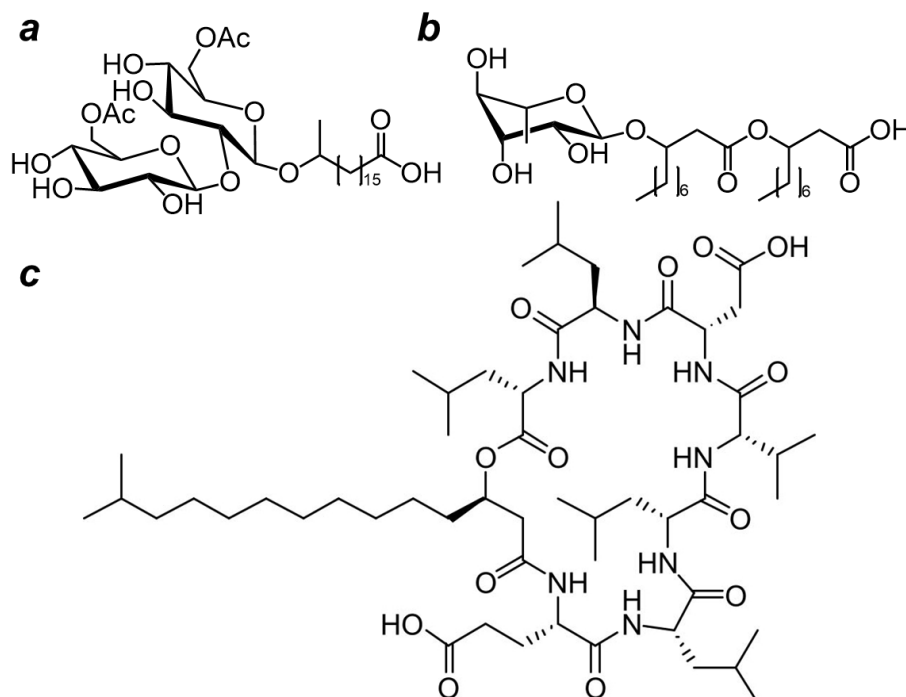


**Figure 1.4.** Examples of natural surfactants obtained through fermentation processes: **a)** Sophorolipid; **b)** Rhamnolipid; **c)** Surfactin®.

- **Surfactants based on a naturally derived “hydrophobic tail”**

Fatty amide ethoxylates and sterol ethoxylates (**Figure 1.5.a** and **1.5.b**) represents the two families of molecules which aroused the greatest interest within this category of biosurfactants.

Specifically, fatty amide ethoxylates have been deeply investigated as they showed excellent packing capacity, due to hydrogen bond formation, and ready biodegradability into amino-terminated poly(ethylene glycols) and fatty acids. Thus, they are considered a valuable alternative to fatty alcohol polyethoxylates. Good packing capacity at the interface was also reported for sterol-based surfactants due to their large hydrophobic group of fully natural origin, whose planar structure of four rings seems to generate strong Van der Waals intermolecular interactions (Holmberg et al., 2001).

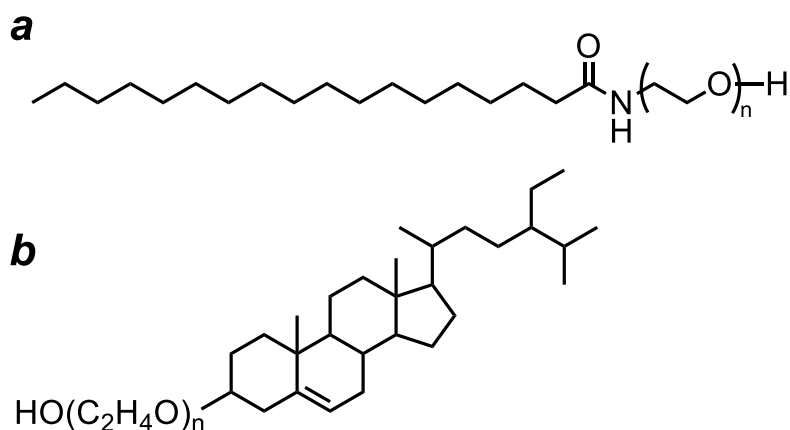


**Figure 1.5.** Examples of surfactants bearing a hydrophobic tail of natural origin: **a**) Stearyl amide ethoxylate; **b**)  $\beta$ -Sitosterol ethoxylates.

- **Surfactants based on a naturally derived “polar head”**

Amino acids and sugars represent the mostly investigated natural polar headgroups. Regarding the former, studies focused on lysine and arginine derivatives. On the other hand, several research efforts were put into the investigation of the promising physico-chemical properties of sugar-based

surfactants, due to their huge application potential in different industrial fields (Holmberg et al., 2001).

Several molecules fall under this category of tensides. One or innumerable saccharide units of all kinds can constitute the hydrophilic head of the surfactant, instead the hydrophobic tail could comprise one or more chains of different length. Moreover, four type of bonds can occur between the hydrophilic sugar headgroup and the hydrophobic alkyl chain (see **Figure 1.7**) (Stubenrauch, 2001).

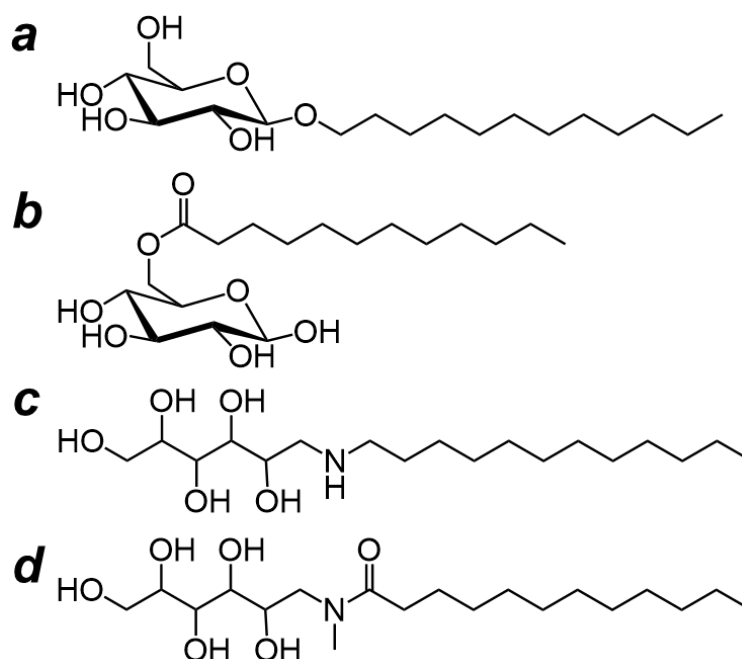


**Figure 1.7.** Examples for the most frequent linkages between the hydrophilic and the hydrophobic moiety in sugar-based surfactants: **a**) ether bond, dodecyl- $\beta$ -D-glucoside; **b**) ester bond, 6-O-lauroyl-D-glucose; **c**) amine bond, N-dodecyl-glucamine; and **d**) amide bond, N-lauroyl-glucamine.

Among all the sugar-based surfactants, the research mostly focused on three classes: alkyl polyglucosides (APGs), alkyl glucamides and sugar fatty acid esters (SFAEs). The former have been extensively studied for their environmentally friendly profile and its mildness to eyes and skin, making APGs well-established ingredients for personal care products. Some alkyl glucamides, *i.e.*, N-decanoyl-N-methylglucamines and cocoyl methyl glucamide, well-known under the trade name GlucoPure<sup>®</sup>, are commercially available non-ionic surfactants, widely used in the detergency sector (Clariant, 2023; Holmberg et

al., 2001). Finally, SFAEs, which represent the main topic of this research, will be discussed in detail in the following **Section 1.3.2**.

### 1.3.2 Sugar fatty acid esters

Sugar Fatty Acid Esters (SFAEs) are non-ionic surfactants comprised by a sugar moiety, which acts as “polar head”, linked *via* an ester bond to a long alkyl “tail” derived from a fatty acid. SFAEs can be labelled as natural and renewable surfactants because both their constituent parts can be derived from natural sources or from waste upgrading (Bhadani et al., 2020).

SFAEs unique physico-chemical properties can be tuned by controlling the nature of the sugar moiety and the type and length of the fatty acid residue, as well as the degree of esterification (Soultani et al., 2003).

Indeed, the customization of the HLB of these biosurfactants translates into a wide range of different applications, *i.e.*, solubilizing agents, lubricants, penetrating enhancers, pore forming agents and O/W or W/O emulsifiers (El-Laithy et al., 2011).

SFAEs displace numerous advantages over petrochemical-derived surfactants as several of them are reported to be non-harmful to the environment, and fully biodegradable. In addition, they exhibit low / no toxicity and are tasteless, odorless and skin-compatible (Ducret et al., 1995).

All these features make SFAEs an industrially relevant class of specialty chemicals, indeed they are used in many market sectors within the fine chemistry, *i.e.*, cosmetics, pharmaceuticals, detergency and food industry (Kennedy et al., 2006).

Nowadays, the only SFAEs commercially available include surfactants derived from sucrose and sorbitan, such as sucrose esters, as well as sorbitan esters and ethoxylated sorbitan esters, well-known under the trade names of Span<sup>®</sup> and Tween<sup>®</sup> (**Figure 1.8**) (Neta et al., 2015).

Recently, several research efforts have been put in the laboratory-scale investigation of the relationship between the nature of the sugar polar head moiety and the unique properties attributable to SFAEs. Many works have focused on the achievement of the target molecules exploiting the use of unsustainable synthetic



strategies, not sufficiently deepening SFAEs alternative productions from renewable and inexpensive resources, which remains an open field of study (El-Laithy et al., 2011).

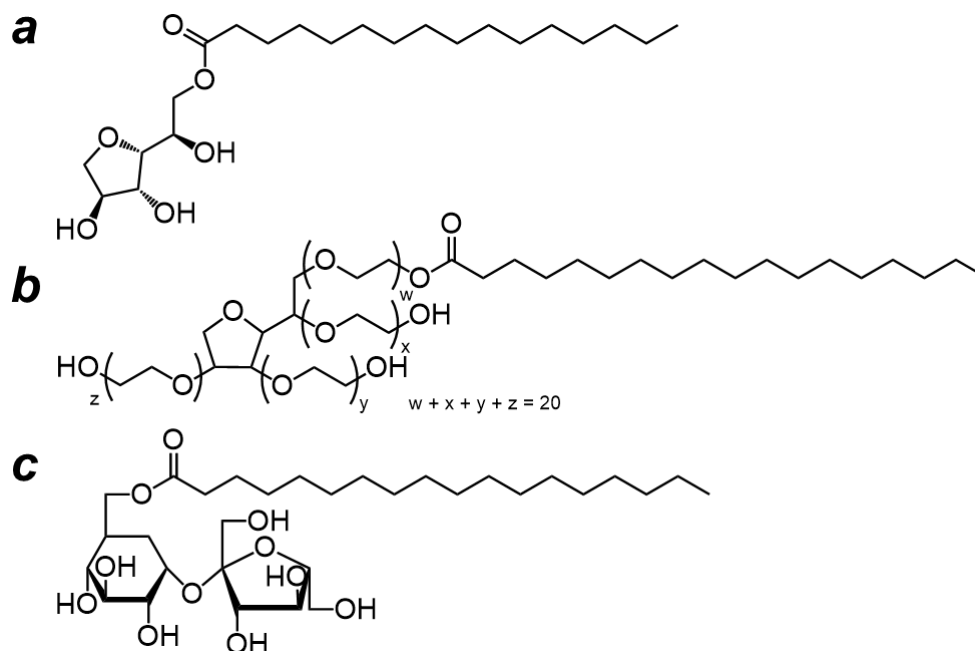


**Figure 1.8.** Examples of commercially available SFAEs: **a)** Sorbitan monopalmitate Span® 40; **b)** Polysorbate or Tween® 60 (polyoxyethylene (20) sorbitan monostearate); **c)** Sucrose monostearate.

### 1.4 Chemical vs enzymatic synthesis of SFAEs

SFAEs currently available on the market are industrially produced through direct esterification or transesterification which require the use of hazardous solvents, strong acid or alkaline metal catalysts, and high temperatures, ranging from 150 to 240 °C (Khan & Rathod, 2015).

These harsh reaction conditions result in high energy consumption and costs for the overall production processes, increasing the formation of undesirable by-products. They can be generated by thermally induced side-reactions on the raw materials *i.e.*, sugar dehydration / caramelization or unsaturated fatty acids polymerisation / oxidation (Ansorge-Schumacher & Thum, 2013).

Moreover, the poor regioselectivity of conventional catalysts towards the various hydroxyl groups bearing similar reactivity of saccharides can led to several SFAEs with different positions of acylation and different degrees of esterification (Yan et al., 2001).

Several species (more than 60) were isolated through gas chromatography analysis of food-grade sorbitan esters. Many of them were identified as isomers of sorbitan and isosorbide, as well as their mono-, di- and tri-esters. In addition, traces of undesirable by-products suspected as allergenic or carcinogenic were also found (Gumel et al., 2011; Sarney & Vulfson, 1995).

Protection / deprotection strategies can enhance the regioselectivity of the chemical synthesis of SFAEs, however, they have been demonstrated not to be economically feasible for the synthesis of surfactants (Björkling et al., 1898).

Dark and sometimes malodorous heterogeneous mixtures are often obtained. Several purification steps are compulsory to achieve the final pure product, *i.e.*, deodorisation by steam-stripping of water-soluble and volatile contaminations, bleaching with reagents like hydrogen peroxide, removal of residual water by drying, and filtration for catalysts, solid by-products and bleaching agents removal (**Figure 1.9.a**) (Ansorge-Schumacher & Thum, 2013).

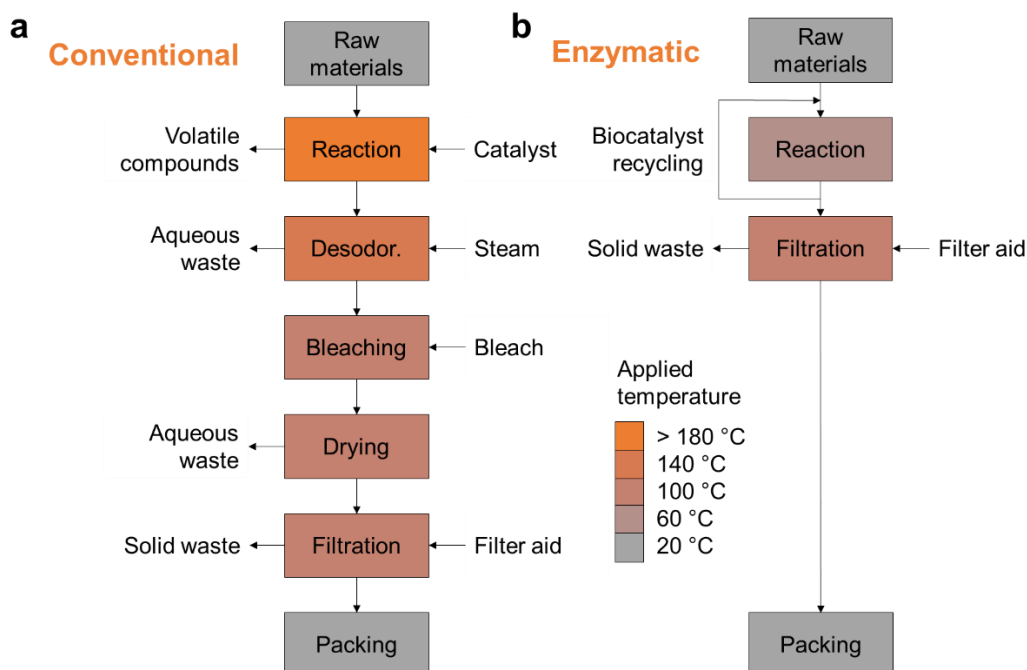


**Figure 1.9.** Simplified scheme of the process steps of **a)** conventional and; **b)** enzymatic esterification to produce SFAEs.

Enzyme-mediated syntheses of SFAEs represent a valid alternative to well-established chemical approaches, by circumventing the above-mentioned drawbacks. Enzymatic reactions usually can be performed under milder conditions (not exceeding 80 °C) and do not require tedious protection / deprotection steps as enzymes generally show high degree of chemo- and regioselectivity (Gumel et al., 2011).

Indeed, SFAEs can be prepared through enzyme-catalyzed esterification / transesterification reactions. (Ren & Lamsal, 2017; Sarmah et al., 2018)

In these cases, the monoester derivatives represent the main products of the reactions, almost completely avoiding the generation of diesters and by-products. Simplified purification procedures can be applied to the obtained mixtures, constituted only of product, enzyme, solvent and unreacted raw materials, thus reducing the generation of waste (Neta et al., 2015).

Enzymes are usually more expensive than conventional catalysts; however, their cost can be amortised by performing their recycling, if they resulted to be sufficiently stable or if they are immobilized onto a solid support. Moreover, the overall SFAEs production costs exploiting biocatalysis can be decreased due to the reduction of

the number of chemical refinement steps and the lower energy requirements, in terms of reaction temperature (**Figure 1.9.b**) (Ansorge-Schumacher & Thum, 2013).

Thus, the exploitation of biocatalysis to produce SFAEs is compliant with several Principles of Green Chemistry, *i.e.*, the use of selective catalysts able to reduce the derivatives produced, the prevention of waste, the design of a safer chemical synthesis, energetically efficient, with improved sustainability and economic savings (Anastas & Warner, 1998). Moreover, it meets the growing market demand for environmentally benign processes and products.

As a matter of fact, the number of synthetic steps in industrial processes conducted with biocatalysts has grown exponentially in the last two decades, as well as the related research aimed at solving shortcomings that sometimes still affect enzyme-mediated synthesis.

### 1.4.1 Lipases as biocatalysts

Lipases (triacyl glycerol hydrolases, EC 3.1.1.3) are ubiquitous enzymes which play a key role in the digestion of fats of several organisms, *i.e.*, bacteria, yeasts, plants and animals (Reis et al., 2009).

In aqueous media, this family of enzymes usually catalyses the hydrolysis of lipids. Their activity is drastically enhanced upon adsorption at the lipid / water interface. Indeed, lipases tend to change their conformation, undergoing interfacial activation (Uppenberg et al., 1995). This conformational change involves the opening of the lid, a mobile amphipathic structure, which usually covers the pocket of the catalytic active site of most lipases (Secundo et al., 2006).

The substrate-selectivity of these enzyme is usually regulated by the steric hinderance of hydrophobic amino acids residues, which cover the inner walls of the catalytic pocket. On the other hand, the activity of lipases is mainly due to the three hydrophilic amino acids situated at the bottom of the pocket. Notably, the catalytic mechanism (**Figure 1.10**) of these enzymes is strictly related to the stabilization of the tetrahedral intermediate generated during the hydrolysis of triglycerides, in the presence of water, by the Ser-His-Asp triad (Anderson et al., 1998).

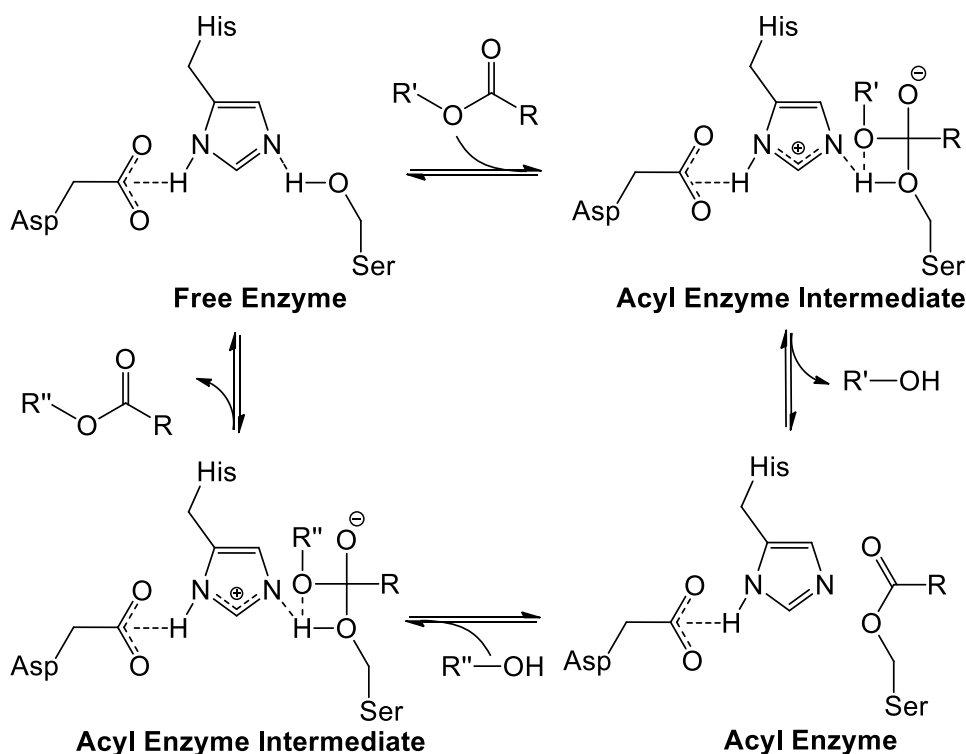


**Figure 1.10.** As first step, histidine and aspartate residues activate serine through deprotonation.

The hydroxyl residue of Ser, showing an enhanced nucleophilicity, is able to attack the carbonyl group of the triglyceride substrate, thus generating an acyl-enzyme intermediate, which is stabilized by the presence of an oxianion hole. During the de-acylation step, the alcohol moiety of the starting ester is released and hosted in the alcohol channel of the catalytic site, while a nucleophile, such as H<sub>2</sub>O, a monoglyceride or a simple alcohol, attacks the acylated enzyme, leading to the release of the product and regeneration of the catalytic site (Reis et al., 2009).

However, lipases behaviour can change in absence of aqueous media, *i.e.*, organic solvents containing traces of water compulsory for enzyme hydration and activity. Indeed, in this condition, the hydrolysis equilibrium reaction catalysed by this family of enzymes can be shifted towards the synthesis of esters (Gumel et al., 2011).

Studies on lipase substrate specificity reported a wide range of substrates well tolerated by these enzymes for the synthesis of esters. Due to their excellent versatility, they can be potentially applied in several industrial sectors, *i.e.*, cosmetic, detergent, food, pharmaceutical, leather, textile, and paper. Indeed, lipases have been acknowledged as the most promising class of enzymes in biotechnology (Reis et al., 2009).

Lipases widespread use is also related to their availability and stability, *i.e.*, bacteria or yeasts fermentation offers the accessibility to large quantity of these enzymes, moreover, most of them are extracellular enzymes, thus making easier their isolation and recovery (Hasan et al., 2006).

The lipase B yielded from the yeast species *Candida antarctica* (CALB) is widely used in several organic reactions and industrial processes due to its broad alcohol substrates scope, high stereo-, enantio-, and regioselectivity, as well as its excellent thermal stability and stability in organic solvents (Staucha et al., 2015).

CALB prefers molecules with straight chains, being not able to accept sterically demanding acyl moieties (Juhl et al., 2010). The rather restricted dimensions of the binding pocket were corroborated by crystallographic studies and molecular modelling (Uppenberg et al., 1995).

Nowadays, it is available on the market in both its free and immobilized forms. The latter is well-known under the trade name of Novozym<sup>®</sup> 435 (Novozymes A/S, Denmark), in which CALB is immobilised on the polymethacrylate carrier Lewatit VP OC 1600 (Lanxess, Germany). In the supported form, CALB demonstrated enhanced thermal and solvent stability, indeed, it can be used up to 60-80°C in presence of organic solvents without any significant loss of activity (Anderson et al., 1998).

Finally, the adoption of immobilized enzymes can bring several advantages at industrial scale, with respect to their free forms, *i.e.*, simple recovery from the product mixture by filtration and potential recycling.

### 1.4.2 SFAEs synthetic strategies

The main obstacle of the enzymatic synthesis of sugar fatty acid esters is related to the striking different polarity of the reagents, *i.e.*, sugars and fatty acids (Khan & Rathod, 2015).

To date, two different strategies can be identified to circumvent this constraint: *i*) selecting a proper solvent or co-solvent able to solubilize both the sugar and the fatty acid moieties without deactivating the enzyme; *ii*) derivatizing the sugar into a less polar precursor (*i.e.*, alkyl glycoside), followed by a solvent-free lipase-mediated esterification (Neta et al., 2015; Sangiorgio et al., 2022, Semproli et al., 2022).

Both strategies bear advantages and disadvantages. The first strategy is more straightforward however few solvents are qualified to dissolve a sufficient amount of both reactants without adversely affecting lipase activity and stability. They must be non-aqueous to promote the esterification reaction, avoiding hydrolysis. Nevertheless organic solvents tend to cause the water stripping of the hydration layer of the enzyme, reducing its mobility and, consequently, its catalytic power, activity and stability (Liu et al., 1999; Šabeder et al., 2006).

The second approach avoids the use of solvents during the esterification reaction, by exploiting the relatively low melting points of several fatty acids or analogues, thus performing the reaction in melt conditions. A preliminary step is compulsory to achieve sufficiently apolar sugar derivatives, therefore, in some cases, running protection / deprotection steps are required (Ansorge-Schumacher & Thum, 2013).

Early works focused on the first strategy found out that relatively polar aprotic solvents were suitable to synthesize SFAEs. Hazardous solvents such as pyridine, dimethyl formamide (DMF) and dimethylpyrrolidone (DMP) were commonly adopted (Akkara et al., 1999; Degn & Zimmermann, 2001; Jia et al., 2010). More sustainable solvents were also successfully employed for this enzymatic esterification, *i.e.*, methyl ethyl ketone (MEK), 2-methyl-2-butanol (2M2B), *tert*-butanol (*t*-BuOH), mixtures of pyridine/*t*-BuOH (45:55) and DMSO/*t*-BuOH (90:10) (Yan et al., 1999; Degn & Zimmermann, 2001; Pappalardo et al., 2017).

Regarding the second strategy, several derivatizations of the sugar moiety were investigated by exploring the use of different reversible lipophilic sugar-based

compounds as esterification substrates, *i.e.*, alkyl glycosides, sugar acetals or organoboronic acids complexes (Adelhorst et al., 1990; Fregapane et al., 1994; Ikeda & Klibanov, 1993). To restore the polar head of the surfactant, the selective hydrolysis of the protecting groups must be carried out. The steps required could complicate the synthesis and the use of auxiliary reagents, thus making the strategy less sustainable, both economically and environmentally.

Therefore, it is fundamental to evaluate, for both the strategies, the most sustainable choices in terms of process design, reagents, catalysts and solvents.

Regarding the latter, solvents represent at least half of the material used in conventional chemical processes. Solvents influence solubility, stability and chemical reactivity of compounds during a chemical reaction. Environmental and health risks related to the toxicity, flammability, volatility and corrosivity of many of them have driven the research towards more innocuous, but still effective ones (Anastas & Warner, 1998; de Marco et al., 2018).

The selection of the “greenest” solvent for a process represents a challenging task because several criteria have to be evaluated, *i.e.*, safety, occupational health, environment, quality and risk of impurities, as well as industrial constraints, such as boiling point, freezing temperature, density, recyclability, and cost.

Prat and co-workers proposed a classification of commonly employed solvents according to six categories of risks which represents a useful tool to guide this choice (**Figure 1.11**) (Prat et al., 2014).

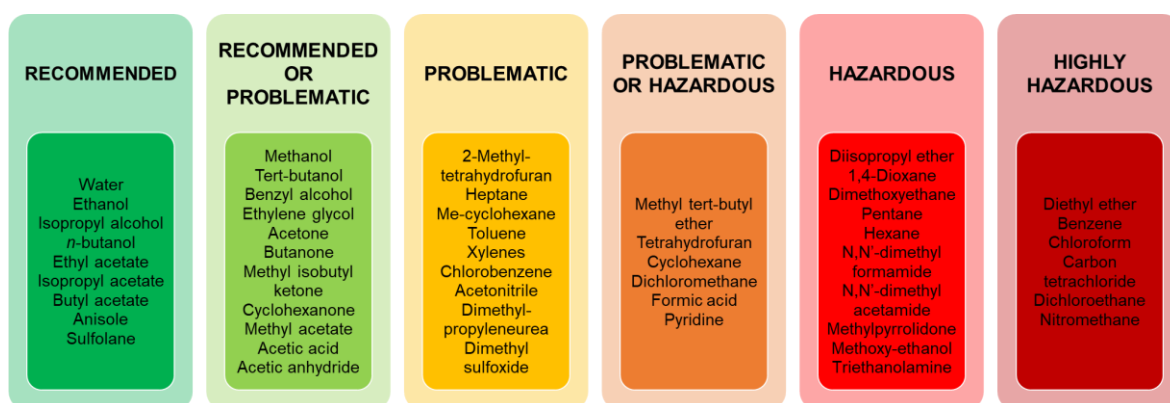


**Figure 1.11.** Green solvents classification.



### 1.5 Exploitation of renewable raw materials

The selection of the starting materials strongly influences the synthetic pathway of production processes, as well as their environmental and health impact. Chemicals originated from processes, which deplete limited natural resource, will result in environmental damage.

Thus, whenever technically and economically practicable, the initial choice should be focused on the exploitation of renewable feedstock and raw materials, rather than depleting ones, according to the seventh Principle of Green Chemistry (Anastas & Warner, 1998).

Nowadays, the society and the chemical processes are still largely dependent on non-renewable fossil resources, *i.e.*, oil, coal and natural gas, whose widespread use to produce chemicals, energy and fuels is unsustainable (Sheldon, 2011).

The transition to a new “circular economy” is becoming compulsory, in which renewable raw materials and waste are managed sustainably by turning them into a resource is becoming compulsory.

#### 1.5.1 Oils and fats as renewable raw materials

Oil and fats, derived from vegetal and animal sources, represent historically and currently essential renewable feedstocks of the chemical industry (Hill, 2000).

The total production of oils and fats has had an exponential growth over the last two decades. In 2016, their worldwide production was estimated to be roughly 204 million tonnes, thus doubling the amount manufactured in 1998 (**Figure 1.12**) (MPOC Malaysian Palm Oil Council, 2023).

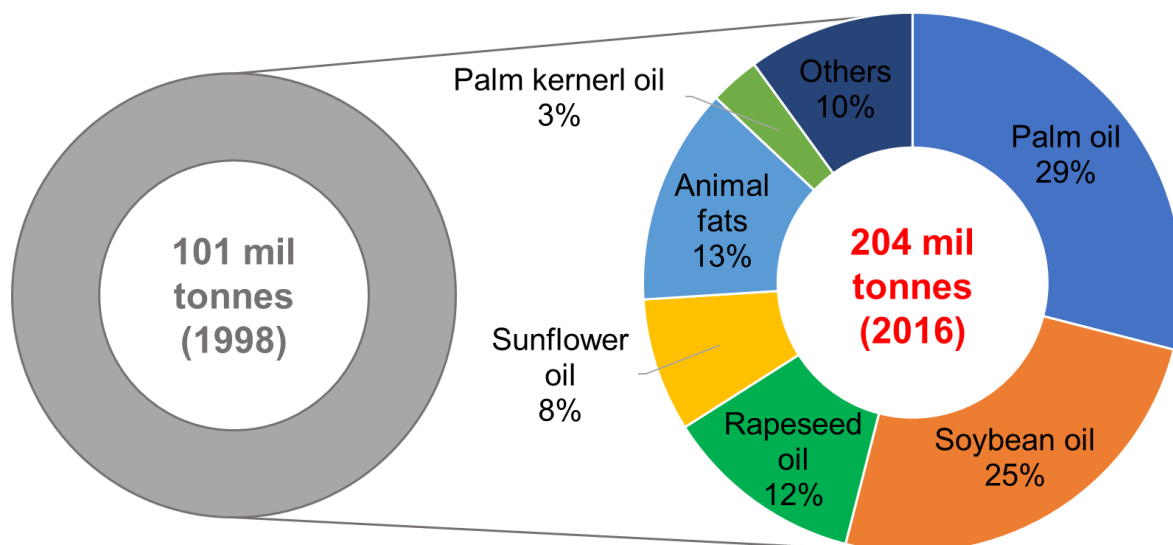


**Figure 1.12.** Global production of fats and oils in 2016, according to the Oil World Database.

On one side, this huge increment meets the demands of the ever-increasing human population. About three-fourths of the worldwide consumption of these fats and oils is related to food applications.

On the other hand, the growing production of biodiesel stimulated their industrial consumption in oleochemistry. In 2016, around 45 million tonnes were made available for this purpose.

Palm oil global production has undergone exponential growth, passing from 18% in 1998 to 29%, which is mainly due to its high and homogeneous content of long-chain fatty acids, *i.e.*, C<sub>16</sub> and C<sub>18</sub>, saturated and unsaturated. Its lipidic profile, as well as those of soybean, rapeseed, and sunflower oil, results in a narrow distribution of fatty acid methyl esters obtained through the conventional and well-established oleochemical process of triglyceride hydrolysis, followed by transesterification, to produce biodiesel (Hill, 2000).

Coconut and palm kernel oils also represent valuable sources of short and medium chain length fatty acids (mainly C<sub>12</sub> and C<sub>14</sub>). They are extremely suitable to generate surfactants for washing and cleansing agents in cosmetics (Biermann et al. 2011). Indeed, the derivatization and the processing of fats and oils to generate a wide variety of products with several potential applications has a long tradition (Neta et al., 2015).

### 1.5.2 Cheese whey valorization

Carbohydrates represent a valuable raw material to produce non-toxic and environmentally friendly specialty chemicals (Tokiwa et al., 2000). However, only few sugars fulfil the criteria of availability, price, and quality to be considered suitable for industrial application. Moreover, the use of first-generation biomass, which are directly or indirectly food competitors, should be avoided, aiming at obtaining sustainable products and processes. Contrarily, the valorization of unavoidable sugar waste biomass, *i.e.*, agricultural, forestry and dairy residues, represents an attractive scenario. Therefore, special attention must be given to sucrose derived from sugarcane bagasse, glucose and its derivatives, *i.e.*, sorbitol, obtained from starches and lignocellulosic feedstock, and lactose from cheese whey (Neta et al., 2015; Sheldon, 2016).

Cheese whey represents the main waste stream of the dairy industry, which is generated during the precipitation and removal of milk casein in cheese making. Indeed, to produce 10 kg of cheese, around 100 kg of milk are used and roughly 90 kg of cheese whey or cheese whey wastewater (CW or CWW) are generated as by-product (FAO Food and Agriculture Organization, 2021). Considering that the global cheese production amounted to about 22.17 million tons, in 2022, CWW resulted to be roughly 200 million tons (Statista, 2023).

Nowadays, CWW is considered an environmental burden due to its large production volumes; furthermore, lactose and fats contained within it require high values of biochemical and chemical oxygen (BOD and COD, respectively) in order to be broken down by microorganisms once disposed (Carvalho et al., 2013; Guimarães et al., 2010).

The dairy industry has faced the CWW surplus as a waste problem, until recently, *i.e.*, piping it into rivers, lakes or the ocean, spreading it over fields, feeding into ruminants, or dumping it into municipal sewage systems. Especially the latter resulted not to be able to handle the high BOD and COD demand required to reduce CWW polluting load, thus creating serious environmental problems (Kosikowski, 1979).

Strict regulations prohibiting its dumping into waterways have been issued consequently to the rising awareness of the polluting problems related to CWW. Moreover, the acknowledgement of its huge potential as source of value-added products became widespread, making interesting its possible valorization (**Figure 1.13**) (Guimarães et al., 2010).

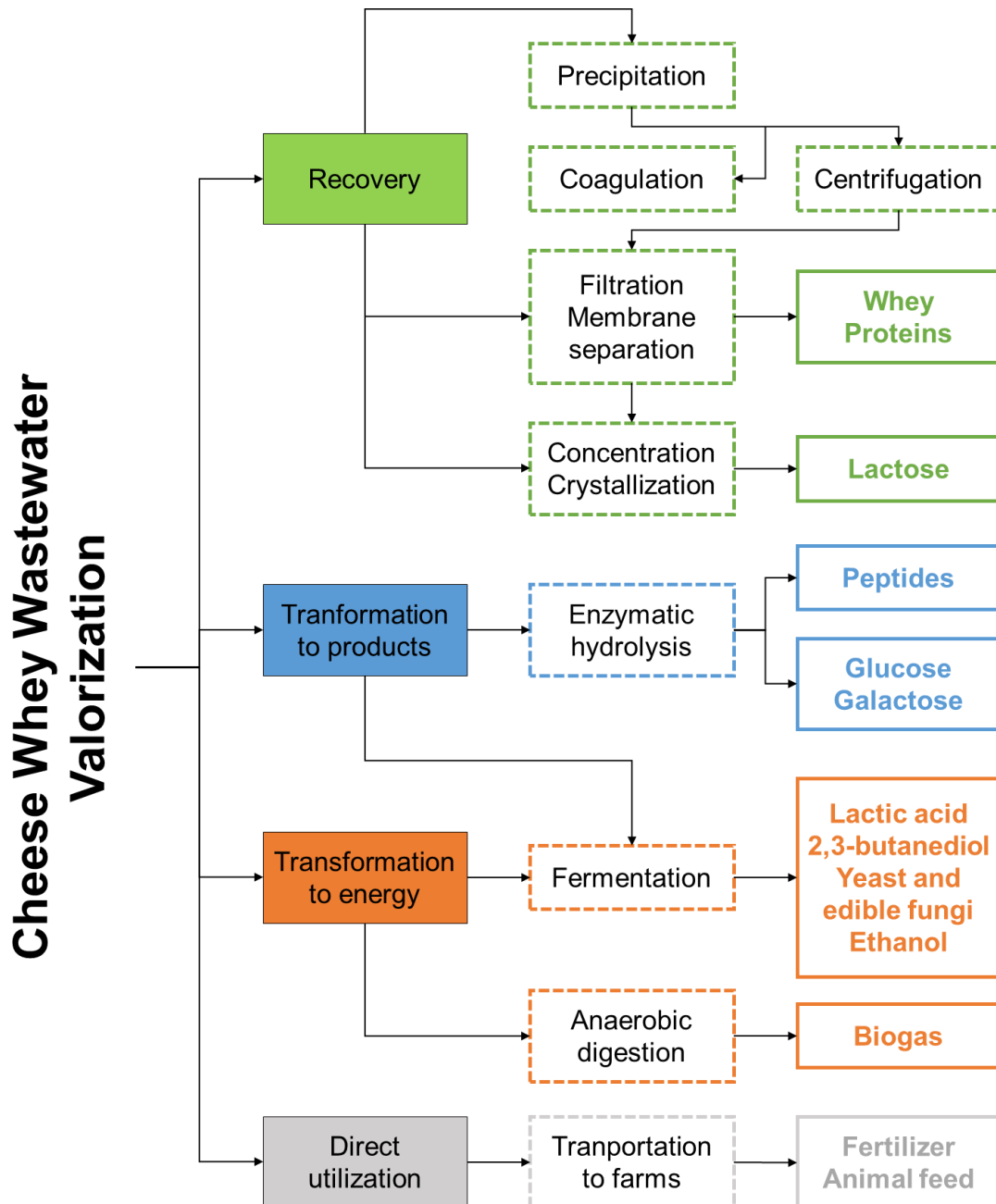


Figure 1.13. Options for the cheese whey wastewater valorization.

Indeed, CWW retains high concentration of lactose (4.5–5.0% w/v), soluble proteins (0.6–0.8% w/v), lipids (0.4–0.5% w/v) and mineral salts (8–10% of dried extract) (Guimarães et al., 2010).

Nutrients, metal traces and high amount of organic matter make CWW a valuable fertilizer or animal feed without the implementation of any treatment. In addition, the application of the anaerobic digestion on CWW leads to the production of biogas. The latter consists of a methane and carbon dioxide mixture obtained through the consecutive organic matter treatments by several groups of microorganisms under anaerobic conditions. Furthermore, valuable compounds, *i.e.*, lactic acid and ethanol, can be yielded by fermentation processes employing CWW as substrate (Lin et al., 2014).

Recovery procedures are the most widespread because CWW is considered a valuable source of milk proteins, which have a wide range of applications in food, cosmetic and pharmaceutical industries (Kosikowski, 1979; Siso, 1996; Audic et al., 2003). The protein fraction of CWW can be recovered through several techniques, *i.e.*, thermal or isoelectric precipitation, coagulation with chitosan, or membrane separation. The former two techniques require high temperatures (90–120 °C) and a pH modification, up to protein denaturation and isoelectric point, respectively. The loss of functionality of the recovered proteins is a challenge for the food industry. Regarding proteins coagulation, chitosan must be regenerated with acids, thus increasing the cost of recovery and decreasing its adsorption efficiency. Therefore, proteins are usually recovered by CWW ultrafiltration through membranes, which is an established technology, whose drawbacks are only related to operational costs for applying the required pressure and for the frequent cleaning of the membranes (Lin et al., 2014).

High volumes of cheese whey permeate (CWP) resulted from the protein recovery through ultrafiltration. CWP still contain high concentration of lactose, up to 45-50 g L<sup>-1</sup> (Prazeres, Carvalho & Rivas, 2012), thus it retains the same disposal problems of CWW, both in terms of volumes produced and polluting load. Therefore, most of the commercially available lactose is recovered from CWP by several processes involving crystallisation procedures. It is essential to deepen the investigation of the

possible uses of lactose in order to solve the problem related to the CWP surplus, thus upcycling this abundant and cheap feedstock, which is independent of season and climate and is not in competition with food (Zall, 1984; Guimarães et al., 2010).

Lactose (4-O- $\beta$ -galactopyranosyl-D-glucopyranose, C<sub>12</sub>H<sub>22</sub>O<sub>11</sub>) is a disaccharide constituted of one molecule of glucose linked to a galactose one with a  $\beta$ -1 $\rightarrow$ 4 glycosidic bond. It is the main component of most mammals' milk and it shows lower solubility and sweetness with respect to other sugars (Gänzle et al., 2008).

Lactose mostly finds application in the food and confectionery industry, as a food ingredient or an additive that prolongs the storage life of products. It is also used as an excipient in the pharmaceutical industry, employed to avoid flavour alteration in formulations both of human and veterinary medicinal products (Yang & Silva, 1995).

Furthermore, lactose can be chemically or enzymatically hydrolysed in its monosaccharide components to yield hydrolysed lactose syrup. The latter one bears greater sweetening power with respect to lactose, due to the presence of free glucose, thus it can act as potential substitute of sucrose or starch syrup in confectionery and ice-cream industries. Moreover, it is widespread in dairy products for lactose-intolerant individuals (Gänzle et al., 2008; Siso, 1996).

The exploitation of lactose or its hydrolysis products as raw materials to produce biosurfactants answers the need for tackling the issue of CWP disposal in dairy industry. Indeed, sugar fatty acid esters represent the result of a product design based on the use of readily accessible, inexpensive, renewable, as well as non-toxic, biodegradable and harmless to the environment resources.

Thus, recently attention has been brought to the use of lactose as raw material in the synthesis of SFAEs. To the best of our knowledge, the number of studies dedicated to the synthesis of lactose-based esters is surprisingly limited (Gonçalves et al., 2021, Liang et al., 2018; Staroń et al., 2018; Verboni et al., 2021; Walsh et al., 2009; Zaidan et al., 2012), thus it still represents an open field of research.

## 2 | Aim of the work

The present research work is part of the BIOSURF project ('Integrated platform for the sustainable production of bio-based surfactants from renewable resources') funded by Fondazione CARIPLO (Call Circular Economy for a sustainable future 2020, ID 2020-1094), whose aim is the development of a sustainable production process to synthesize promising biosurfactants (sugar fatty acid esters, SFAEs) by fully upgrading cheese whey permeate (CWP), the main waste stream of the dairy industry.

The PhD research activity focused on two main topics:

- The investigation of sustainable synthetic strategies, *i.e.*, enzymatic esterification, acetalization or Fischer glycosylation followed by solvent-free esterification, to be used as alternatives to the currently established chemical schemes for the preparation of a small library of performant SFAEs, by exploring the use of challenging substrates, *i.e.*, lactose and CWP;
- The investigation of the physico-chemical properties, such as interfacial tension features, W/O emulsification capability and the relative stability over time, of the prepared biosurfactants to assess their potential application as bio-emulsifiers in the food, pharmaceutical and cosmetic industries.



## 3 | Results and discussion

### 3.1 Green credentials of Sugar Fatty Acid Esters

The research aims at synthesizing bio-based surfactants to be used as emulsifiers in cosmetic and food industries, applying some of the Green Chemistry Principles and focusing on the valorization of industrial waste. Therefore, the building blocks selected for the tenside structure and the chemical conditions for its synthesis must fulfil some green credentials.

In particular, lactose, *i.e.*, the sugar-based polar head of the surfactant, is commonly considered an unavoidable sugar waste biomass, that derives from cheese whey permeate, representing the main residue of the dairy processes (Pires et al., 2021). It is a renewable, inexpensive, and readily accessible feedstock, in compliance with the paradigm of the Circular Economy.

Saturated fatty acids (lauric, palmitic and stearic acids), used as hydrophobic tail of the surfactant, are obtained from fats and oils derivatization processes and they represent one of the most important renewable feedstocks of the chemical industry (Hill & Rhode, 1999; Neta et al., 2015).

The esterification reaction necessary for the surfactant synthesis can be performed in safe and mild chemical conditions, in the presence of non-toxic solvents and highly selective enzymatic catalyst. Regarding the latter, commercially available immobilized lipase obtained from *Candida antarctica* type B (Novozym<sup>®</sup> 435) was selected as biocatalyst within this study. Novozym<sup>®</sup> 435 is the most frequently used lipase in organic reactions due to its high regioselectivity, thermal stability up to 80 °C, stability in organic solvents and its easy recovery and reutilization (Stauch et al., 2015).

As regards for the other reaction conditions, the selection of the solvent is the most critical issue due to the opposite solubility of the reagents and the possibility of causing enzyme denaturation (Khan & Rathod, 2015). Polar aprotic solvents or hindered alcohols (*i.e.*, DMF, THF, pyridine, 2-methyl-2-butanol (2M2B), *t*-BuOH, *etc.*) are widely used for this enzymatic esterification (Chopineau et al., 1998; Khaled et al., 1991; Riva et al., 1988), however, aiming at respecting the Principles

of Green Chemistry, the choice must be restricted to those classified as green and recommended solvents.

According to Prat and co-workers (Prat et al., 2014), a solvent is considered recommended if it meets criteria of safety, environment, occupational health, quality and risk of impurities, as well as general industrial constraints, *i.e.*, boiling point, recyclability, density, freezing temperature, and cost.

Considering these constrains, *t*-BuOH and 2M2B were identified as potential candidates. Moreover, a mixture of DMSO/*t*-BuOH (9:1) was also tested, aiming at improving the low solubility of lactose in organic solvents.

**Figure 3.1** summarizes the green credentials of the selected target molecule and the reaction conditions for its synthesis.

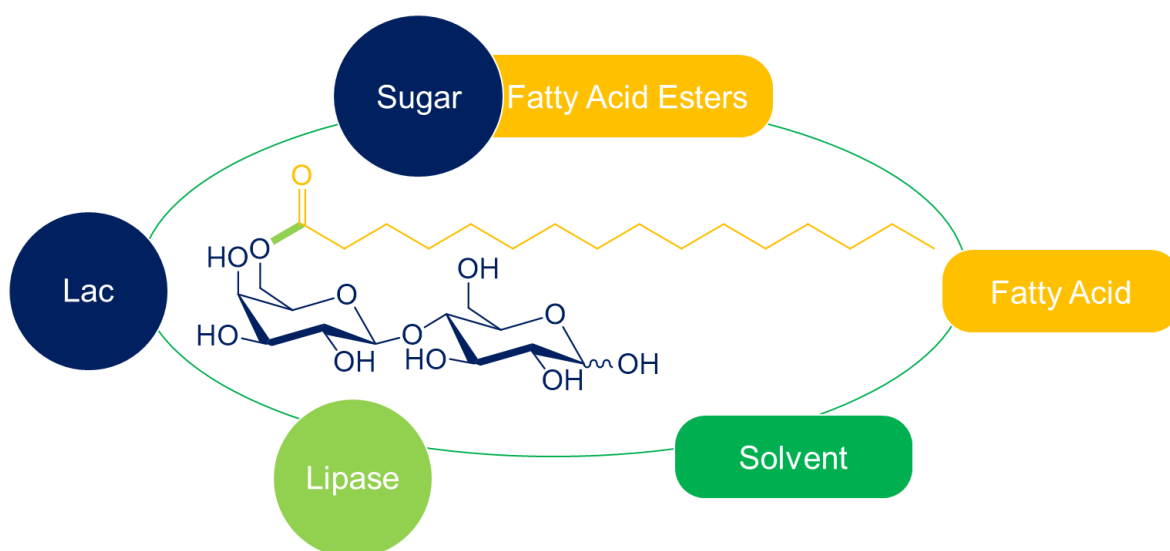


**Figure 3.1.** General overview over the green credentials of sugar fatty acid esters.

## 3.2 Lactose monoesters

### 3.2.1 Sustainable vs chemical synthesis

The reaction conditions for the enzymatic esterification of D-lactose (**1**) (*i.e.*, reactants relative ratio, temperature, time, solvent medium, biocatalyst and molecular sieves loadings) have to be tuned carefully. In particular, lactose and the acyl donor were added in a molar ratio of 1:2 because lipases usually show higher activity in hydrophobic environments than in the hydrophilic ones (Kumar et al., 2016) and 65 °C was identified as the optimal working temperature of the enzyme (Pappalardo et al., 2017). Both Novozym<sup>®</sup> 435 and molecular sieves loadings were selected according to reaction conditions optimization studies carried out on similar substrates (Šabeder et al., 2006).

Several attempts were performed, by varying the acyl donor (*i.e.*, lauric, palmitic and stearic acids, **5-7**; or vinyl laurate, palmitate or stearate, **8-10**) and the reaction solvent (*i.e.*, DMSO/*t*-BuOH (9:1), *t*-BuOH, 2M2B), see **Figure 3.2.** and **Table 3.1.** However, in our hands, none of them led to the formation of the desired products, as confirmed by the absence of possible product spots in the TLCs used to monitor the reaction (DCM/MeOH; 8:2). The absence of lactose monoesters (**2,3,4**) could be due to the low solubility of lactose, if compared to other sugars, in the adopted organic green solvents (Gänzle et al., 2008).

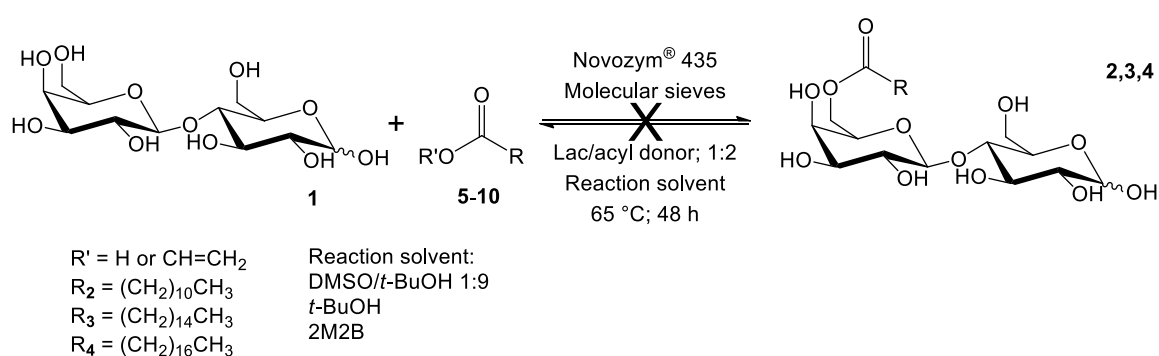


**Figure 3.2.** Sustainable enzymatic esterification of lactose with several acyl donors and different reaction solvents.

**Table 3.1.** Experimental conditions for the attempts performed on the synthesis of lactose monoesters.

<b>Attempt</b>	<b>Esterifying or transesterifying agent</b>	<b>Reaction solvent</b>
2.01		DMSO/ <i>t</i> -BuOH 1:9
2.02	Lauric acid ( <b>5</b> )	<i>t</i> -BuOH
2.03		2M2B
3.01		DMSO/ <i>t</i> -BuOH 1:9
3.02	Palmitic acid ( <b>6</b> )	<i>t</i> -BuOH
3.03		2M2B
4.01		DMSO/ <i>t</i> -BuOH 1:9
4.02	Stearic acid ( <b>7</b> )	<i>t</i> -BuOH
4.03		2M2B
2.04		DMSO/ <i>t</i> -BuOH 1:9
2.05	Vinyl laurate ( <b>8</b> )	<i>t</i> -BuOH
2.06		2M2B
3.04		DMSO/ <i>t</i> -BuOH 1:9
3.05	Vinyl palmitate ( <b>9</b> )	<i>t</i> -BuOH
3.06		2M2B
4.04		DMSO/ <i>t</i> -BuOH 1:9
4.05	Vinyl stearate ( <b>10</b> )	<i>t</i> -BuOH
4.06		2M2B

To the best of our knowledge, only few recent studies have reported the successful enzyme-mediated esterification of lactose to produce SFAEs (Enayati et al., 2018; Liang et al., 2018; Walsh et al., 2009). All the research mostly focused on the production of lactose monolaurate (**2**), using non-sustainable and hardly scalable reaction conditions to favor the solubilization of lactose, *i.e.*, hazardous solvents (a mixture 1:1 of THF/pyridine) and extremely long reaction times (9-12 days). These literature data have highlighted the potential of the surfactant properties of some lactose monoesters, despite the synthetic route used.

Thus, aiming at synthesizing a less investigated lactose-based biosurfactant, namely lactose monopalmitate, the green credentials for the synthesis of SFAEs was temporarily set aside and a chemical approach was pursued.

Following the widely used Fischer esterification reaction conditions (Lou et al., 2011; Wang & Demchenko, 2019), lactose (**1**) was acylated with palmitoyl chloride (**11**) using pyridine as a base and DMF as solvent. After the solvent removal under reduced pressure, an extraction in *n*-BuOH from 10% NaCl aqueous solution and a flash chromatography (DCM/MeOH; 8:2), a mixture of 6- and 6'-O-palmitoyl-D-lactose (**3**) was obtained, see **Figure 3.3**.

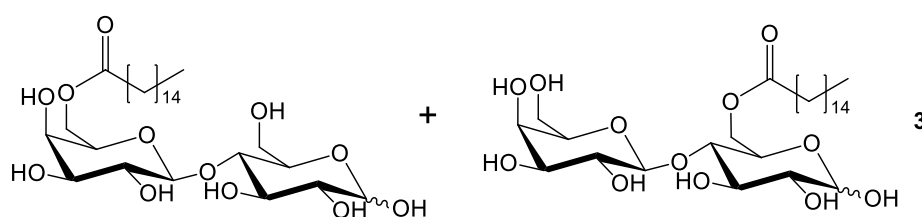


**Figure 3.3.** Mixture of the two isomers of lactose monopalmitate (**3**) obtained by chemical esterification of lactose with palmitoyl chloride, pyridine and DMF.

The isolated isomers of lactose monopalmitate (**3**) were characterized by ESI-MS and  $^1\text{H}$  and  $^{13}\text{C}$  APT NMR analysis, carried out in  $\text{CD}_3\text{OD}$ . NMR signals were partially attributed with the aid of literature data (Liang et al., 2018). The complete interpretation of the spectra was not feasible because of their high complexity, due to the presence of four isomers (two anomers ( $\alpha/\beta$ ) of 6-O-palmitoyl-D-lactose and other two of 6'-O-palmitoyl-D-lactose), which causes signal overlapping.

However, both the data obtained from the partial interpretation of the NMR spectra and the ESI-MS analysis confirmed the presence of only the mono-acylated species in the 6 and 6' positions of lactose, according to the well-known higher reactivity of primary hydroxyl groups in esterification reactions, with respect to the other -OHs of the sugar moiety.

The obtained mixture of isomers of lactose monopalmitate (**3**) was investigated for its emulsion stabilizing capacity, since the synthesis of a biosurfactant with promising emulsifying properties is the scope of the project.

### 3.2.2 Solubility measurements and Hydrophilic-Lipophilic Balance (HLB)

An emulsion is a disperse system of one immiscible liquid (disperse phase) in another (continuous phase). Usually, one of the liquids is aqueous and the other is an oil. Due to the immiscibility of the two phases, an imbalance of intermolecular forces exists at the interface results in an interfacial tension (IFT). Surfactants, due to their amphiphilic nature, are spontaneously adsorbed at the interphase of disperse systems, thus reducing the interfacial tension and stabilizing emulsions

Therefore, as prerequisite, emulsifying agents should have complete solubility in the continuous phase of the system (*i.e.*, solubility in oil in the case of water-in-oil (W/O) emulsions, while in water-for-oil in water (O/W) ones), according to the Bancroft's rule (Schramm, 2005).

The obtained lactose monopalmitate (**3**) was submitted to solubility measurements both in oil and water. Despite the heating step at 80 °C, it showed extremely low solubility, both in oil and water, making complex the evaluation of surface or interfacial tensions.

This result could be explained by calculating the hydrophilic-lipophilic balance (HLB) of the biosurfactant, according to the Griffin method (Zhang et al., 2014).

$$\text{HLB}_{\text{lactose monopalmitate (3)}} = 20 \times \frac{M_H}{M} = 20 \times \frac{341 \text{ g mol}^{-1}}{580 \text{ g mol}^{-1}} = 11.8$$

where  $M_H$  represents the molecular weight of the hydrophilic portion of lactose monopalmitate (**3**) and  $M$  that of the overall biosurfactant.

The HLB concept represents one of the most useful approached to predict the type of emulsion that can be stabilized by a given surfactant.

The HLB is an empiric dimensionless value strictly related to the surfactant solubility because it describes the balance of the size of the hydrophilic and lipophilic groups in an emulsifier. For non-ionic surfactants, the HLB ranges from 0–20. Lipophilic surfactants, soluble in oil, commonly have an HLB value lower than 9, on the other hand, hydrophilic (water soluble) emulsifiers show a HLB higher than 11.

Surfactants with the HLB values boundary (8-12) are usually difficult to be solubilized either in oil or water phase because the two parts of the molecules contribute equally to the HLB of the whole molecule.

Specifically, the HLB value of the synthesized mixture of the two isomers of lactose monopalmitate (**3**) is 11.8, indeed, the compound showed poor solubility in water and in oil, thus making difficult its use as emulsifier.

Liang and co-workers obtained similar data from the solubilization in water and the emulsion stability index studies carried out on single isomers of lactose monoesters, synthesized by the enzymatic transesterification of lactose with different fatty acid vinyl esters (Liang et al., 2018). Lactose monopalmitate showed lower solubility and mediocre surfactants properties, with respect to the other shorter-chained analogues.

Therefore, considering the difficulties encountered in obtaining the target surfactant molecule through green reaction conditions and in its solubilization both in oil and water phase, the use of lactose as polar head of the biosurfactants was not pursued and alternative strategies were followed.



### 3.3 Glucose monoesters

#### 3.3.1 Green credentials of glucose-based fatty acid esters

Lactose (Lac) can be easily hydrolysed, chemically or enzymatically, into its monosaccharide components, glucose (Glc) and galactose (Gal) (Shintani, 2019). Thus, aiming at producing biosurfactants with promising surfactancy, the study focused firstly on the investigation of a suitable synthesis to obtain glucose or galactose-based fatty acid esters, to be used as substrate models for the successive valorization of lactose derived from cheese whey permeate (CWP), which is the main goal of the project.

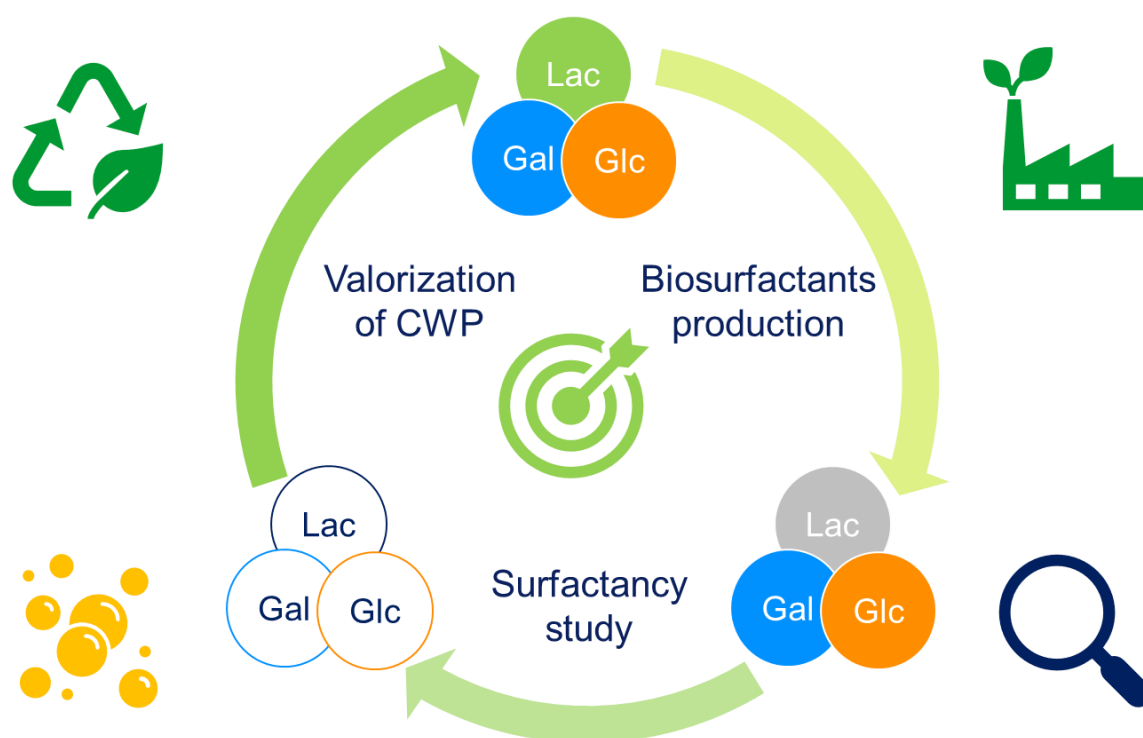


**Figure 3.4.** General overview over the aim of the project.

Both glucose (Glc) and galactose (Gal) are readily available from renewable resources which are not in competition with food production, respecting the paradigm of Circular Economy, in which an unavoidable waste biomass could become a resource, feeding the industrial production system (Sheldon, 2016).

In particular, Gal can be directly isolated from CWP after protein removal, Lac enzymatic hydrolysis and several purification steps, *i.e.*, activated carbon treatment,

electrodialysis, ion purification and simulated moving bed chromatography (Yan et al., 2016).

On the other hand, excluding lactose hydrolysis, Glc could be more easily obtained from starch and lignocellulose feedstock. Moreover, it is one of the few carbohydrates which fulfils the price, quality, and availability criteria to be considered a potential raw material source from an industrial perspective (Hill & Rhode, 1999).

Therefore, the research investigated initially the use of Glc, to enzymatically synthesize glucose fatty acid esters, according to the previously selected green credentials (*i.e.*, the type of saturated fatty acids, the use of a lipase as biocatalyst in green and recommended solvents), see **Section 3.1** and **Figure 3.5**.

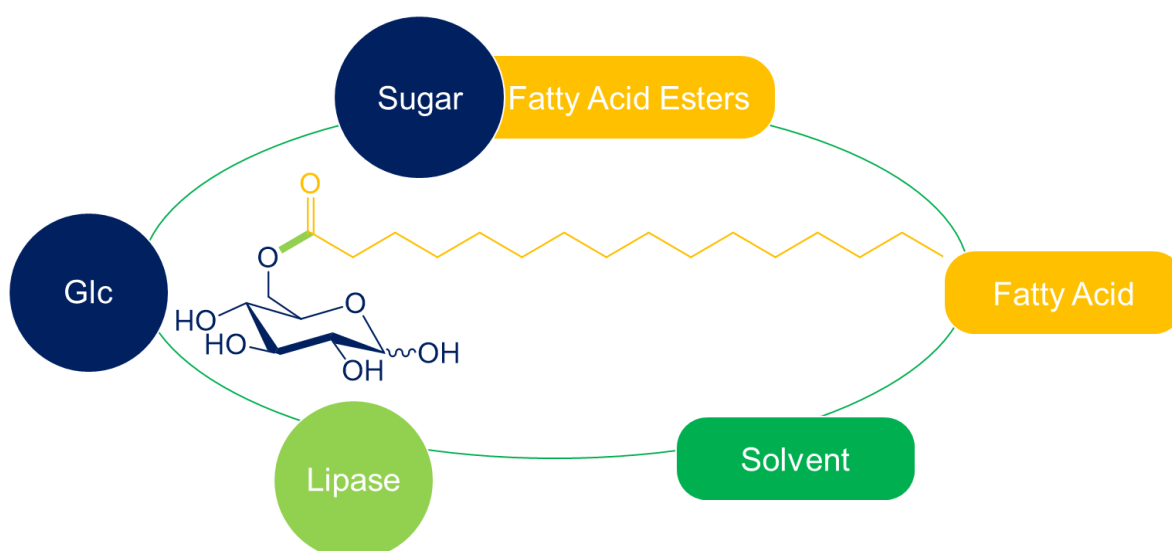


**Figure 3.5.** General overview over the green credentials of glucose-based fatty acid esters.

### 3.3.2 Preliminary experiments

D-Glucose was submitted to experimental conditions similar to those of D-lactose, see **Section 3.2.1**. In these cases, glucose was quite easily esterified with lauric, palmitic and stearic acids (Glc/fatty acid molar ratio; 1:2), at 65 °C, using Novozym<sup>®</sup> 435 as biocatalyst and a mixture of DMSO/*t*-BuOH (9:1) as solvent. After 48 h, the reactions were stopped by filtration of the immobilized enzyme beads and the molecular sieves, then, *t*-BuOH was removed under reduced pressure. Finally, a chromatographic purification (DCM/MeOH; 8.8:1.2) afforded 6-*O*-lauroyl-D-glucose (**13**), 6-*O*-palmitoyl-D-glucose (**14**), and 6-*O*-stearoyl-D-glucose (**15**), see **Figure 3.5**.

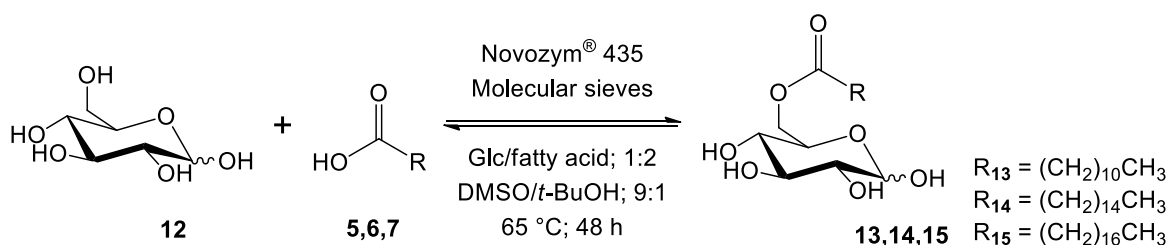


**Figure 3.5.** Preliminary experimental conditions for the synthesis of glucose monoesters.

The isolated products **13**, **14** and **15** were fully characterized by ESI-MS, <sup>1</sup>H and <sup>13</sup>C APT NMR analysis, carried out in DMSO-*d*<sub>6</sub> with one drop of D<sub>2</sub>O, in order to make the exchangeable -OH protons of the sugar moiety disappear from the spectrum. <sup>1</sup>H and <sup>13</sup>C NMR signals were assigned with the aid of <sup>1</sup>H-<sup>1</sup>H and <sup>1</sup>H-<sup>13</sup>C correlation experiments (COSY, HSQC and HMBC).

The spectra recorded shortly after the sample preparation highlighted the presence of almost exclusively the signals related to the α-anomer of the sugars, e.g., see the <sup>1</sup>H NMR of 6-*O*-palmitoyl glucose (**14**) in **Figure 3.6**.

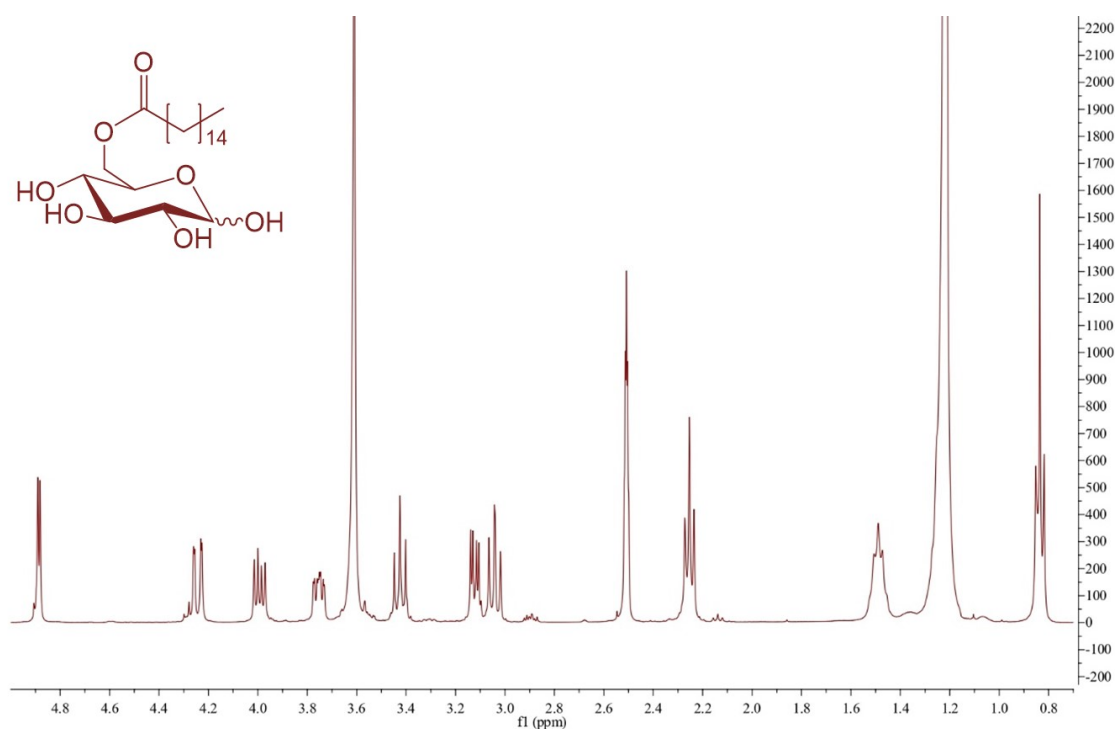


**Figure 3.6.**  $^1\text{H}$  NMR spectrum of 6-O-palmitoyl-D-glucose (**14**), recorded in  $\text{DMSO-d}_6 + \text{D}_2\text{O}$  (one drop).

According to literature data (Arifin et al., 2018), the stabilization of the  $\alpha$ -anomer of glucose is enhanced in DMSO with respect to aqueous solution, due to different solvation effects induced by the two solvents. Moreover, it is reasonable to assume that the long hydrophobic chain of the synthesized products **13**, **14** and **15** could induce variations in the conformational stability of the sugar portions of the molecules, thus resulting in an extremely high stabilization of the  $\alpha$ -anomeric forms.

It is also known that the mutarotation reaction of glucose in DMSO is slow. Indeed, reinvestigation of the same samples after one week showed the increasing of the signals related to the  $\beta$ -anomer (Ballash & Robertson, 1973).

The presence of only the mono-acylated specie was confirmed by ESI-MS analysis. Moreover, the position of the ester linkage was corroborated both by the downfield shift of the two proton signals of the position 6 of the sugar moiety, if compared to free glucose (**Figure 3.7**) (Bock & Thøgersen, 1982), and from their interaction with the carbonyl carbon observed in the  $^1\text{H}$ - $^{13}\text{C}$  heteronuclear multiple bond correlation spectroscopy (HMBC) (**Figure 3.8**).

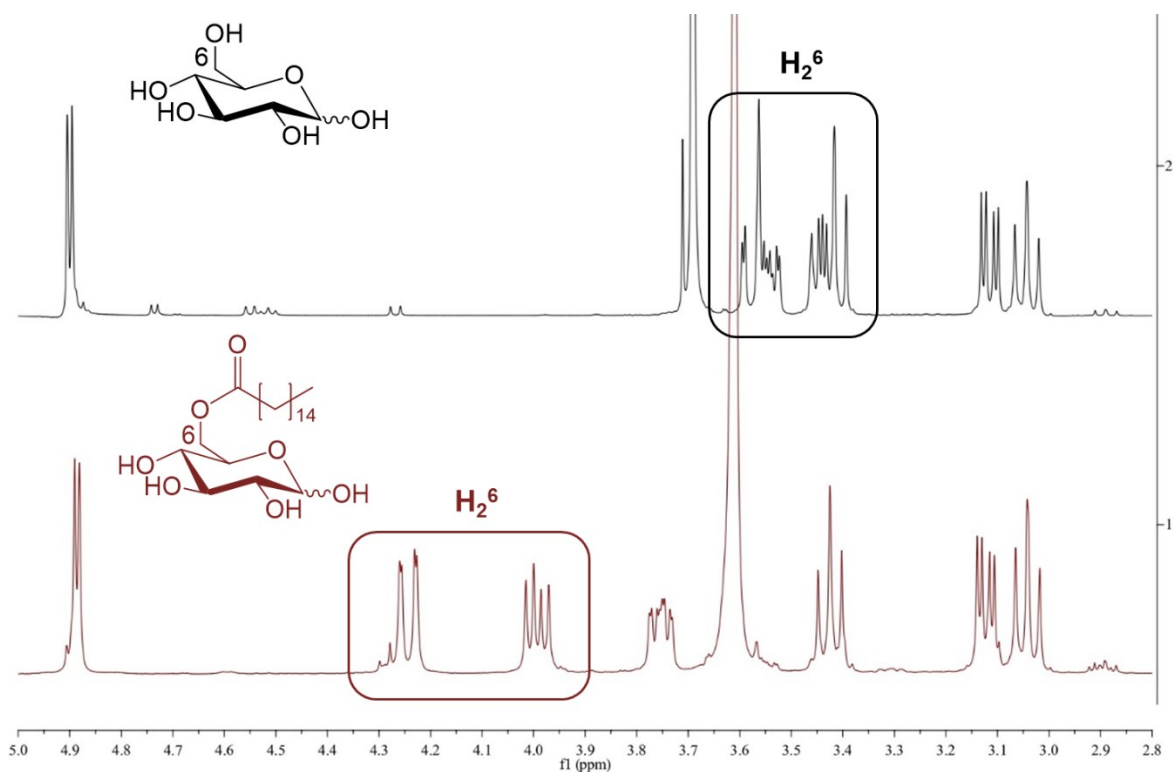


**Figure 3.7.** Comparison of  $^1\text{H}$  NMR spectra of free D-glucose and 6-O-palmitoyl-D-glucose (**14**), both recorded in in  $\text{DMSO-}d_6 + \text{D}_2\text{O}$  (one drop), zoomed in the range 5.0-2.8 ppm.

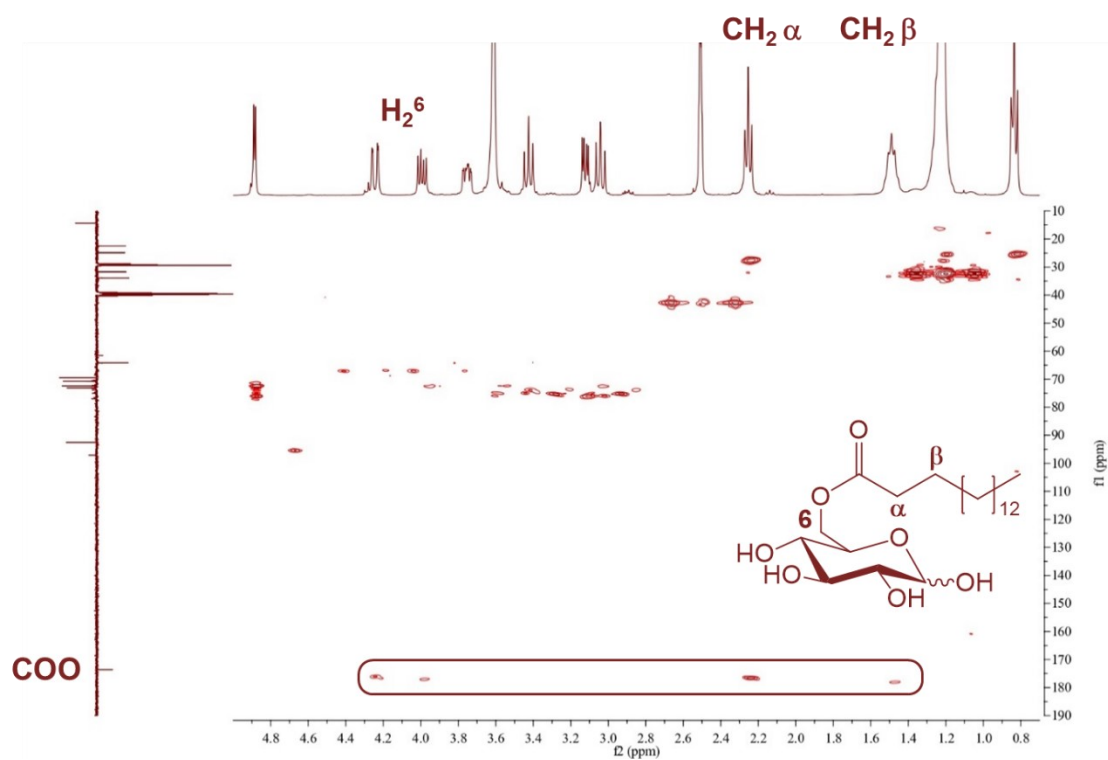


**Figure 3.8.** HMBC of 6-O-palmitoyl-D-glucose (**14**): horizontal and vertical axis indicate the  $^1\text{H}$  and the  $^{13}\text{C}$  APT NMR spectrum, respectively.

### 3 | Results and discussion

---

Despite the high purity of the obtained products **13**, **14** and **15**, their purification through flash column chromatography resulted to be tedious due to difficulties in separating them from DMSO and from the unreacted fatty acids, which were continuously eluted from the column. Moreover, DMSO acted as a co-solvent, slightly modifying the eluent composition and the products elution, thus leading to rather poor yields of purified products.

Therefore, a two-step washing procedure was developed as an alternative method to isolate the target products **13**, **14** and **15**. Indeed, after the *t*-BuOH evaporation under reduced pressure, **13**, **14**, **15** and the unreacted fatty acids were precipitated in H<sub>2</sub>O, thus removing unreacted glucose and DMSO. The precipitates were filtered and dried overnight at room temperature, then, unreacted fatty acids were dissolved in hot *n*-heptane (0.1 v/W<sub>fatty acid</sub>), thus recovering **13**, **14** and **15** with a sufficient degree of purity (all around 90%), after filtration.

Considering the obtained purity and the slight improvement of the yields, which are listed in **Table 3.2**, this purification method was selected as a valid alternative to the purification procedure *via* flash column chromatography.

Moreover, among the three obtained products **13**, **14** and **15**, the one bearing the palmitoyl chain (**14**) resulted in the highest yield (**Table 3.2**), thus, the subsequent optimization experiments were carried out using palmitic acid as acyl donor, assuming a similar trend for the other fatty acids.

**Table 3.2.** Preliminary experimental conditions and obtained yields of the synthesis of glucose monoesters, considering 1 mmol of Glc (**12**).

<b>Compound</b>	<b>Fatty acid (mmol)</b>	<b>Time (h)</b>	<b>Temperature (°C)</b>	<b>Yield (%)</b>
<b>13</b>	2	48	65	<b>15</b>
<b>14</b>	2	48	65	<b>17</b>
<b>15</b>	2	48	65	<b>14</b>

### 3.3.3 Optimization of experimental conditions by Design of Experiment (DoE) approach

To perform a systematic study of optimization of reaction conditions through an experimental design, it is compulsory to identify the variables supposed to be critical in affecting the result of the reaction.

Indeed, the design of experiments (DoE) is a systematic method, alternative to the One-Variable-At-a-Time (OVAT) methodology, used to investigate the cause-and-effect interactions between the critical factors affecting a process and its output, usually to optimize it (Tambe & Bonde, 2017).

The use of DoE is becoming well-established and is gaining significant prominence in several sectors, ranging from the pharmaceutical industry to the biocatalysis research, because it represents a fundamental tool for providing a scientifically grounded evaluation of manufacturing performances to make the most suitable design choices for the processes (Chhatre et al., 2011). Recent literature data reported the successful exploitation of a full factorial DoE in optimizing the transesterification of rapeseed oil with methanol, catalyzed by *Mucor miehei* lipase immobilized onto mesoporous silica materials (Carteret et al., 2018).

The choice of the most appropriate DoE is a key issue, which strictly depends upon the previous knowledge of the process to be optimized, the number of variables to be tested and the available resources (Montgomery, 2004). A full factorial design ( $2^n$ ) can be extremely useful and practical, especially when the critical parameters (n) to investigate are few ( $n \leq 3$ ).

In the considered process, namely the enzymatic esterification of glucose with palmitic acid to synthesize 6-O-palmitoyl-D-glucose (**14**) (**Figure 3.9**), the amount of palmitic acid, the reaction time and the reaction temperature were identified as the three critical parameters. The yield was selected as the process output, while all the other reaction conditions (*i.e.*, amount of solvent and Novozym<sup>®</sup> 435 and molecular sieves loadings) and purification procedures (namely the two-step washing procedure) were standardized in order to minimize variation sources.

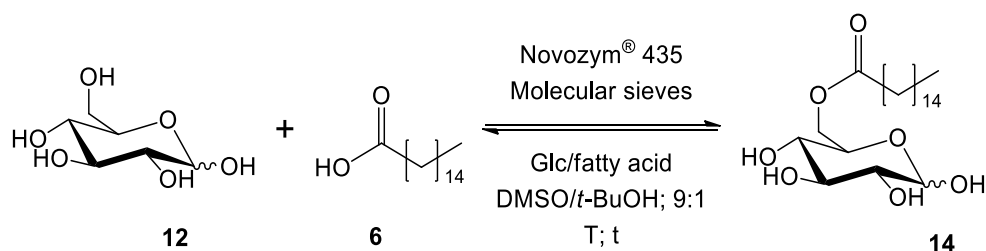


**Figure 3.9.** Experimental design conditions for the synthesis of 6-O-palmitoyl-D-glucose (14).

According to the full factorial design ( $2^3$ ) DoE method, the three identified variables are systematically changed in each experiment, ranging from a selected minimum to a maximum value (*i.e.*, the amount of palmitic acid (1-3 mmol), the reaction time (24-48 h) and the reaction temperature (55-75 °C)), see **Table 3.3**. All these experiments are designed to generate the  $2^3$  matrix, which can be visualized as a cube, in which each dimension represents the variation of a critical parameter, thus making the edges the conditions of each experiment, see **Figure 3.10**.

**Table 3.3.** List of experiments with the parameters variation for the selected  $2^3$  full factorial DoE.

DoE Experiment	$X_1$ , Palmitic acid (mmol)	$X_2$ , Time (h)	$X_3$ , Temperature (°C)
1	1	24	55
2	3	24	55
3	1	48	55
4	3	48	55
5	1	24	75
6	3	24	75
7	1	48	75
8	3	48	75



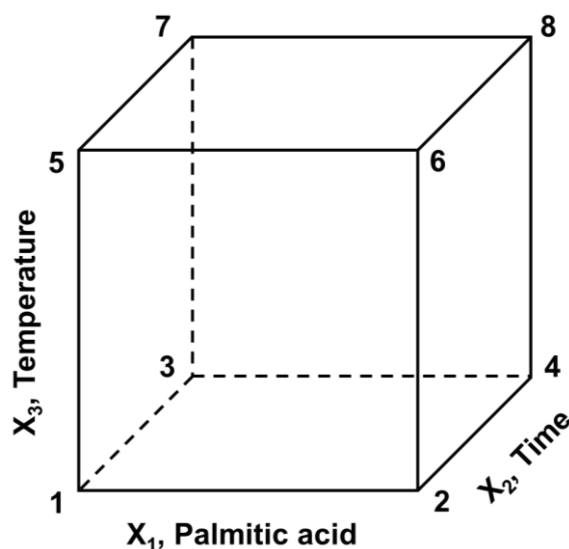


Figure 3.10. Visual representation of the  $2^3$  full factorial matrix.

The elaboration of the experimental responses generates an equation with several coefficients, which is reported in a graphical way (Figure 3.11). Each coefficient represents the contribute of each of the three critical variables ( $X_1$ ,  $X_2$ ,  $X_3$ ) and their interactions ( $X_1X_2$ ,  $X_1X_3$ ,  $X_2X_3$ ,  $X_1X_2X_3$ ) to the yield response.

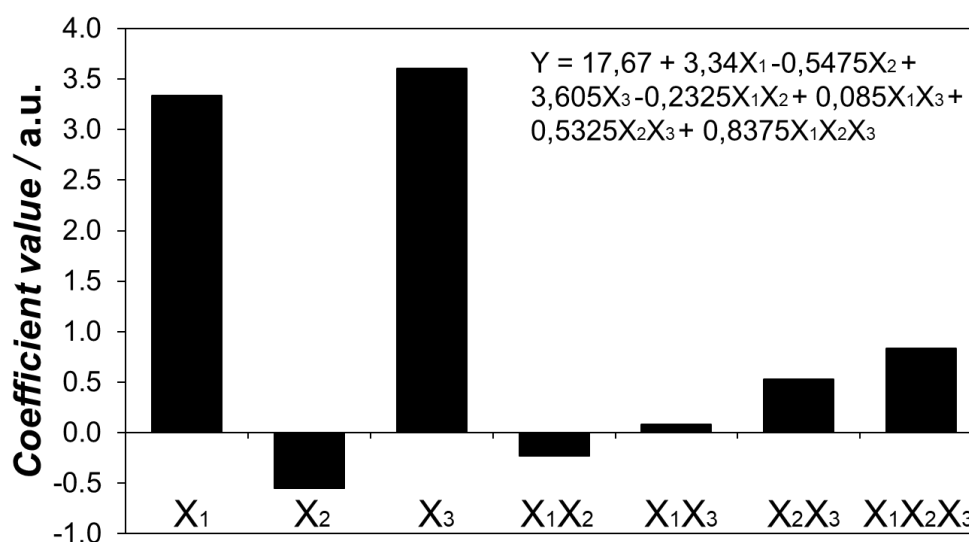


Figure 3.11. Experimental design conditions for the synthesis of 6-O-palmitoyl glucose (14).

From the preliminary analysis of the results, it is possible to observe that the three critical parameters are independent from each other. The interaction between the pairs of factors is minimal: in particular, the one between the amount of palmitic acid and temperature. This implies that by increasing both, the yield is influenced in a positive but non-additive way.

Another interlocutory data is represented by the low value of the time coefficient, if compared to the other two critical parameters. Taking into account that esterification is an equilibrium, it could have been reached just after 24 h, thus leading to reaction yields similar to those of longer reaction time (48 h), especially at 75 °C. Therefore, time can be considered as an irrelevant variable and reaction should always be carried out for the time selected as minimum value (24 h).

Summing up, further experiments should be performed to get a better knowledge of these reaction conditions and to understand if the model has predictive validity. However, this preliminary study allowed the highest reaction yield, by using a glucose/palmitic acid molar ratio of 1:3, at 75 °C for 24 h. Therefore, these reaction conditions were considered suitable to perform further investigations.

### 3.3.4 Influence of solvents

Aiming at improving the reaction yield, the use of different solvents was investigated. Solvents have strong influence on reactants solubility, chemical reactivity and reaction rates (Reichardt, 2007), indeed, the selection of the optimal solvent or solvent mixture for the synthesis of SFAEs is a key issue, see **Section 3.1**.

An appropriate solvent medium for the enzymatic esterification of sugars and fatty acids must solubilize a sufficient amount of both reagents, which have opposite polarity, without affecting the enzyme activity or being a substrate of the biocatalyst. (Liu et al., 1999; Šabeder et al., 2006).

Moreover, in view of the potential application of the final products as emulsifiers in food or cosmetic industries, these experiments focused on solvents included in the “recommended” category, according to the table of Prat and co-workers (Prat et al., 2014). The typical solvents of enzymatic esterification of sugars and fatty acids, *i.e.*, DMF, THF and pyridine, were ruled out as they are classified as hazardous.

Therefore, the influence of *t*-BuOH, 2M2B and DMSO on the reaction yield was tested, by carrying out the experiments in the reaction conditions optimized by the DoE approach, see **Figure 3.12**.

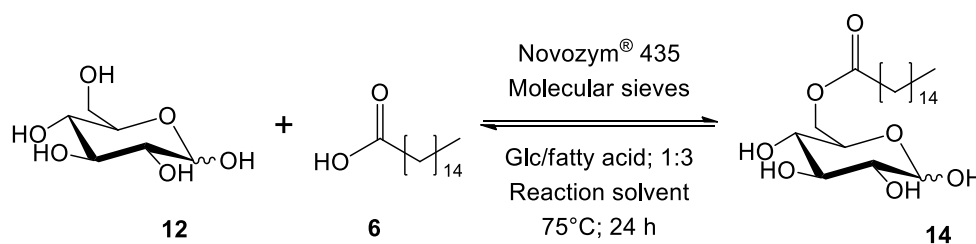


**Figure 3.12.** Synthesis of 6-O-palmitoyl-D-glucose (14) in different solvents.

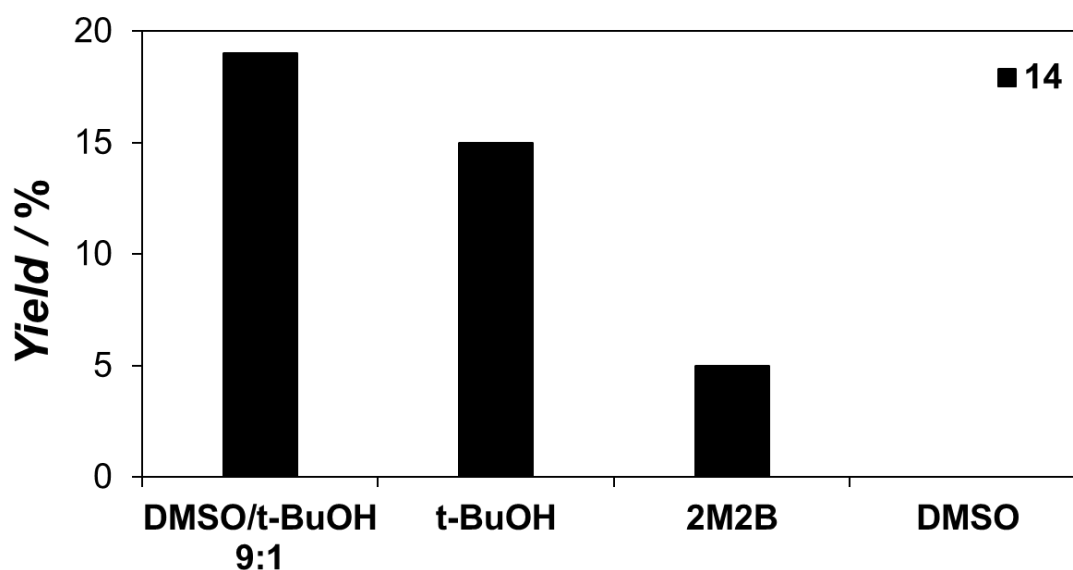


*Figure 3.13.* Comparison of the yields of 6-O-palmitoyl-D-glucose obtained with different solvents.

The obtained results (**Figure 3.13**) evinced that DMSO causes strong deactivating effect on enzymes activity, probably due to its capacity of stripping water molecules from the protein surface and from the active site (Croitoru et al., 2012).

However, its use in low amount acts as a hydrophilic cosolvent, thus increasing the sugar solubility, as corroborated by other studies (Pappalardo et al., 2017). Therefore, it is evident that a percentage of DMSO has a positive influence of the overall reaction yield.

However, considering that DMSO is classified as a problematic solvent, its optimal concentration should be further investigated, as well as possible alternative strategies to increase the solubility of the reagents and the reaction yield.

### 3.3.5 Optimized synthesis

The improvement in the yield of 6-O-palmitoyl-D-glucose (**14**), obtained using the reaction conditions found through the DoE approach, was investigated also for the other SFAEs, *i.e.*, 6-O-lauroyl-D-glucose (**13**) and 6-O-stearoyl-D-glucose (**15**).

Therefore, the enzymatic esterification of glucose with lauric and stearic acids (**5,7**) was performed according to the optimized reaction conditions, *i.e.*, Glc/fatty acid molar ratio 1:3; 75 °C and 24 h, see **Figure 3.14**. The resulting overall yields were compared to those obtained with the initially selected conditions, *i.e.*, Glc/fatty acid molar ratio 1:2; 65 °C and 48 h (**Figure 3.15**).

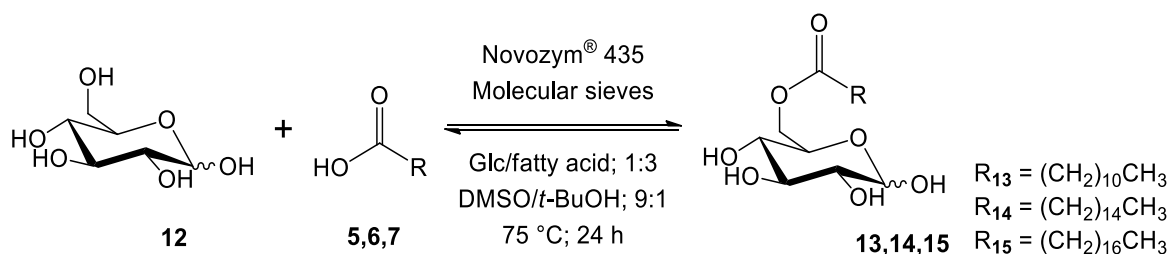


**Figure 3.14.** Optimized conditions for the synthesis of glucose monoesters (**13,14,15**).

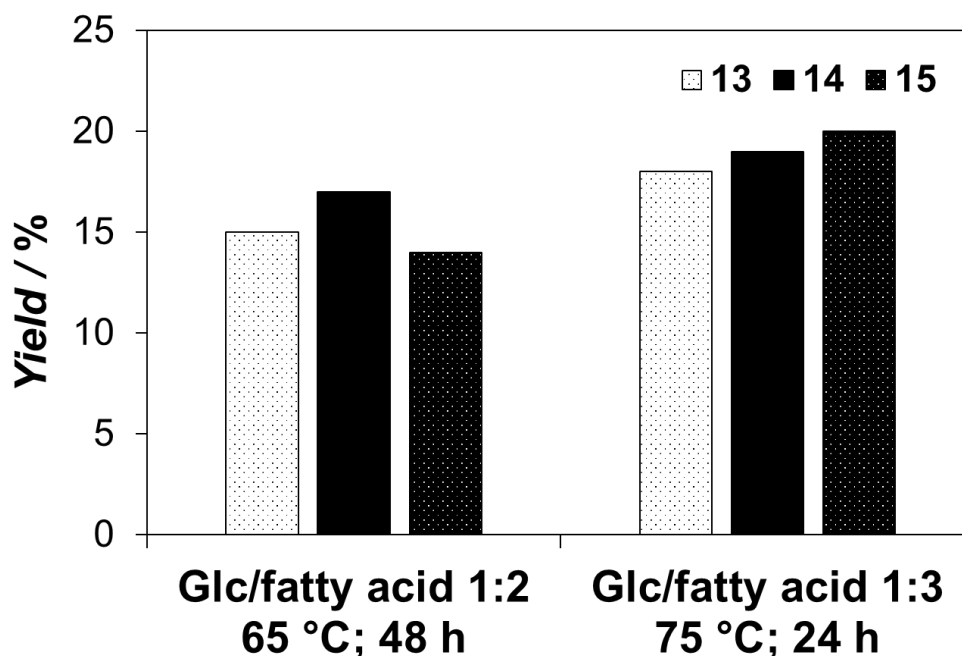


**Figure 3.15.** Comparison of the yields of glucose monoesters (**13,14,15**) obtained from the initially selected experimental conditions and the optimized ones.

In all the three cases, the reaction conditions optimized through the experimental design led to higher yields, corroborating the validity of the DoE model independently on the fatty acid used.

Moreover, the most marked improvement in the yield (from 14% to 20%) was obtained for the reaction carried out with the stearic acid using the newly selected conditions. Furthermore, it is possible to notice a levelling of the obtained overall yields (18%, 19% and 20% for SFAE **13**, **14** and **15**, respectively) in the experimentally designed reaction conditions. These data corroborate the ability of CALB to catalyse esterification reactions independently of the chain length of the fatty acid used (Kumar et al., 2005).

However, despite the improvement in the overall yields obtained by carrying out the enzymatic esterification in the reaction conditions identified through the DoE approach, the yields of the three SFAEs are still modest.

This result can be due to the low solubility of glucose in the selected reaction conditions, making further studies compulsory, especially those that involve the investigation of an alternative synthetic pathway based on the modification of the sugar moiety to make it less polar.

### 3.3.6 Physico-chemical characterization

The surfactant properties of the synthesized glucose monoesters were investigated, in view of their potential application as emulsifiers in cosmetic or food sectors.

Being the solubilization of a tenside either in the water or oil phase a prerequisite for its emulsifying capacity, the solubility of 6-O-lauroyl-D-glucose (**13**), 6-O-palmitoyl-D-glucose (**14**), and 6-O-stearoyl-D-glucose (**15**), was investigated.

Particularly, all the three products showed very low water solubility, making surface tension measurements of the surfactants difficult to be evaluated. Moreover, also their oil solubility, both in edible and industrial waste oils (*i.e.*, sunflower, rapeseed, rice and tall ones), was poor to conduct interfacial tension studies.

Once again, these results were corroborated by the HLB values of the three SFAEs calculated according to the Griffin method, see **Table 3.3**. All the three biosurfactants showed intermediate HLB values ranging from 8-10, indicating that both the sugar heads and the fatty long chains equally contribute to the molecules polarity, making complex their solubilization.

**Table 3.3.** HLB and contact angle values of synthesized glucose monoesters (**13,14,15**); all the values are averaged across three repetitions.

<b>Compound</b>	<b>HLB</b>	<b>Water</b>	<b>Diiodomethane</b>
		$\theta / ^\circ$	$\theta / ^\circ$
<b>13</b>	9.9	88 ± 2	61 ± 2
<b>14</b>	8.5	89 ± 2	61 ± 2
<b>15</b>	8.0	91 ± 1	57 ± 3

Therefore, in order to investigate the wettability of the biotensides, contact angle measurements were carried out (**Table 3.3** and **Figure 3.16**). Aiming at evaluating the hydrophilicity and lipophilicity of the SFAEs **13**, **14** and **15**, water and diiodomethane were used, respectively.

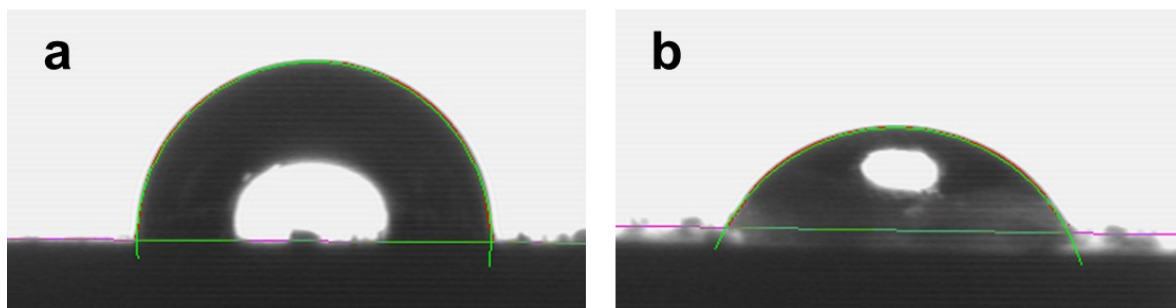


**Figure 3.16.** Side view pictures obtained from the high-resolution camera of the Krüss Easy instrument taken immediately after the syringe tip left a 5  $\mu$ L drop of **a)** water and; **b)** diiodomethane onto the surface of 6-O-palmitoyl glucose (**14**).

The measured contact angle values were similar to those recently reported in the literature. Moreover, the data were in accordance with the calculated HLB index. Indeed, the higher the HLB values, the lower the hydrophilicity and the greater the lipophilicity measured (Ren & Lamsal, 2017).

By comparing the results obtained for SFAEs **13**, **14** and **15**, it is possible to infer a quite comparable degree of either hydrophilicity (very similar contact angles were detected, around  $90^\circ$ ) and lipophilicity ( $\cong 60^\circ$ ). Thus, the different chain length of the three tested biosurfactants did not strongly influence their surface wettability.

To sum up, although the strategy of enzymatically synthesizing SFAEs by dissolving a sugar and a fatty acid in the presence of a lipase is straightforward, difficulties in obtaining high concentration of both reactants within a single phase are such that the overall yield is poor, see **Graph 3.3**. Moreover, the obtained SFAEs (**13**, **14**, **15**) showed poor surfactant features, due again to problems of their solubilization both in oil and water phases. Thus, our study changed the target molecules and the synthetic strategy once again.



### 3.4 6-O-palmitoyl-1,2-O-isopropylidene- $\alpha$ -D-glucofuranose

#### 3.4.1 Acetalization strategy

Considering the difficulties encountered both in the synthesis and application as emulsifiers of the synthesized SFAEs based on the free sugar moiety, the study focused on the investigation of an alternative strategy based on the modification of the saccharide component.

Indeed, a suitable derivatization of the sugar moiety could be an efficient strategy to reduce sugars polarity, allowing to perform the successive enzymatic esterification step, compulsory to generate a tenside, without any solvent and obtaining a biosurfactants with improved emulsifying properties.

Aiming at respecting some of the 12 Principles of the Green Chemistry (Anastas & Warner, 1998), the sugar derivatizations should be performed using safe, environmentally friendly and non-toxic reagents, solvents and catalysts, moreover they should be carried out in mild conditions.

It is important to underline that the reactions used in this strategy are designed to improve the miscibility of reactants and they have to be distinguished from the conventional protecting / deprotecting strategies commonly employed in regioselective organic synthesis, which are hardly acceptable for industrial production of surfactants (Pérez et al., 2017).

Therefore, among the various strategies to decrease the polarity of sugars, two reactions were identified, *i.e.*, acetalization and Fischer glycosylation (which will be discussed in detail in **Section 3.5**).

The former approach relies on the preparation of sugar acetals. In the presence of an acid catalyst, aldehydes and ketones react with suitably arranged diols of saccharide derivatives to give cyclic acetals. In case of ketones, the formation of a 5-membered ring is so favoured that some sugars, as glucose, modify their conventional pyranose ring structure in order to get to the most stable one (Collins & Ferrier, 1995).

Specifically, it is known that in the presence of acetone, glucose preferentially gives the diacetonide derivative (see **Section 3.4.2**). However, this fully protected glucose compound has to be selectively hydrolyzed to perform the enzymatic esterification, allowing the generation of the target biosurfactant. Indeed, the selected lipase was proven to be extremely regioselective towards primary hydroxyl group of the saccharide moiety, see **Section 3.3.2**.

**Figure 3.17** summarizes the step of the acetalization strategy to obtain biosurfactants.

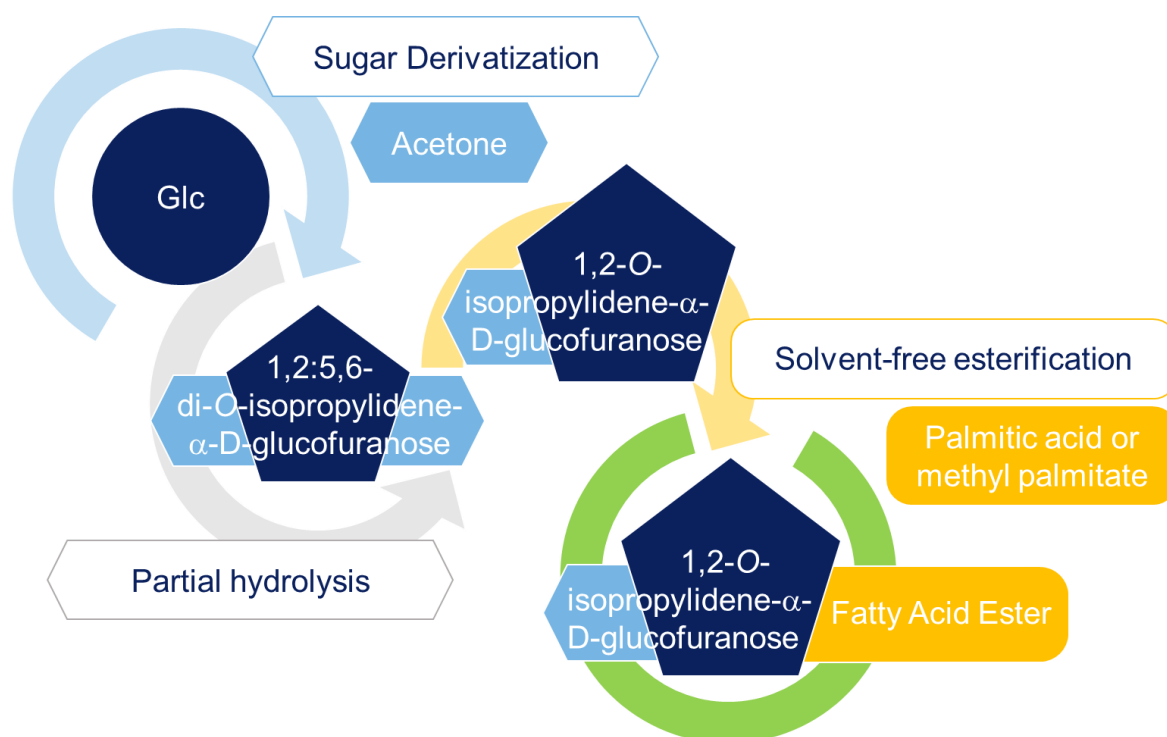


**Figure 3.17.** General overview over the acetalization strategy.

### 3.4.2 Well-known vs alternative synthesis

As first attempt, D-glucose (**12**) was submitted to the well-known protocol of sugar acetalization (de Belder, 1965). It involves the use of a Glc suspension in dry acetone at room temperature, *p*-toluenesulfonic acid monohydrate (PTSA) as acid catalyst and the presence of a small amount of 2,2-dimethoxypropane (2,2-DMP) as scavenger molecule for the water produced during reaction, see **Figure 3.18**.

After 24 h, the reaction was quenched with 1 M NaOH solution, the solvent was removed under reduced pressure and an extraction in EtOAc from a saturated aqueous solution of NaHCO<sub>3</sub>, followed by a flash column chromatography (*n*-hexane/EtOAc; 1:1) afforded 1,2:5,6-di-*O*-isopropylidene- $\alpha$ -D-glucofuranose (**16**) in good yield (40%).

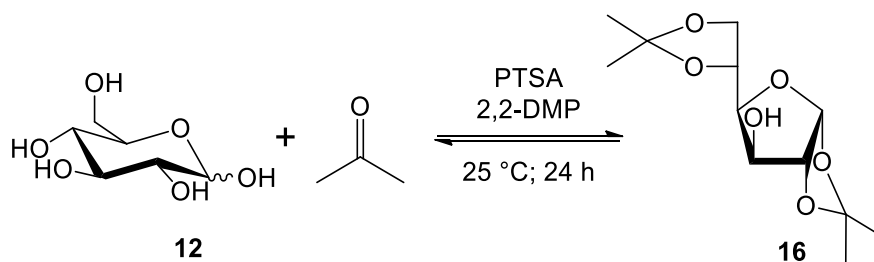


**Figure 3.18.** Acetalization of Glc (**12**) carried out using the de Belder reaction conditions.

The product **16** was fully characterized by ESI-MS and NMR analyses that are in good agreement with previously reported data (Ghosh et al., 2018). This *O*-isopropylidene Glc derivative has a long tradition as compound of commercial interest, important in multi-step syntheses in organic, medicinal, and carbohydrate chemistry (Khan & Khan, 2010), moreover, it is well known for its low toxicity, anti-inflammatory and antipyretic activities (Goi et al., 1979).

As described above, the typical synthesis of *O*-isopropylidene-derivatives of sugars is carried out in anhydrous conditions by using acetone in the presence of an acid catalyst, *i.e.*, PTSA or concentrated H<sub>2</sub>SO<sub>4</sub>. However, considering the industrial relevance of compound **16**, it is not surprising that many research efforts have been put during the years in finding alternative catalysts to prepare this product in significant quantities.

So far, a wide variety of catalysts have been explored, including iodine (Kantha 1986) and various Lewis acidic metal salts, *i.e.*, CuSO<sub>4</sub> (Hering et al., 2005), FeCl<sub>3</sub> (Singh et al., 1977), AlCl<sub>3</sub> (Lal et al., 1989) and many others. More recently, the use of deep eutectic solvents (DES) based on choline chloride and malonic acid was also investigated (Rokade & Bhate, 2017), moreover, several heterogeneous catalysts have been employed, *i.e.*, montmorillonite K10 clay (Asakura et al., 1996), vanadyl triflate (Lin et al., 2006) and H<sub>2</sub>SO<sub>4</sub>-functionalized silica (Krishna et al., 2018).

However, some of these methods possess drawbacks that make them unsustainable, both in the environmental and economic terms, *i.e.*, low yields, use of non-recyclable catalyst, mandatory neutralization step, moisture sensitivity and high cost of the catalysts, and harsh reaction condition. Therefore, in view of designing a sustainable process to produce biosurfactants, the study focused on the investigation of some cation exchange resins.

Indeed, ion exchange resins have been known for many years and they are widely used catalyst in several industrially relevant organic reactions (Whistler & Wolfrom, 1963). They offer several advantages with respect to the other catalysts mentioned above, *i.e.*, ease of separation from the reaction mixtures and possibility of recycling, control of side-reactions, non-necessity of special corrosion resistant equipments or special safety measurements and many of them are cheap and commercially available, thus reducing the overall economics of the process (Nair et al., 1981).

The research focused on two main type of cation exchange strongly acid resins: Amberlyst<sup>®</sup> 15 and Amberlite<sup>®</sup> IR-120. Both are widely employed, even at industrial scale, as heterogeneous catalysts in a broad range of non-aqueous organic syntheses (Boz et al., 2015). They are commercially available macroreticular resins, produced through styrene cross-linking with divinyl benzene followed by sulfonation. Amberlite<sup>®</sup> IR-120 and Amberlyst<sup>®</sup> 15 mostly differ for their particle size (0.62 - 0.83 and 0.30 mm, respectively), crosslinking degree (8 vs 20%), acid sites concentration (4.40 and 4.53 meq g<sup>-1</sup>, respectively) and surface area (1.53 vs 45 m<sup>2</sup> g<sup>-1</sup>) (Taddeo et al., 2022).

Therefore, the acetalization of D-glucose (**12**) was carried out using the two selected resins Amberite<sup>®</sup> IR-120 and Amberlyst<sup>®</sup> 15. The purification protocol was easier,

with respect to that of the well-known method based on PTSA: the reactions were stopped by the filtration of the supported catalysts, then an extraction in EtOAc from a saturated aqueous solution of NaHCO<sub>3</sub> afforded 1,2:5,6-di-O-isopropylidene- $\alpha$ -D-glucofuranose (**16**), see **Figure 3.19**.

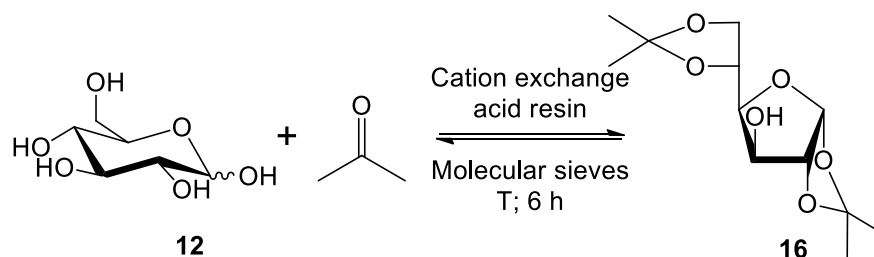


**Figure 3.19.** Acetalization of Glc (**12**) carried out using alternative reaction conditions.

ESI-MS and NMR analysis were in accordance with previously reported data and demonstrated that no further purifications were needed.

Therefore, a short optimization study of the reaction conditions was performed. Reaction yields were increased, reaching values around 50% for both Amberlite® IR-120 and Amberlyst® 15, by reducing the Glc concentration in dry acetone and carrying out the reaction under reflux conditions, see **Table 3.4**.

**Table 3.4.** Optimization study of 1,2:5,6-di-O-isopropylidene- $\alpha$ -D-glucofuranose (**16**) synthesis.

<b>Experiment</b>	<b>Cation exchange acid resin</b>	<b>% w<sub>12</sub>/v<sub>acetone</sub> (%)</b>	<b>Temperature (°C)</b>	<b>Yield (%)</b>
16.01		3.6	50	27
16.02	Amberlite® IR-120	3.6	65, reflux	29
<b>16.03</b>		1.8	65, reflux	<b>50</b>
16.04		3.6	50	18
16.05	Amberlyst® 15	3.6	65, reflux	25
<b>16.06</b>		1.8	65, reflux	<b>51</b>

At higher temperature, the two resins led to similar yields, however, the study on Amberlite® IR-120 was not pursued because it produced a slightly more colored product **16**, with respect to that obtained with Amberlyst® 15. In the cosmetic field, the color of the final product is a fundamental aspect to consider in order to meet the customer's demands.

### 3.4.3 Partial hydrolysis

As mentioned in the **Section 3.3.2**, CALB is a lipase well-known for its extremely high regioselectivity towards the primary hydroxyl group. Therefore, a selective hydrolysis of 1,2:5,6-di-O-isopropylidene- $\alpha$ -D-glucofuranose (**16**) is compulsory to deprotect the primary -OH group of the sugar moiety, thus allowing the successive esterification step and the production of the biosurfactant.

Indeed, it is known that the 5,6-O-isopropylidene group of compound **16** can be selectively hydrolysed in mild conditions in the presence of an aqueous solution of acetic acid (AcOH/H<sub>2</sub>O 7:3) (Silva et al., 2013), affording the partially protected 1,2-O-isopropylidene- $\alpha$ -D-glucofuranose (**17**), see **Figure 3.20** and **Figure 3.21**.

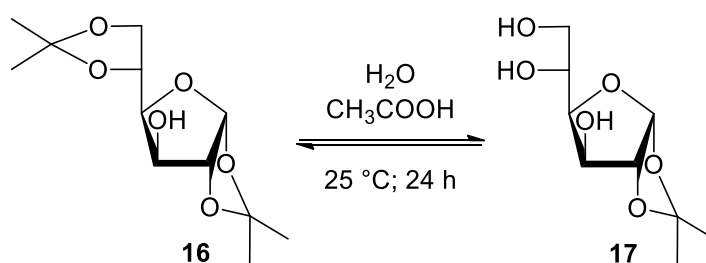


**Figure 3.20.** Selective hydrolysis of 1,2:5,6-di-O-isopropylidene- $\alpha$ -D-glucofuranose (**16**).

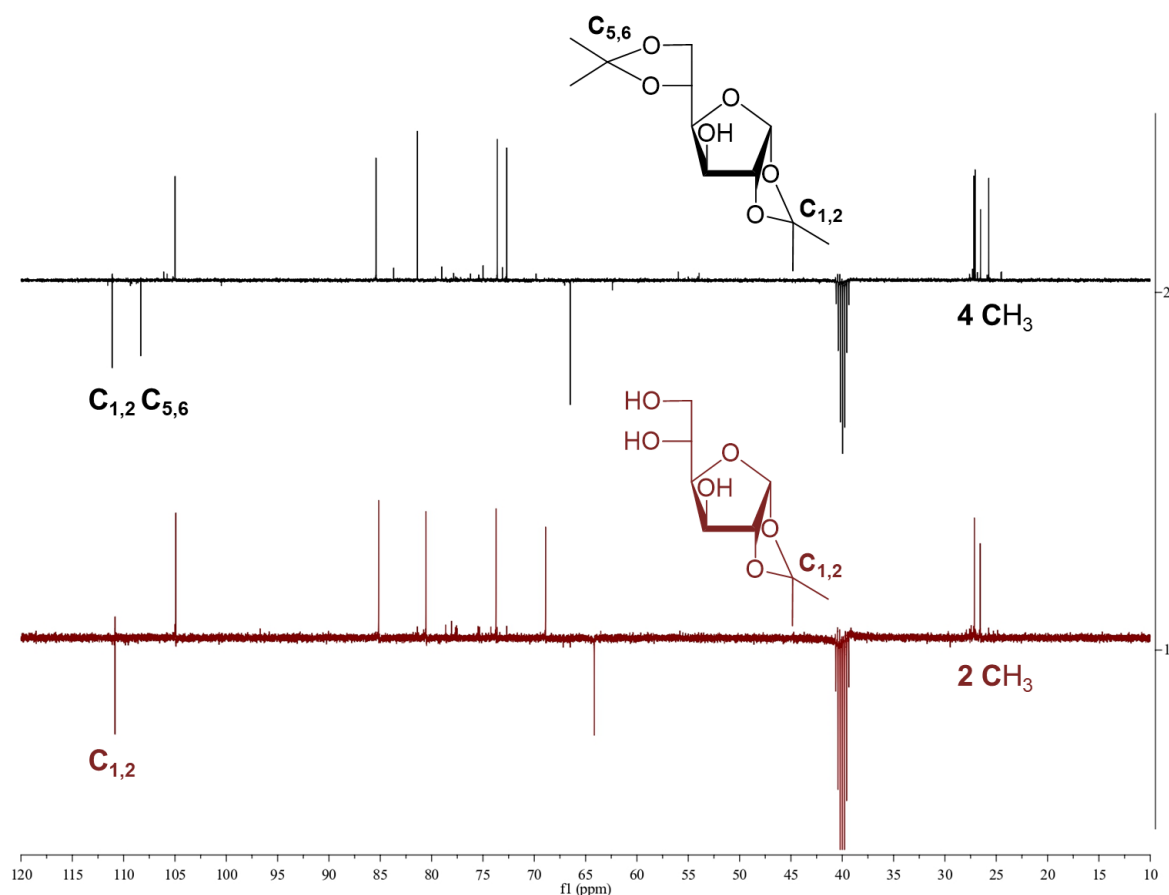


**Figure 3.21.** <sup>13</sup>C APT NMR analysis comparison between 1,2:5,6-di-O-isopropylidene- $\alpha$ -D-glucofuranose (**16**) and 1,2-O-isopropylidene- $\alpha$ -D-glucofuranose (**17**).

However, this reaction was not straightforward. Difficulties related to the purification procedure based on chromatographic separation were encountered in obtaining the pure product **17**, leading to poor isolated yield (18%). However, considering the promising tenside structure that could be generated using **17** as polar head, the study focused on the subsequent enzymatic esterification. Indeed, the identification of the suitable reaction conditions for the selective 5,6-O-ketal cleavage were postponed to the synthesis of the biosurfactants and the study of its emulsifying properties.

### 3.4.4 Enzymatic esterification

As stated in the **Section 3.4.1**, the generation of a sugar derivative apolar enough to allow the enzymatic esterification to be carried out without any solvent could solve the problems related to the selection of the optimal medium for this enzymatic reaction, moreover, leading to a SFAE with improved surfactant features.

Indeed, the enzymatic esterification of 1,2-O-Isopropylidene- $\alpha$ -D-glucofuranose (**17**) was performed in molten conditions at 80 °C in a glass oven B-585 Kugelrohr, in order to avoid magnetic stirring, that can wreck enzyme beads.

The conditions were selected on the basis of the DoE study conducted on the enzymatic esterification of glucose and palmitic acid, with slight modifications. Thus, sugar derivative **17**, methyl palmitate (**19**) or palmitic acid (**6**) (in molar ratio 1:3), Novozym<sup>®</sup> 435 (10% w/w<sub>sugar</sub>) and molecular sieves (10% w/w<sub>sugar</sub>) were charged in a flask and reacted in the glass oven at 80 °C for 24 h. Then, the reaction mixture was filtered, to remove the immobilized enzyme and the molecular sieves, and a flash chromatographic separation (*n*-hexane/EtOAc; 6:4) afforded 6-O-palmitoyl-1,2-O-isopropylidene- $\alpha$ -D-glucofuranose (**18**), see **Figure 3.22**.

ESI-MS and NMR analysis of **18** confirmed that the enzymatic esterification is highly regioselective for the primary hydroxyl group, without affecting the acetonide group, as corroborated by HMBC analysis, carried out in DMSO-*d*<sub>6</sub>, see **Figure 3.23**.

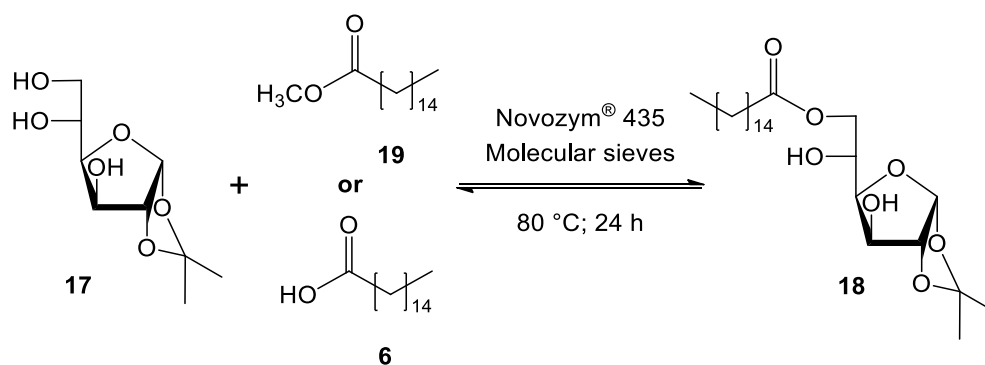


**Figure 3.22.** Enzymatic esterification of 1,2-O-isopropylidene- $\alpha$ -D-glucofuranose (**17**) and methyl palmitate (**19**) or palmitic acid (**6**) in molten conditions in the glass oven B-585 Kugelrohr.



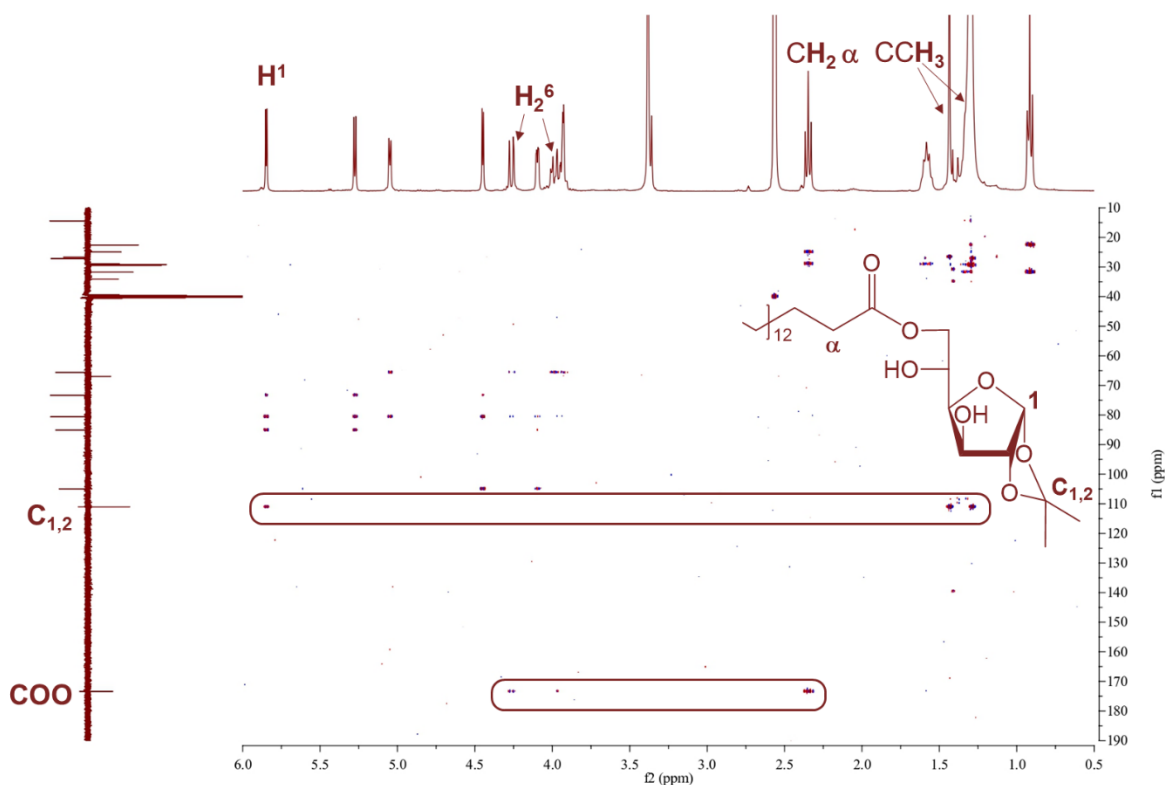


**Figure 3.23.** HMBC of 6-O-Palmitoyl-1,2-O-isopropylidene- $\alpha$ -D-glucofuranose (**18**): horizontal and vertical axis indicate the  $^1\text{H}$  and the  $^{13}\text{C}$  APT NMR spectrum, respectively.

It is known that CALB could perform transesterification reactions (Wafti et al., 2021), thus, methyl palmitate (**19**) was firstly used as acyl donor, in place of palmitic acid (**6**), considering the lower boiling point of the methanol (65 °C) generated as the by-product of the reaction, with respect to that of water. In theory, carrying out the reaction at 80 °C, the formed methanol is more easily removed from the reaction system, with respect to water, thus shifting the equilibrium of the transesterification reaction towards the product formation.

However, the reaction yield obtained from the use of methyl palmitate (**19**) as acyl donor resulted to be lower, with respect to that with palmitic acid (**6**) (20 and 27%, respectively). This result was corroborated by Chen and Wu, who observed that linear alcohols are toxic to the immobilized lipase, with a degree of deactivation inversely proportional to the number of carbon atom (Chen & Wu, 2003). Indeed, methanol rapidly inactivate CALB by stripping off water molecule from the protein surface and the active site, imposing structural rigidity (Lotti et al., 2014).

Furthermore, despite it is known that hydrophobic environments are favored by lipases (Kumar et al., 2016), the molar ratio between the fatty acid and the sugar moieties was reduced from 3:1 to 1:1. The reduction of the amount of reagents used in a reaction respects the atom economy principle (Anastas & Warner, 1998), according to which synthetic methods should be designed to maximize the incorporation of all materials used in the process into the final product, thus reducing the production costs and simplifying the purification procedure.

Therefore, a further attempt of the solvent-free enzymatic esterification was performed using the sugar derivative **17** and palmitic acid (**6**) in molar ratio 1:1 and the product 6-*O*-palmitoyl-1,2-*O*-isopropylidene- $\alpha$ -D-glucofuranose (**18**) was obtained in similar yield with respect to that using the higher reactants ratio, probably due to the simplification in the purification protocol.

Thus, despite further studies to improve the synthetic route of SFAE **18** are needed, the investigation of its surfactants properties was put ahead.

### 3.4.5 Physico-chemical characterization

With the purpose of investigating the emulsifying properties of 6-O-Palmitoyl-1,2-O-isopropylidene- $\alpha$ -D-glucofuranose (**18**), preliminary solubility tests and HLB calculation were performed.

Compound **18** was easily dissolved in sunflower oil, on the other hand, it showed low solubility in water, according to the calculated HLB value (7.7).

The HLB is an empirical indicator of the emulsifying characteristics of an emulsifier, thus, surfactants having an HLB index lower than 8 will tend to promote water in oil (W/O) emulsions, according to the rule of thumb described in the **Section 1.2.1**.

Therefore, 6-O-palmitoyl-1,2-O-isopropylidene- $\alpha$ -D-glucofuranose (**18**) was roughly studied for its ability in stabilizing W/O emulsions. **18** was firstly solubilized in commercial sunflower oil (4.5 mM), then it was emulsified with a laboratory equipment working at 3000 rpm, by slowly adding milli-Q water at different phase volumes ( $\phi_V$ : 0.04, 0.1, 0.2), for a mixing time of 15 min. Then, emulsion formation and stability were checked, see **Figure 3.24**.

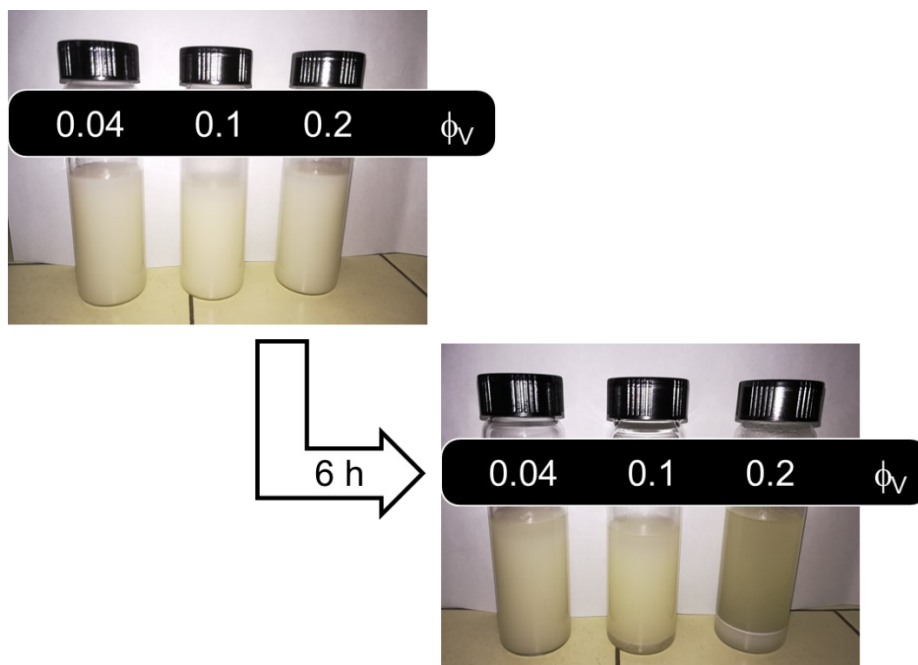


**Figure 3.24.** Stability within 6 h of W/O emulsions generated with 6-O-palmitoyl-1,2-O-isopropylidene- $\alpha$ -D-glucofuranose (**18**) at surfactant concentration of 4.5 mM and different phase volumes ( $\phi_V = 0.04, 0.1, 0.2$ ).

Emulsions are dispersed systems thermodynamically unstable, indeed they tend to undergo emulsion breaking processes over time due to various physicochemical mechanisms, *i.e.*, Ostwald ripening, flocculation, particle coalescence, gravitational separation, coalescence, and, finally, phase separation (McClements & Jafari, 2018).

Different types of stabilizers are generally included in commercially available emulsion recipes, which cooperate, acting on different aspects of the formulation, to improve its long-term stability. Few examples are texture modifiers, weighting agents, ripening inhibitors, and emulsifiers (McClements, 2011).

It is important to underline that the emulsion systems tested in this study, in which only the investigated surfactant acts as stabilizing agent of the disperse system, is an unrealistic model, assumed to isolate the contribute of the tenside to the emulsion stabilization. Despite it showed limitations and the created emulsion will tend to breakdown, this model allows a simple and quick evaluation of the emulsifier capacity of the biosurfactant, by evaluating the amount of phase volume the system can withstand and the time to obtain the separation of phases.

Regarding the former aspect, the smaller is the amount of water to be incorporated in the W/O emulsion (the smaller is the phase volume), the easier is the stabilization of the disperse system, at equal surfactant concentration and using the same emulsification technique.

Indeed, during the formation of a W/O emulsion, water is dispersed into small droplets, leading to a high increment of the surface area of the dispersed phase. Considering the intrinsic instability of the system, to prevent droplets against coalescence, it is necessary to obtain a full coverage of droplets surface with a layer of the surfactant (Maindarkar et al., 2015).

Therefore, the lower is the phase volume, the lower resulted to be the surface of the droplets to be covered by the emulsifier.

Furthermore, the surface coverage of the dispersed phase droplets is strongly influenced by the interfacial layer generated by the surfactant adsorbed to the oil-water interface. Indeed, the interactions, the molecular dimensions and the packing

capacity of the adsorbed emulsifier molecules largely determine the stability of emulsions (Bos & van Vliet, 2001).

Considering the W/O emulsions prepared with 6-*O*-Palmitoyl-1,2-*O*-isopropylidene- $\alpha$ -D-glucofuranose (**18**), it is evident that the systems showed poor stability. Only the emulsion prepared with a phase volume of 0.04 maintained its stability within the first 6 h, but it also underwent complete sedimentation after less than 24 h.

This instability could be due either to the surfactant concentration (too low to be able to cover all the surface of the droplets), or to its poor packing capacity at the interface.

Probably the sugar polar head of compound **18** was too hindered to properly pack at the oil-water interface, due to the acetonide group, thus resulting in an impossibility of generating a compact interlayer, compulsory to generate a stable emulsion.

Therefore, due to the poor emulsifying results obtained, the research focused on an alternative strategy of the sugar derivatization based on the Fisher glycosylation, which could generate compounds with a less hindered structure.

### 3.5 Alkyl D-glucosides

#### 3.5.1 Fischer glycosylation strategy

The second strategy selected for the derivatization of the sugar moiety is based on the synthesis of glycosides. They are saccharide derivatives in which a sugar is bonded to a non-sugar moiety (aglycone) *via* a glycosidic bond. When the latter is formed between a sugar and an alcohol, in the presence an acid catalyst, O-glycosides are generated as products, according to the Fischer glycosidation reaction (Collins & Ferrier, 1995).

This well-known and industrially relevant reaction is generally catalyzed by a homogenous acid catalyst, *i.e.*, sulphamic acid or *p*-toluenesulfonic acid, which requires a neutralization step (Kinanti et al., 2021). Aiming at improving the sustainability of the derivatization step, Amberlyst® 15, already described in the **Section 3.4.2**, was selected as acid catalyst. Indeed, this cation exchange strongly acidic resin can be filtered, recovered and eventually recycled, moreover, troublesome acid neutralizations and resulting salt formation at the end of the reactions are avoided (Whistler & Wolfrom, 1963).

Naturally occurring alcohols were selected as aglycones of the glycosides, aiming at employing recommended solvents / reagents with low toxicity and non-hazardous.

The generated glycosides, due to their reduced polarity with respect to unprotected sugars, showed improved solubility in molten fatty acids, thus allowing the solvent-free enzymatic esterification step, which is mandatory to produce alkyl glycoside fatty acid esters (AGFAEs) biosurfactants.

In particular, two families of AGPAEs were synthesised by varying the type of sugar (Glc and Gal), the naturally occurring alcohols used in the Fischer glycosylation (using linear and branched alcohols from EtOH to 1-HexOH) and the saturated fatty acid of the solvent-free enzymatic esterification (lauric, palmitic and stearic acid), see **Figure 3.25**.

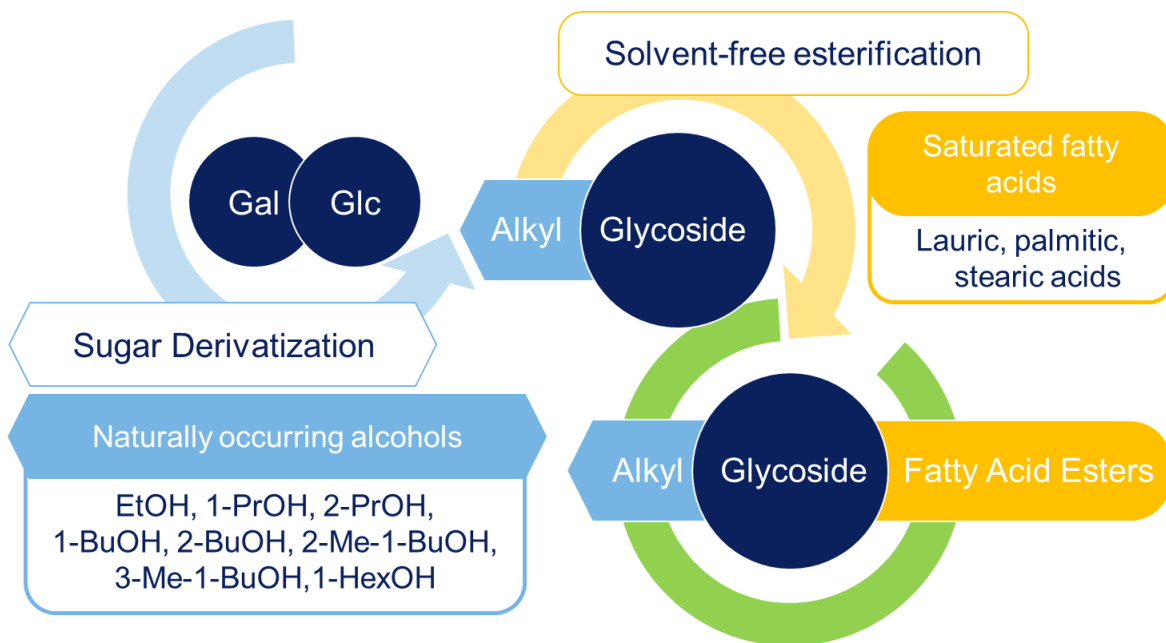


**Figure 3.25.** General overview over the Fischer glycosylation strategy.

## 3.5.2 Synthesis

According to the preparative scale Fischer glycosylation protocol (Whistler & Wolfrom, 1963), D-glucose (**12**) suspended in dry naturally occurring alcohols (**28-35**) in the presence of the strongly acidic cation exchange resin Amberlyst® 15 and molecular sieves under reflux or at 120 °C. The reactions were stopped after a certain time (ranging from 1.5 to 6.0 h), depending on the alcohol, by filtration of the solid catalyst. Then, the alcohols were removed under reduced pressure, and the reaction mixtures were submitted to flash column chromatography (DCM/MeOH 8.8:1.2) to give alkyl D-glucosides (**20ad-27ad**) in good yields, with few exceptions, see **Figure 3.26** and **Table 3.5**.

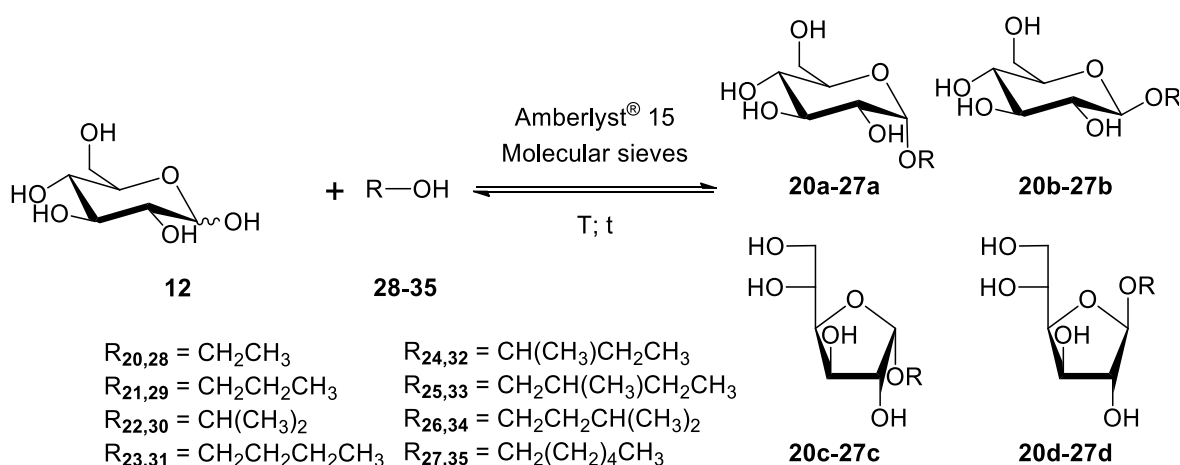


**Figure 3.26.** Synthesis of alkyl D-glucosides (**20ad-27ad**).

**Table 3.5.** Experimental conditions for the synthesis of alkyl D-glucoside (**20ad-27ad**).

Compound	R-OH	Temperature (°C)	Time (h)	Yield (%)
<b>20ad</b>	EtOH ( <b>28</b> )	90	4	65
<b>21ad</b>	1-PrOH ( <b>29</b> )	100	3	71
<b>22ad</b>	2-PrOH ( <b>30</b> )	90	6	67
<b>23ad</b>	1-BuOH ( <b>31</b> )	120	2.5	91
<b>24ad</b>	2-BuOH ( <b>32</b> )	120	6	87
<b>25ad</b>	2-Me-1-BuOH ( <b>33</b> )	120	1.5	70
<b>26ad</b>	3-Me-1-BuOH ( <b>34</b> )	120	2	89
<b>27ad</b>	1-HexOH ( <b>35</b> )	120	1.5	73



Since the temperature has a strong impact on Glc solubility in the listed alcohols, it was selected as high as possible, according to the alcohol boiling points and the maximum working temperature of the resin (120 °C).

Few experiments allowed the identification of the optimal reaction time for the reactions carried out. Exceeding the reported times led to the formation of undesired by-products, deriving from side-reactions, such as sugar dehydration and caramelization.

The lowest yields of 65% and 67% were obtained from the Fischer glycosylation of Glc (**12**) with EtOH (**28**) and 2-PrOH (**30**), respectively. These results could be due both to the lower temperature set for the reactions, according to the boiling points of the two alcohols, and to their higher solubility with water, with respect to the other alcohols. These factors could have complicated the water removal from the reaction mixture, thus disadvantaging the shift of the equilibrium towards the product formation. On the contrary, high yields (70-91%) were achieved for all the other alcohols, both branched and linear.

### 3.5.3 MS and NMR characterization

It is known that Fischer glycosylation reactions led to isomeric mixture of four isomers, which differ for their ring sizes (pyranose or furanose) and configuration at the anomeric position ( $\alpha/\beta$ ), thus obtaining  $\alpha/\beta$ -pyranosides, labelled as **a/b**; and  $\alpha/\beta$ -furanosides, **c/d** (Collins & Ferrier, 1995).

All the synthesized isomeric mixtures (**20ad-27ad**) were fully characterized by ESI-MS and NMR analysis that allowed the estimation of the isomeric ratios. In particular, they were obtained by  $^1\text{H}$  NMR analysis, carried out in  $\text{D}_2\text{O}$ , as the ratio of the areas of anomeric proton signals of each isomer present in the reaction mixture, see **Figure 3.27** as an example. NMR anomeric proton signals were identified by comparison with data reported in the literature (Straathof et al., 1987).

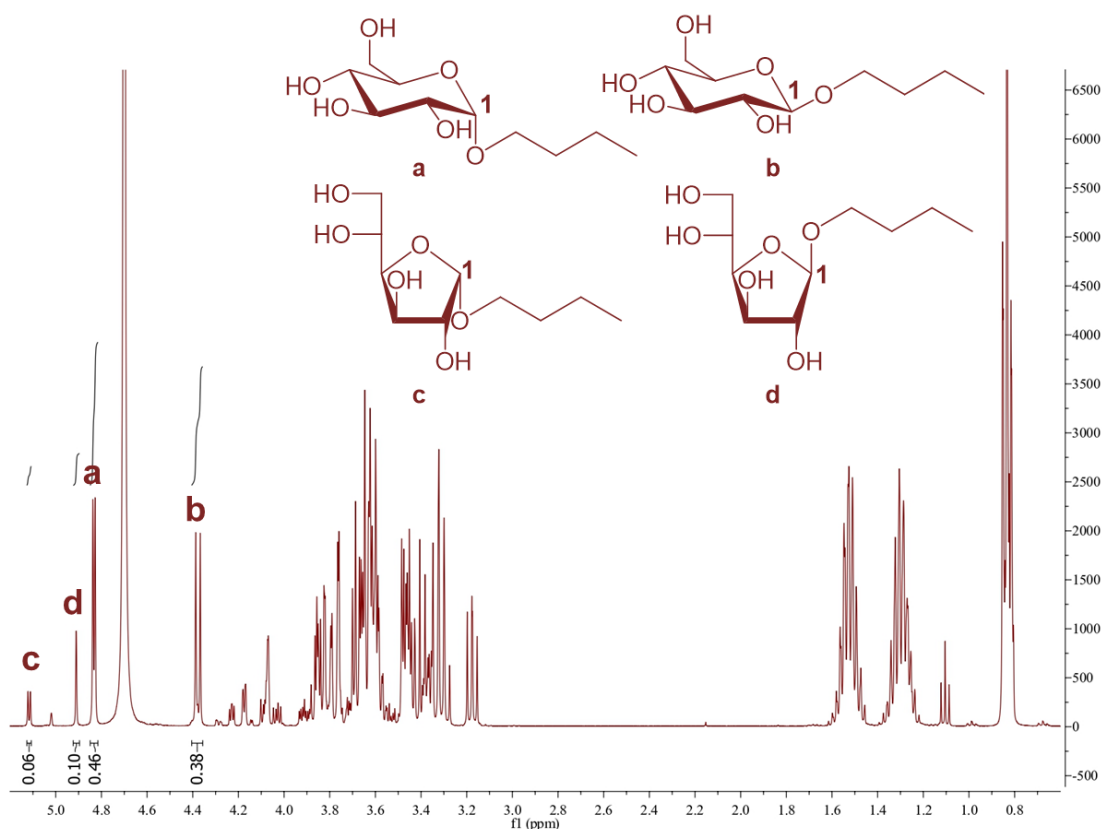



**Figure 3.27.**  $^1\text{H}$  NMR (400 MHz) spectrum of 1-butyl D-glucoside isomeric mixture (**23ad**) recorded in  $\text{D}_2\text{O}$  with highlighted integrals of the anomeric proton signals.

The ratio of the four glycosidic forms present at the equilibrium is strongly influenced by the temperature, the catalyst, the type of the sugar and the chain length of the alcohol (Collins & Ferrier, 1995).

### 3 | Results and discussion

According to the results obtained, a high amount of furanoside derivatives is produced with short chained alcohols (*i.e.*, EtOH, 1-PrOH and 2-PrOH). On the other hand, in the case of longer chained alcohols (*i.e.*, 1-BuOH, 3-Me-1-BuOH, 2-Me-1-BuOH and 1-HexOH), it is possible to observe a reverse trend, indeed pyranosides are usually more than double the amount of furanosides, see **Table 3.6**.

**Table 3.6.** Isomeric ratio of the synthesized of alkyl D-glucoside (**20ad-27ad**).

Compound	R-OH	Isomeric ratio a/b/c/d (%)	
<b>20ad</b>	EtOH ( <b>28</b> )	13/20/27/40	
<b>21ad</b>	1-PrOH ( <b>29</b> )	24/27/19/30	
<b>22ad</b>	2-PrOH ( <b>30</b> )	18/20/28/34	
<b>23ad</b>	1-BuOH ( <b>31</b> )	46/38/6/10	
<b>24ad</b>	2-BuOH ( <b>32</b> )	36/32/12/20	
<b>25ad</b>	2-Me-1-BuOH ( <b>33</b> )	37/29/14/20	
<b>26ad</b>	3-Me-1-BuOH ( <b>34</b> )	43/34/10/13	
<b>27ad</b>	1-HexOH ( <b>35</b> )	37/32/14/17	

These results can be explained by looking into the mechanism of the Fischer glycosylation reaction. Indeed, it well-known that the conversion of the free sugar to pyranosides occurs *via* furanosides (Mowery, 1955). Therefore, by using milder reaction conditions, as in the case of synthesis of ethyl, 1-propyl and 2-propyl D-glucosides (**20**, **21**, and **22**), the reaction mixtures will be richer in furanosides.

Instead, focusing on the pyranosides, their anomeric equilibrium ratio is strongly influenced by the anomeric effect. It is a stereoelectronic effect that explains the preferential allocation of the hydroxyl substituent in the anomeric position of pyranoid monosaccharides in the *axial* orientation, instead of the less hindered *equatorial* orientation, that would be expected from steric considerations (Edward, 1955; Lemieux & Chü, 1958).

This effect is mainly due to hyperconjugative interactions between the axial unshared lone pairs of electrons on the ring oxygen atoms and the antibonding  $\sigma^*$ -orbitals of the C-X bond, where X is the hydroxyl substituent in the anomeric

position. These stabilizing interactions, able to lower the overall energy of the structure, can occur only when X is axially oriented because the donating lone pair of electrons resulted antiperiplanar ( $180^\circ$ ) to the exocyclic C-X  $\sigma^*$ -orbitals (Alabugin et al., 2021), see **Figure 3.28**.

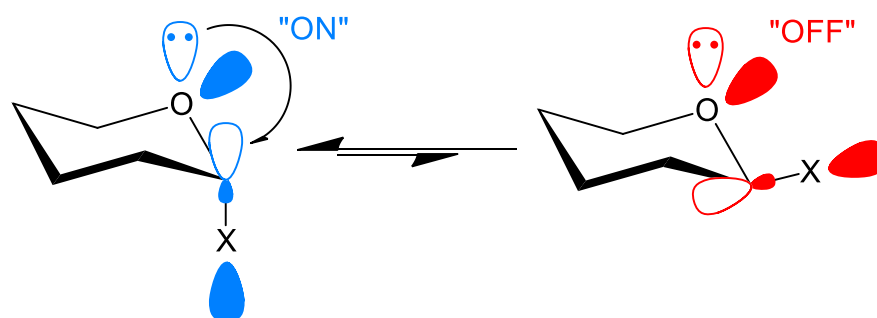


**Figure 3.28.** Hyperconjugative model of the anomeric effect.

This preference for the  $\alpha$ -anomer decreases in solvents of increasing polarity (Collins & Ferrier, 1995), corroborating the obtained data.

Among all the synthesized alkyl glucosides, 1-butyl D-glucoside isomeric mixture (**23ad**) was selected as substrate model for the successive enzymatic esterification step, because it was afforded with one of the highest yields and it showed an intermediate value of polarity, with respect to the other compounds.

### 3.6 1-Butyl 6-O-acyl-D-glucosides

#### 3.6.1 Enzymatic esterification with different fatty acids

Aiming at evaluating possible differences in the interfacial properties according to the surfactant tail, lauric, palmitic and stearic acids (**5,6,7**) were selected as acyl donors for the enzymatic solvent free esterification of 1-butyl D-glucosides (**23ad**), in the presence of the immobilized lipase Novozym<sup>®</sup> 435, see **Figure 3.29**.

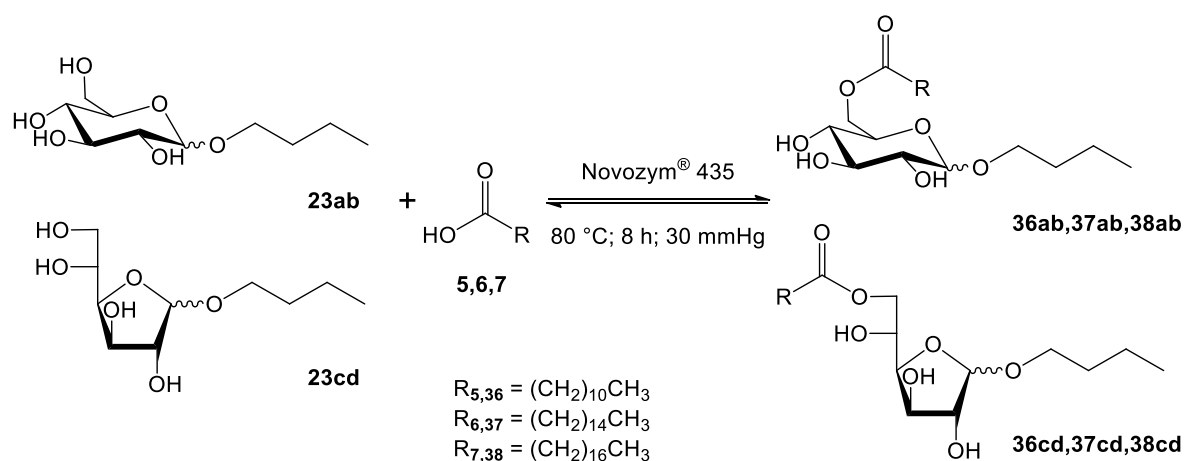


**Figure 3.29.** Enzymatic synthesis of 1-butyl 6-O-acyl-D-glucosides (**36ad**, **37ad**, and **38ad**).

Also in these cases, the reactions were carried out at 80 °C in a glass oven B-585 Kugelrohr, to avoid magnetic stirring, however, considering the modest previous results, it was decided to work under reduced pressure (30 mmHg), thus further favouring the water removal, with respect to the use of molecular sieves.

After 8 h, reaction mixtures were taken up in EtOAc and the immobilized enzyme was removed by filtration. Then, the esters were extracted in EtOAc (2 times) from 1 M NaOH. The striking difference in polarity between pyranoside- and furanoside-based derivatives enabled the separation of the two species through flash chromatography (*n*-hexane/EtOAc; 2:8), thus affording three 1-butyl 6-O-acyl-D-glucopyranosides (**36ab**, **37ab**, and **38ab**) and three 1-butyl 6-O-acyl-D-glucofuranosides (**36cd**, **37cd**, and **38cd**).

Yields are listed in the **Table 3.7**, as well as the isomeric ratios of the anomers, which were estimated by <sup>1</sup>H NMR analysis, carried out in DMSO-*d*<sub>6</sub>, as the ratio of the areas of the two anomeric proton signals.

### 3 | Results and discussion

Table 3.5. Yields and isomeric ratios of 1-butyl 6-O-acyl-D-glucosides.

Compound	Yield ab (%)	Yield cd (%)	Ratio ab/cd (%)	Isomeric ratio a/b/c/d (%)
36ad	37	5	88/12	60/28/7/5
37ad	47	10	82/18	52/30/10/8
38ad	52	13	80/20	50/30/11/9

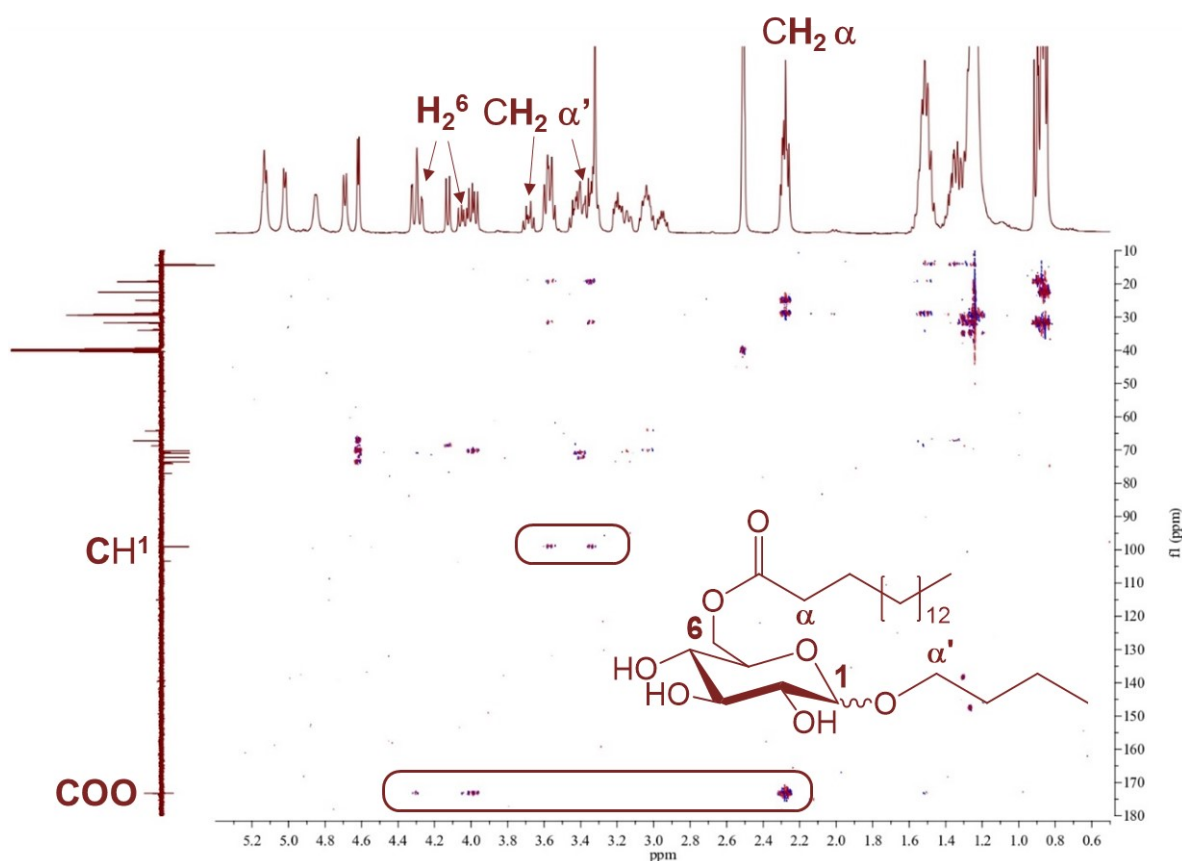


Figure 3.30. Enzymatic synthesis of 1-butyl 6-O-acyl-D-glucosides (36ad, 37ad, and 38ad).

ESI-MS and NMR analysis also demonstrated that the enzymatic esterification is highly regioselective for the primary hydroxyl group of the sugar moiety. Indeed, the HMBC spectrum showed the interactions of the carbonyl ester group (COO) with the two protons of the 6 position of the sugar (H<sub>2</sub><sup>6</sup>) and the two protons of the carbon in α position relative to the carbonyl group (CH<sub>2</sub> α), see **Figure 3.30** as example. Moreover, the reaction did not promote the glucoside hydrolysis, as confirmed, in

the same spectrum, by the persistence of the interactions of the anomeric carbons ( $\text{CH}^1$ ) with the two protons in  $\alpha'$  position of the aglycone ( $\text{CH}_2 \alpha'$ ).

Observing the obtained yields, pyranosides esters (**36ab**, **37ab**, **38ab**) prevailed over the furanosides ones (**36cd**, **37cd**, **38cd**) with a relative ratio of roughly 80:20.

### 3.6.2 Physico-chemical characterization

Considering the higher amount of 1-butyl 6-O-acyl-D-glucopyranosides (**36ab**, **37ab**, and **38ab**) obtained from the enzymatic esterification with respect to their furanoside-based derivatives, the research firstly focused on the investigation of their physico-chemical properties.

Compounds **36ab**, **37ab** and **38ab** were submitted to solubility tests and they resulted to be soluble in sunflower oil (up to 6.0 mM), but poorly soluble in water. These results were in accordance with their HLB value of 8.5, 7.5 and 7.1, respectively, calculated according to the Griffin method.

As previously stated in **Section 3.2.2**, the stabilization of a disperse system, such as an emulsion, can be achieved by reducing the interfacial tension (IFT) between oil and water. Indeed, the thermodynamically unfavourable contact between the oil and water molecules in an emulsion causes high IFT at the oil/water interface (van Oss, 2007). Surfactants can modify the IFT by adsorbing at the interface, thus reducing the scarce interactions between the oil and water phases (Somasundaran & Huang, 2000).

Therefore, the ability of reducing the IFT is usually investigated by du Noüy tensiometric measurements. It is a well-established method commonly used for the measurement of both surface and interfacial tensions (du Noüy, 1925). This method relies on the measurement of the force necessary to detach a platinum ring from the surface of a liquid, according to the equation:

$$\gamma = \frac{F\beta}{4\pi r} + F_A$$

where  $\gamma$  is surface tension, expressed in  $\text{mN m}^{-1}$ ,  $F$  represents the force at the point of detachment, measured using a balance connected to a proper software,  $r$  is the average diameter of the ring,  $F_A$  the buoyancy force, and  $\beta$  is a tabulated correction factor, compulsory to take into account for the complex shape of the liquid before the break-away, the non-vertical surface tension forces and the weight of the upraised liquid.



To obtain this simplified equation, it is assumed a contact angle of  $0^\circ$  of the liquid onto the ring surface, which is guaranteed by the material of the ring (the Pt/Ir alloy assures the complete wettability of the ring), moreover, it must lie flat on a quiescent liquid surface (Schramm, 2005).

For interfacial tension measurements, see **Figure 3.31**, it is possible to apply the same equation, however, further parameters have to be introduced, *i.e.*, liquid density, platinum ring and wire radii, according to the Harkins-Jordan correction (Harkins & Jordan, 1930).

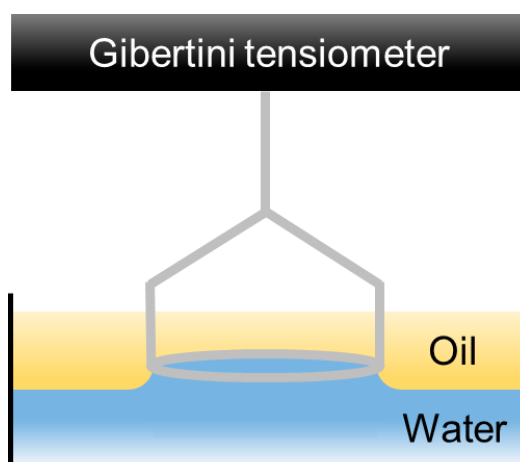


**Figure 3.31.** Illustration of water/oil interfacial tension measurements according to the du Noüy ring method: moment of the ring detachment from the water surface.

Therefore, the IFT reduction between water (milli-Q) and sunflower oil was evaluated by means of a Gibertini tensiometer, as reported elsewhere (Lotierzo et al., 2016). 1-butyl 6-O-lauroyl- (**36ab**), 6-O-palmitoyl- (**37ab**) and 6-O-stearoyl- (**38ab**) D-glucopyranosides (**Figure 3.32**), were dissolved in the oil phase at increasing concentration (0.1, 1.0, 3.0, 4.5, 6.0 mM), up to the solubility limit of some of them. Then, the oil/water IFT was measured as a function of the biosurfactants concentrations, see **Figure 3.33**.

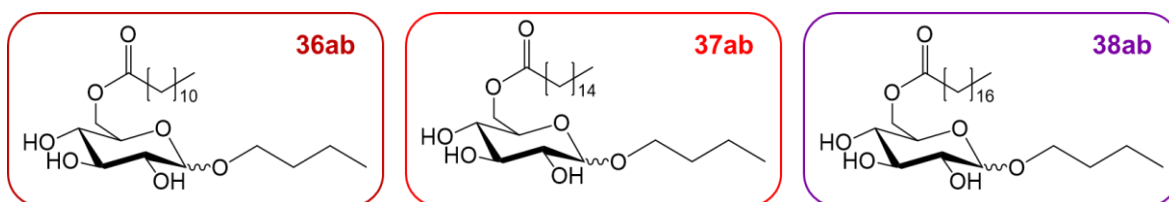


**Figure 3.32.** 1-butyl 6-O-lauroyl-, 6-O-palmitoyl-, and 6-O-stearoyl-D-glucopyranosides (**36ab, 37ab, 38ab**).

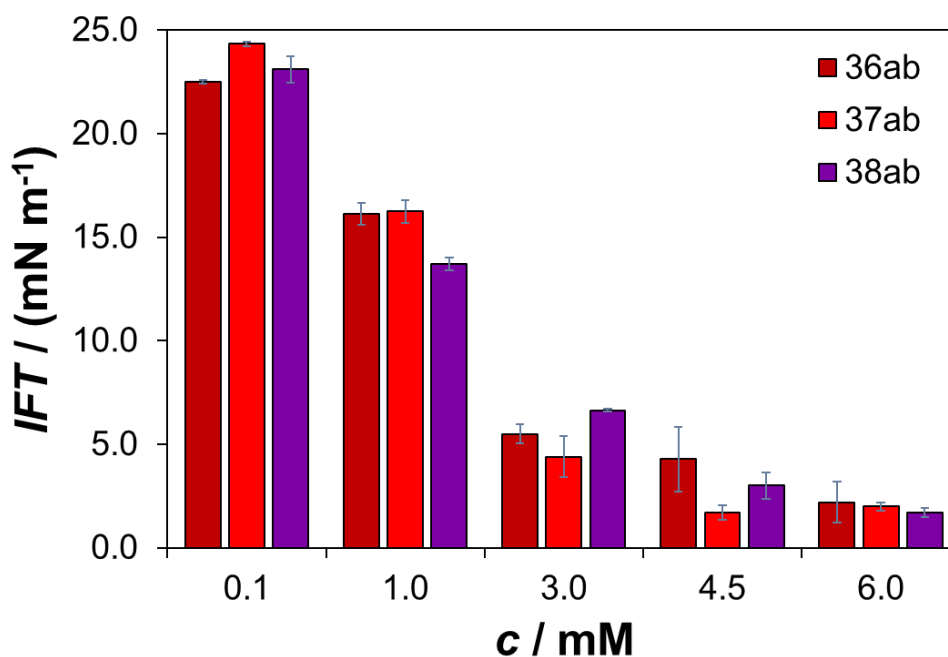


**Figure 3.33.** Comparison of sunflower oil/water interfacial tension (IFT) data by varying the concentration of **36ab**, **37ab** and **38ab** in the range 0.1-6.0 mM in oil. Data were reported as average values on three different replicates at room temperature.

All the tensides allowed to reduce the sunflower oil/water IFT from 26 mN m<sup>-1</sup> (which represents the sunflower oil/water IFT without any surfactant) to values lower than 4 mN m<sup>-1</sup> at concentrations of 6.0 mM. These results seem to be in agreement with previously reported data obtained with similar surfactants (Bai et al, 2018; Opawale & Burges 1998).

### 3.6.3 Emulsifying properties and stability over time

To corroborate these promising interfacial features, the emulsifying behaviour of the three biosurfactants (**36ab**, **37ab** and **38ab**) was investigated. As already described in the **Section 3.4.5**, ionic surfactant molecules with HLB lower than 8 should act as emulsifiers in W/O emulsions.

Thus, water (milli-Q) in sunflower oil (W/O) emulsions were prepared using a Thermo Fisher Q700 sonicator equipped with a 3 mm-titanium alloy microtip. The operative conditions were selected on the basis of previous work (Cionti et al., 2022) and they contemplate a frequency of 20 kHz in pulsed mode (3 s on and 3 s off) at 50% amplitude for 45 s. The pulsed ultrasound mode avoids the generation of uncontrolled heat that can cause emulsion breaking processes, moreover, for further dissipating heat, the emulsions were refrigerated in a cold-water bath during the whole procedure.

Aiming at optimizing the emulsion phase volume ( $\phi_v$ ) and the surfactant concentration ( $c$ ), preliminary tests were carried out on 1-butyl 6-O-palmitoyl-D-glucopyranosides (**37ab**), selected as a substrate model. Three phase volumes, commonly used in commercial formulations ( $\phi_v = 0.16, 0.14$  and  $0.13$ ), and two different concentrations, identified from the IFT study ( $c = 4.5$  and  $6.0$  mM, solubilized in sunflower oil at  $80$  °C), were adopted, see **Table 3.6**.

**Table 3.6.** Optimization of emulsion parameters.

<b>Emulsion</b>	<b><math>c</math> (mM)</b>	<b>Phase volume, <math>\phi_v</math></b>
<b>1</b>	4.5	0.16
<b>2</b>	4.5	0.14
<b>3</b>	4.5	0.13
<b>4</b>	6.0	0.16
<b>5</b>	6.0	0.14
<b>6</b>	6.0	0.13

### 3 | Results and discussion

The prepared W/O emulsions were checked for their stability within 24 h (**Figure 3.34**). Examination of the fresh emulsions (picture on the left) reveals that traces of water are immediately released from the formulations with 0.16  $\phi_v$  (samples **1** and **3**), therefore, lower phase volumes should be selected. After 24 h, all the other prepared emulsions (**2**, **3**, **4** and **6**) resulted to be similar (picture on the right), thus a phase volume of 0.14 is well tolerated and a  $c$  of 4.5 mM is enough to generate a relatively stable emulsion (emulsion **2**).

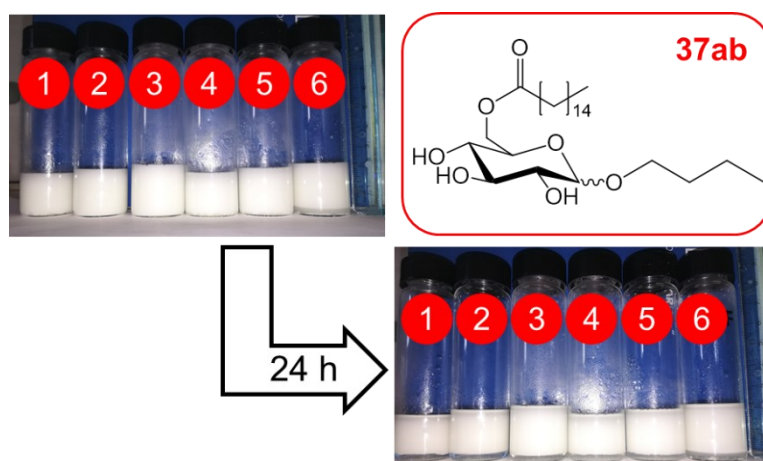


**Figure 3.34.** Stability within 24 h of W/O emulsions generated with 1-butyl 6-O-palmitoyl-D-glucopyranosides (**37ab**) at different surfactant concentration and phase volumes (**1-6**), prepared using a Thermo Fisher Q700 sonicator equipped with a 3 mm-titanium alloy microtip.

Once optimized the experimental conditions ( $c = 4.5$  mM,  $\phi_v = 0.14$ ), W/O emulsions were prepared with the three selected biosurfactants 1-butyl 6-O-lauroyl-, 6-O-palmitoyl- and 6-O-stearoyl-D-glucopyranosides (**36ab**, **37ab**, **38ab**) and their stability within 72 h was assessed by means of turbidimetric measurements (Aizawa, 2014).

The evaluation of the stability of an emulsion is a key issue for many industrial processes and products. During the years, several methods have been extensively investigated to determine the extent of emulsion-breaking processes over time, *i.e.*, droplet size analyses, measurements of physical properties, accelerated tests, light-scattering, and the turbidimetric method (Song et al., 2000).

Regarding the latter, it is a simple and relatively fast method based on absorbance measurements. Basically, light scatters whenever it hits dispersed droplets, by passing through an emulsion. Thus, turbidity is related to the size and number of

dispersed droplets present in the emulsion (Aizawa, 2014). The theoretical turbidity ( $\tau$ ) of a monodisperse emulsion can be expressed as a function of the total scattering coefficient ( $K$ ) with respect to the dispersed droplets diameter ( $d$ ), according to the Goulden equation (Goulden, 1958):

$$\tau = k \frac{K}{d}$$

Emulsion-breaking processes (*i.e.*, coalescence or flocculation) cause the shift from small to larger droplets up to the complete separation of the two phases. Therefore, considering the inversely proportional relationship of the turbidity ( $\tau$ ) with the dispersed droplets diameter ( $d$ ), it is possible to state that a decrease in turbidity over time, at any wavelength, is strictly related to emulsion destabilization phenomena (Song et al., 2000).

The stability of the generated W/O emulsion were assessed by following their absorbance value at a fixed wavelength (500 nm), in a 1 cm path length optical cell ( $l$ ), using a Shimadzu UV–Vis spectrophotometer UV-2600. Then,  $\tau$  can be easily calculated according to the equation (Aizawa, 2014):

$$\tau = \ln(10) A$$

To compare the results obtained, normalized turbidity values ( $\tau / \tau_0$ , where  $\tau_0$  is the turbidity at 0 min) were studied as a function of time within 72 h, see **Figure 3.35**.

6-*O*-Palmitoyl- and 6-*O*-stearoyl-based compounds (**37ab** and **38ab**) exhibit gradually decreasing curves, whereas a sharp normalized turbidity reduction is appreciable for lauroyl-based surfactant **36ab**. Indeed, both **37ab** and **38ab** resulted sufficiently stable up to 72 h, whereas **36ab** molecule caused the sedimentation of the water droplets already after 48 h.

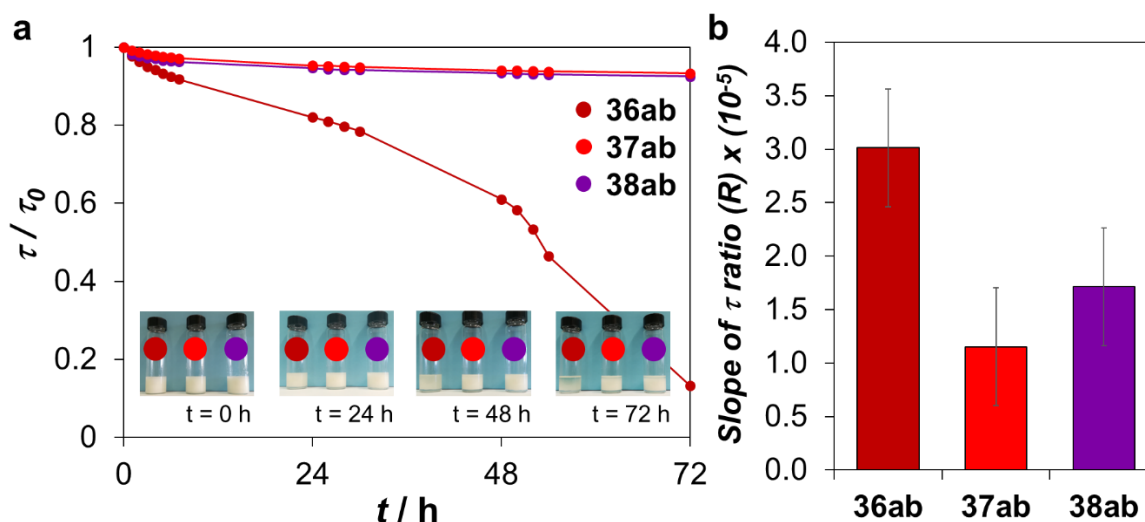


**Figure 3.35.** **a)** Normalized turbidity ( $\tau / \tau_0$ ) of W/O emulsions generated with 1-butyl 6-O-lauroyl-, 6-O-palmitoyl- and 6-O-stearoyl-D-glucopyranosides (**36ab**, **37ab**, **38ab**) at optimized surfactant concentration and phase volumes ( $c = 4.5$  mM and  $\phi_v = 0.14$ ) within 72 h. Insets: photos of the three samples at 0, 24, 48 and 72 h; **b)** slope of turbidity ratio ( $R$ ) values as a function of the adopted surfactant (**36ab**, **37ab**, **38ab**).

In order to confirm the previous outcomes, the slope of the stability index or turbidity ratio ( $R$ ) was investigated. This parameter represents a useful, rapid and simple tool to evaluate emulsions stability against sedimentation within a relatively short period of time.  $R$  is defined as the ratio of turbidity at high and low wavelengths (in this case 700 and 450 nm,  $R = \tau_{700} / \tau_{450}$ ). Then, the slope of  $R$  over time can be calculated within 50 min (Song et al., 2000). To avoid emulsion modifications, no samples dilution was performed (Bai et al., 2018).

As already stated, a reduction of the turbidity over time is related to emulsion-breaking processes. The faster  $\tau$  decreases, the higher is the difference between values of  $R$  calculated at each interval of time (10 min), thus, the slope of the ratio of turbidity over time increases. In the studied cases, the slope of  $R$  was minimized by adding **37ab** and **38ab** biosurfactant to the W/O emulsions, thus indicating higher emulsion stabilization capacity with respect to **36ab**.

### 3.6.4 Confocal microscopy images of W/O emulsions

The promising results obtained from the turbidimetric measurements were further corroborated by confocal microscopy images of fresh and aged W/O emulsions generated with the three 1-butyl 6-*O*-lauroyl-, 6-*O*-palmitoyl-, and 6-*O*-stearoyl-*D*-glucopyranosides (**36ab**, **37ab**, and **38ab**).

Before the analysis, emulsions were stained with Rhodamine B, which is a fluorescent dye emitting in the red, soluble only in the water phase. Images were acquired by a Nikon A1 laser scanning confocal microscope (LSCM) working in oil immersion (NA1.4), equipped with a 60 $\times$  objective, see **Figure 3.36.a-k**.

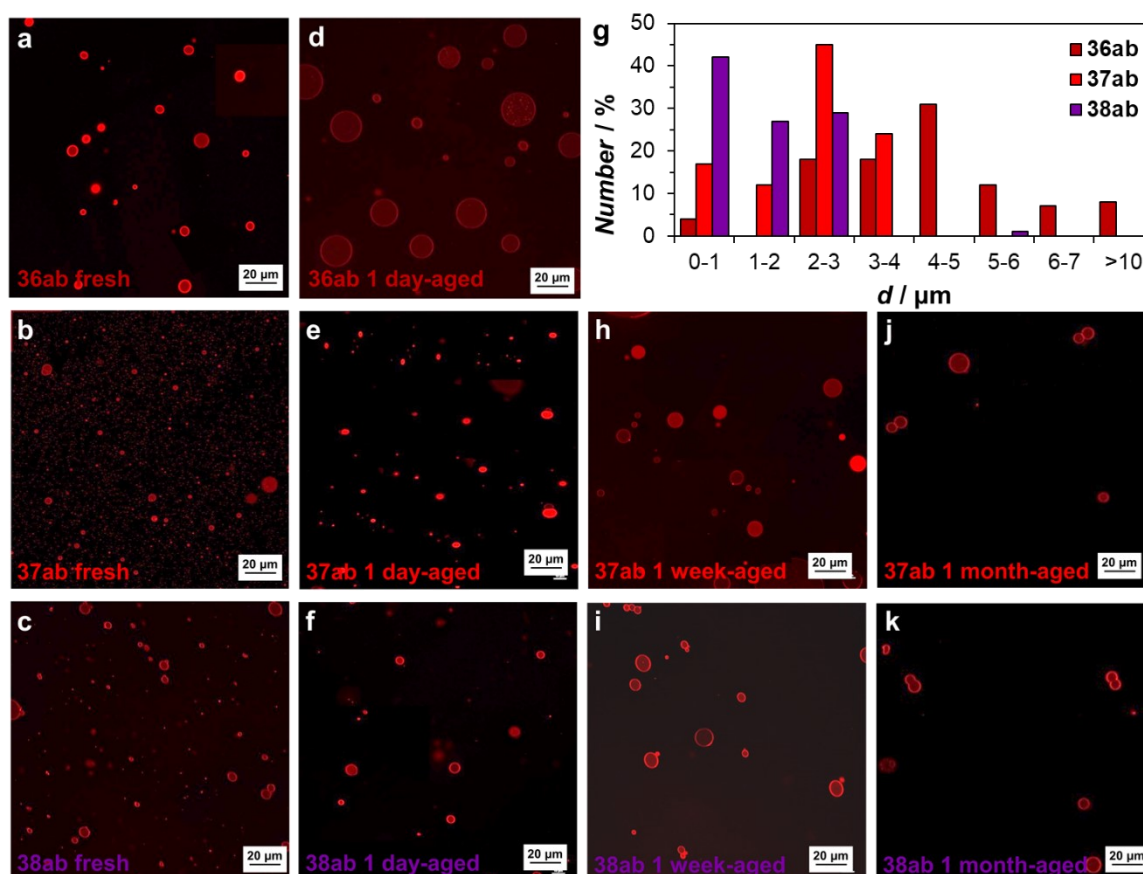


**Figure 3.36.** LSCM images of **a-c**) freshly prepared, **d-f**) 1 day-aged, **h-i**) 1 week-aged, and **j-k**) 1 month-aged 1-butyl 6-*O*-lauroyl- (**36ab**), 6-*O*-palmitoyl- (**37ab**) and 6-*O*-stearoyl- (**38ab**) *D*-glucopyranosides W/O emulsions; **g**) relative droplets size distribution (as number percentage) of the fresh samples.

Indeed, examination of the images resulting from the freshly prepared W/O emulsions with **36ab**, **37ab**, and **38ab** (*Figure 3.36.a-c*) confirmed the type of the emulsion (red water droplets surrounded by black oil phase) and it revealed very small droplets for all the three systems (average diameter <20  $\mu\text{m}$ ).

This is the result of the ultrasound-assisted emulsification technique used. By generating hydrodynamic shear forces, causing cavitation and collapse of gas bubbles, the ultrasound process can reduce the interfacial tension between the two phases, favouring the surfactants adsorption at the interface and thus resulting in stable emulsions characterized by very small droplet size (Silva & Sato, 2019).

However, the droplets diameter distribution between the three fresh W/O emulsions was quite different. Droplets size distribution was evaluated by processing the three images of *Figure 3.36.a-c* with the ImageJ software, thus obtaining the relative abundance of each droplet diameter. The emulsions obtained with **37ab** and **38ab** exhibit an average diameter lower than 3  $\mu\text{m}$ , on the other hand, the disperse system derived from **36ab** was characterized by a wider size distribution, with a maximum centred around 4–5  $\mu\text{m}$ , see *Figure 3.36.g*.

Furthermore, the emulsions stability was assessed over time to be compared with the turbidity results. After 1 day of ageing, a visible enlargement of droplets diameter (average  $d \geq 20 \mu\text{m}$ ) can be observed only in the case of the emulsion prepared with the lauroyl-based derivative **36ab**, see *Figure 3.36.d*. This fast growth of droplets, caused by Ostwald ripening, underwent complete water sedimentation in less than 1 week. Conversely, both the **37ab**- and **38ab**-based emulsions resulted only in a noticeable droplets size increase by five-fold, after 1 week of aging, see *Figure 3.36.h,i*.

A further destabilization of the systems obtained in the presence of the biosurfactants **37ab** and **38ab** was revealed after 1 month, clearly observing a huge decrease of the droplets number with the concomitant droplets aggregation into larger ones for **38ab**-based emulsion (*Figure 3.36.k*). On the other hand, the palmitoyl moiety of **37ab** seems to preserve the drops interlayer, thus resulting in a slightly better emulsion stabilization ability against sedimentation (*Figure 3.36.j*).



### 3 | Results and discussion

These different emulsifying capacities of **36ab**, **37ab** and **38ab** can be clarified by studying the fatty acid profile of the commercial sunflower oil used as continuous phase of the W/O emulsions. The percentage composition of each fatty acid residue was evaluated by GC/MS analysis carried out after base-catalyzed transmethylation of triglycerides, according to the protocol FIL-IDF 182:1999 (ISO 15884:2002 - IDF 182:2002, 2002), see **Table 3.7**.

*Table 3.7. Fatty acid profile of commercial sunflower oil by GC/MS analysis.*

<i>Fatty acid methyl ester</i>	<i>Chain carbon atoms: insaturation</i>	<i>Composition (%)</i>
Methyl Palmitate	C16:0	7
Methyl Linoleate	C18:2	61
Methyl Oleate	C18:1	29
Methyl Octadecenoate	C18:1	< 1
Methyl Stearate	C18:0	3
Methyl Eicosenoate	C20:1	< 0.5
Methyl Arachidate	C20:0	< 0.5
Methyl Behenate	C22:0	< 0.5

The poor stability of the W/O emulsion prepared with the lauroyl-based biosurfactant **36ab** is probably due to the presence in sunflower oil of lauric acid derivatives only in traces (Orsavova et al., 2015). Moreover, its shorter alkyl chain, with respect to the other sugar-based tensides, could limit its affinity with the oil phase, as further indicated by its intermediate HLB value of 7.8.

Using the same approach, the slightly higher emulsifying capacity of **37ab** with respect to **38ab** can be related to its higher affinity with the sunflower oil used because of the higher content of palmitoyl-based triglycerides, which is usually twice that of stearoyl-based ones (6 - 9 % and 3 - 5 % of C16:0 and C18:0 component, respectively, as further confirmed by literature data (Rabail et al., 2021)).

### 3.7 Alkyl 6-O-palmitoyl-D-glucosides

#### 3.7.1 Enzymatic esterification

Considering the promising surfactancy of the obtained molecules, the study went back to the synthesis of the other biosurfactants, aiming at producing a broad family of alkyl glucoside fatty acid esters to be tested for their physico-chemical properties.

Thus, all the other alkyl D-glucoside (**20ad-27ad**) previously reported were submitted to the same enzymatic esterification protocol, using Novozym<sup>®</sup> 435 as biocatalyst and palmitic acid (**6**) as acyl donor, which demonstrated higher affinity for the oil phase of the emulsion, moreover, is usually considered the most abundant saturated fatty acid in nature.

Reaction conditions were kept constant (the use of a glass oven B-585 Kugelrohr, working at 80 °C, under reduced pressure, for 8 h), as well as the purification procedure (extraction in EtOAc from 1 M NaOH and flash chromatography (*n*-hexane/EtOAc; 2:8)), thus obtaining couples of alkyl 6-O-palmitoyl-D-glucopyranosides (**37ab,39ab-45ab**) and D-glucofuranosides (**37cd,39cd-45cd**), see **Figure 3.37**.

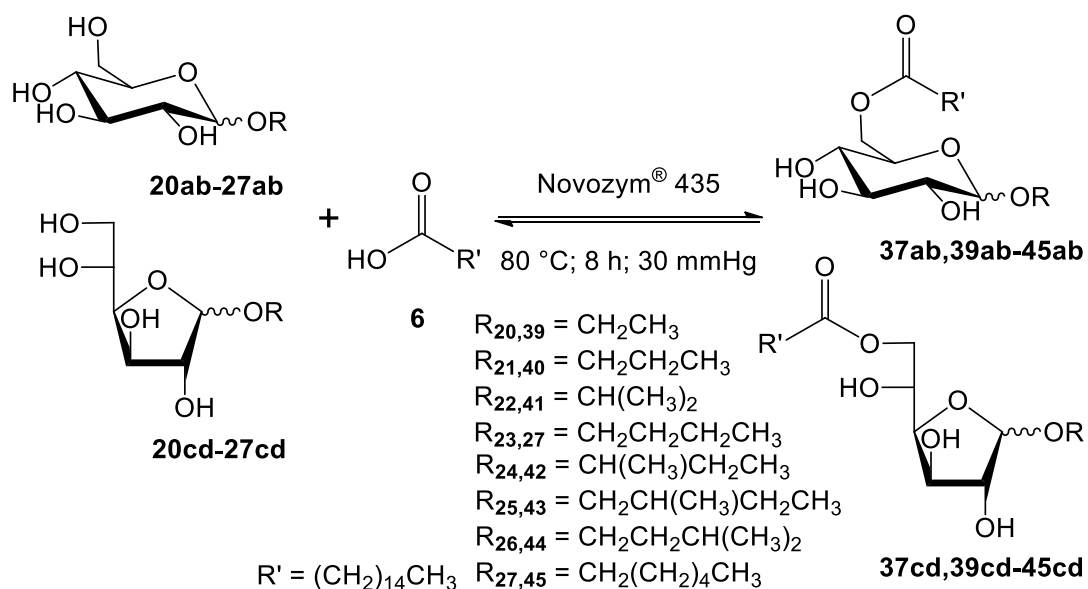


**Figure 3.37.** Enzymatic synthesis of alkyl 6-O-palmitoyl-D-glucosides (**37ad**, **39ad-45ad**).

Data reported in **Table 3.8** reveal that lower yields are obtained for shorter chained alkyl D-glucosides (36%, 36% and 23% for **39ad**, **40ad** and **41ad**, respectively). Probably, the aglycones (EtOH, 1-PrOH and 2-PrOH, respectively) did not sufficiently influence the sugar polarity, thus these glucosides resulted to be less soluble in the molten palmitic acid.

Moreover, it is possible to appreciate higher yields when linear aglycone-based D-glucosides are used as substrates (57% and 52% for 1-BuOH and 1-HexOH (**37ad**, **45ad**)) with respect to branched ones (49%, 41% and 47% for 2-BuOH, 2-Me-1-BuOH and 3-Me-1-BuOH (**42ad**, **43ad** and **44ad**)). This is probably related to the higher steric hinderance of branched glucosides which resulted in less favourable interactions in the catalytic site of the immobilized lipase.

Finally, considering the trend observed for the relative abundance of each isomer obtained from the Fisher glycosylation, it seems to be maintained after the esterification reaction, as confirmed by the estimation of the isomeric ratios by <sup>1</sup>H NMR analysis, carried out in DMSO-*d*<sub>6</sub>, as the ratio of the areas of the two anomeric proton signals in each isomeric couple.

**Table 3.8.** Yields and isomeric ratios of alkyl 6-O-palmitoyl-D-glucosides.

<b>Compound</b>	<b>R-OH</b>	<b>Yield ad (%)</b>	<b>Ratio ab/cd (%)</b>	<b>Isomeric ratio a/b/c/d (%)</b>
<b>39ad</b>	EtOH	36	28/72	16/12/35/37
<b>40ad</b>	1-PrOH	36	42/58	25/17/30/28
<b>41ad</b>	2-PrOH	23	30/70	17/13/43/27
<b>37ad</b>	1-BuOH	57	82/18	52/30/10/8
<b>42ad</b>	2-BuOH	49	73/27	42/31/19/8
<b>43ad</b>	2-Me-1-BuOH	41	66/34	34/32/18/16
<b>44ad</b>	3-Me-1-BuOH	47	85/15	53/32/9/6
<b>45ad</b>	1-HexOH	52	73/27	44/29/16/11

### 3.7.2 Physico-chemical characterization: pyranosides vs furanosides

In view of a potential industrial application of these biosurfactants as food and cosmetic emulsifiers, it is important to avoid expensive purification steps such as chromatographic separations during the production. However, to deeply investigate the surfactant properties of the isomeric mixtures obtained from the process, it is compulsory to study the contribute of the different isomers.

Thus, aiming at investigating possible differences in the physico-chemical properties according to the surfactant aglycone, all the synthesized alkyl 6-O-palmitoyl-D-glucopyranosides (**37ab,39ab-45ab**) and D-glucofuranosides (**37cd,39cd-45cd**) were submitted to solubility tests in water (Milli-Q) and in commercial sunflower oil. Moreover, the HLB of each isomeric mixture was calculated according to the Griffin method, see **Table 3.9**.

**Table 3.9.** Oil solubility and HLB of alkyl 6-O-palmitoyl-D-glucopyranosides (**37ab,39ab-45ab**) and D-glucofuranosides (**37cd,39cd-45cd**).

<b>Compound</b>	<b>ab solubility<sup>‡</sup> in sunflower oil</b>	<b>cd solubility<sup>‡</sup> in sunflower oil</b>	<b>HLB</b>
<b>39</b>	O	+	8.0
<b>40</b>	O	+	7.7
<b>41</b>	O	+	7.7
<b>37</b>	+	++	7.5
<b>42</b>	+	++	7.5
<b>43</b>	+	++	7.3
<b>44</b>	+	++	7.3
<b>45</b>	+	++	7.1

<sup>‡</sup> Legend: ++ very soluble; + soluble; O sparingly soluble.

All the tensides exhibited very low solubility in water, according to the calculated HLB values, all lower than 8.0, which indicate lipophilic or oil soluble surfactants. Indeed, all the compounds **37ad, 39ad-45ad** showed greater oil solubility, by increasing the number of carbon atom of the aglycone, corroborating the decreasing values of HLB obtained.

However, despite pyranosides and furanosides derivatives are constitutional isomers (sharing the same raw formula and HLB value), some differences were observed in their solubilization in sunflower oil. Furanosides-based derivatives (**cd**) seem to show higher affinity towards the oil phase with respect to pyranosides analogues (**ab**), corroborating their higher  $R_f$  value obtained through the TLC analysis (*n*-hexane/EtOAc; 2:8), all in the range 0.39-0.50, with respect to 0.26-0.34, for **cd** and **ab** compounds, respectively.

Then, the water/oil IFT reduction capability of the biosurfactants was measured (Lotierzo et al., 2016). All the alkyl 6-O-palmitoyl-D-glucopyranosides (**37ab**, **39ab-45ab**) and alkyl 6-O-palmitoyl-D-glucofuranosides (**37cd**, **39cd-45cd**) were dissolved in sunflower oil at the same concentration (3 mM).

**Table 3.10.** Oil / water IFT of alkyl 6-O-palmitoyl-D-glucopyranosides (**37ab,39ab-45ab**) and D-glucofuranosides (**37cd,39cd-45cd**), measured at 3 mM biosurfactants concentration. Data were reported as average values on three different replicates at room temperature.

<b>Compound</b>	<b>R-OH</b>	<b>IFT ab (mN m<sup>-1</sup>)</b>	<b>IFT cd (mN m<sup>-1</sup>)</b>
<b>39ad</b>	EtOH	2.0 ± 0.9	11.2 ± 0.4
<b>40ad</b>	1-PrOH	< 1	16.5 ± 0.1
<b>41ad</b>	2-PrOH	1.8 ± 0.1	14.9 ± 0.1
<b>37ad</b>	1-BuOH	4.4 ± 1.0	17.9 ± 0.1
<b>42ad</b>	2-BuOH	3.1 ± 0.3	17.8 ± 0.1
<b>43ad</b>	2-Me-1-BuOH	4.5 ± 0.8	18.9 ± 0.3
<b>44ad</b>	3-Me-1-BuOH	4.6 ± 0.8	18.4 ± 0.1
<b>45ad</b>	1-HexOH	8.1 ± 0.1	18.4 ± 0.1

**Table 3.10** reports strong differences in the interfacial proprieties, according to both the ring size and the aglycone of the selected compounds. All the pyranosides-based derivatives (**ab**) seem to induce a huge variation of the IFT, whose value passes from 26 mN m<sup>-1</sup>, in the absence of any tenside, down to 2.0-8.1 mN m<sup>-1</sup> values. On the contrary, furanoside-based ones (**cd**) provoke a much lower IFT reduction, ranging from 11.2 to 18.4 mN m<sup>-1</sup>.

Moreover, a decreasing trend of IFT reduction can be appreciated by increasing the number of carbon atoms of the aglycone from 2 to 6, both in the case of **ab** and **cd** molecules.

Generally speaking, the IFT reduction capacity of surfactant molecules is strictly related to their surface or interfacial activity, which should be considered a dynamic phenomenon of equilibrium between their adsorption and desorption (due to thermal motions) (Schramm, 2005).

The main driving forces for tensides to adsorb at fluid interfaces are the reduction of the interfacial free energy of the system, the surfactant concentration in the bulk and its hydrophobic interactions with the oil phase, together with other factors, *i.e.*, ionic strength, pH, salinity, and temperature (Belhaj et al., 2020; Eastoe & Dalton, 2000).

Within the IFT study, the biosurfactants concentration was maintained constant, thus, the less decreasing of the IFT related to the increasing number of carbon atom in the aglycone chain could be explained by considering the less intense hydrophobic interactions with the oil phase generated by the longer-chained surfactant molecules, *i.e.*, **45ad**. Their higher affinity towards the bulk of the oil phase, corroborated by the lower HLB calculated and their easier dissolution in oil, could result in a lower tensides adsorption at the interface, thus provoking an increase of the IFT.

Among all the alkyl 6-O-palmitoyl-D-glucosides tested (**37ad**, **39ad-45ad**), three compounds were selected to further investigate the reasons behind this extremely different interfacial behaviour. Taking into account that the pyranoside-based isomers of **40ad** resulted in the lowest IFT value, **37ad** was obtained with the highest yield (57%) and all the isomers of **45ad** showed the highest and worst IFT measure, thus their isomeric forms were submitted to preliminary computational studies.

Particularly, the MacroModel suite of Schrodinger computer software, based on OPLS2005 force field and, the GB/SA continuum solvation model for water was used. The conformational searches were carried out using the systematic pseudo-MonteCarlo procedure SPMC and the TNCC (Truncated Newton Conjugate

Gradient) algorithm for the energy minimization. Only conformers that differed from the global minimum by no more than 50 kJ mol<sup>-1</sup> were saved. Duplicate conformations, as defined by RMS comparison of all the heavy atoms, were discarded. Searches were considered complete when all low-energy conformers (within 1 kcal mol<sup>-1</sup>) were severally sampled.

All the most stable conformations of furanoside-based surfactants (**40cd**, **37cd**, **45cd**), individuated according to the calculation of the global energetic minimum of each system, resulted in a steric energy of around 45-60 kJ mol<sup>-1</sup> higher than those of pyranoside-based ones (**40ab**, **37ab**, **45ab**).

Higher energy values of the optimized conformations of **cd** molecules, due mainly to their higher torsional component induced by the 5-membered ring, are strictly related to their lower stability in an aqueous medium, with respect to **ab** analogues. Indeed, the geometrical arrangement of **cd** alkyl chains resulted to be more twisted, as they are wrapped on themselves, contrarily to those of **ab**, which are more elongated.

In the molecular mechanics force field studies, each surfactant molecule is assumed as isolated, however, in a real system, at the oil / water interface, several molecules must be considered, as well as their conformations and intermolecular interactions.

It is possible to suppose that the twisted conformation of furanoside-based tensides may result in a lower tendency to generate intermolecular interactions with other molecules, thus resulting in a less compact surfactant layer at the interface giving rise to lower IFT reduction capacity.

Further studies of molecular dynamic are compulsory to deepen the intermolecular interactions in this complex system. Preliminary results are reported in the **Section 3.7.4**, however additional investigations are still ongoing.

### 3.7.3 Physico-chemical characterization: pyranosides vs isomeric mixtures

The study proceeded by investigating the IFT reduction induced by the isomeric mixture of the three previously selected biosurfactants 1-propyl, 1-butyl and 1-hexyl 6-O-palmitoyl-D-glucosides (**40ad**, **37ad**, **45ad**). Their IFT values were assessed once again at 3 mM concentration, and then compared to those resulting from only pyranoside-based derivatives (**40ab**, **37ab**, **45ab**), see **Table 3.11**.

**Table 3.11.** Oil / water IFT of 1-propyl, 1-butyl and 1-hexyl 6-O-palmitoyl-D-glucopyranosides (**40ab**, **37ab**, **45ab**) and D-glucosides isomeric mixture (**40ad**, **37ad**, **45ad**), measured at 3 mM biosurfactants concentration and the pyranosides / furanosides isomeric ratio in **ad**. Data were reported as average values on three different replicates at room temperature.

Compound	R-OH	IFT ab (mN m <sup>-1</sup> )	IFT ad (mN m <sup>-1</sup> )	Ratio ab/cd in ad (%)
<b>40ad</b>	1-PrOH	< 1	8.2 ± 0.2	42/58
<b>37ad</b>	1-BuOH	4.4 ± 1.0	1.7 ± 0.9	82/18
<b>45ad</b>	1-HexOH	8.1 ± 0.1	3.5 ± 0.4	73/27

The previously observed trend in pyranoside-based surfactants (**ab**), which was strictly dependent on the number of carbon atoms of the alkyl chain of the aglycone, is completely different in the case of the isomeric mixtures (**ad**).

1-propyl 6-O-palmitoyl-D-glucopyranosides (**40ab**), which alone demonstrated the best IFT reduction capacity, resulted in a worse result when all the four isomers are present (**40ad**). On the contrary, 1-butyl and 1-hexyl 6-O-palmitoyl-D-glucopyranosides (**37ab**, **45ab**) showed improved interfacial behaviour, being able to reduce the IFT values of 61% and 57% when analysed in mixture (**37ad**, **45ad**).

These surprising results can be probably related to the different percentages of furanoside-based derivatives (**cd**) inside the mixtures (**ad**). Indeed, the highest IFT value was measured in the case of the 1-propyl-based mixture (**40ad**) whose relative ratio between pyranoside and furanoside is roughly 1:1. On the contrary, a synergistic effect, probably due to the presence of a small amount of **cd**-based derivatives (roughly 20% and 30%, respectively), can be appreciated for the other two 1-butyl and 1-hexyl-based mixtures (**37ad** and **45ad**). Indeed, the presence of



**cd** seems to induce an even further IFT reduction, with respect to those obtained in the presence of pyranosides-based components alone (**37ab**, **45ab**).

To corroborate these features, W/O emulsions were prepared with all the selected biosurfactants (**40ab**, **37ab**, **45ab**, **40ad**, **37ad**, **45ad**), using the already reported optimized conditions and the ultrasound-assisted emulsification method. Their stability within 72 h was then evaluated by means of turbidimetric measurements (**Figure 3.37**).

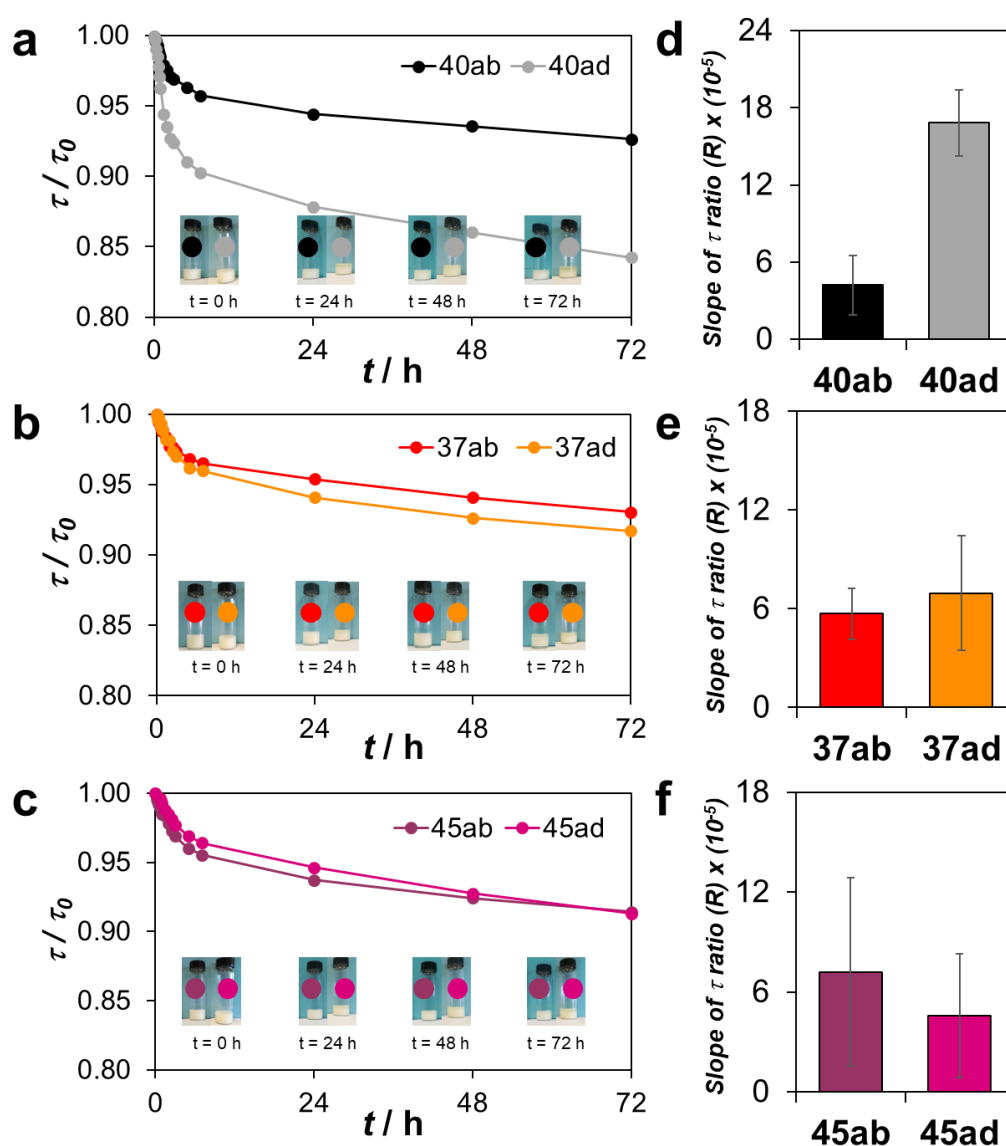


**Figure 3.37.** **a,b,c**) Normalized turbidity ( $\tau/\tau_0$ ) of W/O emulsions generated with 1-propyl, 1-butyl, 1-hexyl 6-O-palmitoyl-D-glucopyranosides (**40ab**, **37ab**, **45ab**) and 1-propyl, 1-butyl, 1-hexyl 6-O-palmitoyl-D-glucoside isomeric mixtures (**40ad**, **37ad**, **45ad**) at optimized surfactant concentration and phase volumes ( $c = 3.0$  mM and  $\phi_v = 0.14$ ) within 72 h. Insets: photos of the six samples at 0, 24, 48 and 72 h; **d,e,f**) slope of turbidity ratio ( $R$ ) values as a function of the adopted surfactant.

### 3 | Results and discussion

Both the normalized turbidity trend of W/O emulsions within time (**Figure 3.37.a,b,c**) and slope of the turbidity ratio (R) (**Figure 3.37.d,e,f**) corroborated the data obtained from the IFT study. All the generated emulsions resulted stable within 72 h, as indicated by the slight decrease of the obtained curves, as well as the low value of R calculated. The only exception is represented by the emulsion produced in the presence of 1-propyl 6-O-palmitoyl-D-glucoside isomeric mixture (**40ad**), which underwent faster destabilization, as confirmed by the higher R value estimated.

To further investigate the extent of the furanosides percentage influence, artificial mixtures (**ad<sub>artificial</sub>**) of the three selected compounds were created by varying the ratio of pyranosides and furanosides spontaneously obtained from the synthetic protocol (**ad<sub>real</sub>**). Then, IFT data were assessed in the same conditions and compared with previous results, see **Table 3.12**.

**Table 3.12.** Oil / water IFT of 1-propyl, 1-butyl and 1-hexyl 6-O-palmitoyl-D-glucosides isomeric mixture (**40ad,37ad,45ad**) real and artificial, measured at 3 mM biosurfactants concentration and the pyranosides / furanosides isomeric ratio in **ad**. Data were reported as average values on three different replicates at room temperature.

<b>Compound</b>	<b>R-OH</b>	<b>ab/cd in ad<sub>real</sub> (%)</b>	<b>IFT ad real (mN m<sup>-1</sup>)</b>	<b>ab/cd in ad<sub>artificial</sub> (%)</b>	<b>IFT ad artificial (mN m<sup>-1</sup>)</b>
<b>40ad</b>	1-PrOH	1/1	8.2 ± 0.2	8/2	< 1
<b>37ad</b>	1-BuOH	8/2	1.7 ± 0.9	1/1	5.5 ± 1.6
<b>45ad</b>	1-HexOH	7/3	3.5 ± 0.4	1/1	3.4 ± 0.6

These results highlight the strong influence related to the percentage of furanoside-based derivatives (**cd**) inside the mixture (**ad**). Isomeric ratios of  $\cong 1/1$  seem to induce lower IFT reduction, both in the case of **40ad<sub>real</sub>** and **37ad<sub>artificial</sub>**. On the contrary, when the ratio is shifted towards the pyranoside derivatives (8/2), no negative effect on the IFT can be observed. **45ad** represents an exception: the IFT value was maintained unchanged for both the tested ratio (7/3 and 1/1 for **ad<sub>real</sub>** and **ad<sub>artificial</sub>**). It is possible to suppose that the influence of the ring size on the IFT reduction capacity decreases at increasing aglycone chain length, probably because the contribute of intermolecular interactions becomes dominant.

### 3.7.4 Preliminary molecular dynamic simulations

To further investigate the interactions between the molecules of these biosurfactants, 1-butyl 6-*O*-palmitoyl-*D*-glucoside isomeric mixture and its isomeric components of pyranoside and furanosides (**37ad** and **37ab**, **37cd**) were selected as substrate models for preliminary molecular dynamic simulations, again performed with the MacroModel suite of Schrodinger computer software, the OPLS2005 force field and the GB/SA continuum solvation model for water.

They were carried out using the stochastic SD algorithm, with a time-step of 1 fs, the algorithm SHAKE on for C-H bonds and a coupling bath constant of 0.2 ps. Van der Waals and electrostatic cut-offs of 25 Å, together with a hydrogen bond cut-off of 15 Å, were used. All SD simulations were run at a constant temperature of 300 K.

All the simulations were performed on 10 molecules for a total run time of 50 ns, evaluating the variation of the distances between selected carbon atoms. Specifically, the distances were evaluated between the terminal carbon atoms of the two alkyl chains (C<sub>4</sub>–C<sub>16</sub>) and between the carbonyl carbon and the end carbon of the fatty alkyl “tail” of the surfactant molecules (C=O–C<sub>16</sub>), in order to evaluate the interactions between the two chains and the elongation of the palmitoyl residue. These distances were firstly calculated for the most stable conformation of each isomeric species obtained through computational studies, and then compared to those obtained from the dynamic simulations. The latter were performed on model systems, recreating the pyranoside and furanoside mixtures experimentally isolated with a defined isomeric ratio evaluated by NMR analysis. Thus, two molecular dynamic simulations were performed: one for the pyranosides mixture (**37ab**), constituted of 6 molecules of 1-butyl 6-*O*-palmitoyl- $\alpha$ -*D*-glucopyranoside (**37a**) and 4 of the  $\beta$ -analogue (**37b**); and the other related to the furanosides mixture (**37cd**), formed by 5 + 5 molecules of the two furanoside-based anomers (**37c** and **37d**).

The variation of these distances, passing from a single molecule to a series of 10, implies the tendency of the surfactant molecules to interact with each other. The

more the molecules tend to interact, the greater will be their final packing, as well as their tendency to generate a compact system able to stabilize the O/W interphase.

Specifically, in both the dynamic simulations, the C<sub>4</sub>–C<sub>16</sub> distances increased for all the isomers by 22%, 66%, 107% and 25% for **37a**, **37b**, **37c** and **37d**, respectively. Indeed, the butyl chain of all the isomers tend to move with respect to their starting configurations, aiming at interacting with other surfactant molecules.

However, the tendency of the molecules to create Van der Waals interactions is strongly dependent on the straightness of the surfactant “tails”. The  $\beta$ -pyranoside-based surfactant (**37b**) showed already a hairpin-like conformation, thus the variation of the C=O–C<sub>16</sub> distance resulted negligible, on the contrary, the tail of its  $\alpha$ -analogue (**37a**) tends to unravel, thus resulting in an increasing of the 45% of the C=O–C<sub>16</sub> distance. The more linear conformation assumed by pyranoside-based surfactant alkyl chains can favour intermolecular interactions, thus enhancing their packing capacity and resulting in a compact and almost spherical aggregate of molecules (**37ab**).

On the contrary, it is not possible to appreciate a similar variation of the C=O–C<sub>16</sub> distances in the case of both the  $\alpha$ - and the  $\beta$ -furanoside-based molecules (**37c** and **37d**). At the end of the molecular dynamic simulation of the furanosides mixture, each single isomeric molecule maintains a globular structure, thus reducing the possibility of generating intermolecular interactions. The system results to be less aggregated and some molecules seem separate from others during the simulation, thus indicating a less compact system, which difficultly can stabilize an interface.

Then, the system got complicated, recreating the real mixture obtained from the production process, thus a mixture (**37ad**) composed by 5 molecules of the  $\alpha$ -pyranoside-based derivative (**37a**), 3 of the  $\beta$ -pyranoside one (**37b**) and 1 + 1 of the two furanoside anomers (**37c** and **37d**).

This system (**37ad**) resulted in less aggregated, with respect to that obtained after the simulation of the pyranosides mixture (**37ab**), however it remained compact. A small amount of furanoside-based derivatives, acting as co-surfactant, seems to

favour the generation of a system with higher degree of disorder, which could potentially induce a stronger contribution to the entropy of the overall system.

Indeed, generally, the IFT reduction is strongly driven by the degree of disorder of the interfacial film, which is related to the interfacial entropic contributions of water / oil / surfactant molecules. At the interface, in absence of a surfactant, oil and water molecules partially lose some degrees of freedom due to the instauration between the two phases of parallel alignments induced by strong short-range van der Waals interactions. On the contrary, oily molecules are pushed away from the water surface by the adsorption of a surfactant, making the three-dimensional structure of the water more disordered, by increasing their rotational and translational modes (Bui et al., 2021).

Thus, aiming at achieving a situation closer to the reality, computational studies carried out in the presence of triglycerides are still ongoing.

## 3.8 Alkyl 6-O-palmitoyl-D-galactosides

### 3.8.1 Fischer glycosylation

During the last years, the demand for manufacturing monosaccharides from a cheap and abundant source, such as cheese whey permeate (CWP), is strongly increasing (Vera et al., 2022). As already stated in **Section 3.3.1**, D-galactose can be directly isolated from CWP, following a precise purification procedure recently patented (Yan et al., 2016).

Since the valorization of CWP is the main goal of the project, the study focused also on the use of galactose to produce alkyl glycoside fatty acid esters (AGFAEs), which has been scarcely reported to date.

Therefore, D-galactose (**46**) was submitted to the preparative scale Fischer glycosylation (Whistler & Wolfrom, 1963) with naturally occurring alcohols (**28-35**), in the presence of the strongly acidic cation exchange resin Amberlyst® 15. Reaction conditions similar to those used for the synthesis of alkyl D-glucosides were selected, by varying temperature and time according to the alcohol used. Supported catalyst filtration, solvent removal and flash column chromatography (DCM/MeOH 8.8:1.2) afforded alkyl D-galactosides (**47ad-54ad**), see **Figure 3.38** and **Table 3.13**.

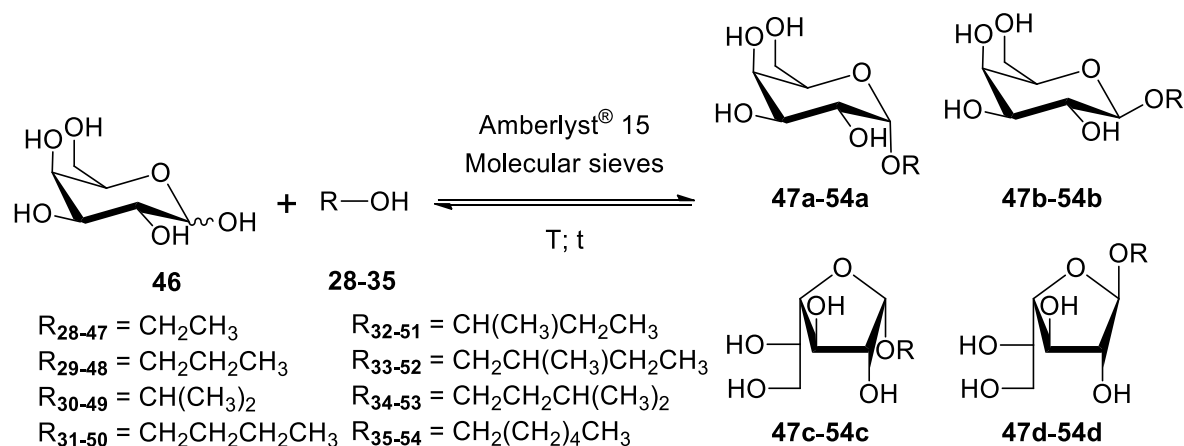


**Figure 3.38.** Synthesis of alkyl D-galactosides (**47ad-54ad**).

*Table 3.13. Experimental conditions for the synthesis of alkyl D-galactosides (47ad-54ad).*

<b>Compound</b>	<b>R-OH</b>	<b>Temperature (°C)</b>	<b>Time (h)</b>	<b>Yield (%)</b>
<b>47ad</b>	EtOH ( <b>28</b> )	90	4	73
<b>48ad</b>	1-PrOH ( <b>29</b> )	100	3	78
<b>49ad</b>	2-PrOH ( <b>30</b> )	90	6	36
<b>50ad</b>	1-BuOH ( <b>31</b> )	120	2.5	81
<b>51ad</b>	2-BuOH ( <b>32</b> )	120	6	88
<b>52ad</b>	2-Me-1-BuOH ( <b>33</b> )	120	1.5	95
<b>53ad</b>	3-Me-1-BuOH ( <b>34</b> )	120	2	88
<b>54ad</b>	1-HexOH ( <b>35</b> )	120	1.5	32

As in the case of Glc, the temperature was kept as high as possible, depending on the alcohol boiling point, up to 120 °C, to increase the Gal solubility in the selected naturally occurring alcohols. Moreover, reaction times were monitored trying to avoid the generation of by-products due to sugar dehydration side-reactions.

In general, the yields were in the same order of magnitude as those obtained with glucose, except for the reaction carried out with 2-PrOH (**30**) and 1-HexOH (**35**), resulting in 36% and 32% yields for **49ad** and **54ad**, respectively. Steric hinderance effects, in the case of **30**, and very low sugar solubility in **35** can explain the obtained results.

Conversely, good yields (73-93%) were afforded for all the other alkyl D-galactosides (**47ad,48ad,50ad-53ad**).

## 3.8.2 MS and NMR characterization

The alkyl D-galactosides were obtained as isomeric mixtures of four structural isomers:  $\alpha$ -/ $\beta$ -pyranosides (**a/b**) and  $\alpha$ -/ $\beta$ -furanosides (**c/d**). All the isomeric mixtures (**47ad-54ad**) were characterized by ESI-MS and NMR analysis. However, some  $^1\text{H}$  NMR peaks were not completely resolved because of the instrument resolution and signals overlapping. Thus, isomeric ratios were estimated by  $^1\text{H}$  NMR analysis, carried out both in  $\text{D}_2\text{O}$  and in  $\text{DMSO-}d_6$ , as the ratio of the areas of anomeric proton signals of each isomer present in the reaction mixture. Specifically, NMR anomeric proton signals were identified by comparison with data reported in the literature (Cinget & Schmidt, 1993; Chioconi et al., 1996) and  $\text{DMSO-}d_6$  was used to resolve the anomeric proton signals related to the  $\alpha$ -/ $\beta$ -furanosides (**c/d**), which are overlapped in the spectrum carried out in  $\text{D}_2\text{O}$ , see **Figure 3.39** as an example.

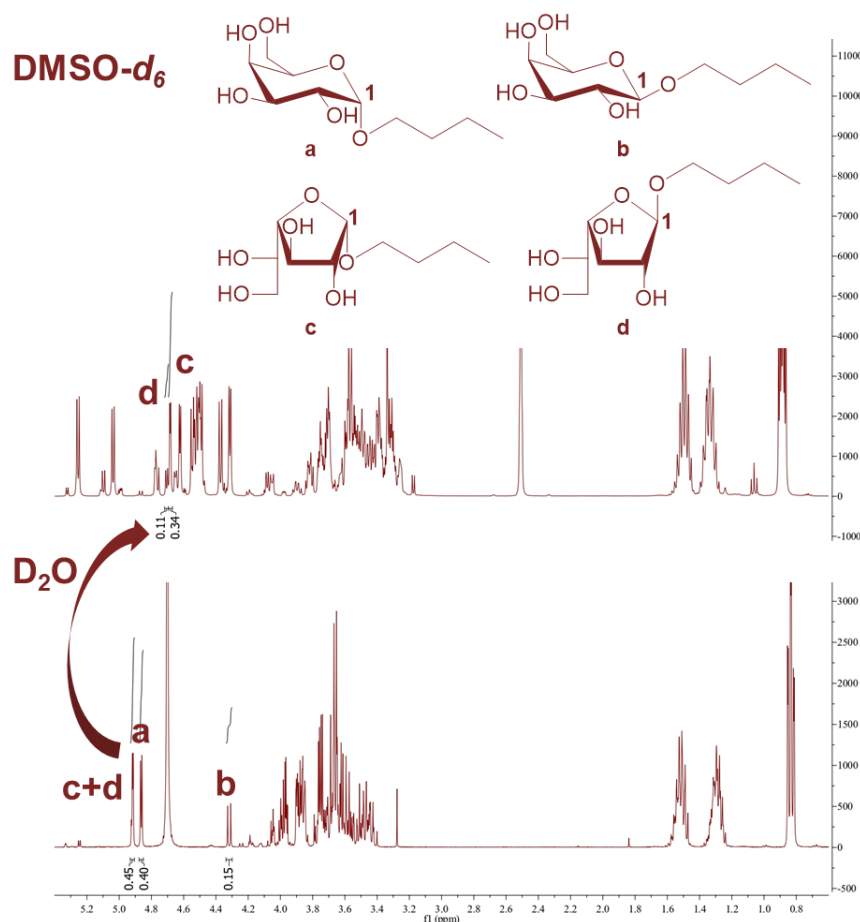


**Figure 3.39.**  $^1\text{H}$  NMR (400 MHz) spectrum of 1-butyl D-galactoside isomeric mixture (**50ad**) recorded both in  $\text{D}_2\text{O}$  and  $\text{DMSO-}d_6$  with highlighted integrals of the anomeric proton signals.



As reported in the **Section 3.5.3**, the ratio of the four glycosidic forms is extremely influenced by the temperature, the catalyst, the chain length of the alcohol and the type of the sugar (Collins & Ferrier, 1995).

Obtained yields resemble those obtained for alkyl D-glucoside (**Table 3.6**): high amount of furanoside derivatives is produced with short chained alcohols (*i.e.*, EtOH, 1-PrOH and 2-PrOH). However, with longer chained alcohols (*i.e.*, 1-BuOH, 3-Me-1-BuOH, 2-Me-1-BuOH and 1-HexOH), a plateau of the relative ratio between the two structural isomeric forms of about 1:1 is reached, see **Table 3.14**.

**Table 3.14.** Isomeric ratio of the synthesized of alkyl D-galactosides (**47ad-54ad**).

<b>Compound</b>	<b>R-OH</b>	<b>Isomeric ratio a/b/c/d (%)</b>	
<b>47ad</b>	EtOH ( <b>28</b> )	13/6/31/50	
<b>48ad</b>	1-PrOH ( <b>29</b> )	25/10/16/49	
<b>49ad</b>	2-PrOH ( <b>30</b> )	24/12/21/43	
<b>50ad</b>	1-BuOH ( <b>31</b> )	40/15/34/11	
<b>51ad</b>	2-BuOH ( <b>32</b> )	36/12/16/36	
<b>52ad</b>	2-Me-1-BuOH ( <b>33</b> )	29/12/17/42	
<b>53ad</b>	3-Me-1-BuOH ( <b>34</b> )	38/15/11/36	
<b>54ad</b>	1-HexOH ( <b>35</b> )	31/13/14/42	

Significant statements can be drawn also by the comparison of the relative isomeric ratios obtained from the Fischer glycosylation of galactose and glucose.

The higher amount of D-galactofuranosides derivatives obtained independently on the chain length of the alcohol, with respect to those of D-glucofuranosides, can be related to their higher thermodynamic stability. Indeed, D-galactofuranosides have the vicinal *trans*-relationship for the C-2, C-3 and C-4 groups, which induce stabilization effects, thus resulting in higher amount of these glycosidic modifications. Contrarily, D-glucofuranosides possess an unfavourable *cis*-interaction between the substituents at C-3 and C-4 and are consequently relatively unstable.

Furthermore, the lower amount of D-galactopyranosides is also related to the axial group at C-4, when the molecules adopt the  ${}^4C_1$  chair conformation, which induces destabilization effects. On the contrary, glucopyranosides are extremely favoured because their  ${}^4C_1$  chair conformation allocates all the ring substituents (C-2–C-5) in equatorial position.

Finally, in both cases, a preference of the  $\alpha$ -anomer due to the anomeric effect can be easily appreciated (Collins & Ferrier, 1995).

## 3.8.3 Enzymatic esterification

In order to produce biosurfactants, all the synthesized alkyl D-galactosides (**47ad-54ad**) were submitted to the already reported enzymatic esterification using palmitic acid (**6**) as acyl donor and Novozym<sup>®</sup> 435 as biocatalyst. Reaction conditions (the use of a glass oven B-585 Kugelrohr, working at 80 °C, under reduced pressure, for 8 h), as well as the purification procedure were carried out in the same way (extraction in EtOAc from 1 M NaOH and flash chromatography (*n*-hexane/EtOAc; 2:8)), thus resulting in couples of alkyl 6-O-palmitoyl-D-galactopyranosides (**55ab-62ab**) and D-galactofuranosides (**55cd-62cd**), see **Figure 3.40** and **Table 3.15**.

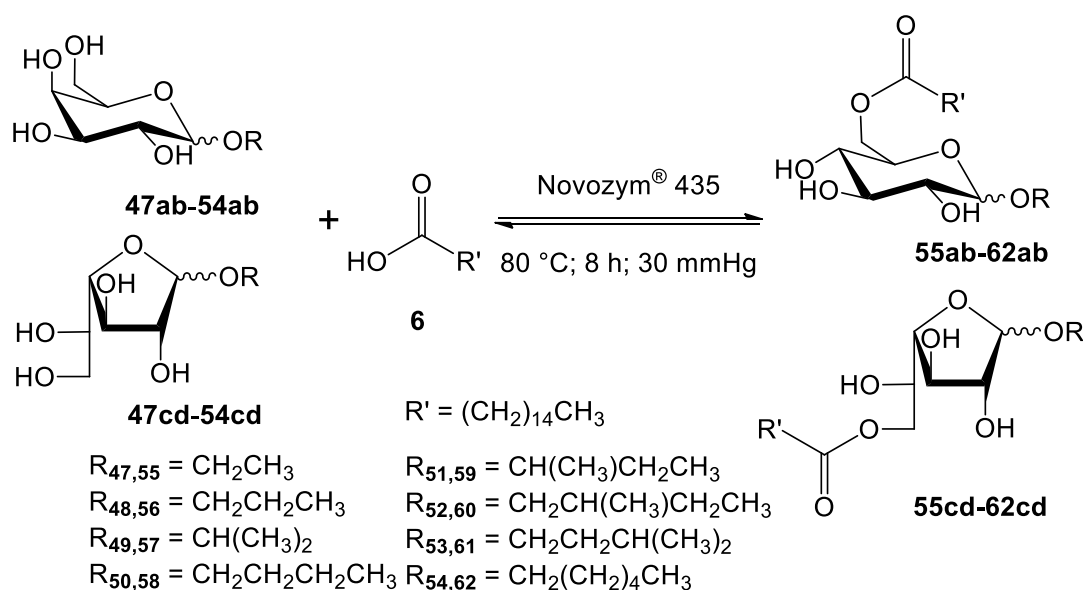


**Figure 3.40.** Enzymatic synthesis of alkyl 6-O-palmitoyl-D-galactosides (**55ad-62ad**).

**Table 3.15.** Yields and isomeric ratios of alkyl 6-O-palmitoyl-D-galactosides.

Compound	R-OH	Yield ad (%)	Ratio ab/cd (%)	Isomeric ratio a/b/c/d (%)
<b>55ad</b>	EtOH	35	20/80	15/5/32/48
<b>56ad</b>	1-PrOH	29	31/69	29/2/30/39
<b>57ad</b>	2-PrOH	32	16/84	9/7/34/50
<b>58ad</b>	1-BuOH	35	60/40	56/4/8/32
<b>59ad</b>	2-BuOH	35	41/59	40/1/27/32
<b>60ad</b>	2-Me-1-BuOH	10	40/60	34/6/5/55
<b>61ad</b>	3-Me-1-BuOH	30	53/47	44/9/18/29
<b>62ad</b>	1-HexOH	34	47/53	41/6/15/38

Examination of the **Table 3.15** reveals comparable yields (all around 35%) for all the synthesized alkyl galactoside fatty acid esters independently on the aglycone of the sugar moiety with the sole exception of **60ad**, which was obtained with a poor yield (10%). 2-Me-1-BuOH is a bulky branched aglycone, thus, probably, **52ad** could not properly fit into the active site of the enzyme due to steric hinderance.

Moreover, comparing these data with the ones previously obtained with glucose as sugar moiety (**Table 3.8**), it is possible to observe that the overall yields of galactose-based derivatives resulted to be lower. These data can be related to the only difference in the chemical structure between the two families of biosurfactants: they are epimers in the C-4 position of the sugars. Probably the axially oriented hydroxyl group OH(4) of galactose-based molecules induces less favourable interactions with the active site of the immobilized lipase with respect to those of an OH(4) equatorially oriented, as in the case of glucose-based analogues, thus resulting in lower yields.

Finally, considering the relative abundance of each isomer obtained, it seems that  $\beta$ -D-galactopyranosides derivatives resulted in decreased amount, with respect to the relative percentages obtained from the Fischer glycosylation. This result can be also attributed to the unfavourable interactions of the  $\beta$ -D-galactopyranosides with the enzymatic active site.

### 3.8.4 Physico-chemical characterization: D-galactosides vs D-glucosides

Among all the synthesized biosurfactants, the study focused on the investigation of the surfactant features of 1-butyl 6-O-palmitoyl-D-galactosides (**58ad**) to be compared with those of 1-butyl 6-O-palmitoyl-D-glucosides (**37ad**), having selected them as substrate models for the more complex mixture obtained from cheese whey permeate.

Both these alkyl glycoside fatty acid esters (AGFAEs) represent mixtures of interest to be deeply investigated for their emulsifying properties because they were obtained in the highest yields, with respect to the other biosurfactants synthesized. Moreover, their aglycone is considered a green and recommended solvent (Prat et al., 2014), thus obeying to environmental credentials.

Despite the use of a mixture of surfactants is strongly recommended in industrial realities, the identification of the contribute of each isomer to the final surfactancy is compulsory. Therefore, considering that the two families of AGFAEs have the same HLB (7.5) and showed similar behaviours in terms of solubility in oil, the study focused on the interfacial tension (IFT) analysis.

IFT reduction studies were carried out on a Gibertini tensiometer, according to the du Noüy ring method, dissolving the selected biosurfactants (1-butyl 6-O-palmitoyl-D-galactopyranosides (**58ab**) and 1-butyl 6-O-palmitoyl-D-galactofuranosides (**58cd**)), their isomeric mixture (1-butyl 6-O-palmitoyl-D-galactosides (**58ad**)) and their glucoside-based analogues (pyranosides, **37ab**, furanosides, **37cd**, and the isomeric mixture, **37ad**), in sunflower oil (3 mM), see **Figure 3.41** and **Figure 3.42**.

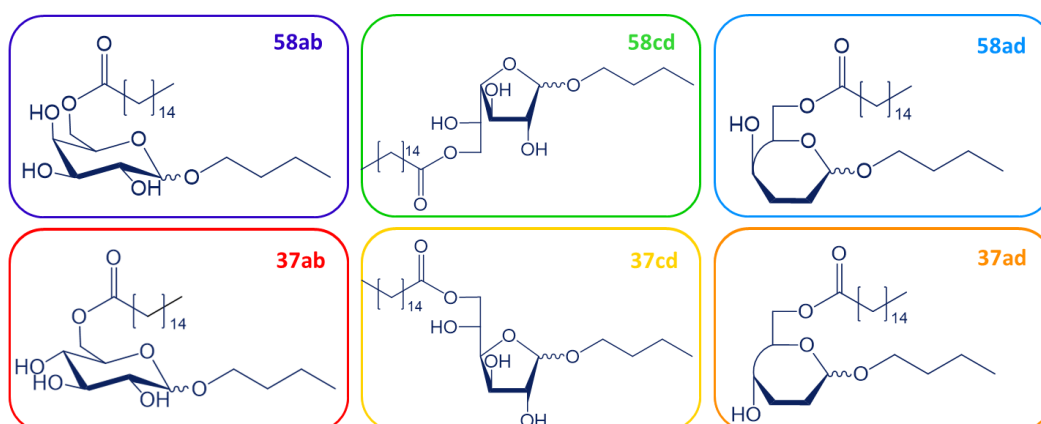


**Figure 3.41.** AGFAEs selected for the IFT study.

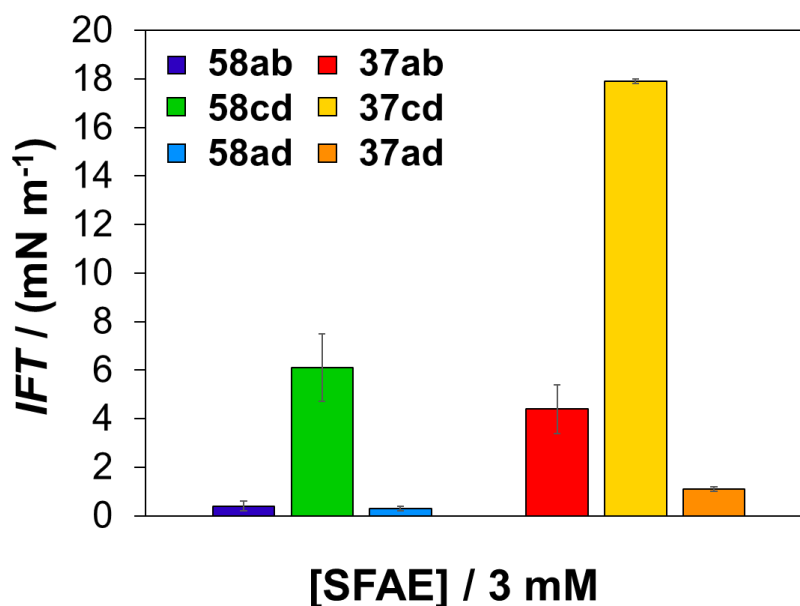


**Figure 3.42.** Comparison of IFT reduction capacity between 1-butyl 6-O-palmitoyl-D-galactopyranosides (**58ab**), D-galactofuranosides (**58cd**), their isomeric mixture (**58ad**) and their glucoside-based analogues (pyranosides, **37ab**, furanosides, **37cd**, and the isomeric mixture, **37ad**). Data were reported as average values on three different replicates at room temperature.

**Figure 3.42** reveals the different ability in reducing the IFT according to the ring size of the tested biosurfactants. Both the pyranoside-based derivatives (**58ab** and **37ab**) at 3 mM concentration led to low IFT values (4.4 and 0.4 mN m<sup>-1</sup>, respectively), on the contrary, furanoside-based ones (**58cd** and **37cd**) cannot induce such variation. This result may be due to a better surfactant chain orientation in the case of **58ab** and **37ab**, which favours their packing capacity at the interface, thus reducing the IFT significantly. Indeed, in **Section 3.7.4**, preliminary molecular dynamic simulation studies corroborated the formation of a more aggregated surfactants system in the case of glucopyranoside-based surfactants, with respect to that of glucofuranosides analogues.

It is also possible to appreciate that both the mixture of the four isomers (**58ad** and **37ad**) generate a similar or even higher IFT reduction. The presence of different types of surfactant molecules (**58ad** is composed of **58ab** and **58cd** in a relative ratio of 6:4; instead **37ad** of **37ab/37cd** in ratio 8/2) seems to preserve the interfacial properties of the system, on the contrary, the presence of a small amount of a co-tenside could better cover the interface layer, generating a denser tenside film, further reducing the IFT.

Moreover, all the galactoside-based surfactants (**58**) seem to lead to extremely low values of IFT, if compared to their glucoside-based analogues (**37**). This result could be explained by looking into the only difference in the chemical structure between the two surfactants: **58** and **37** family are epimers in C-4 position. Sugars with axial OH(4) group, such as galactose, match the three-dimensional water structure much worse than sugars with equatorially-oriented OH(4), as glucose (Penkov, 2021). The mismatch, see **Figure 3.43**, causes a distortion of the water structure in the primary hydration shell, which is also transmitted to the more distant layers, inducing a more disordered structure in the water configuration and, consequently, the increase in the total entropy of the system, favouring an extremely lowering ability of the IFT (Bui et al., 2021).

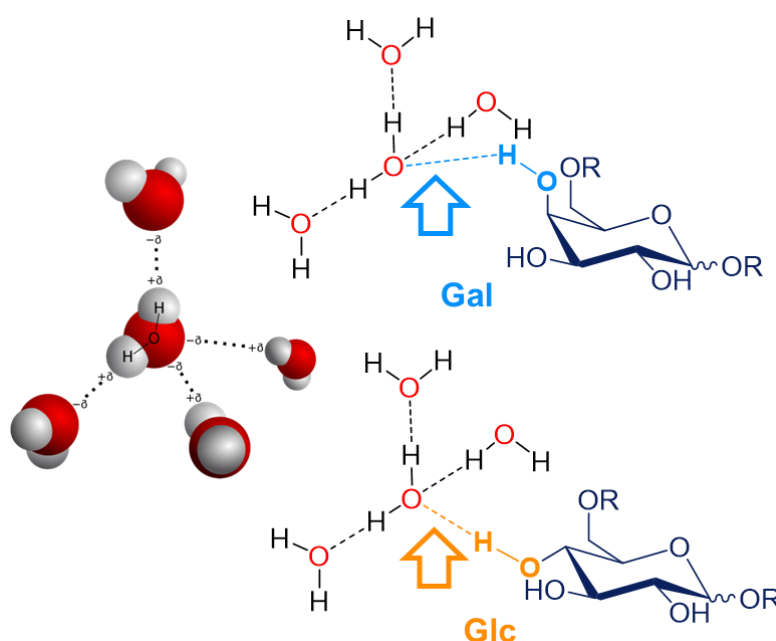


**Figure 3.43.** Comparison of galactoside- (**58**) and glucoside-based surfactants (**37**) matching with the 3D structure of water.

### 3.8.5 Emulsifying properties and stability over time

However, the previously obtained results can be only partially translated in the case of more complex and dynamic systems, as emulsions. W/O emulsions of the three selected biosurfactants (1-butyl 6-O-palmitoyl-D-galactopyranosides (**58ab**), D-galactofuranosides (**58cd**) and the isomeric mixture (**58ad**)) were prepared under the optimized conditions and using the ultrasound-assisted technique. Their stability over time was then assessed by turbidimetric measurements, see **Figure 3.44**.

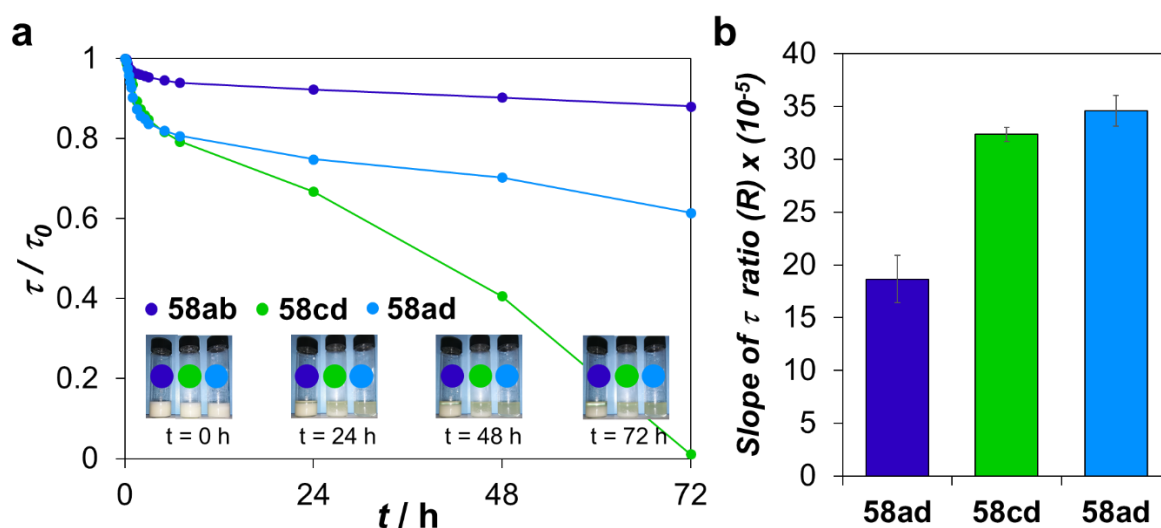


**Figure 3.44.** a) Normalized turbidity ( $\tau / \tau_0$ ) of W/O emulsions generated with 1-butyl 6-O-palmitoyl-D-galactopyranosides (**58ab**), D-galactofuranosides (**58cd**) and their isomeric mixture (**58ad**), at optimized surfactant concentration and phase volumes ( $c = 3.0$  mM and  $\phi_v = 0.14$ ) within 72 h. Insets: photos of the three samples at 0, 24, 48 and 72 h; b) slope of turbidity ratio ( $R$ ) values as a function of the adopted surfactant (**58ab**, **58cd**, **58ad**).

As expected from the previous IFT data, the W/O emulsion prepared with the galactofuranoside-based surfactant (**58cd**) resulted to be the least stable one. A sharp decrease in the normalized turbidity, as well as the emulsion sedimentation can be appreciated in the **Graph 3.8.a** and in its insets. On the contrary, the emulsion generated with the pyranoside-based analogues (**58ab**) showed relatively good stability within 72 h, as corroborated by the lower slope of turbidity ratio ( $R$ ) calculated, see **Graph 3.8.b**.

However, the isomeric mixture (**58ad**), which showed the best IFT reduction ability, produced a partially stable W/O emulsion, which resulted in a fast destabilization within the first hour of the emulsion generation, as highlighted by the high  $R$



obtained. This could be probably explained by focusing on the isomeric ratio between pyranoside (**ab**) and furanoside-based (**cd**) derivatives contained in the mixture. The presence of the 40% of the **cd** molecules could partially hinder the **ab** surfactant capacity, thus favouring emulsion breaking processes.

**58ad** could lead to a less compact surfactant system probably due to a less favourable molecules' chain orientation, which are not able to form proper intermolecular interactions. However, these hypotheses will be confirmed by molecular dynamic simulation analysis, which are still ongoing.

### 3.9 Preliminary study on the valorization of cheese whey permeate

#### 3.9.1 Enzymatic hydrolysis of cheese whey permeate

Finally, on the basis of the obtained data, the study went back to the main goal of the project, namely the valorization of lactose found in cheese whey permeate (CWP). The use of lactose as tenside polar-head was previously ruled out (**Section 3.2.2**) since reaction conditions for the synthesis of lactose-based biosurfactants were not sustainable, moreover, they resulted in poor surfactancy.

Thus, considering the promising synthetic pathways designed and the surfactant features demonstrated by the biosurfactants produced both with glucose and galactose as sugar polar head, the research focused on the enzymatic hydrolysis of CWP, to afford lactose monosaccharides.

Cheese whey permeate represents the main waste stream of the dairy industry, containing high concentration of lactose (around 50 g L<sup>-1</sup>) (Prazeres et al., 2012). It is generated as a by-product of the cheese whey ultrafiltration, used to recover valuable milk proteins, thus resulting in a very low protein content in CWP (N%: 1.12%). Such small protein residue, together with the ashes naturally contained in CWP, contribute to its slightly acid pH of 6.0, which is a key parameter in enzymatic reactions.

Indeed, D-lactose (**1**) of CWP, provided from Latteria Soresina, was enzymatically hydrolyzed with the food-grade commercially available  $\beta$ -galactosidase Saphera<sup>®</sup> 2600 L. The reaction was carried out at optimum enzyme/substrate ratio, pH and temperature (2.4% w/w, pH 6.0 and 50 °C, respectively), according to the manufacturer datasheet (Novozymes, 2023), see **Figure 3.45.a**.

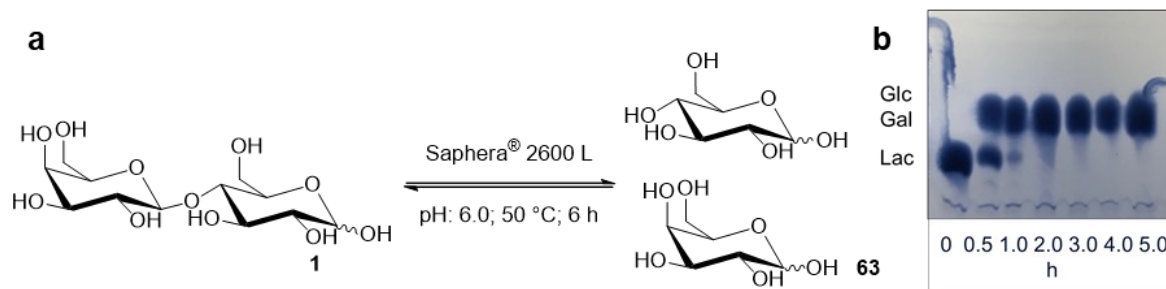


**Figure 3.45.** *a*) Enzymatic hydrolysis of D-lactose (**1**) found in cheese whey permeate; *b*) Reaction monitoring by TLC ( $\text{CH}_3\text{CN}/\text{H}_2\text{O}$ ; 8:2).

The reaction was monitored by TLC ( $\text{CH}_3\text{CN}/\text{H}_2\text{O}$ ; 8:2), see **Figure 3.45.b** and it is possible to appreciate the complete disappearance of the spot associated to D-lactose within the first 5.0 h of hydrolysis. Thus, after 6 h, the enzyme was inactivated by heat treatment at 85 °C for 15 min. Then, the reaction mixture was filtered to remove the ash naturally contained in the cheese whey permeate and freeze-dried to obtain a mixture of D-glucose / D-galactose (**63**).

Comparison of  $^1\text{H}$  NMR spectra carried out in  $\text{D}_2\text{O}$  of Lac, Glc, Gal and the obtained mixture **63** corroborated the complete hydrolysis of lactose into its monosaccharide components and the presence of the two sugars in a 1:1 ratio, see **Figure 3.46**.

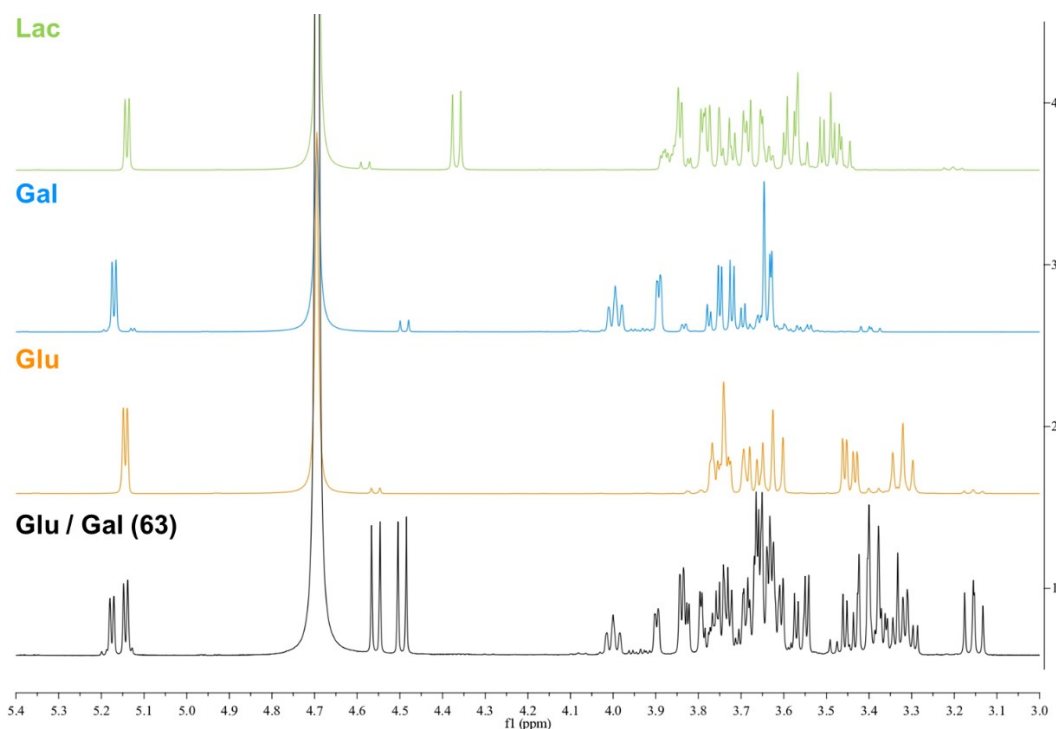


**Figure 3.46.** Comparison of  $^1\text{H}$  NMR spectra carried out in  $\text{D}_2\text{O}$  of Lac, Glc, Gal and the obtained mixture of Glc/Gal **63**.

### 3.9.2 Fischer glycosylation

Aiming at producing biosurfactants to valorize cheese whey permeate, a preliminary study focused on the application of the designed Fischer glycosylation strategy (see **Section 3.5.1**) was performed on the mixture of Glc/Gal (**63**) derived from the enzymatic hydrolysis of CWP D-lactose (**1**).

Thus, the obtained sugar mixture **63** was submitted the deeply investigated preparative scale Fischer glycosylation with dry *n*-butanol (**31**), in the presence of the strongly acidic cation exchange resin Amberlyst® 15 and molecular sieves, see **Figure 3.47**.

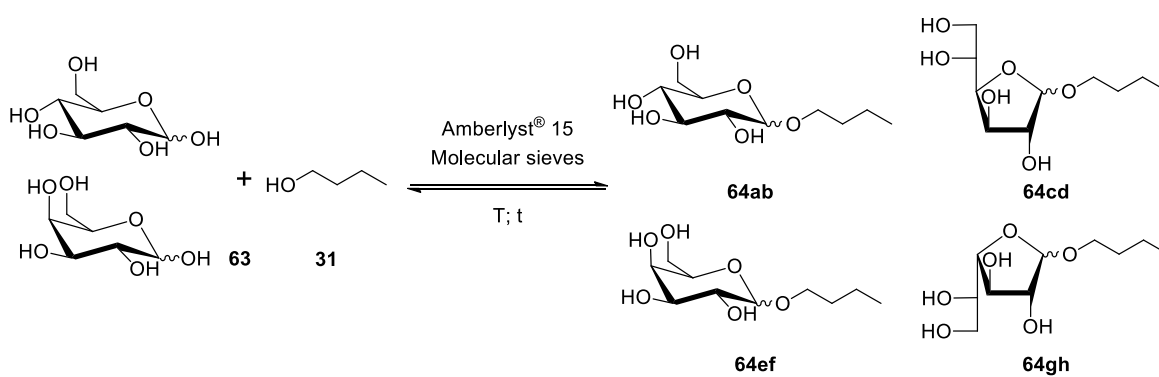


**Figure 3.47.** Synthesis of 1-butyl D-glycosides isomeric mixture (**64ah**).

However, the production of 1-butyl D-glycosides isomeric mixture (**64ah**) was not straightforward, as in the case of purified sugars (see **Sections 3.5.2** and **3.8.1**). The mixture of Glc/Gal **63** obtained from the hydrolysis of CWP still contained protein and ashes traces, which seemed to negatively affect the Fischer glycosylation, by inducing side-reactions. Any preliminary attempt in removing these impurities (*i.e.*, ion exchange column chromatography and filtration on Whatman filters) resulted to be unsuccessful. Moreover, product **63** was extremely moisture sensitive, further complicating its handling.

Thus, few attempts were performed on the obtained sugar mixture **63**, by varying reaction temperature and time, aiming at reducing side reactions. However, despite an improvement in reaction yield was observed by reducing the reaction temperature (from 120 to 80 °C) and increasing the time (from 3 to 24 h), the reaction yields resulted to be not reproducible (ranging from 15-34%), probably due to the non-homogeneous condition of the starting material, see **Table 3.16**.

### 3 | Results and discussion

**Table 3.16.** Experimental conditions for the synthesis of 1-butyl D-glycoside isomeric mixture (**64ah**).

Attempt	Temperature (°C)	Time (h)	Yield (%)
64.01	120	3	8
64.02	50	6.5	9
64.03			34
64.04	80	24	15
64.05			22
64.06			24

On the contrary, isomeric ratios of 1-butyl D-glycoside isomeric mixture (**64ah**) obtained in the same improved reaction conditions, resulted to be similar, see **Figure 3.48** as an example. They were estimated by  $^1\text{H}$  NMR analysis, carried out in  $\text{D}_2\text{O}$ , as the ratio of the areas of anomeric proton signals of each isomer present in the reaction mixture. Anomeric proton signals were identified by comparison with previously synthesized products.

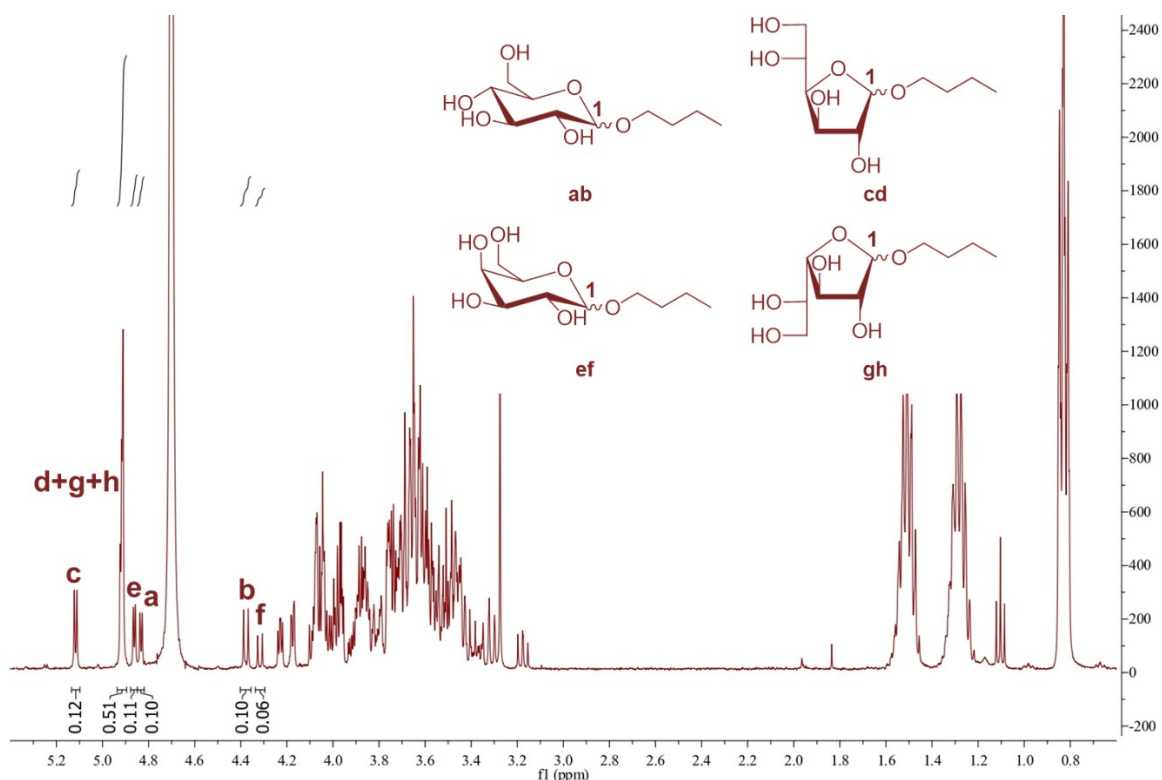


**Figure 3.48.**  $^1\text{H}$  NMR spectrum of 1-butyl D-glycosides isomeric mixture (**64ah**) carried out in  $\text{D}_2\text{O}$ .

Despite the overlapping of some signals (related to **d**, **g** and **h** isomers), examination of the  $^1\text{H}$  NMR spectrum reveals higher amount of furanoside derivatives, both for Glc and Gal (relative ratio **abef/cdgh**: 37/63). This result can be probably related to the mechanism of the Fischer glycosylation, see **Section 3.5.3**, which favours the formation of furanosides in milder reaction conditions (Mowery, 1955). However, interactions of the non-purified sugars mixture **63** with the catalyst cannot be excluded, considering the huge difference in isomeric ratios between pyranoside and furanoside species produced and those obtained from purified sugars.

Therefore, despite the investigation of optimized reaction conditions is compulsory, the study postponed it, focusing instead on the subsequent enzymatic esterification and on the evaluation of the surfactancy of the product.

### 3.9.3 Solvent-free enzymatic esterification

The already reported solvent-free lipase-mediated esterification was carried out on the synthesized 1-butyl D-glycosides isomeric mixture (**64ah**), using palmitic acid (**6**) as acyl donor and Novozym<sup>®</sup> 435 as biocatalyst, see **Figure 3.49**.

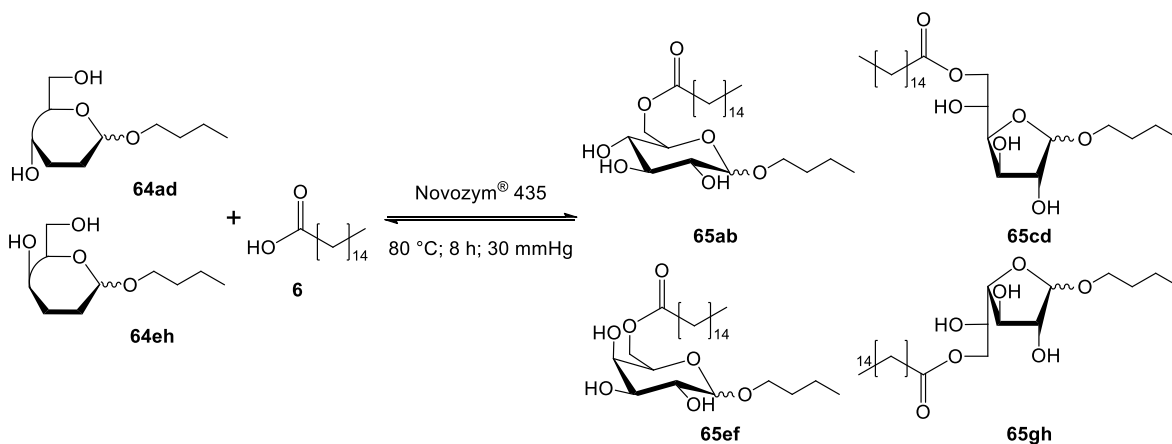


**Figure 3.49.** Synthesis of 1-butyl 6-O-palmitoyl-D-glycosides isomeric mixture (**65ah**).

Preliminary attempts resulted in poor yields of 1-butyl 6-O-palmitoyl-D-glycosides (**65ah**, 15%). Despite reaction conditions were maintained equal to those of purified sugars (see **Sections 3.7.1** and **3.8.3**), difficulties were encountered during purification procedures (extraction in EtOAc from 1 M NaOH solution and flash column chromatography), probably due to the more complex reaction mixture.

Regarding the isomeric ratio between pyranosides and furanosides, calculated by <sup>1</sup>H NMR analysis, carried out DMSO-*d*<sub>6</sub> + D<sub>2</sub>O (1 drop), as the ratio of the areas of anomeric proton signals, it was roughly maintained from the previous Fischer glycosylation (isomeric ratio **abef/cdgh**: 32/68). However, examination of the <sup>1</sup>H spectrum, see **Figure 3.50**, reveals only traces of the proton signals related to the D-galactopyranosides (**e** and **f**), indicating less favourable interactions of those species with the active site of the lipase, probably due to the axially oriented OH(4) of galactose-based molecules.

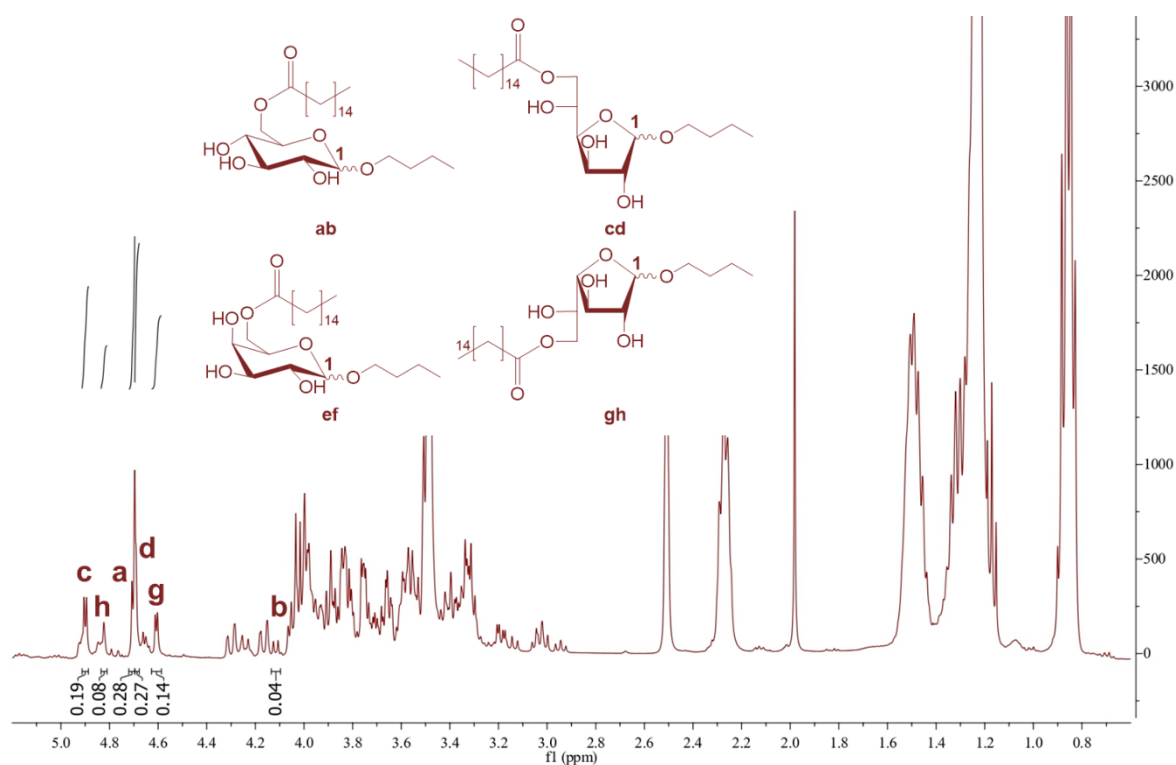


**Figure 3.50.**  $^1\text{H}$  NMR spectrum of 1-butyl 6-O-palmitoyl-D-glycosides isomeric mixture (**65ah**), carried out in  $\text{DMSO-d}_6 + \text{D}_2\text{O}$  (1 drop).

Further studies have to be performed to improve reaction yields and purification procedures, however, the preliminary study of the CWP valorization focused on the investigation of the interfacial and emulsifying behaviour of the generated biosurfactant mixture (**65ah**).



### 3.9.4 Preliminary results of the physico-chemical characterization

Considering the promising surfactant features of the previously obtained alkyl glucoside and galactoside fatty acid esters, the research performed preliminary studies on the interfacial tension (IFT) reduction capacity and on the emulsifying properties of the synthesized biosurfactants mixture **65ah** derived from cheese whey permeate.

Going into details, the IFT reduction between water (milli-Q) and sunflower oil was evaluated by adding the biosurfactants 1-butyl 6-O-palmitoyl-D-glycoside isomeric mixture **65ah** at increasing concentration (0.1-7.5 mM in sunflower oil), see **Figure 3.51.a**.

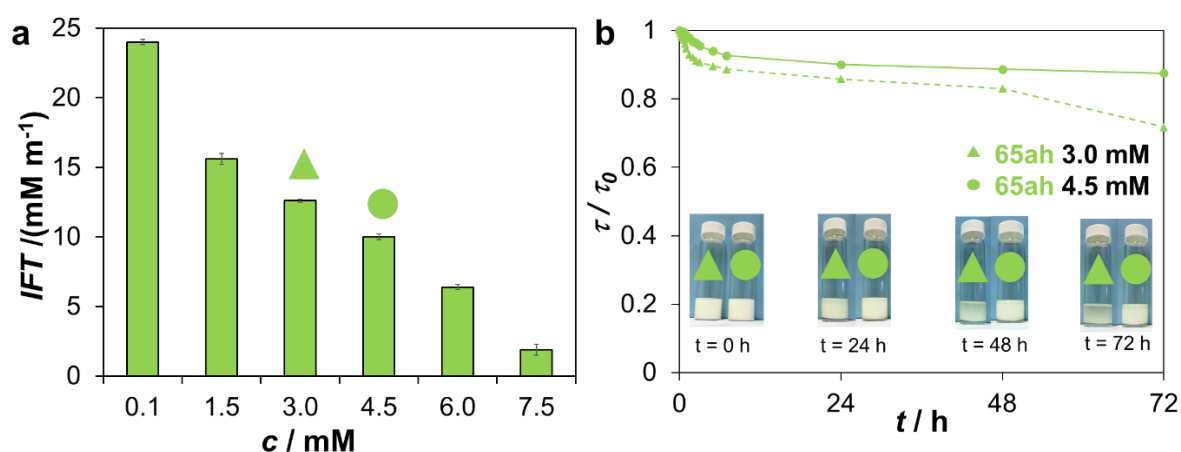


**Figure 3.51.** **a)** Sunflower oil/water interfacial tension (IFT) data by varying the concentration of **65ah** in the range 0.1-7.5 mM in oil. Data were reported as average values on three different replicates at room temperature; **b)** Normalized turbidity ( $\tau / \tau_0$ ) of W/O emulsions generated with **58ah** at 3.0 and 4.5 mM concentration within 72 h. Insets: photos of the two samples at 0, 24, 48 and 72 h.

**Figure 3.51** shows the lower ability of **65ah** in reducing the IFT according to the surfactant concentration, if compared to both the isomeric mixtures of 1-butyl 6-O-palmitoyl-D-glucosides (**37ad**) and D-galactosides (**58ad**), see **Section 3.8.4**. Only a concentration of 7.5 mM led to the sunflower oil/water IFT reduction to a value lower than 2 mN m<sup>-1</sup>, contrarily to **37ad** and **58ad**, which required concentrations of 4.5 mM and 3.0 mM, respectively, to reach the same IFT reduction. This result corroborates the strong impact of the pyranoside/furanoside isomeric ratio on the IFT reduction capacity of the biosurfactant mixture.

However, the use of a complex mixture of biosurfactants allowed to produce novel and relatively stable W/O emulsions, already at 4.5 mM concentration of surfactant in oil, see **Figure 3.51.b**.

Thus, preliminary results of this physico-chemical characterization study of **58ah** showed promising surfactancy, both in the case of IFT reduction ability and emulsion stabilization, thus confirming the present protocols for the achievement of sustainable and performing biosurfactants.

# **4 | Conclusions and future perspectives**

## 4 | Conclusions and future perspectives

---

The main goals of the present research are:

- A suitable and sustainable protocol for the synthesis of sugar-based biosurfactants was successfully used to produce several glucoside and galactoside-based tensides;
- Their physico-chemical properties, in terms of sunflower oil/water interfacial tension reduction and emulsifying capability, have been deeply investigated;
- These results were used for a preliminary study related to the valorization of cheese whey permeate (CWP).

However, these results highlighted the need for further studies, which are still ongoing, *i.e.*:

- The improvement of the reaction yields and the purification downstream of CWP derived biosurfactants, by exploiting process intensification techniques, *i.e.*, performing the chemo-enzymatic synthesis with the flow reactor technology often able to overcome the typical constraints associated to batch reactions;
- The adsorption modes of the synthesized surfactants have to be studied in detail (thanks to molecular dynamics simulations), in order to explain their different behaviours;
- Finally, these tensides will be used in complex formulation recipes for their industrial applications as emulsifiers in food and cosmetics.

## 5 | Experimental section

### 5.1 Materials and methods

#### *Solvents and reagents*

All solvents and reagents were purchased from Merck Life Science (Milano, Italy) and were used without further purification, unless specified elsewhere.  $\beta$ -Lactose, D-(+)-glucose, D-(+)-galactose, Amberlite<sup>®</sup> IR-120, Amberlyst<sup>®</sup> 15 and 3 Å molecular sieves were dried at 90 °C overnight prior to use.

Commercial immobilized lipase from *Candida antarctica* lipase B (CALB, Novozym<sup>®</sup> 435) and bacterial  $\beta$ -galactosidase Saphera<sup>®</sup> 2600 L liquid formulation were kindly supplied by Novozymes (Bagsvard, Denmark).

Cheese whey permeate was gently provided by Latteria Soresina (Soresina, Italy).

#### *Analytical and flash column chromatography*

Analytical TLC was performed on silica gel F<sup>254</sup> precoated aluminum sheets (0.2 mm layer, Merck); components were detected by spraying with CeSO<sub>4</sub> / (NH<sub>4</sub>)<sub>6</sub>Mo<sub>7</sub>O<sub>24</sub> x H<sub>2</sub>O solution, followed by heating at 150°C. Silica gel 60, 40-63  $\mu$ m (Merck, Darmstadt, Germany) was used for flash column chromatography.

#### *NMR spectroscopy*

<sup>1</sup>H and <sup>13</sup>C NMR spectra were recorded at 400.13 and 100.61 Hz, respectively, on a Bruker AVANCE 400 spectrometer equipped with TOPSPIN software package (Bruker, Karlsruhe, Germany) at 300 K, unless stated otherwise. <sup>1</sup>H and <sup>13</sup>C chemical shifts ( $\delta$ ) are given in parts per million and were referenced to the solvent signals ( $\delta^H$  3.31 -  $\delta^C$  49.00,  $\delta^H$  2.50 -  $\delta^C$  39.52 and  $\delta^H$  4.79 ppm from tetramethylsilane (TMS) for CD<sub>3</sub>OD, DMSO-*d*<sub>6</sub> and D<sub>2</sub>O, respectively).

<sup>1</sup>H NMR signals were assigned with the aid of <sup>1</sup>H-<sup>1</sup>H correlation spectroscopy (<sup>1</sup>H-<sup>1</sup>H COSY). <sup>13</sup>C NMR signal multiplicities were based on APT (Attached proton test) spectra. <sup>13</sup>C NMR signals were assigned with the aid of <sup>1</sup>H-<sup>13</sup>C correlation experiments (Heteronuclear single quantum correlation spectroscopy, HSQC, and Heteronuclear multiple bond correlation spectroscopy, HMBC).

### *Mass spectrometry*

Electrospray ionization mass spectra (ESI-MS) were recorded on the Thermo Finnigan LCQ Advantage spectrometer (Hemel Hempstead, Hertfordshire, U.K.).

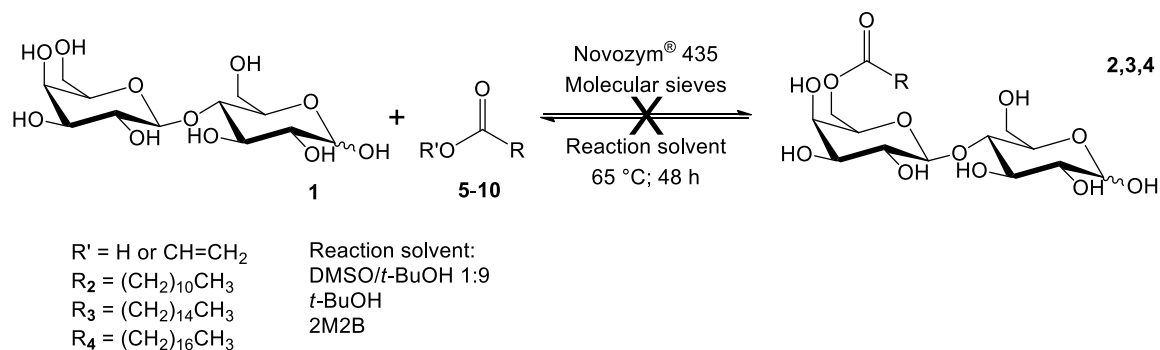
### *Equipment*

Some enzymatic reactions were performed in a glass oven B-585 Kugelrohr (BUCHI Italia s.r.l., Cornaredo, Italy).

Centrifuge 5804-R (Eppendorf S.r.l., Milan, Italy).

## 5.2 Synthesis of lactose monoesters

### 5.2.1 Enzymatic synthesis of lactose monoesters



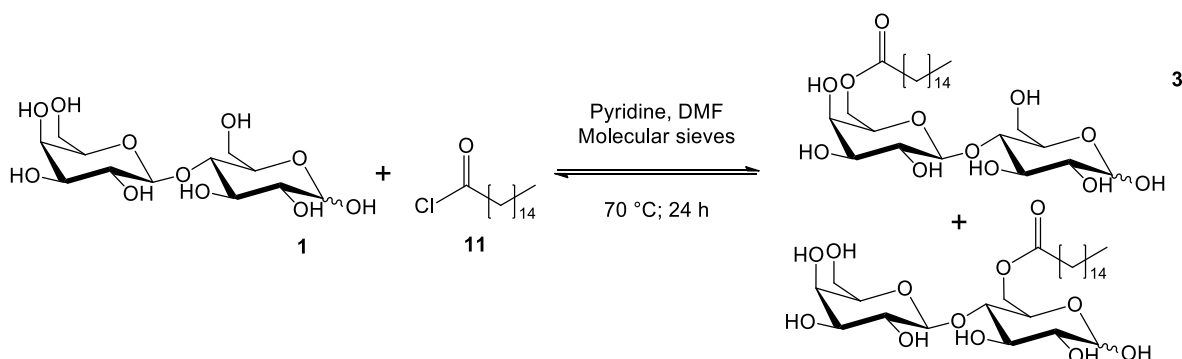
$\beta$ -D-Lactose (**1**) and saturated fatty acids (lauric acid, **5**; palmitic acid, **6**; and stearic acid, **7**) or activated acyl donors (vinyl laurate, **8**; vinyl palmitate, **9**; and vinyl stearate, **10**) in molar ratio 1:2, were suspended in different solvents and solvent mixtures (3.6% w/v), see **Table 5.1**, under magnetic stirring (400 rpm), at 65 °C. After 15 minutes, Novozym<sup>®</sup> 435 (10% w/w) and 3 Å molecular sieves (12% w/w) were added to start the reactions. After 48 h, reactions were monitored by TLC (DCM/MeOH; 8:2), but lactose monoesters formation was not observed.



## 5 | Experimental section

**Table 5.1.** Experimental conditions for the synthesis of lactose monoesters.

<b>Attempt</b>	<b>Esterifying or transesterifying agent</b>	<b>Reaction solvent</b>
2.01		DMSO/ <i>t</i> -BuOH 1:9
2.02	Lauric acid ( <b>5</b> )	<i>t</i> -BuOH
2.03		2M2B
3.01		DMSO/ <i>t</i> -BuOH 1:9
3.02	Palmitic acid ( <b>6</b> )	<i>t</i> -BuOH
3.03		2M2B
4.01		DMSO/ <i>t</i> -BuOH 1:9
4.02	Stearic acid ( <b>7</b> )	<i>t</i> -BuOH
4.03		2M2B
2.04		DMSO/ <i>t</i> -BuOH 1:9
2.05	Vinyl laurate ( <b>8</b> )	<i>t</i> -BuOH
2.06		2M2B
3.04		DMSO/ <i>t</i> -BuOH 1:9
3.05	Vinyl palmitate ( <b>9</b> )	<i>t</i> -BuOH
3.06		2M2B
4.04		DMSO/ <i>t</i> -BuOH 1:9
4.05	Vinyl stearate ( <b>10</b> )	<i>t</i> -BuOH
4.06		2M2B

5.2.2 Chemical synthesis of 6- and 6'-O-palmitoyl-D-lactose (**3**)

$\beta$ -D-Lactose (**1**, 684 mg, 2 mmol) was suspended in anhydrous dimethylformamide (DMF, 17 mL), then pyridine (0.16 mL), molecular sieves (343 mg, 50% w/w) and palmitoyl chloride (**11**, 0.304 mL, 1 mmol) were added and the reaction mixture was stirred (700 rpm) at 70 C° overnight.

After 24 h, the reaction was monitored by TLC (DCM/MeOH; 8:2), the molecular sieves were filtered, and the solvent was removed under reduced pressure. The product was extracted in 1-BuOH (2 x 75 mL) from 10% NaCl aqueous solution. The organic phases were collected, dried over Na<sub>2</sub>SO<sub>4</sub> and the solvent was removed under reduced pressure. A flash column chromatography (DCM/MeOH; 8:2) afforded a mixture of **6**- and **6'**-O-palmitoyl-D-lactose (**3**, 197 mg, 0.34 mmol) as a yellowish solid.

**Yield:** 34%

**R<sub>f</sub>** (eluent: DCM/MeOH; 8:2): 0.32.

**<sup>1</sup>H NMR (CD<sub>3</sub>OD, 400 MHz):**  $\delta$  (ppm) 4.99 (m, CH<sup>1 $\alpha$</sup> ), 4.48 – 4.32 (m, CH<sup>1 $\beta$</sup> , CH<sub>2</sub><sup>6</sup>COO), 4.31 – 4.21 (m, CH<sup>1'</sup>, CH<sub>2</sub><sup>6</sup>COO), 4.21 – 4.15 (m, CH<sup>1'</sup>, CH<sub>2</sub><sup>6</sup>COO), 4.00 (dd, J = 10.1, 2.7 Hz, CH), 3.93 – 3.86 (m, CH), 3.84 – 3.75 (m, CH, CH, CH<sub>2</sub><sup>6</sup>), 3.75 – 3.65 (m, 8 CH, CH<sub>2</sub><sup>6</sup>), 3.65 – 3.52 (m, 5 CH, CH<sub>2</sub><sup>6</sup>), 3.50 – 3.37 (m, 8 CH), 3.37 – 3.30 (m, 5 CH), 3.14 – 3.07 (m, CH, CH), 2.35 – 2.21 (m, COOCH<sub>2</sub>), 2.17 (t, J = 7.4 Hz, HCOOCH<sub>2</sub>), 1.50 (m, COOCH<sub>2</sub>CH<sub>2</sub>), 1.19 (br s, (CH<sub>2</sub>)<sub>12</sub>), 0.80 (t, J = 6.8 Hz, CH<sub>3</sub>).

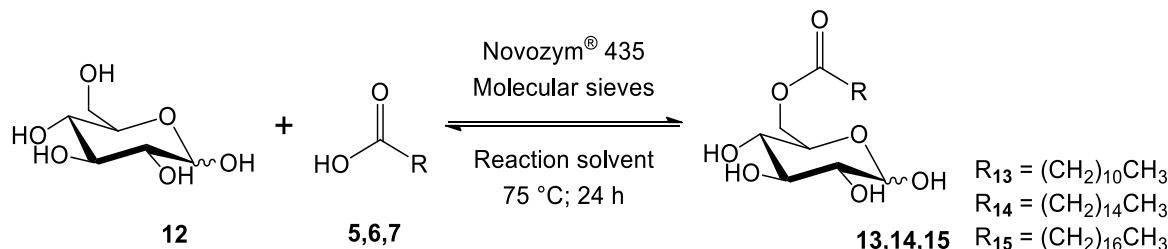
**$^{13}\text{C}$  NMR ( $\text{CD}_3\text{OD}$ , 101 MHz):**  $\delta$  (ppm) 176.35 (HCOO), 174.02, 174.01, 174.00, 173.99 (4 COO), 103.92, 103.91, 103.88, 103.87 (4  $\text{CH}^{1'}$ ), 96.65, 96.62 (2  $\text{CH}^{1\beta}$ ), 92.30, 92.24 (2  $\text{CH}^{1\alpha}$ ), 80.66, 80.39, 79.93, 79.56, 75.80, 75.57, 75.00, 74.97, 74.95, 74.59, 74.41, 73.38, 73.37, 73.17, 73.15, 72.95, 72.58, 72.23, 72.02, 71.78, 71.03, 70.99, 70.86, 70.83, 69.95, 69.83, 69.32, 68.86, 68.84, 68.78, 68.76, 67.75 (32 CH), 63.21, 63.20, 62.89, 62.83 (4  $\text{CH}_2^6\text{COO}$ ), 61.16, 61.13, 60.77, 60.69 (4  $\text{CH}_2^6$ ), 33.67, 33.61, 33.42, 33.41 (4  $\text{COOCH}_2$ ), 31.67, 29.40, 29.39, 29.38, 29.37, 29.36, 29.31, 29.25, 29.23, 29.21, 29.07, 29.03, 28.86, 28.84 ( $(\text{CH}_2)_{12}$ ), 24.72 ( $\text{COOCH}_2\text{CH}_2$ ), 22.33 ( $(\text{CH}_2)_{12}$ ), 13.05 ( $\text{CH}_3$ ).

**MS (ESI<sup>+</sup>):** *m/z* calcd for  $[\text{C}_{28}\text{H}_{52}\text{O}_{12}]$ : 580.35; found: 603.61  $[\text{M}+\text{Na}]^+$ , 1183.11  $[2\text{M}+\text{Na}]^+$ .

**MS (ESI<sup>-</sup>):** *m/z* calcd for  $[\text{C}_{28}\text{H}_{52}\text{O}_{12}]$ : 580.35; found: 580.08  $[\text{M}-\text{H}]^-$ , 1160.26  $[2\text{M}-\text{H}]^-$ .

## 5.3 6-O-lauroyl-, 6-O-palmitoyl-, 6-O-stearoyl-D-glucose

### 5.3.1 Optimized enzymatic synthesis of glucose monoesters



D-(+)-glucose (**12**) and saturated fatty acids (lauric acid, **5**; palmitic acid, **6**; and stearic acid, **7**), in molar ratio 1:3, were suspended in different solvents and solvent mixtures (3.6%  $w_{\text{sugar}}/v$ ), as reported in the **Table 5.2**, under magnetic stirring (400 rpm), at 75 °C. After 15 minutes, Novozym® 435 (10% w/w) and 3 Å molecular sieves (12% w/w) were added to start the reactions.

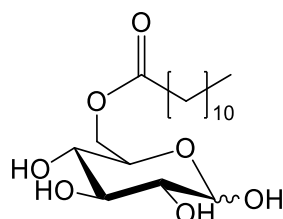
After 24 h, the reaction mixtures were filtered to separate the immobilized enzyme beads and the molecular sieves, and solvents were removed under reduced pressure. The ester products and the unreacted fatty acids were precipitated in H<sub>2</sub>O, thus favouring the removal of unreacted glucose and DMSO. The precipitates obtained from the filtration were dried overnight at room temperature.

Then, unreacted fatty acids were dissolved in hot *n*-heptane (0.1  $v/w_{\text{fatty acid}}$ ) and **6-O-lauroyl-D-glucose** (**13**, Purity: 90%); **6-O-palmitoyl-D-glucose** (**14**, Purity: 89%); and **6-O-stearoyl-D-glucose** (**15**, Purity: 89%) were recovered by filtration as white powders.

**Table 5.2.** Experimental conditions for the synthesis of glucose monoesters.

<b>Attempt</b>	<b>Reaction solvent</b>	<b>Yield (%)</b>
<b>13.01</b>	DMSO/t-BuOH 1:9	<b>18</b>
<b>14.01</b>	DMSO/t-BuOH 1:9	<b>19</b>
14.02	t-BuOH	15
14.03	2M2B	5
14.04	DMSO	-
<b>15.01</b>	DMSO/t-BuOH 1:9	<b>20</b>

## 5.3.2 Characterization of 6-O-lauroyl-D-glucose (13)



$R_f$  (eluent: DCM/MeOH; 8.8:1.2): 0.28.

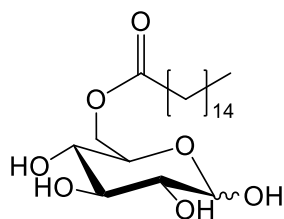
**$^1\text{H NMR}$  (DMSO- $d_6$  +  $\text{D}_2\text{O}$  (1 drop), 400 MHz):**  $\delta$  (ppm) 4.89 (d,  $J = 3.3$  Hz, 1H,  $\text{CH}^1$ ), 4.25 (d,  $J = 11.5$  Hz, 1H,  $\text{CH}_2^{6'}$ ), 3.99 (dd,  $J = 11.6, 6.1$  Hz, 1H,  $\text{CH}_2^{6''}$ ), 3.75 (m, 1H,  $\text{CH}^5$ ), 3.43 (t,  $J = 9.1$  Hz, 1H,  $\text{CH}^3$ ), 3.12 (dd,  $J = 9.4, 3.3$  Hz, 1H,  $\text{CH}^2$ ), 3.04 (t,  $J = 9.3$  Hz, 1H,  $\text{CH}^4$ ), 2.26 (t,  $J = 7.1$  Hz, 2H,  $\text{COOCH}_2$ ), 1.50 (m, 2H,  $\text{COOCH}_2\text{CH}_2$ ), 1.23 (br s, 16H,  $(\text{CH}_2)_8$ ), 0.84 (t,  $J = 6.2$  Hz, 3H,  $\text{CH}_3$ ).

**$^{13}\text{C NMR}$  (DMSO- $d_6$  +  $\text{D}_2\text{O}$  (1 drop), 101 MHz):**  $\delta$  (ppm) 176.36 ( $\text{COO}$ ), 95.47 ( $\text{CH}^1$ ), 75.99 ( $\text{CH}^3$ ), 75.31 ( $\text{CH}^2$ ), 73.68 ( $\text{CH}^4$ ), 72.41 ( $\text{CH}^5$ ), 67.09 ( $\text{CH}_2^6$ ), 36.77 ( $\text{COOCH}_2$ ), 34.59 ( $\text{CH}_2\text{CH}_2\text{CH}_3$ ), 43.64 - 41.68 ( $(\text{CH}_2)_6$ ), 27.76 ( $\text{COOCH}_2\text{CH}_2$ ), 25.39 ( $\text{CH}_2\text{CH}_3$ ), 17.25 ( $\text{CH}_3$ ).

**MS (ESI $^+$ ):**  $m/z$  calcd for  $[\text{C}_{18}\text{H}_{34}\text{O}_7]$ : 362.23; found: 385.41  $[\text{M}+\text{Na}]^+$ , 747.29  $[2\text{M}+\text{Na}]^+$ .

**MS (ESI $^-$ ):**  $m/z$  calcd for  $[\text{C}_{18}\text{H}_{34}\text{O}_7]$ : 362.23; found: 361.74  $[\text{M}-\text{H}]^-$ , 723.61  $[2\text{M}-\text{H}]^-$ .

## 5.3.3 Characterization of 6-O-palmitoyl-D-glucose (14)



**R<sub>f</sub>** (eluent: DCM/MeOH; 8.8:1.2): 0.28.

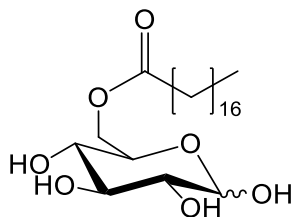
**<sup>1</sup>H NMR (DMSO-*d*<sub>6</sub> + D<sub>2</sub>O (1 drop), 400 MHz):** δ (ppm) 4.89 (d, *J* = 3.6 Hz, 1H, CH<sup>1</sup>), 4.24 (dd, *J* = 11.6, 6.0 Hz, 1H, CH<sub>2</sub><sup>6'</sup>), 3.99 (dd, *J* = 11.7, 6.0 Hz, 1H, CH<sub>2</sub><sup>6''</sup>), 3.75 (ddd, *J* = 1.7, 5.9, 9.6 Hz 1H, CH<sup>5</sup>), 3.43 (t, *J* = 9.2 Hz, 1H, CH<sup>3</sup>), 3.12 (dd, *J* = 9.6, 3.7 Hz, 1H, CH<sup>2</sup>), 3.04 (t, *J* = 9.4 Hz, 1H, CH<sup>4</sup>), 2.25 (t, *J* = 7.3 Hz, 2H, COOCH<sub>2</sub>), 1.49 (m, 2H, COOCH<sub>2</sub>CH<sub>2</sub>), 1.23 (br s, 24H, (CH<sub>2</sub>)<sub>12</sub>), 0.84 (t, *J* = 6.8 Hz, 3H, CH<sub>3</sub>).

**<sup>13</sup>C NMR (DMSO-*d*<sub>6</sub> + D<sub>2</sub>O (1 drop), 101 MHz):** δ (ppm) 173.56 (COO), 92.56 (CH<sup>1</sup>), 73.07 (CH<sup>3</sup>), 72.38 (CH<sup>2</sup>), 70.73 (CH<sup>4</sup>), 69.50 (CH<sup>5</sup>), 64.14 (CH<sub>2</sub><sup>6</sup>), 33.88 (COOCH<sub>2</sub>), 31.70 (CH<sub>2</sub>CH<sub>2</sub>CH<sub>3</sub>), 29.83 - 28.49 ((CH<sub>2</sub>)<sub>10</sub>), 24.86 (COOCH<sub>2</sub>CH<sub>2</sub>), 22.50 (CH<sub>2</sub>CH<sub>3</sub>), 14.35 (CH<sub>3</sub>).

**MS (ESI<sup>+</sup>):** *m/z* calcd for [C<sub>22</sub>H<sub>42</sub>O<sub>7</sub>]: 418.29; found: 441.25 [M+Na]<sup>+</sup>, 858.81 [2M+Na]<sup>+</sup>.

**MS (ESI<sup>-</sup>):** *m/z* calcd for [C<sub>22</sub>H<sub>42</sub>O<sub>7</sub>]: 418.29; found: 417.26 [M-H]<sup>-</sup>, 834.93 [2M-H]<sup>-</sup>.

## 5.3.4 Characterization of 6-O-stearoyl-D-glucose (15)



**R<sub>f</sub>** (eluent: DCM/MeOH; 8.8:1.2): 0.29.

**<sup>1</sup>H NMR (DMSO-*d*<sub>6</sub> + D<sub>2</sub>O (1 drop), 400 MHz):** δ (ppm) 4.90 (d, *J* = 3.6 Hz, 1H, CH<sup>1</sup>), 4.26 (dd, *J* = 11.7, 1.7 Hz, 1H, CH<sub>2</sub><sup>6\*</sup>), 4.02 (dd, *J* = 11.7, 5.9 Hz, 1H, CH<sub>2</sub><sup>6\*\*</sup>), 3.76 (m, 1H, CH<sup>5</sup>), 3.45 (t, *J* = 9.2 Hz, 1H, CH<sup>3</sup>), 3.15 (dd, *J* = 9.6, 3.6 Hz, 1H, CH<sup>2</sup>), 3.07 (t, *J* = 9.4 Hz, 1H, CH<sup>4</sup>), 2.25 (t, *J* = 7.3 Hz, 2H, COOCH<sub>2</sub>), 1.50 (m, 2H, COOCH<sub>2</sub>CH<sub>2</sub>), 1.23 (s, 36H, (CH<sub>2</sub>)<sub>14</sub>), 0.84 (t, *J* = 6.6 Hz, 3H, CH<sub>2</sub>CH<sub>3</sub>).

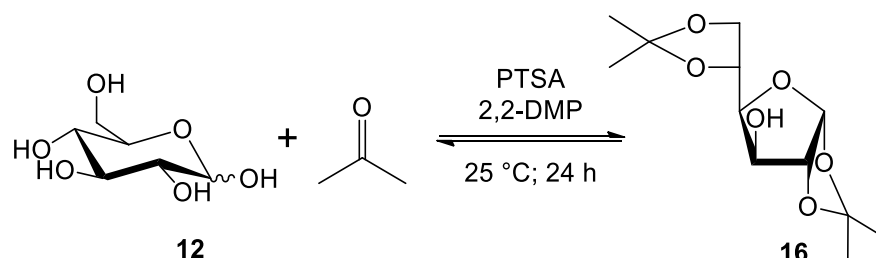
**<sup>13</sup>C NMR (DMSO-*d*<sub>6</sub> + D<sub>2</sub>O (1 drop), 101 MHz):** δ (ppm) 176.40 (COO), 95.45 (CH<sup>1</sup>), 76.08 (CH<sup>3</sup>), 75.34 (CH<sup>2</sup>), 73.70 (CH<sup>4</sup>), 72.45 (CH<sup>5</sup>), 67.01 (CH<sub>2</sub><sup>6</sup>), 36.79 (COOCH<sub>2</sub>), 34.50 (CH<sub>2</sub>CH<sub>2</sub>CH<sub>3</sub>), 32.68 – 31.37 ((CH<sub>2</sub>)<sub>12</sub>), 27.70 (COOCH<sub>2</sub>CH<sub>2</sub>), 25.28 (CH<sub>2</sub>CH<sub>3</sub>), 17.11 (CH<sub>3</sub>).

**MS (ESI<sup>+</sup>):** *m/z* calcd for [C<sub>24</sub>H<sub>46</sub>O<sub>7</sub>]: 446.32; found: 469.74 [M+Na]<sup>+</sup>, 915.46 [2M+Na]<sup>+</sup>.

**MS (ESI<sup>-</sup>):** *m/z* calcd for [C<sub>24</sub>H<sub>46</sub>O<sub>7</sub>]: 446.32; found: 445.17 [M-H]<sup>-</sup>, 891.24 [2M-H]<sup>-</sup>.

## 5.4 1,2:5,6-Di-O-isopropylidene- $\alpha$ -D-glucofuranose

### 5.4.1 Chemical synthesis of 1,2:5,6-di-O-isopropylidene- $\alpha$ -D-glucofuranose (**16**)

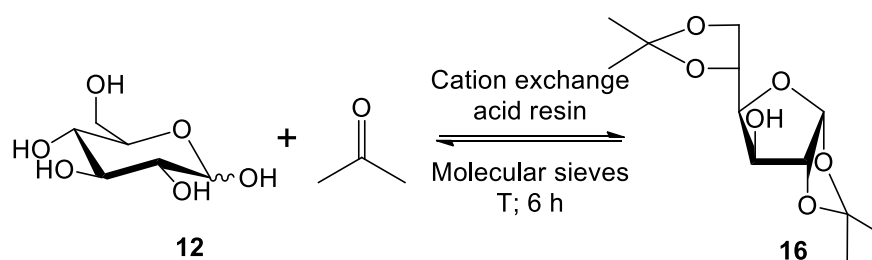


D-(+)-glucose (**12**, 1.8 g, 10 mmol) was suspended in dry acetone (50 mL), then 2,2-dimethoxypropane (2,2-DMP, 30 mmol) and *p*-toluenesulfonic acid monohydrate (PTSA, 1 mmol) were added and the reaction mixture was stirred at room temperature overnight.

After 24 h, the reaction was monitored by TLC (*n*-hexane/EtOAc; 1:1), the reaction was quenched with 1 M NaOH solution and the solvent was removed under reduced pressure. The reaction product was extracted in EtOAc (2 x 20 mL) from a saturated aqueous solution of NaHCO<sub>3</sub> (20 mL). The organic phases were collected, dried over Na<sub>2</sub>SO<sub>4</sub> and the solvent was removed under reduced pressure. A flash column chromatography (*n*-hexane/EtOAc; 1:1) afforded pure **1,2:5,6-di-O-isopropylidene- $\alpha$ -D-glucofuranose** (**16**, 1.06 g, 4 mmol) as a yellowish solid.

**Yield:** 40%



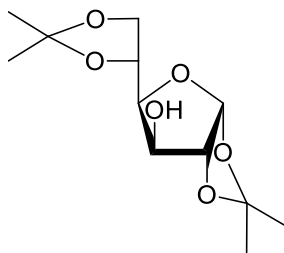
5.4.2 Alternative synthesis of 1,2:5,6-di-*O*-isopropylidene- $\alpha$ -D-glucofuranose (16)

D-(+)-glucose was suspended in dry acetone (different weight/volume percentages were tested, see **Table 3.3**), then cation exchange acid resins (Amberite<sup>®</sup> IR-120 or Amberlyst<sup>®</sup> 15, 10% w/w<sub>sugar</sub>) and 3 Å molecular sieves (25% w/w<sub>sugar</sub>) were added, and the reaction mixture was stirred (700 rpm) at different temperatures (see **Table 5.3**).

After 6 h, the reaction was monitored by TLC (*n*-hexane/EtOAc; 1:1) and the reaction mixture was filtered to remove the immobilized acid catalyst and the molecular sieves, and the solvent was removed under reduced pressure. The product was extracted in EtOAc (2 times) from saturated aqueous solution of NaHCO<sub>3</sub>, the organic phases were collected, dried over Na<sub>2</sub>SO<sub>4</sub> and the solvent was removed under reduced pressure, thus obtaining **1,2:5,6-di-*O*-isopropylidene- $\alpha$ -D-glucofuranose (16)** as a yellowish solid. No further purification was needed.

**Table 5.3.** Experimental conditions for the synthesis of the glucose derivative.

<b>Attempt</b>	<b>Cation exchange acid resin</b>	<b>% w/v (%)</b>	<b>Temperature (°C)</b>	<b>Yield (%)</b>
16.01		3.6	50	27
16.02	Amberite <sup>®</sup> IR-120	3.6	65, reflux	29
16.03		1.8	65, reflux	50
16.04		3.6	50	18
16.05	Amberlyst <sup>®</sup> 15	3.6	65, reflux	25
<b>16.06</b>		1.8	65, reflux	<b>51</b>

5.4.3 Characterization of 1,2:5,6-di-*O*-isopropylidene- $\alpha$ -D-glucofuranose (16)

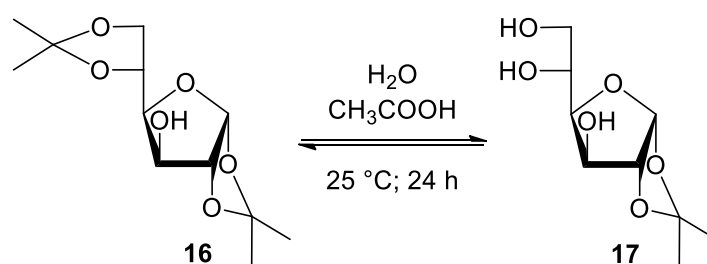
$R_f$  (eluent: *n*-hexane/EtOAc; 1:1): 0.34.

$^1\text{H NMR}$  (DMSO-*d*<sub>6</sub>, 400 MHz):  $\delta$  (ppm) 5.82 (d,  $J = 3.6$  Hz, 1H, CH<sup>1</sup>), 5.39 (d,  $J = 4.8$  Hz, 1H, OH<sup>3</sup>), 4.40 (d,  $J = 3.7$  Hz, 1H, CH<sup>2</sup>), 4.23 (q,  $J = 6.4$  Hz, 1H, CH<sup>5</sup>), 4.00 – 3.93 (m, 3H, CH<sup>3,4</sup>, CH<sub>2</sub><sup>6'</sup>), 3.81 (dd,  $J = 8.4, 6.0$  Hz, 1H, CH<sub>2</sub><sup>6''</sup>), 1.38 (s, 3H, CH<sup>1</sup>OCCH<sub>3</sub>'), 1.32 (s, 3H, CH<sub>2</sub><sup>6</sup>OCCH<sub>3</sub>'), 1.27 (s, 3H, CH<sub>2</sub><sup>6</sup>OCCH<sub>3</sub>''), 1.24 (s, 3H, CH<sup>1</sup>OCCH<sub>3</sub>'').

$^{13}\text{C NMR}$  (DMSO-*d*<sub>6</sub>, 101 MHz):  $\delta$  (ppm) 111.10 (CH<sup>1</sup>C), 108.34 (CH<sub>2</sub><sup>6</sup>C), 104.99 (CH<sup>1</sup>), 85.42 (CH<sup>2</sup>), 81.38 (CH<sup>3</sup>), 73.60 (CH<sup>4</sup>), 72.69 (CH<sup>5</sup>), 66.49 (CH<sub>2</sub><sup>6</sup>), 27.18 (CH<sup>1</sup>OCCH<sub>3</sub>'), 27.06 (CH<sub>2</sub><sup>6</sup>OCCH<sub>3</sub>'), 26.53 (CH<sub>2</sub><sup>6</sup>OCCH<sub>3</sub>''), 25.73 (CH<sup>1</sup>OCCH<sub>3</sub>'').

$\text{MS (ESI}^+)$ :  $m/z$  calcd for [C<sub>12</sub>H<sub>20</sub>O<sub>6</sub>]: 260.13; found: 260.64 [M+Na]<sup>+</sup>.

$\text{MS (ESI}^-)$ :  $m/z$  calcd for [C<sub>12</sub>H<sub>20</sub>O<sub>6</sub>]: 260.13; found: 259.21 [M-H]<sup>-</sup>, 519.08 [2M-H]<sup>-</sup>.

5.5 1,2-*O*-Isopropylidene- $\alpha$ -D-glucofuranose

1,2:5,6-Di-*O*-isopropylidene- $\alpha$ -D-glucofuranose (**16**, 260 mg, 1 mmol) was suspended in a 60% acetic acid aqueous solution (CH<sub>3</sub>COOH, 4 mL) and the reaction mixture was stirred (700 rpm) at room temperature, overnight.

After 24 h, the reaction was monitored by TLC (DCM/MeOH; 9:1) and it was quenched by 1 M NaOH aqueous solution (few drops to reach pH 7.0) and freeze-dried. The product mixture was purified by flash column chromatography (DCM/MeOH; 9:1), obtaining **1,2-*O*-isopropylidene- $\alpha$ -D-glucofuranose (17**, 40 mg, 0,18 mmol) as a whitish powder.

**Yield:** 18%

**R<sub>f</sub>** (eluent: DCM/MeOH; 9:1): 0.44.

**<sup>1</sup>H NMR (DMSO-*d*<sub>6</sub>, 400 MHz):**  $\delta$  (ppm) 5.79 (d,  $J$  = 3.7 Hz, 1H, CH<sup>1</sup>), 5.12 (d,  $J$  = 4.7 Hz, 1H, OH<sup>3</sup>), 4.64 (d,  $J$  = 5.7 Hz, 1H, OH<sup>5</sup>), 4.43 (t,  $J$  = 5.6 Hz, 1H, OH<sup>6</sup>), 4.37 (d,  $J$  = 3.7 Hz, 1H, CH<sup>2</sup>), 4.03 (dd,  $J$  = 4.4, 2.6 Hz, 1H, CH<sup>3</sup>), 3.83 (dd,  $J$  = 8.5, 2.6 Hz, 1H, CH<sup>4</sup>), 3.72 – 3.65 (m, 1H, CH<sup>5</sup>), 3.55 (m,  $J$  = 11.0, 5.3, 3.0 Hz, 1H, CH<sub>2</sub><sup>6'</sup>), 3.40 – 3.35 (m, 1H, CH<sub>2</sub><sup>6''</sup>), 1.37 (s, 3H, CH<sup>1</sup>OCCH<sub>3</sub>'), 1.23 (s, 3H, CH<sup>1</sup>OCCH<sub>3</sub>'').

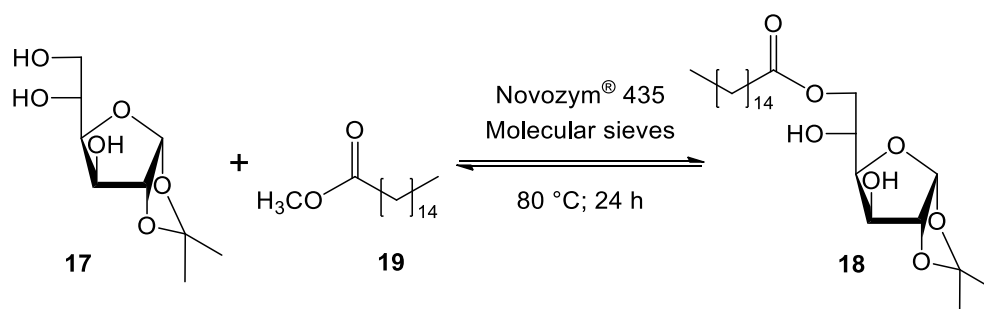
**<sup>13</sup>C NMR (DMSO-*d*<sub>6</sub>, 101 MHz):**  $\delta$  (ppm) 110.84 (OCCH<sub>3</sub>), 104.91 (CH<sup>1</sup>), 85.16 (CH<sup>2</sup>), 80.55 (CH<sup>4</sup>), 73.73 (CH<sup>3</sup>), 68.90 (CH<sup>5</sup>), 64.15 (CH<sub>2</sub><sup>6</sup>), 27.13 (CH<sup>1</sup>OCCH<sub>3</sub>'), 26.57 (CH<sup>1</sup>OCCH<sub>3</sub>'').

**MS (ESI<sup>+</sup>):**  $m/z$  calcd for [C<sub>9</sub>H<sub>16</sub>O<sub>6</sub>]: 220.09; found: 243.00 [M+Na]<sup>+</sup>, 462.73 [2M+Na]<sup>+</sup>.

**MS (ESI<sup>-</sup>):**  $m/z$  calcd for [C<sub>9</sub>H<sub>16</sub>O<sub>6</sub>]: 220.09; found: 219.10 [M-H]<sup>-</sup>, 438.86 [2M-H]<sup>-</sup>.

## 5.6 6-O-Palmitoyl-1,2-O-isopropylidene- $\alpha$ -D-glucofuranose

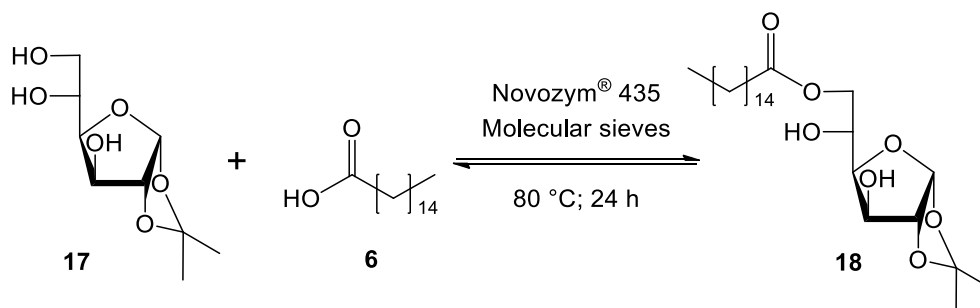
### 5.6.1 Enzymatic synthesis of 6-O-palmitoyl-1,2-O-isopropylidene- $\alpha$ -D-glucofuranose (**18**) with methyl palmitate as acyl donor



1,2-O-Isopropylidene- $\alpha$ -D-glucofuranose (**17**, 220 mg, 1 mmol) and methyl palmitate (**19**, 810 mg, 3 mmol), Novozym<sup>®</sup> 435 (10% w/w<sub>sugar</sub>) and 3 Å molecular sieves (10% w/w<sub>sugar</sub>) were mixed together and charged into a round-bottom flask. The mixture was heated to 80 °C while rotating the flask by means of a glass oven B-585 Kugelrohr.

After 24 h, the reaction mixture was taken up in EtOAc, monitored by TLC (*n*-hexane/EtOAc; 6:4) and filtered to remove the immobilized enzyme beads and the molecular sieves. A flash column chromatography (*n*-hexane/EtOAc; 6:4) afforded pure **6-O-palmitoyl-1,2-O-isopropylidene- $\alpha$ -D-glucofuranose** (**18**, 92 mg, 0.2 mmol) as a whitish solid.

**Yield:** 20%

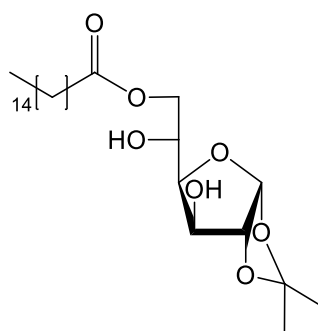
**5.6.2 Enzymatic synthesis of 6-O-palmitoyl-1,2-O-isopropylidene- $\alpha$ -D-glucofuranose (18) with palmitic acid as acyl donor**

1,2-O-Isopropylidene- $\alpha$ -D-glucofuranose (**17**, 220 mg, 1 mmol) and palmitic acid (**6**, 768 mg, 3 mmol or 256 mg, 1 mmol), Novozym<sup>®</sup> 435 (10% w/w<sub>sugar</sub>) and 3 Å molecular sieves (10% w/w<sub>sugar</sub>) were mixed together and charged into a round-bottom flask. The mixture was heated to 80 °C while rotating the flask by means of a glass oven B-585 Kugelrohr.

After 24 h, the reaction mixture was taken up in EtOAc, monitored by TLC (*n*-hexane/EtOAc; 6:4) and filtered to remove the immobilized enzyme beads and the molecular sieves. A flash column chromatography (*n*-hexane/EtOAc; 6:4) afforded pure **6-O-palmitoyl-1,2-O-isopropylidene- $\alpha$ -D-glucofuranose (18**, 124 mg, 0.27 mmol) as a whitish solid.

**Yield:** 27%

### 5.6.3 Characterization of 6-O-palmitoyl-1,2-O-isopropylidene- $\alpha$ -D-glucofuranose (18)



$R_f$  (eluent: *n*-hexane/EtOAc; 6:4): 0.41.

**$^1\text{H NMR}$  (DMSO- $d_6$ , 400 MHz):**  $\delta$  (ppm) 5.79 (d,  $J = 3.6$  Hz, 1H,  $\text{CH}^1$ ), 5.22 (d,  $J = 4.9$  Hz, 1H,  $\text{OH}^3$ ), 4.99 (d,  $J = 4.9$  Hz, 1H,  $\text{OH}^5$ ), 4.39 (d,  $J = 3.6$  Hz, 1H,  $\text{CH}^2$ ), 4.21 (d,  $J = 10.3$  Hz, 1H,  $\text{CH}_2^{6'}$ ), 4.04 (d,  $J = 3.3$  Hz, 1H,  $\text{CH}^3$ ), 3.98 – 3.81 (m, 3H,  $\text{CH}^4$ ,  $\text{CH}^5$ ,  $\text{CH}_2^{6''}$ ), 2.29 (t,  $J = 7.4$  Hz, 2H,  $\text{COOCH}_2$ ), 1.59 – 1.46 (m, 2H,  $\text{COOCH}_2\text{CH}_2$ ), 1.38 (s, 3H,  $\text{CH}^1\text{OCCH}_3'$ ), 1.27 – 1.23 (br s, 29H,  $(\text{CH}_2)_{12}$ ,  $\text{CH}^1\text{OCCH}_3''$ ), 0.86 (t,  $J = 6.8$  Hz, 3H,  $\text{CH}_3$ ).

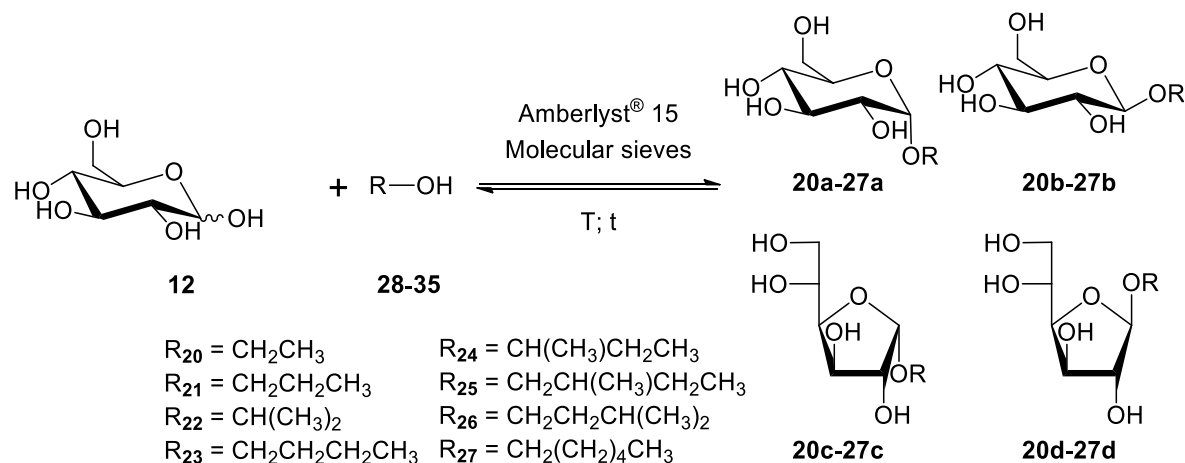
**$^{13}\text{C NMR}$  (DMSO- $d_6$ , 101 MHz):**  $\delta$  (ppm) 173.38 ( $\text{COO}$ ), 111.04 ( $\text{OCCH}_3$ ), 104.96 ( $\text{CH}^1$ ), 85.11 ( $\text{CH}^2$ ), 80.61 ( $\text{CH}^4$ ), 73.33 ( $\text{CH}^3$ ), 66.93 ( $\text{CH}_2^6$ ), 65.64 ( $\text{CH}^5$ ), 34.06 ( $\text{COOCH}_2$ ), 28.94 – 29.50 ( $(\text{CH}_2)_{12}$ ), 27.16 ( $\text{CH}^1\text{OCCH}_3'$ ), 26.63 ( $\text{CH}^1\text{OCCH}_3''$ ), 24.93 ( $\text{COOCH}_2\text{CH}_2$ ), 14.42 ( $\text{CH}_3$ ).

**MS (ESI $^+$ ):**  $m/z$  calcd for  $[\text{C}_{25}\text{H}_{46}\text{O}_7]$ : 458.32; found: 481,71  $[\text{M}+\text{Na}]^+$ , 939,30  $[2\text{M}+\text{Na}]^+$ .

**MS (ESI $^-$ ):**  $m/z$  calcd for  $[\text{C}_{25}\text{H}_{46}\text{O}_7]$ : 458.32; found: 457.22  $[\text{M}-\text{H}]^-$ , 915.50  $[2\text{M}-\text{H}]^-$ .

## 5.7 Alkyl D-glucoside isomeric mixtures

### 5.7.1 Sustainable synthesis of alkyl D-glucosides (20ad-27ad)



D-(+)-Glucose (**12**) was suspended in dry naturally occurring alcohols (**28-35**) (1.8% w/v) in the presence of the strongly acidic cation exchange resin Amberlyst<sup>®</sup> 15 (10 %, w/w) and 3 Å molecular sieves (25 %, w/w), under reflux or at 120 °C, according to the alcohol boiling points.

After reaction times reported in **Table 5.4**, the reactions were stopped by filtration of the solid catalyst, the alcohols were removed under reduced pressure and the reaction mixtures were submitted to flash chromatography (DCM/MeOH; 9:1) to give **alkyl D-glucoside isomeric mixtures (20ad-27ad)** as viscous syrups.

All products were fully characterized by TLC, ESI-MS and NMR analysis. Some <sup>1</sup>H and <sup>13</sup>C peaks are not completely resolved because of the instrument resolution.

Isomeric ratios of each alkyl D-glucoside isomeric mixture were estimated by <sup>1</sup>H NMR analysis, carried out in D<sub>2</sub>O, as the ratio of the areas of anomeric proton signals of each isomer present in the reaction mixture. NMR anomeric proton signals were identified by comparison with data reported in the literature (Straathof et al., 1987).

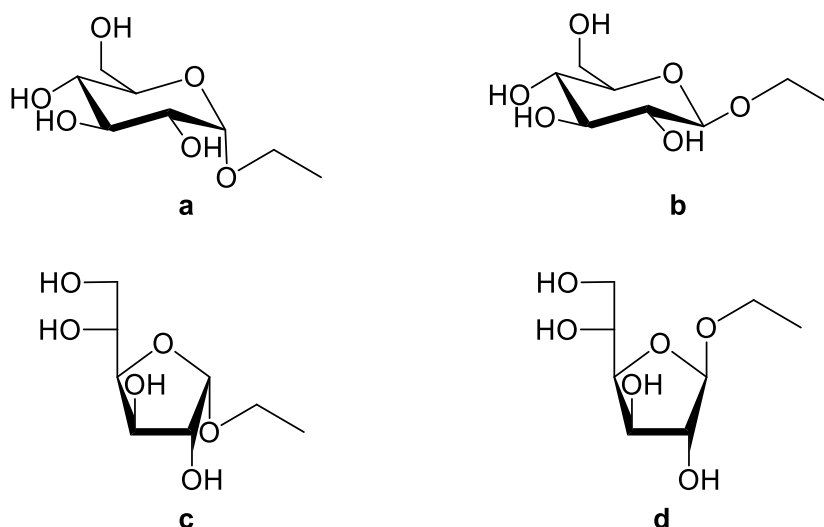
## 5 | Experimental section

**Table 5.4.** Experimental conditions for the synthesis of alkyl D-glucoside isomeric mixtures.

<b><i>R-OH</i></b>	<b><i>Temperature</i></b> <b>(°C)</b>	<b><i>Time</i></b> (h)	<b><i>Yield</i></b> (%)	<b><i>Isomeric ratio</i></b> <b><i>a/b/c/d</i></b> (%)
EtOH ( <b>28</b> )	90	4	65	13/20/27/40
1-PrOH ( <b>29</b> )	100	3	71	24/27/19/30
2-PrOH ( <b>30</b> )	90	6	67	18/20/28/34
1-BuOH ( <b>31</b> )	120	2.5	91	46/38/6/10
2-BuOH ( <b>32</b> )	120	6	87	36/32/12/20
2-Me-1-BuOH ( <b>33</b> )	120	1.5	70	37/29/14/20
3-Me-1-BuOH ( <b>34</b> )	120	2	89	43/34/10/13
1-HexOH ( <b>35</b> )	120	1.5	73	37/32/14/17



## 5.7.2 Characterization of ethyl D-glucoside isomeric mixture (20ad)



$R_f$  (eluent: DCM/MeOH; 9:1): 0.26, 0.35, 0.40.

Isomeric ratio a/b/c/d: 13/20/27/40.

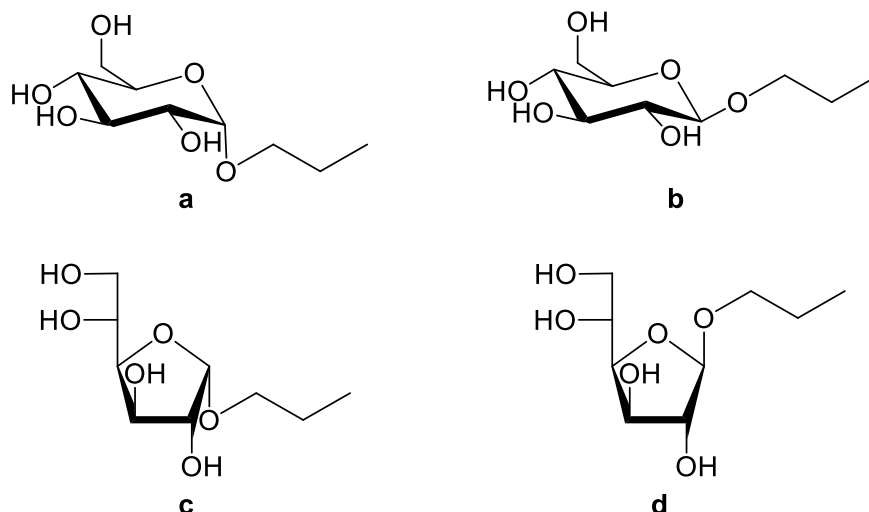
$^1\text{H NMR}$  (DMSO- $d_6$ , 400 MHz):  $\delta$  (ppm) 5.28 (d,  $J = 3.6$  Hz, OH), 5.04 (d,  $J = 4.2$  Hz, OH), 4.97 (d,  $J = 4.9$  Hz, OH), 4.93 (d,  $J = 4.0$  Hz,  $\text{CH}^1_{\alpha\text{-Fu}}$ ), 4.88 (d,  $J = 4.8$  Hz, OH), 4.84 (d,  $J = 5.5$  Hz, OH), 4.70 (br s,  $\text{CH}^1_{\beta\text{-Fu}}$ ), 4.62 (m,  $\text{CH}^1_{\alpha\text{-Py}}$ , OH), 4.52 (m, OH), 4.41 (m, OH), 4.11 (d,  $J = 7.8$  Hz,  $\text{CH}^1_{\beta\text{-Py}}$ ), 3.99 (br d,  $J = 3.3$  Hz, CH), 3.90 (br t,  $J = 3.7$  Hz, CH), 3.85 (dd,  $J = 8.0, 4.3$  Hz, CH, CH), 3.80 (m, CH, CH,  $\text{OCH}_2$ ), 3.77 – 3.69 (m, CH), 3.69 – 3.53 (m, CH, CH, CH, CH,  $\text{CH}_2^6$ ,  $\text{OCH}_2$ ), 3.52 – 3.42 (m,  $\text{CH}_2^6$ ,  $\text{OCH}_2$ ), 3.42 – 3.32 (m, CH, CH,  $\text{OCH}_2$ ), 3.20 – 3.14 (m, CH), 3.14 – 3.09 (m, CH), 3.09 – 3.00 (m, CH, CH), 2.96 – 2.89 (m, CH), 1.19 – 1.06 (m,  $\text{CH}_3$ ).

$^{13}\text{C NMR}$  (DMSO- $d_6$ , 101 MHz):  $\delta$  (ppm) 109.06 ( $\text{CH}^1_{\beta\text{-Fu}}$ ), 103.07 ( $\text{CH}^1_{\beta\text{-Py}}$ ), 102.38 ( $\text{CH}^1_{\alpha\text{-Fu}}$ ), 98.76 ( $\text{CH}^1_{\alpha\text{-Py}}$ ), 81.54, 81.09, 78.64, 77.57, 77.26, 77.22, 76.10, 75.88, 73.88, 73.78, 73.15, 72.39, 70.86, 70.54, 70.40, 70.29 (16 CH), 64.29 ( $\text{CH}_2^6$ ), 64.14, 63.90, 63.77, 63.09 (4  $\text{OCH}_2$ ), 62.70, 61.54, 61.47 (3  $\text{CH}_2^6$ ), 15.68, 15.61, 15.58, 15.50 (4  $\text{CH}_3$ ).

$\text{MS (ESI}^+)$ :  $m/z$  calcd for  $[\text{C}_8\text{H}_{16}\text{O}_6]$ : 208.09; found: 231.18  $[\text{M}+\text{Na}]^+$ , 438.84  $[\text{2M}+\text{Na}]^+$ .

$\text{MS (ESI}^-)$ :  $m/z$  calcd for  $[\text{C}_8\text{H}_{16}\text{O}_6]$ : 208.09; found: 207.68  $[\text{M}-\text{H}]^-$ , 415.55  $[\text{2M}-\text{H}]^-$ .

## 5.7.3 Characterization of 1-propyl D-glucoside isomeric mixture (21ad)



$R_f$  (eluent: DCM/MeOH; 9:1): 0.28; 0.39; 0.44.

Isomeric ratio a/b/c/d: 24/27/19/30.

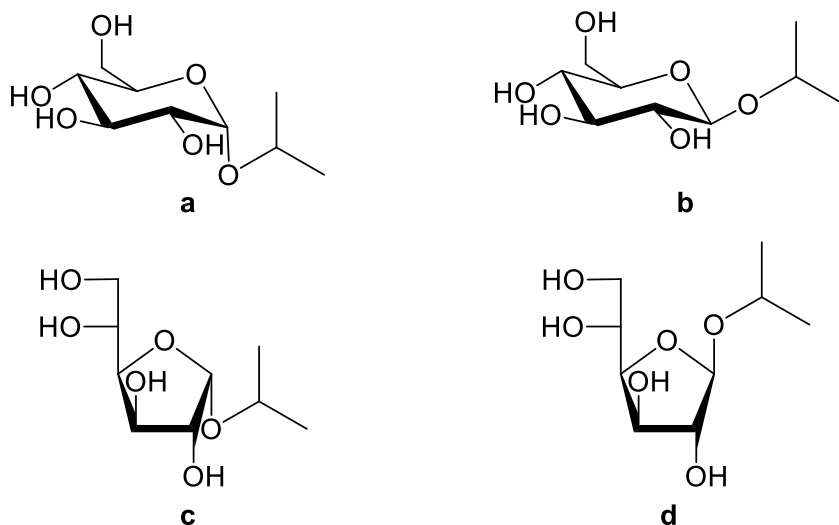
$^1\text{H NMR}$  (DMSO- $d_6$ , 400 MHz):  $\delta$  (ppm) 5.27 (t,  $J = 4.0$  Hz, OH), 5.03 (d,  $J = 4.8$  Hz, OH), 4.94 (d,  $J = 4.9$  Hz, OH), 4.91 (d,  $J = 4.0$  Hz,  $\text{CH}^1_{\alpha\text{-Fu}}$ ), 4.87 (d,  $J = 4.7$  Hz, OH), 4.84 (d,  $J = 5.4$  Hz, OH), 4.71 (d,  $J = 6.6$  Hz,  $\text{CH}^1_{\beta\text{-Fu}}$ ), 4.61 (m, OH), 4.58 (m,  $\text{CH}^1_{\alpha\text{-Py}}$ , OH), 4.54 – 4.34 (m, OH), 4.10 (d,  $J = 7.8$  Hz,  $\text{CH}^1_{\beta\text{-Py}}$ ), 4.00 (dd,  $J = 8.0, 4.5$  Hz, CH), 3.91 (m, CH), 3.88 – 3.78 (m, CH, CH, CH, CH), 3.76 – 3.68 (m, CH,  $\text{OCH}_2$ ), 3.68 – 3.60 (m, CH,  $\text{CH}_2^6$ ), 3.60 – 3.48 (m,  $\text{CH}_2^6$ ,  $\text{OCH}_2$ ), 3.48 – 3.34 (m, CH, CH, CH, CH,  $\text{CH}_2^6$ ,  $\text{OCH}_2$ ), 3.32 – 3.23 (m,  $\text{OCH}_2$ ), 3.20 – 3.15 (m, CH), 3.14 – 3.09 (m, CH), 3.09 – 3.00 (m, CH, CH), 2.94 (td,  $J = 8.4, 4.9$  Hz, CH), 1.59 – 1.44 (m,  $\text{OCH}_2\text{CH}_2$ ), 0.92 – 0.81 (m,  $\text{CH}_3$ ).

$^{13}\text{C NMR}$  (DMSO- $d_6$ , 101 MHz):  $\delta$  (ppm) 109.21 ( $\text{CH}^1_{\beta\text{-Fu}}$ ), 103.30 ( $\text{CH}^1_{\beta\text{-Py}}$ ), 102.43 ( $\text{CH}^1_{\alpha\text{-Fu}}$ ), 98.91 ( $\text{CH}^1_{\alpha\text{-Py}}$ ), 81.59, 81.03, 78.58, 77.68, 77.29, 77.24, 76.12, 75.89, 73.91, 73.74, 73.19, 72.46, 70.84 (13 CH), 70.58 ( $\text{OCH}_2$ ), 70.55, 70.47, 70.30 (3 CH), 69.96, 69.29, 68.85 (3  $\text{OCH}_2$ ), 64.15, 63.89, 61.55, 61.47 (4  $\text{CH}_2^6$ ), 23.01, 22.98, 22.89, 22.83 ( $\text{OCH}_2\text{CH}_2$ ), 11.13, 11.04, 10.98, 10.92 (4  $\text{CH}_3$ ).

$\text{MS (ESI}^+)$ :  $m/z$  calcd for  $[\text{C}_9\text{H}_{18}\text{O}_6]$ : 222.11; found: 245.15  $[\text{M}+\text{Na}]^+$ .

$\text{MS (ESI}^-)$ :  $m/z$  calcd for  $[\text{C}_9\text{H}_{18}\text{O}_6]$ : 222.11; found: 221.43  $[\text{M}-\text{H}]^-$ .

## 5.7.4 Characterization of 2-propyl D-glucoside isomeric mixture (22ad)



$R_f$  (eluent: DCM/MeOH; 9:1): 0.27; 0.39; 0.44.

Isomeric ratio a/b/c/d:18/20/28/34.

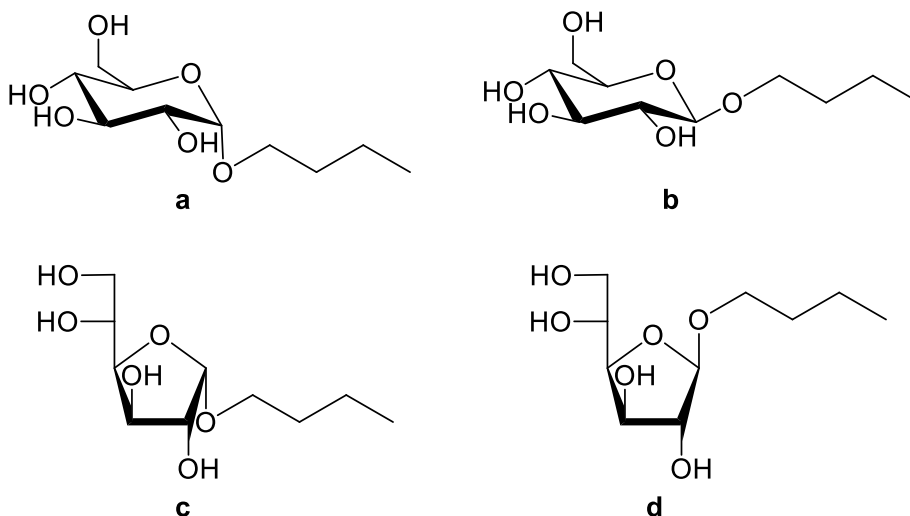
**$^1\text{H NMR}$  (DMSO- $d_6$ , 400 MHz):**  $\delta$  (ppm) 5.26 (d,  $J = 2.2$  Hz, OH), 5.03 (d,  $J = 4.0$  Hz,  $\text{CH}^1_{\alpha\text{-Fu}}$ ), 4.85 (d,  $J = 3.9$  Hz, OH), 4.79 (br s,  $\text{CH}^1_{\beta\text{-Fu}}$ ), 4.73 (d,  $J = 3.8$  Hz,  $\text{CH}^1_{\alpha\text{-Py}}$ ), 4.52 (d,  $J = 4.7$  Hz, OH), 4.48 – 4.34 (m, OH), 4.17 (d,  $J = 7.8$  Hz,  $\text{CH}^1_{\beta\text{-Py}}$ ), 3.98 (br s, CH), 3.91 (m, CH, CH), 3.87 – 3.80 (m, CH, CH, CH, OCH), 3.80 – 3.70 (m, CH, CH, OCH, OCH), 3.67 – 3.53 (m, CH,  $\text{CH}_2^6$ ), 3.46 – 3.31 (m, CH, CH, CH, OCH), 3.19 – 3.14 (m, CH), 3.14 – 3.10 (m, CH), 3.09 – 2.99 (m, CH, CH), 2.89 (m, CH), 1.15 (t,  $J = 5.2$  Hz,  $\text{CH}_3$ ), 1.09 (m,  $\text{CH}_3$ ).

**$^{13}\text{C NMR}$  (DMSO- $d_6$ , 101 MHz):**  $\delta$  (ppm) 107.41 ( $\text{CH}^1_{\beta\text{-Fu}}$ ), 101.48 ( $\text{CH}^1_{\beta\text{-Py}}$ ), 100.93 ( $\text{CH}^1_{\alpha\text{-Fu}}$ ), 97.27 ( $\text{CH}^1_{\alpha\text{-Py}}$ ), 81.40, 81.34, 78.54, 77.83, 77.31, 77.19, 76.06, 75.97, 73.95, 73.72, 73.20, 72.31, 70.92, 70.61 (14 CH), 70.40, 70.39, 70.34 (3 OCH), 70.28 (CH), 69.35 (OCH), 69.06 (CH), 64.15, 63.96, 61.58, 61.50 (4  $\text{CH}_2^6$ ), 23.99, 23.91, 23.89, 23.80, 22.50, 22.19, 22.12, 21.88 (8  $\text{CH}_3$ ).

**MS (ESI $^+$ ):**  $m/z$  calcd for  $[\text{C}_9\text{H}_{18}\text{O}_6]$ : 222.11; found: 245.34  $[\text{M}+\text{Na}]^+$ .

**MS (ESI $^-$ ):**  $m/z$  calcd for  $[\text{C}_9\text{H}_{18}\text{O}_6]$ : 222.11; found: 221.23  $[\text{M}-\text{H}]^-$ , 443.03  $[2\text{M}-\text{H}]^-$ .

## 5.7.5 Characterization of 1-butyl D-glucoside isomeric mixture (23ad)



$R_f$  (eluent: DCM/MeOH; 9:1): 0.32; 0.40; 0.47.

Isomeric ratio a/b/c/d: 46/38/6/10.

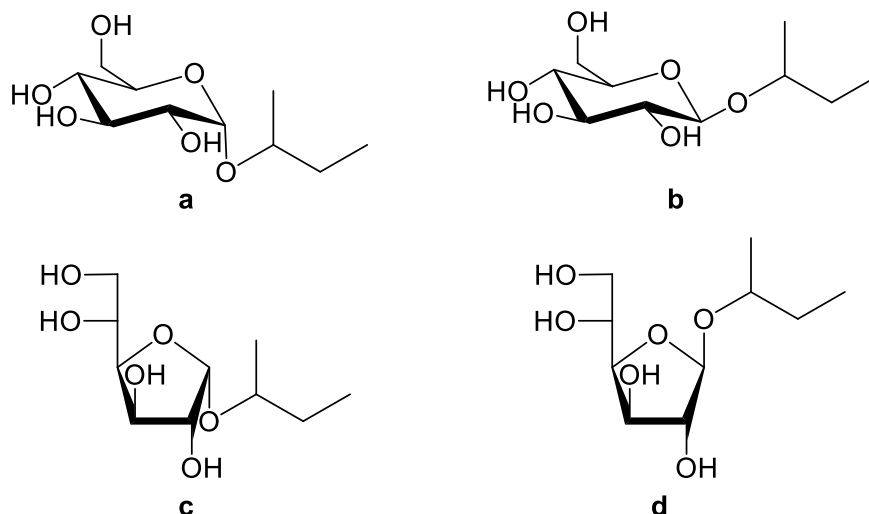
$^1\text{H NMR}$  (DMSO- $d_6$ , 400 MHz):  $\delta$  (ppm) 5.27 (d,  $J = 3.9$  Hz, OH), 5.03 (d,  $J = 4.8$  Hz, OH), 4.93 (d,  $J = 4.9$  Hz, OH), 4.90 (m, OH,  $\text{CH}^1_{\alpha\text{-Fu}}$ ), 4.87 (d,  $J = 4.8$  Hz, OH), 4.85 (d,  $J = 5.4$  Hz, OH), 4.72 (d,  $J = 4.8$  Hz, OH), 4.69 (br s,  $\text{CH}^1_{\beta\text{-Fu}}$ ), 4.61 (m,  $\text{CH}^1_{\alpha\text{-Py}}$ , OH), 4.60 – 4.55 (m, OH), 4.53 (d,  $J = 5.4$  Hz, OH), 4.50 (d,  $J = 5.3$  Hz, OH), 4.49 – 4.36 (m, OH), 4.10 (d,  $J = 7.9$  Hz,  $\text{CH}^1_{\beta\text{-Py}}$ ), 4.00 (dd,  $J = 8.0, 4.6$  Hz, CH), 3.91 (m, CH), 3.88 – 3.77 (m, CH, CH, CH, CH, CH), 3.77 – 3.69 (m, CH,  $\text{OCH}_2$ ), 3.68 – 3.52 (m, CH, CH, CH, CH, CH,  $\text{CH}_2^6$ ,  $\text{OCH}_2$ ), 3.48 – 3.39 (m, CH, CH, CH,  $\text{CH}_2^6$ ,  $\text{OCH}_2$ ), 3.36 – 3.27 (m, CH,  $\text{CH}_2^6$ ,  $\text{OCH}_2$ ), 3.20 – 3.15 (m, CH), 3.15 – 3.08 (m, CH), 3.08 – 3.00 (m, CH, CH), 2.97 – 2.90 (m, CH), 1.58 – 1.41 (m,  $\text{OCH}_2\text{CH}_2$ ), 1.41 – 1.22 (m,  $\text{OCH}_2\text{CH}_2\text{CH}_2$ ), 0.94 – 0.83 (m,  $\text{CH}_3$ ).

$^{13}\text{C NMR}$  (DMSO- $d_6$ , 101 MHz):  $\delta$  (ppm) 109.19 ( $\text{CH}^1_{\beta\text{-Fu}}$ ), 103.30 ( $\text{CH}^1_{\beta\text{-Py}}$ ), 102.39 ( $\text{CH}^1_{\alpha\text{-Fu}}$ ), 98.92 ( $\text{CH}^1_{\alpha\text{-Py}}$ ), 81.59, 80.99, 78.58, 77.69, 77.25, 77.23, 76.12, 75.87, 73.90, 73.73, 73.18, 72.43, 70.80, 70.54, 70.45, 70.28 (16 CH), 68.68, 67.95, 67.28, 66.92 (4  $\text{OCH}_2$ ), 64.14, 63.89, 61.54, 61.44 (4  $\text{CH}_2$ ), 31.81 – 31.67 ( $\text{OCH}_2\text{CH}_2$ ), 19.40 – 19.09 ( $\text{OCH}_2\text{CH}_2\text{CH}_2$ ), 14.27 – 14.17 ( $\text{CH}_3$ ).

$\text{MS (ESI}^+)$ :  $m/z$  calcd for  $[\text{C}_{10}\text{H}_{20}\text{O}_6]$ : 236.13; found: 259.08  $[\text{M}+\text{Na}]^+$ .

$\text{MS (ESI}^-)$ :  $m/z$  calcd for  $[\text{C}_{10}\text{H}_{20}\text{O}_6]$ : 236.13; found: 471.14  $[2\text{M}-\text{H}]^-$ .

## 5.7.6 Characterization of 2-butyl D-glucoside isomeric mixture (24ad)



$R_f$  (eluent: DCM/MeOH; 9:1): 0.34; 0.40; 0.47.

Isomeric ratio a/b/c/d: 36/32/12/20.

**$^1\text{H NMR}$  (DMSO- $d_6$ , 400 MHz):**  $\delta$  (ppm) 5.29 (d,  $J = 4.5$  Hz, OH), 5.25 (d,  $J = 3.8$  Hz, OH), 5.01 (m,  $\text{CH}^1_{\alpha\text{-Fu}}$ ), 4.95 (d,  $J = 4.0$  Hz, OH), 4.91 – 4.82 (m, OH), 4.78 (br s,  $\text{CH}^1_{\beta\text{-Fu}}$ ), 4.74 (d,  $J = 3.8$  Hz,  $\text{CH}^1_{\alpha\text{-Py}}$ ), 4.72 (d,  $J = 3.8$  Hz,  $\text{CH}^1_{\alpha\text{-Py}}$ ), 4.68 (d,  $J = 4.8$  Hz, OH), 4.54 – 4.43 (m, OH), 4.43 – 4.33 (m, OH), 4.17 (d,  $J = 7.6$  Hz,  $\text{CH}^1_{\beta\text{-Py}}$ ), 4.09 – 4.07 (m, CH), 4.07 – 3.97 (m, CH, CH, CH,  $\text{CH}_2^6$ ), 3.93 – 3.86 (m, CH,  $\text{CH}_2^6$ ), 3.86 – 3.76 (m, 7 CH), 3.76 – 3.72 (m, CH), 3.72 – 3.49 (m, 7 CH,  $\text{CH}_2^6$ , 8 OCH), 3.49 – 3.35 (m, 5 CH,  $\text{CH}_2^6$ ), 3.17 – 3.15 (m, CH), 3.15 – 2.98 (m, CH, CH, CH, CH), 2.95 – 2.87 (m, CH, CH), 1.58 – 1.45 (m, OCHCH<sub>2</sub>), 1.46 – 1.34 (m, OCHCH<sub>2</sub>), 1.17 – 1.11 (m, OCHCH<sub>3</sub>), 1.11 – 1.03 (m, OCHCH<sub>3</sub>), 0.91 – 0.81 (m, CH<sub>3</sub>).

**$^{13}\text{C NMR}$  (DMSO- $d_6$ , 101 MHz):**  $\delta$  (ppm) 108.74 ( $\text{CH}^1_{\beta\text{-Fu}}$ ), 104.43 ( $\text{CH}^1_{\beta\text{-Fu}}$ ), 102.82 ( $\text{CH}^1_{\beta\text{-Py}}$ ), 102.10 ( $\text{CH}^1_{\alpha\text{-Fu}}$ ), 101.20 ( $\text{CH}^1_{\beta\text{-Py}}$ ), 99.97 ( $\text{CH}^1_{\alpha\text{-Py}}$ ), 98.87 ( $\text{CH}^1_{\alpha\text{-Py}}$ ), 96.41 ( $\text{CH}^1_{\alpha\text{-Py}}$ ), 81.65, 81.44, 80.96, 80.35, 78.64, 78.46, 78.01, 77.35, 77.31, 77.19, 77.15, 77.03, (12 CH), 76.28 (OCH), 76.21, 76.03, 75.86, 75.79 (4 CH), 75.51, 75.44, 74.89, 74.47 (4 OCH), 74.23, 74.12, 73.94, 73.70, 73.65 (5 CH), 73.46 (OCH), 73.37 (CH), 73.25, 73.05 (2 OCH), 72.55, 72.30, 70.93, 70.83, 70.67, 70.64, 70.57, 70.44, 70.27, 70.13 (10 CH), 66.76, 65.43, 64.19, 64.16, 63.95, 61.66, 61.63, 61.51, 61.45 (8  $\text{CH}_2^6$ ), 30.11, 30.06, 30.04, 30.03 29.97, 29.44, 29.06, 29.03 (8

## 5 | Experimental section

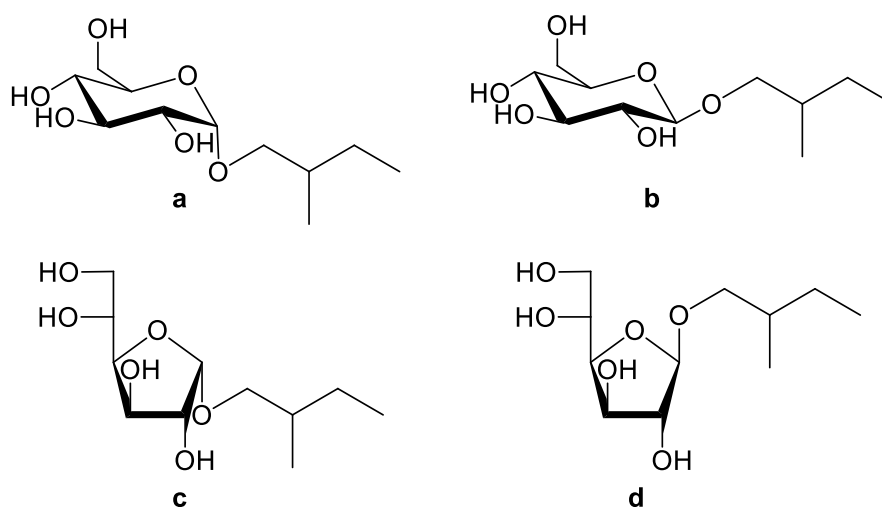
---

OCHCH<sub>2</sub>), 21.50, 21.46, 21.33, 21.26, 19.63, 19.34, 19.28, 18.93 (8 OCHCH<sub>3</sub>), 10.61, 10.60, 10.29, 10.27, 10.12, 10.00, 9.85, 9.81 (8 CH<sub>3</sub>).

**MS (ESI<sup>+</sup>):** *m/z* calcd for [C<sub>10</sub>H<sub>20</sub>O<sub>6</sub>]: 236.13; found: 259.37 [M+Na]<sup>+</sup>, 495.24 [2M+Na]<sup>+</sup>.

**MS (ESI<sup>-</sup>):** *m/z* calcd for [C<sub>10</sub>H<sub>20</sub>O<sub>6</sub>]: 236.13; found: 235.99 [M-H]<sup>-</sup>, 471.73 [2M-H]<sup>-</sup>.

## 5.7.7 Characterization of 2-methyl-1-butyl D-glucoside isomeric mixture (25ad)



$R_f$  (eluent: DCM/MeOH; 9:1): 0.34; 0.41; 0.48.

Isomeric ratio a/b/c/d: 37/29/14/20.

$^1\text{H NMR}$  (DMSO- $d_6$ , 400 MHz):  $\delta$  (ppm) 5.27 (d,  $J = 3.9$  Hz, OH), 5.03 (d,  $J = 4.8$  Hz, OH), 4.91 (d,  $J = 5.2$  Hz, OH), 4.89 – 4.87 (m,  $\text{CH}^1_{\alpha\text{-Fu}}$ ), 4.85 (d,  $J = 5.6$  Hz, OH), 4.72 (d,  $J = 4.8$  Hz, OH), 4.69 (s,  $\text{CH}^1_{\beta\text{-Fu}}$ ), 4.60 (d,  $J = 3.0$  Hz,  $\text{CH}^1_{\alpha\text{-Py}}$ ), 4.58 (s, OH), 4.57 – 4.51 (m, OH), 4.49 (d,  $J = 5.3$  Hz, OH), 4.47 – 4.34 (m, OH), 4.11 (d,  $J = 5.2$  Hz,  $\text{CH}^1_{\beta\text{-Py}}$ ), 4.08 (d,  $J = 4.9$  Hz, CH), 4.01 (dd,  $J = 8.2, 4.1$  Hz, CH), 3.92 (t,  $J = 4.6$  Hz, CH), 3.89 – 3.78 (m, CH, CH, CH, CH), 3.74 (dd,  $J = 5.5, 2.8$  Hz, CH), 3.69 – 3.61 (m, CH,  $\text{CH}_2^6$ ,  $\text{OCH}_2$ ), 3.62 – 3.52 (m,  $\text{CH}_2^6$ ,  $\text{OCH}_2$ ), 3.49 – 3.33 (m, 6 CH,  $\text{CH}_2^6$ ,  $\text{OCH}_2$ ), 3.27 (dd,  $J = 9.5, 6.3$  Hz,  $\text{OCH}_2$ ), 3.20 – 3.14 (m, CH,  $\text{OCH}_2$ ), 3.14 – 3.07 (m, CH,  $\text{OCH}_2$ ), 3.08 – 3.01 (m, CH, CH, CH), 2.95 (td,  $J = 8.3, 5.0$  Hz, CH), 1.66 – 1.51 (m,  $\text{OCH}_2\text{CH}$ ), 1.51 – 1.34 (m,  $\text{OCH}_2\text{CHCH}_2$ ), 1.18 – 1.01 (m,  $\text{OCH}_2\text{CHCH}_2$ ), 0.91 – 0.81 (m,  $\text{CH}_3$ ).

$^{13}\text{C NMR}$  (DMSO- $d_6$ , 101 MHz):  $\delta$  (ppm) 109.33, 109.26 (2  $\text{CH}^1_{\beta\text{-Fu}}$ ), 103.68, 103.54 (2  $\text{CH}^1_{\beta\text{-Py}}$ ), 102.43, 102.33 (2  $\text{CH}^1_{\alpha\text{-Py}}$ ), 99.14, 99.06 (2  $\text{CH}^1_{\alpha\text{-Py}}$ ), 81.64, 80.94, 80.35, 78.64, 78.52, 78.50, 77.82, 77.79, 77.28, 76.13, 75.88 (11 CH), 74.18, 74.12 (2  $\text{OCH}_2$ ), 73.95, 73.93, 73.69, 73.27, 73.26 (5 CH), 73.16, 72.64, 72.59 (3  $\text{OCH}_2$ ), 72.48 (CH), 72.30, 72.29 (2  $\text{OCH}_2$ ), 70.78, 70.57, 70.54, 70.28 (4 CH), 64.15, 63.88, 61.55, 61.44 (4  $\text{CH}_2^6$ ), 34.97, 34.89, 34.87, 34.83, 34.78 (5  $\text{OCH}_2\text{CH}$ ), 26.22, 26.12,

## 5 | Experimental section

---

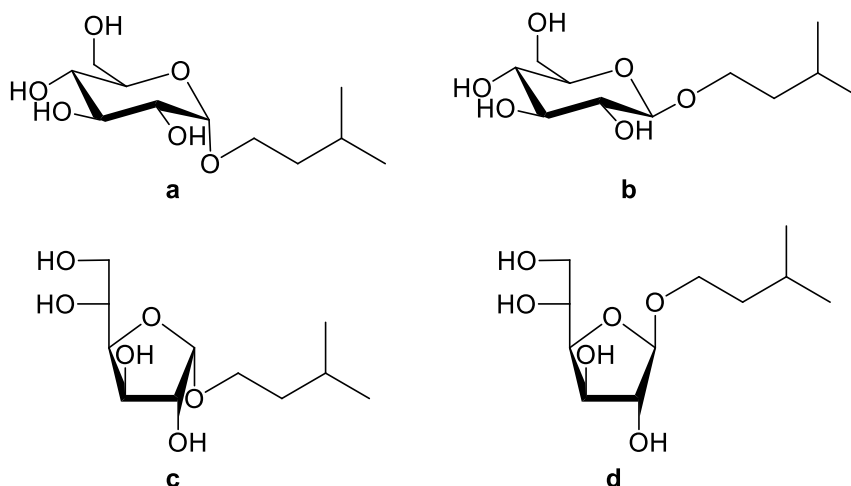
26.10, 26.06 (4 OCH<sub>2</sub>CHCH<sub>2</sub>), 17.13, 16.97, 16.92, 16.88, 16.85, 16.82 (6 OCH<sub>2</sub>CHCH<sub>3</sub>), 11.77, 11.63, 11.60, 11.56, 11.54, 11.52 (CH<sub>3</sub>).

**MS (ESI<sup>+</sup>):** *m/z* calcd for [C<sub>11</sub>H<sub>22</sub>O<sub>6</sub>]: 250.14; found: 273.42 [M+Na]<sup>+</sup>, 523.12 [2M+Na]<sup>+</sup>.

**MS (ESI<sup>-</sup>):** *m/z* calcd for [C<sub>11</sub>H<sub>22</sub>O<sub>6</sub>]: 250.14; found: 249.89 [M-H]<sup>-</sup>, 499.30 [2M-H]<sup>-</sup>.



### 5.7.8 Characterization of 3-methyl-1-butyl D-glucoside isomeric mixture (26ad)



$R_f$  (eluent: DCM/MeOH; 9:1): 0.34; 0.41; 0.48.

Isomeric ratio a/b/c/d: 43/34/10/13.

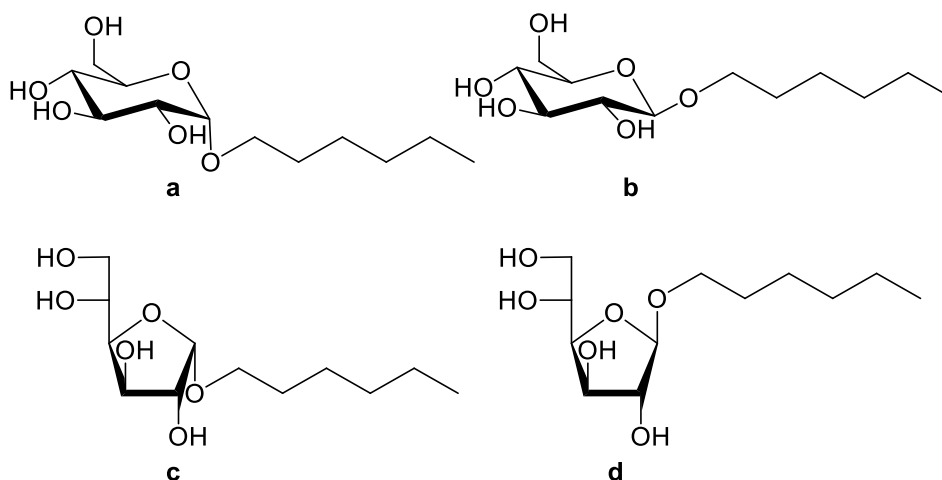
$^1\text{H NMR}$  (DMSO- $d_6$ , 400 MHz):  $\delta$  (ppm) 5.28 (d,  $J = 4.6$  Hz, OH), 5.26 (d,  $J = 3.9$  Hz, OH), 5.02 (d,  $J = 4.8$  Hz, OH), 4.91 (m,  $\text{CH}^1_{\alpha\text{-Fu}}$ , OH), 4.87 (d,  $J = 4.8$  Hz, OH), 4.84 (d,  $J = 5.4$  Hz, OH), 4.72 (d,  $J = 4.8$  Hz, OH), 4.69 (br s,  $\text{CH}^1_{\beta\text{-Fu}}$ ), 4.61 (d,  $J = 3.7$  Hz,  $\text{CH}^1_{\alpha\text{-Py}}$ ), 4.59 (d,  $J = 6.2$  Hz, OH), 4.57 – 4.34 (m, OH), 4.12 – 4.07 (m,  $\text{CH}^1_{\beta\text{-Py}}$ , CH), 4.01 – 3.98 (m, CH), 3.93 – 3.89 (m, CH), 3.88 – 3.84 (m, CH), 3.83 – 3.76 (m, CH,  $\text{OCH}_2$ ), 3.75 – 3.71 (m, CH), 3.69 – 3.55 (m, CH, CH,  $\text{CH}_2^6$ ,  $\text{OCH}_2$ ), 3.48 – 3.38 (m, CH,  $\text{CH}_2^6$ ,  $\text{OCH}_2$ ), 3.37 – 3.30 (m, CH,  $\text{OCH}_2$ ), 3.21 – 3.14 (m, CH), 3.14 – 3.09 (m, CH), 3.09 – 3.01 (m, CH, CH), 2.96 – 2.89 (m, CH), 1.76 – 1.62 (m,  $\text{CH}(\text{CH}_3)_2$ ), 1.52 – 1.34 (m,  $\text{OCH}_2\text{CH}_2$ ), 0.87 (m,  $(\text{CH}_3)_2$ ).

$^{13}\text{C NMR}$  (DMSO- $d_6$ , 101 MHz):  $\delta$  (ppm) 109.21 ( $\text{CH}^1_{\beta\text{-Fu}}$ ), 103.32 ( $\text{CH}^1_{\beta\text{-Py}}$ ), 102.34 ( $\text{CH}^1_{\alpha\text{-Fu}}$ ), 99.02 ( $\text{CH}^1_{\alpha\text{-Py}}$ ), 81.59, 80.98, 78.58, 77.70, 77.27, 77.26, 76.13, 75.85, 73.89, 73.72, 73.25, 72.41, 70.78, 70.55, 70.47, 70.25 (16 CH), 67.36, 66.56, 65.90, 65.66 ( $\text{OCH}_2$ ), 64.13, 63.91 (2  $\text{CH}_2^6$ ), 38.58, 38.56, 38.51, 38.49 ( $\text{OCH}_2\text{CH}_2$ ), 24.97, 24.88, 24.87, 24.86 (4  $\text{CH}(\text{CH}_3)_2$ ), 23.20, 23.02, 22.99, 22.83, 22.80, 22.76 (6  $\text{CH}_3$ ).

$\text{MS (ESI}^+)$ :  $m/z$  calcd for  $[\text{C}_{11}\text{H}_{22}\text{O}_6]$ : 250.14; found: 273.28  $[\text{M}+\text{Na}]^+$ .

$\text{MS (ESI}^-)$ :  $m/z$  calcd for  $[\text{C}_{11}\text{H}_{22}\text{O}_6]$ : 250.14; found: 250.07  $[\text{M}-\text{H}]^-$ .

## 5.7.9 Characterization of 1-hexyl D-glucoside isomeric mixture (27ad)



$R_f$  (eluent: DCM/MeOH; 9:1): 0.34; 0.43; 0.50.

Isomeric ratio a/b/c/d: 37/32/14/17.

$^1\text{H NMR}$  (DMSO- $d_6$ , 400 MHz):  $\delta$  (ppm) 5.29 (d,  $J = 4.5$  Hz, OH), 5.26 (d,  $J = 3.9$  Hz, OH), 5.03 (d,  $J = 4.9$  Hz, OH), 4.93 (d,  $J = 4.9$  Hz, OH), 4.90 (d,  $J = 4.5$  Hz,  $\text{CH}^1_{\alpha\text{-Fu}}$ ), 4.85 (m, OH), 4.72 (d,  $J = 4.8$  Hz, OH), 4.69 (br s,  $\text{CH}^1_{\beta\text{-Fu}}$ ), 4.60 (m,  $\text{CH}^1_{\alpha\text{-Py}}$ , OH), 4.44 (m, OH), 4.09 (m,  $\text{CH}^1_{\beta\text{-Py}}$ ), 4.07 – 4.04 (m, CH), 4.01 – 3.98 (m, CH), 3.93 – 3.89 (m, CH), 3.88 – 3.84 (m, CH), 3.84 – 3.79 (m, CH, CH, CH), 3.80 – 3.72 (m, CH,  $\text{OCH}_2$ ), 3.70 – 3.54 (m, CH,  $\text{CH}_2^6$ ,  $\text{OCH}_2$ ), 3.47 – 3.28 (m, CH, CH,  $\text{CH}_2^6$ ,  $\text{OCH}_2$ ), 3.21 – 3.14 (m, CH), 3.14 – 3.09 (m, CH), 3.09 – 3.01 (m, CH, CH), 2.93 (td,  $J = 8.3, 5.0$  Hz, CH), 1.58 – 1.45 (m,  $\text{OCH}_2\text{CH}_2$ ), 1.36 – 1.20 (m,  $(\text{CH}_2)_3$ ), 0.87 (m,  $\text{CH}_3$ ).

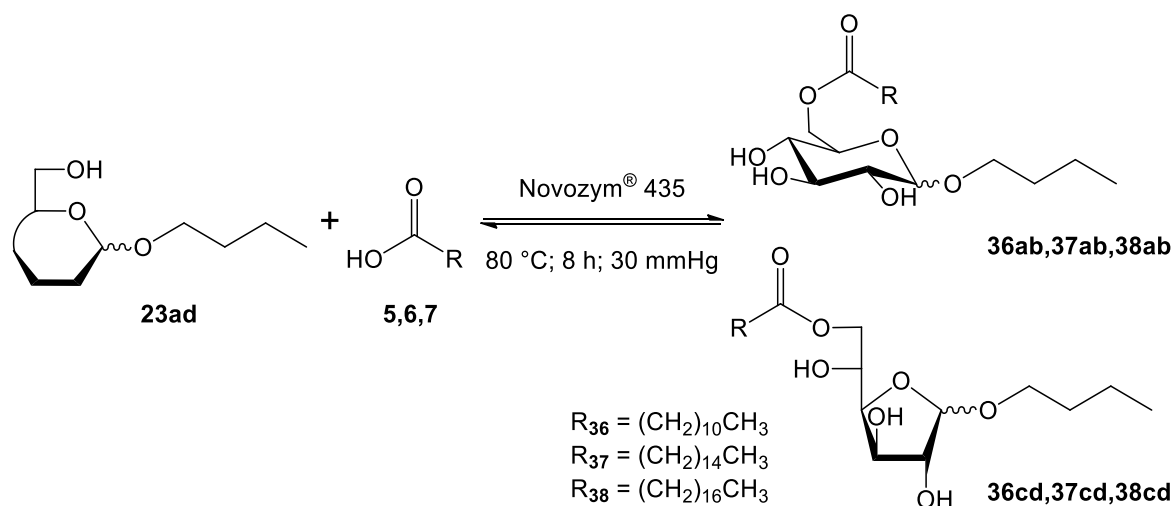
$^{13}\text{C NMR}$  (DMSO- $d_6$ , 101 MHz):  $\delta$  (ppm) 109.22 ( $\text{CH}^1_{\beta\text{-Fu}}$ ), 103.31 ( $\text{CH}^1_{\beta\text{-Py}}$ ), 102.41 ( $\text{CH}^1_{\alpha\text{-Fu}}$ ), 98.95 ( $\text{CH}^1_{\alpha\text{-Py}}$ ), 81.57, 81.00, 80.35, 78.60, 77.68, 77.28, 77.25, 76.12, 75.88, 73.90, 73.72, 73.20, 72.43, 70.79, 70.55, 70.27 (16 CH), 69.02, 68.30, 67.64, 67.26 (4  $\text{OCH}_2$ ), 61.55, 61.44, 61.19 (3  $\text{CH}_2^6$ ), 31.67, 31.63, 31.56 ( $(\text{CH}_2)_3$ ), 29.83, 29.71, 29.59, 29.54 (4  $\text{OCH}_2\text{CH}_2$ ), 25.83, 25.77, 25.67, 25.64, 22.62, 22.55 ( $(\text{CH}_2)_3$ ), 14.40 ( $\text{CH}_3$ ).

$\text{MS (ESI}^+)$ :  $m/z$  calcd for  $[\text{C}_{12}\text{H}_{24}\text{O}_6]$ : 264.16; found: 287.40  $[\text{M}+\text{Na}]^+$ , 531.63  $[2\text{M}+\text{Na}]^+$ .

$\text{MS (ESI}^-)$ :  $m/z$  calcd for  $[\text{C}_{12}\text{H}_{24}\text{O}_6]$ : 264.16; found: 263.21  $[\text{M}-\text{H}]^-$ , 526.89  $[2\text{M}-\text{H}]^-$ .

## 5.8 Alkyl 6-O-acyl-D-glucoside isomeric mixtures

### 5.8.1 Enzymatic synthesis of 1-butyl 6-O-lauroyl-, 6-O-palmitoyl-, 6-O-stearoyl-D-glucosides (36ad-38ad)



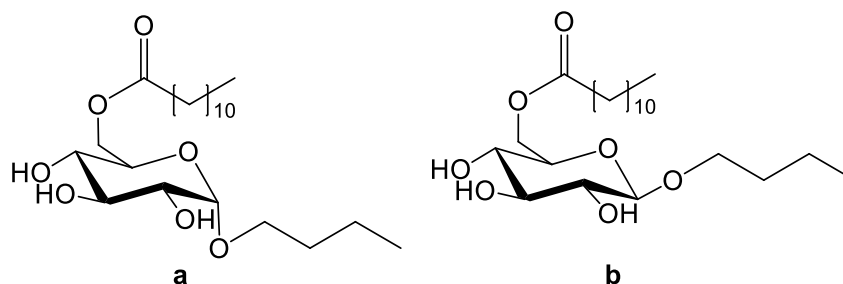
Isomeric mixture of 1-butyl D-glucosides (**23ad**), fatty acids (lauric, **5**, palmitic, **6**, and stearic acid, **7**), in molar ratio 1:1, and Novozym<sup>®</sup> 435 (10 %, w/w) were mixed together and charged into a round-bottom flask. The mixtures were heated to 80 °C while rotating the flask by means of a glass oven B-585 Kugelrohr. After fatty acids melted, the reactions were performed under reduced pressure (30 mmHg).

After 8 h, reaction mixtures were taken up in EtOAc and the immobilized enzyme was removed by filtration. Then, the esters were extracted in EtOAc (2 times) from 1 M NaOH, the organic phases were collected, dried over Na<sub>2</sub>SO<sub>4</sub> and the solvent was removed under reduced pressure. Couple of isomers were isolated by flash chromatography (*n*-hexane/EtOAc; 2:8), thus affording six 1'-butyl 6-O-acyl-glucosides: **1-butyl 6-O-lauroyl-D-glucopyranosides (36ab)**, **1-butyl 6-O-lauroyl-D-glucofuranosides (36cd)**, **1-butyl 6-O-palmitoyl-D-glucopyranosides (37ab)**, **1-butyl 6-O-palmitoyl-D-glucofuranosides (37cd)**, **1-butyl 6-O-stearoyl-D-glucopyranosides (38ab)**, and **1-butyl 6-O-stearoyl-D-glucofuranosides (38cd)**. All products were fully characterized by TLC, ESI-MS and NMR analysis. Yields and isomeric ratios of each isomeric couple, estimated by <sup>1</sup>H NMR analysis, carried out in DMSO-*d*<sub>6</sub>, as the ratio of the areas of the two anomeric proton signals, are listed in **Table 3.5**.

*Table 3.5. Yields and isomeric ratios of 1-butyl 6-O-acyl-D-glucosides.*

<i>Compound</i>	<i>Yield (%)</i>	<i>Isomeric ratio (%)</i>	<i>Compound</i>	<i>Yield (%)</i>	<i>Isomeric ratio (%)</i>
<b>36ab</b>	<b>37</b>	68/32	<b>36cd</b>	5	59/41
<b>37ab</b>	<b>47</b>	63/37	<b>37cd</b>	10	55/45
<b>38ab</b>	<b>52</b>	62/38	<b>38cd</b>	13	56/44

## 5.8.2 Characterization of 1-butyl 6-O-lauroyl-D-glucopyranosides (36ab)



$R_f$  (eluent: *n*-hexane/EtOAc; 2:8): 0.33.

Isomeric ratio a/b: 68/32.

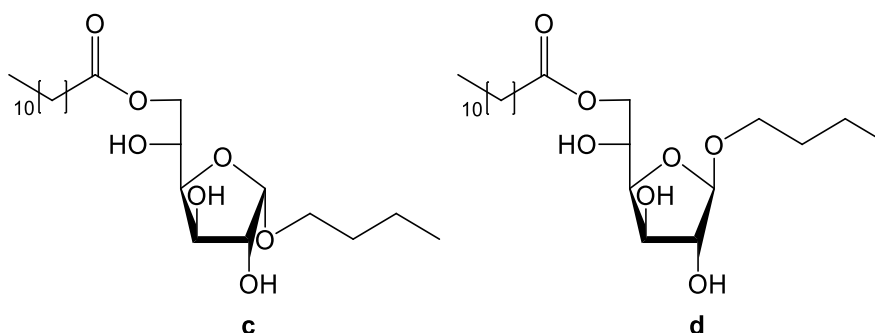
$^1\text{H NMR}$  (DMSO- $d_6$ , 400 MHz):  $\delta$  (ppm) 5.12 (br s, OH), 5.02 (br s, OH), 4.69 (br s, OH), 4.62 (d,  $J = 3.6$  Hz,  $\text{CH}^1_\alpha$ ), 4.30 (m,  $\text{CH}_2^{6'}_\alpha$ ,  $\text{CH}_2^{6'}_\beta$ ), 4.13 (d,  $J = 7.8$  Hz,  $\text{CH}^1_\beta$ ), 4.02 (m,  $\text{CH}_2^{6''}_\alpha$ ,  $\text{CH}_2^{6''}_\beta$ ), 3.69 (dt,  $J = 9.7, 6.7$  Hz,  $\text{OCH}_2^2_\beta$ ), 3.61 – 3.51 (m,  $\text{CH}^5_\alpha$ ,  $\text{OCH}_2^2_\alpha$ ), 3.47 – 3.36 (m,  $\text{CH}^3_\alpha$ ,  $\text{OCH}_2^2_\beta$ ), 3.36 – 3.28 (m,  $\text{CH}^5_\beta$ ,  $\text{OCH}_2^2_\alpha$ ), 3.23 – 3.16 (m,  $\text{CH}^2_\alpha$ ), 3.14 (d,  $J = 8.9$  Hz,  $\text{CH}^3_\beta$ ), 3.09 – 2.99 (m,  $\text{CH}^4_\alpha$ ,  $\text{CH}^4_\beta$ ), 2.95 (t,  $J = 8.3$  Hz,  $\text{CH}^2_\beta$ ), 2.28 (br td,  $J = 7.3, 4.4$  Hz,  $\text{COOCH}_2$ ), 2.18 (t,  $J = 7.4$  Hz,  $\text{HCOOCH}_2$ ), 1.59 – 1.43 (m,  $\text{COOCH}_2\text{CH}_2$ ,  $\text{OCH}_2\text{CH}_2$ ), 1.42 – 1.31 (m,  $\text{OCH}_2\text{CH}_2\text{CH}_2$ ), 1.31 – 1.17 (br s,  $(\text{CH}_2)_8$ ), 0.93 – 0.81 (m,  $\text{CH}_3$ ).

$^{13}\text{C NMR}$  (DMSO- $d_6$ , 101 MHz):  $\delta$  (ppm) 174.95 (HCOO), 173.24 ( $\text{COO}_\beta$ ), 173.18 ( $\text{COO}_\alpha$ ), 103.33 ( $\text{CH}^1_\beta$ ), 99.02 ( $\text{CH}^1_\alpha$ ), 76.93 ( $\text{CH}^3_\beta$ ), 74.04 ( $\text{CH}^5_\beta$ ), 73.78 ( $\text{CH}^2_\beta$ ), 73.56 ( $\text{CH}^3_\alpha$ ), 72.26 ( $\text{CH}^2_\alpha$ ), 71.00 ( $\text{CH}^4_\alpha$ ), 70.65 ( $\text{CH}^4_\beta$ ), 70.25 ( $\text{CH}^5_\alpha$ ), 68.75 ( $\text{OCH}_2_\beta$ ), 67.17 ( $\text{OCH}_2_\alpha$ ), 64.21 ( $\text{CH}_2^{6'}_\alpha$ ), 64.03 ( $\text{CH}_2^{6'}_\beta$ ), 34.12 (HCOOCH<sub>2</sub>), 34.04 (COOCH<sub>2</sub>), 31.84 ( $\text{OCH}_2\text{CH}_2_\beta$ ), 31.76 ( $\text{OCH}_2\text{CH}_2_\alpha$ ), 29.46 – 28.90 ( $(\text{CH}_2)_{12}$ ), 24.95 ( $\text{COOCH}_2\text{CH}_2$ ), 22.56 ( $\text{CH}_2\text{CH}_3$ ), 19.39 ( $\text{OCH}_2\text{CH}_2\text{CH}_2_\alpha$ ), 19.13 ( $\text{OCH}_2\text{CH}_2\text{CH}_2_\beta$ ), 14.41, 14.16 ( $\text{CH}_3$ ).

**MS (ESI<sup>+</sup>):**  $m/z$  calcd for  $[\text{C}_{22}\text{H}_{42}\text{O}_7]$ : 418.29; found: 441.50  $[\text{M}+\text{Na}]^+$ ; 859.30  $[2\text{M}+\text{Na}]^+$ .

**MS (ESI<sup>-</sup>):**  $m/z$  calcd for  $[\text{C}_{22}\text{H}_{42}\text{O}_7]$ : 418.29; found: 417.22  $[\text{M}-\text{H}]^-$ , 835.49  $[2\text{M}-\text{H}]^-$ .

## 5.8.3 Characterization of 1-butyl 6-O-lauroyl-D-glucofuranosides (36cd)



$R_f$  (eluent: *n*-hexane/EtOAc; 2:8): 0.60.

Isomeric ratio c/d: 59/41.

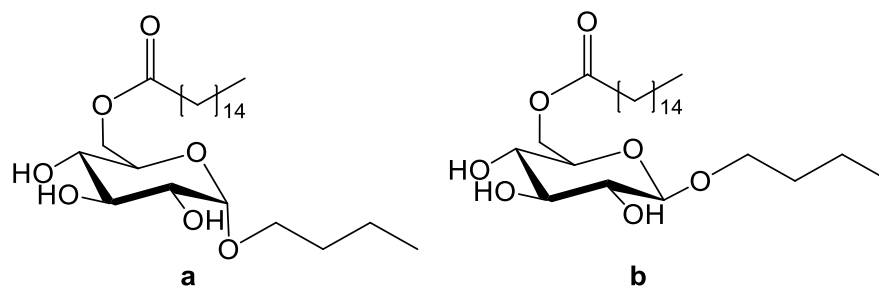
**$^1\text{H NMR}$  (DMSO- $d_6$ , 400 MHz):**  $\delta$  (ppm)  $\delta$  5.34 (d,  $J = 3.9$  Hz, OH), 5.13 (d,  $J = 4.7$  Hz, OH), 4.96 (d,  $J = 4.0$  Hz,  $\text{CH}^{1\alpha}$ ), 4.82 (m, OH), 4.75 (br s,  $\text{CH}^{1\beta}$ ), 4.70 (d,  $J = 5.0$  Hz, OH), 4.65 (d,  $J = 5.4$  Hz, OH), 4.30 (q,  $J = 5.4$  Hz,  $\text{CH}_2^{6\alpha}$ ), 4.27 – 4.20 (m,  $\text{CH}_2^{6\beta}$ ), 4.07 – 3.97 (m, CH, CH, CH,  $\text{CH}_2^{6''}$ ), 3.95 – 3.84 (m, 5 CH), 3.69 – 3.57 (m,  $\text{OCH}_2'$ ), 3.47 (dt,  $J = 9.8, 6.6$  Hz,  $\text{OCH}_2''$ ), 3.40 – 3.33 (m,  $\text{OCH}_2''$ ), 2.34 (td,  $J = 7.4, 2.9$  Hz,  $\text{COOCH}_2$ ), 1.63 – 1.47 (m,  $\text{COOCH}_2\text{CH}_2$ ,  $\text{OCH}_2\text{CH}_2$ ), 1.43 – 1.25 (m,  $(\text{CH}_2)_8$ ,  $\text{OCH}_2\text{CH}_2\text{CH}_2$ ), 0.97 – 0.88 (m,  $\text{CH}_3$ ).

**$^{13}\text{C NMR}$  (DMSO- $d_6$ , 101 MHz):**  $\delta$  (ppm) 173.42 ( $\text{COO}_\beta$ ), 173.41 ( $\text{COO}_\alpha$ ), 109.27 ( $\text{CH}^{1\beta}$ ), 102.42 ( $\text{CH}^{1\alpha}$ ), 81.93, 80.96, 78.69, 77.80, 75.77, 75.63 (6 CH), 67.95, 67.34 (2  $\text{OCH}_2$ ), 67.23 (CH), 67.10 ( $\text{CH}_2^6$ ), 66.96 (CH), 66.73 ( $\text{CH}_2^6$ ), 34.02 ( $\text{COOCH}_2$ ), 31.84, 31.75 (2  $\text{OCH}_2\text{CH}_2$ ), 29.45, 29.44, 29.35, 29.34, 29.17, 29.16, 29.15, 28.94, 28.92 ( $(\text{CH}_2)_8$ ), 24.95, 24.92 (2  $\text{COOCH}_2\text{CH}_2$ ), 19.26, 19.23 (2  $\text{OCH}_2\text{CH}_2\text{CH}_2$ ), 14.40, 14.16, 14.13 (3  $\text{CH}_3$ ).

**MS (ESI $^+$ ):**  $m/z$  calcd for  $[\text{C}_{22}\text{H}_{42}\text{O}_7]$ : 418.29; found: 441.68  $[\text{M}+\text{Na}]^+$ ; 859.00  $[2\text{M}+\text{Na}]^+$ .

**MS (ESI $^-$ ):**  $m/z$  calcd for  $[\text{C}_{22}\text{H}_{42}\text{O}_7]$ : 418.29; found: 417.78  $[\text{M}-\text{H}]^-$ .

## 5.8.4 Characterization of 1-butyl 6-O-palmitoyl-D-glucopyranosides (37ab)



$R_f$  (eluent: *n*-hexane/EtOAc; 2:8): 0.33.

Isomeric ratio a/b: 63/37.

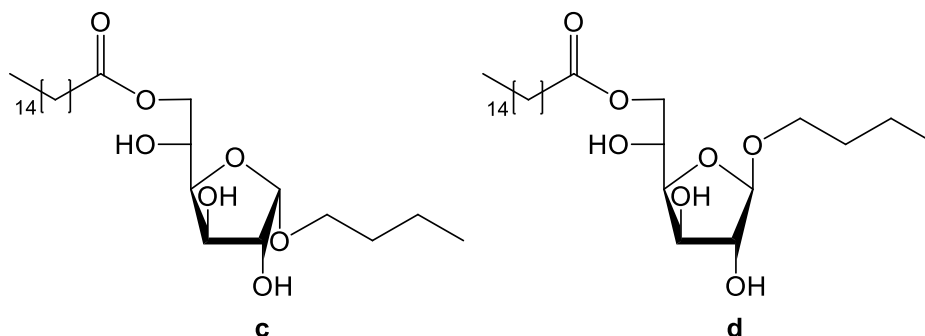
$^1\text{H NMR}$  (DMSO- $d_6$ , 400 MHz):  $\delta$  (ppm) 5.13 (d,  $J = 5.2$  Hz, OH), 5.02 (d,  $J = 4.8$  Hz, OH), 4.85 (d,  $J = 3.6$  Hz, OH), 4.69 (d,  $J = 6.2$  Hz, OH), 4.62 (d,  $J = 3.6$  Hz,  $\text{CH}^1_\alpha$ ), 4.30 (m,  $\text{CH}_2^{6\prime}_\alpha$ ,  $\text{CH}_2^{6\prime}_\beta$ ), 4.13 (d,  $J = 7.8$  Hz,  $\text{CH}^1_\beta$ ), 4.02 (ddd,  $J = 23.5, 11.7, 7.1$  Hz,  $\text{CH}_2^{6''}_\alpha$ ,  $\text{CH}_2^{6''}_\beta$ ), 3.69 (dt,  $J = 9.7, 6.7$  Hz,  $\text{OCH}_2'\beta$ ), 3.61 – 3.53 (m,  $\text{CH}^5_\alpha$ ,  $\text{OCH}_2'\alpha$ ), 3.47 – 3.36 (m,  $\text{CH}^3_\alpha$ ,  $\text{OCH}_2''\beta$ ), 3.36 – 3.29 (m,  $\text{CH}^5_\beta$ ,  $\text{OCH}_2''\alpha$ ), 3.23 – 3.16 (m,  $\text{CH}^2_\alpha$ ), 3.16 – 3.11 (m,  $\text{CH}^3_\beta$ ), 3.09 – 2.99 (m,  $\text{CH}^4_\alpha$ ,  $\text{CH}^4_\beta$ ), 2.95 (td,  $J = 8.5, 5.0$  Hz,  $\text{CH}^2_\beta$ ), 2.32 – 2.24 (m,  $\text{COOCH}_2$ ), 1.57 – 1.45 (m,  $\text{COOCH}_2\text{CH}_2$ ,  $\text{OCH}_2\text{CH}_2$ ), 1.41 – 1.31 (m,  $\text{OCH}_2\text{CH}_2\text{CH}_2$ ), 1.31 – 1.17 (br s,  $(\text{CH}_2)_{12}$ ), 0.93 – 0.82 (m,  $\text{CH}_3$ ).

$^{13}\text{C NMR}$  (DMSO- $d_6$ , 101 MHz):  $\delta$  (ppm) 173.19 (COO), 103.33 ( $\text{CH}^1_\beta$ ), 99.03 ( $\text{CH}^1_\alpha$ ), 76.93 ( $\text{CH}^3_\beta$ ), 74.05 ( $\text{CH}^5_\beta$ ), 73.78 ( $\text{CH}^2_\beta$ ), 73.56 ( $\text{CH}^3_\alpha$ ), 72.26 ( $\text{CH}^2_\alpha$ ), 71.01 ( $\text{CH}^4_\alpha$ ), 70.66 ( $\text{CH}^4_\beta$ ), 70.25 ( $\text{CH}^5_\alpha$ ), 68.75 ( $\text{OCH}_2\beta$ ), 67.16 ( $\text{OCH}_2\alpha$ ), 64.22 ( $\text{CH}_2^{6\prime}_\alpha$ ), 64.04 ( $\text{CH}_2^{6\prime}_\beta$ ), 34.04 ( $\text{COOCH}_2$ ), 31.85 ( $\text{OCH}_2\text{CH}_2\beta$ ), 31.75 ( $\text{OCH}_2\text{CH}_2\alpha$ ), 29.49 - 28.90 ( $(\text{CH}_2)_{12}$ ), 24.95 ( $\text{COOCH}_2\text{CH}_2$ ), 22.56 ( $\text{CH}_2\text{CH}_3$ ), 19.39 ( $\text{OCH}_2\text{CH}_2\text{CH}_2\alpha$ ), 19.14 ( $\text{OCH}_2\text{CH}_2\text{CH}_2\beta$ ), 14.41, 14.17 ( $\text{CH}_3$ ).

**MS (ESI $^+$ ):**  $m/z$  calcd for  $[\text{C}_{26}\text{H}_{50}\text{O}_7]$ : 474.36; found: 497.25  $[\text{M}+\text{Na}]^+$ ; 971.18  $[2\text{M}+\text{Na}]^+$ .

**MS (ESI $^-$ ):**  $m/z$  calcd for  $[\text{C}_{26}\text{H}_{50}\text{O}_7]$ : 474.36; found: 473.05  $[\text{M}-\text{H}]^-$ ; 947.35  $[2\text{M}-\text{H}]^-$ .

## 5.8.5 Characterization of 1-butyl 6-O-palmitoyl-D-glucofuranosides (37cd)



$R_f$  (eluent: *n*-hexane/EtOAc; 2:8): 0.60.

Isomeric ratio c/d: 55/45.

**$^1\text{H NMR}$  (DMSO- $d_6$ , 400 MHz):**  $\delta$  (ppm) 5.30 (br s, OH), 5.08 (br d,  $J = 17.4$  Hz, OH), 4.91 (d,  $J = 3.7$  Hz,  $\text{CH}^{1\alpha}$ ), 4.80 (br d,  $J = 9.1$  Hz, OH), 4.70 (br s,  $\text{CH}^{1\beta}$ ), 4.65 (br d,  $J = 17.3$  Hz, OH), 4.29 – 4.22 (m,  $\text{CH}_2^{6\alpha}$ ), 4.22 – 4.15 (d,  $J = 11.4$  Hz,  $\text{CH}_2^{6\beta}$ ), 4.08 – 3.91 (m, CH, CH,  $\text{CH}_2^{6''}$ ), 3.91 – 3.79 (m, 6 CH), 3.54 – 3.52 (d,  $J = 6.7$  Hz,  $\text{OCH}_2'$ ), 3.46 – 3.39 (dd,  $J = 11.3, 4.7$  Hz,  $\text{OCH}_2''$ ), 3.35 – 3.29 (m,  $\text{OCH}_2''$ ), 2.29 (br s,  $\text{COOCH}_2$ ), 1.59 – 1.42 (m,  $\text{COOCH}_2\text{CH}_2$ ,  $\text{OCH}_2\text{CH}_2$ ), 1.38 – 1.14 (m,  $(\text{CH}_2)_{12}$ ,  $\text{OCH}_2\text{CH}_2\text{CH}_2$ ), 0.87 (dd,  $J = 14.3, 7.0$  Hz,  $\text{CH}_3$ ).

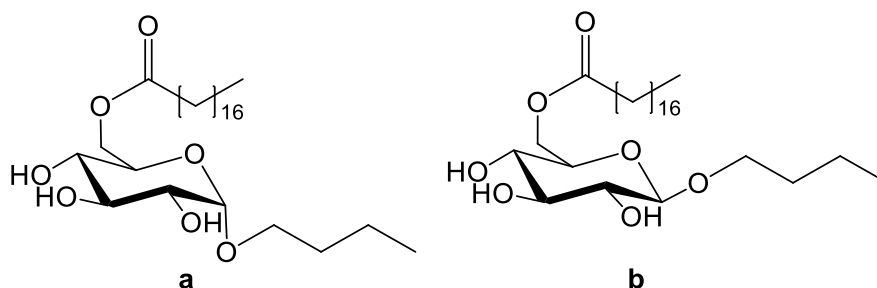
**$^{13}\text{C NMR}$  (DMSO- $d_6$ , 101 MHz):**  $\delta$  (ppm) 173.43 (COO), 109.28 ( $\text{CH}^{1\beta}$ ), 102.44 ( $\text{CH}^{1\alpha}$ ), 81.94, 80.95, 78.69, 77.77, 75.73, 75.58 (6 CH), 67.95, 67.34 (2  $\text{OCH}_2$ ), 67.18 (CH), 67.11 ( $\text{CH}_2^6$ ), 66.91 (CH), 66.73 ( $\text{CH}_2^6$ ), 34.01 ( $\text{COOCH}_2$ ), 31.84, 31.76 (2  $\text{OCH}_2\text{CH}_2$ ), 29.50, 29.36, 29.17, 28.93 ( $(\text{CH}_2)_{12}$ ), 24.95, 24.93 (2  $\text{COOCH}_2\text{CH}_2$ ), 19.26, 19.24 (2  $\text{OCH}_2\text{CH}_2\text{CH}_2$ ), 14.41, 14.17, 14.14 (3  $\text{CH}_3$ ).

**MS (ESI $^+$ ):**  $m/z$  calcd for  $[\text{C}_{26}\text{H}_{50}\text{O}_7]$ : 474.36; found: 497.98  $[\text{M}+\text{Na}]^+$ ; 971.38  $[2\text{M}+\text{Na}]^+$ .

**MS (ESI $^-$ ):**  $m/z$  calcd for  $[\text{C}_{26}\text{H}_{50}\text{O}_7]$ : 474.36; found: 473.82  $[\text{M}-\text{H}]^-$ ; 948.31  $[2\text{M}-\text{H}]^-$ .



## 5.8.6 Characterization of 1-butyl 6-O-stearoyl-D-glucopyranosides (38ab)



$R_f$  (eluent: *n*-hexane/EtOAc; 2:8) 0.34.

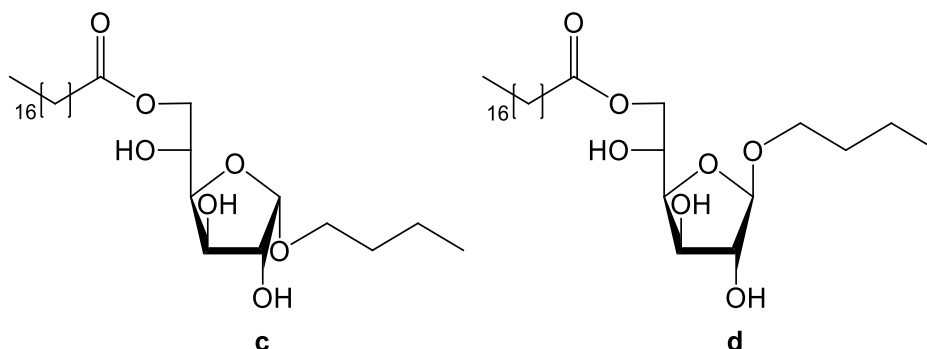
Isomeric ratio a/b: 62/38.

**$^1\text{H NMR}$  (DMSO- $d_6$ , 400 MHz):**  $\delta$  (ppm) 5.12 (t,  $J = 5.8$  Hz, OH), 5.01 (d,  $J = 4.9$  Hz, OH), 4.84 (d,  $J = 4.8$  Hz, OH), 4.67 (d,  $J = 6.3$  Hz, OH), 4.61 (d,  $J = 3.6$  Hz,  $\text{CH}^1_\alpha$ ), 4.30 (t,  $J = 10.1$  Hz,  $\text{CH}_2^{6\prime}_\alpha$ ,  $\text{CH}_2^{6\prime}_\beta$ ), 4.12 (d,  $J = 7.8$  Hz,  $\text{CH}^1_\beta$ ), 4.01 (ddd,  $J = 24.8$ , 11.6, 7.4 Hz,  $\text{CH}_2^{6\prime\prime}_\alpha$ ,  $\text{CH}_2^{6\prime\prime}_\beta$ ), 3.68 (dt,  $J = 9.6$ , 6.7 Hz,  $\text{OCH}_2'_\beta$ ), 3.63 – 3.53 (m,  $\text{CH}^5_\alpha$ ,  $\text{OCH}_2'_\alpha$ ), 3.47 – 3.36 (m,  $\text{CH}^3_\alpha$ ,  $\text{OCH}_2''_\beta$ ), 3.36 – 3.29 (m,  $\text{CH}^5_\beta$ ,  $\text{OCH}_2''_\alpha$ ), 3.24 – 3.17 (m,  $\text{CH}^2_\alpha$ ), 3.16 – 3.11 (m,  $\text{CH}^3_\beta$ ), 3.08 – 2.99 (m,  $\text{CH}^4_\alpha$ ,  $\text{CH}^4_\beta$ ), 2.99 – 2.92 (m,  $\text{CH}^2_\beta$ ), 2.31 – 2.22 (m,  $\text{COOCH}_2$ ), 1.58 – 1.45 (m,  $\text{COOCH}_2\text{CH}_2$ ,  $\text{OCH}_2\text{CH}_2$ ), 1.41 – 1.31 (m,  $\text{OCH}_2\text{CH}_2\text{CH}_2$ ), 1.31 – 1.17 (br s,  $(\text{CH}_2)_{14}$ ), 0.93 – 0.81 (m,  $\text{CH}_3$ ).

**$^{13}\text{C NMR}$  (DMSO- $d_6$ , 101 MHz):**  $\delta$  (ppm) 173.09 ( $\text{COO}_\beta$ ), 173.03 ( $\text{COO}_\alpha$ ), 103.34 ( $\text{CH}^1_\beta$ ), 99.04 ( $\text{CH}^1_\alpha$ ), 76.95 ( $\text{CH}^3_\beta$ ), 74.07 ( $\text{CH}^5_\beta$ ), 73.76 ( $\text{CH}^2_\beta$ ), 73.57 ( $\text{CH}^3_\alpha$ ), 72.25 ( $\text{CH}^2_\alpha$ ), 71.06 ( $\text{CH}^4_\alpha$ ), 70.71 ( $\text{CH}^4_\beta$ ), 70.25 ( $\text{CH}^5_\alpha$ ), 68.72 ( $\text{OCH}_2_\beta$ ), 67.15 ( $\text{OCH}_2_\alpha$ ), 64.31 ( $\text{CH}_2^{6\prime}_\alpha$ ), 64.11 ( $\text{CH}_2^{6\prime}_\beta$ ), 34.03 ( $\text{COOCH}_2_\alpha$ ), 34.00 ( $\text{COOCH}_2_\beta$ ), 31.86 ( $\text{OCH}_2\text{CH}_2_\beta$ ), 31.81 ( $\text{OCH}_2\text{CH}_2_\alpha$ ), 29.56 – 28.96 ( $(\text{CH}_2)_{14}$ ), 25.00 ( $\text{COOCH}_2\text{CH}_2$ ), 22.58 ( $\text{CH}_2\text{CH}_3$ ), 19.39 ( $\text{OCH}_2\text{CH}_2\text{CH}_2_\alpha$ ), 19.14 ( $\text{OCH}_2\text{CH}_2\text{CH}_2_\beta$ ), 14.33, 14.11, 14.09 ( $\text{CH}_3$ ).

**MS (ESI $^+$ ):**  $m/z$  calcd for  $[\text{C}_{28}\text{H}_{54}\text{O}_7]$ : 502.39; found: 525.65  $[\text{M}+\text{Na}]^+$ ; 1027.22  $[2\text{M}+\text{Na}]^+$ .

**MS (ESI $^-$ ):**  $m/z$  calcd for  $[\text{C}_{28}\text{H}_{54}\text{O}_7]$ : 502.39; found: 501.53  $[\text{M}-\text{H}]^-$ , 1003.50  $[2\text{M}-\text{H}]^-$ .

5.8.7 Characterization of 1-butyl 6-*O*-stearyl-D-glucofuranosides (38cd)

$R_f$  (eluent: *n*-hexane/EtOAc; 2:8) 0.62.

Isomeric ratio c/d: 56/44.

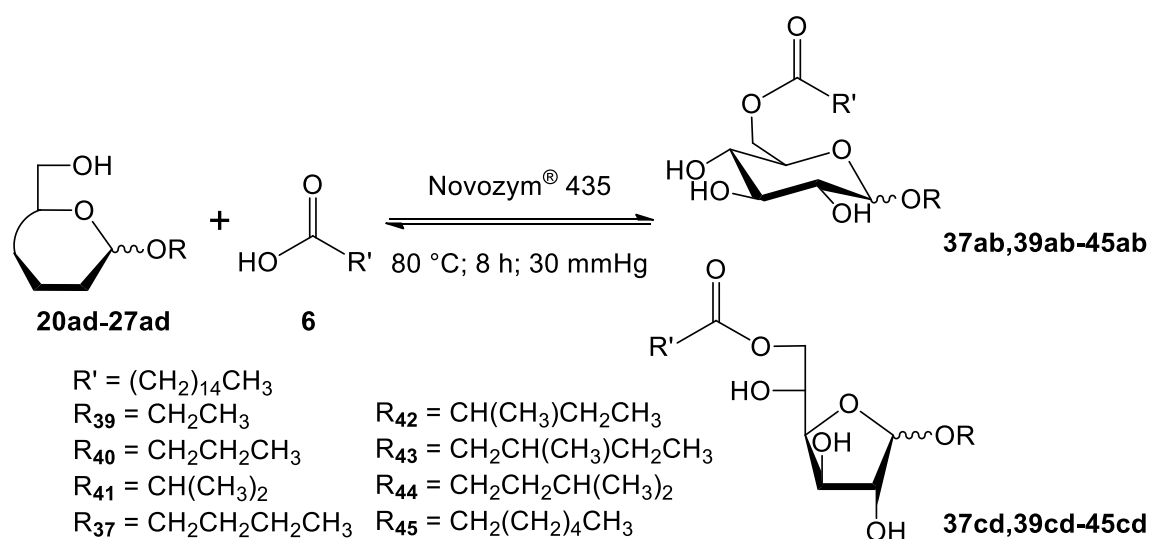
**$^1\text{H NMR}$  (DMSO- $d_6$ , 400 MHz):**  $\delta$  (ppm) 5.29 (d,  $J = 3.9$  Hz, OH), 5.08 (d,  $J = 4.8$  Hz, OH), 4.92 (d,  $J = 4.0$  Hz,  $\text{CH}^{1\alpha}$ ), 4.77 (dd,  $J = 5.1, 3.1$  Hz, OH), 4.71 (br s,  $\text{CH}^{1\beta}$ ), 4.65 (d,  $J = 5.1$  Hz, OH), 4.59 (d,  $J = 5.4$  Hz, OH), 4.26 (q,  $J = 5.5$  Hz,  $\text{CH}_2^{6\alpha}$ ), 4.19 (m,  $\text{CH}_2^{6\beta}$ ), 4.04 – 3.92 (m, CH, CH, CH,  $\text{CH}_2^{6''}$ ), 3.91 – 3.80 (m, 5 CH), 3.65 – 3.53 (m,  $\text{OCH}_2'$ ), 3.43 (dt,  $J = 9.8, 6.6$  Hz,  $\text{OCH}_2''$ ), 3.37 – 3.31 (m,  $\text{OCH}_2''$ ), 2.30 (td,  $J = 7.4, 2.9$  Hz,  $\text{COOCH}_2$ ), 1.59 – 1.43 (m,  $\text{COOCH}_2\text{CH}_2$ ,  $\text{OCH}_2\text{CH}_2$ ), 1.39 – 1.20 (m,  $(\text{CH}_2)_{14}$ ,  $\text{OCH}_2\text{CH}_2\text{CH}_2$ ), 0.93 – 0.84 (m,  $\text{CH}_3$ ).

**$^{13}\text{C NMR}$  (DMSO- $d_6$ , 101 MHz):**  $\delta$  (ppm) 173.40 (COO), 109.29 ( $\text{CH}^{1\beta}$ ), 102.43 ( $\text{CH}^{1\alpha}$ ), 81.94, 80.97, 78.69, 77.81, 75.78, 75.63 (6 CH), 67.96, 67.35 ( $\text{OCH}_2$ ), 67.24 ( $\text{CH}_2^{6\alpha}$ ), 67.11 (CH), 66.96 ( $\text{CH}_2^{6\beta}$ ), 66.74 (CH), 34.03 ( $\text{COOCH}_2$ ), 31.76, 31.73 (2  $\text{OCH}_2\text{CH}_2$ ), 29.49, 29.37, 29.17, 28.96 ( $(\text{CH}_2)_{12}$ ), 24.96 ( $\text{COOCH}_2\text{CH}_2$ ), 19.25 ( $\text{OCH}_2\text{CH}_2\text{CH}_2$ ), 14.40, 14.17 (2  $\text{CH}_3$ ).

**MS (ESI<sup>+</sup>):**  $m/z$  calcd for  $[\text{C}_{28}\text{H}_{54}\text{O}_7]$ : 502.39; found: 525.93  $[\text{M}+\text{Na}]^+$ ; 1027.46  $[\text{2M}+\text{Na}]^+$ .

**MS (ESI<sup>-</sup>):**  $m/z$  calcd for  $[\text{C}_{28}\text{H}_{54}\text{O}_7]^-$ : 502.39; found: 501.57  $[\text{M}-\text{H}]^-$ ; 1003.95  $[\text{M}-\text{H}]^-$ .

## 5.8.8 Enzymatic synthesis of alkyl 6-O-palmitoyl-D-glucoside isomeric mixtures (37ad,39ad-45ad)



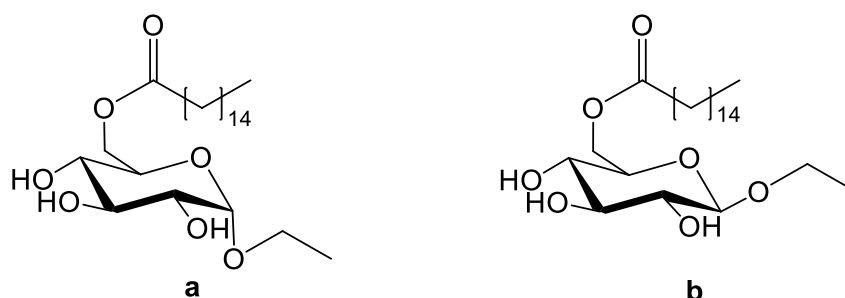
Isomeric mixtures of alkyl D-glucosides (**20ad-27ad**), palmitic acid (**6**), in molar ratio 1:1, and Novozym<sup>®</sup> 435 (10 %, w/w) were mixed together and charged into a round-bottom flask. The mixtures were heated to 80 °C while rotating the flask by means of a glass oven B-585 Kugelrohr. After palmitic acid melted, the reactions were performed under reduced pressure (30 mmHg).

After 8 h, reaction mixtures were taken up in EtOAc and the immobilized enzyme was removed by filtration. Then, the esters were extracted in EtOAc (2 times) from 1 M NaOH, the organic phases were collected, dried over Na<sub>2</sub>SO<sub>4</sub> and the solvent was removed under reduced pressure. Couple of isomers were isolated by flash chromatography (*n*-hexane/EtOAc; 2:8), thus affording **alkyl 6-O-palmitoyl-D-glucopyranosides (37ab,39ab-45ab)** and **alkyl 6-O-palmitoyl-D-glucofuranosides (37cd,39cd-45cd)**. All products were fully characterized by TLC, ESI-MS and NMR analysis. Some <sup>1</sup>H and <sup>13</sup>C peaks are not completely resolved because of the instrument resolution. Yields and isomeric ratios of each isomeric couple, estimated by <sup>1</sup>H NMR analysis, carried out in DMSO-*d*<sub>6</sub>, as the ratio of the areas of the two anomeric proton signals, are reported in **Table 5.5**.

*Table 5.5. Yields and isomeric ratios of alkyl 6-O-palmitoyl-D-glucosides.*

<i>Compound</i>	<i>Yield (%)</i>	<i>Isomeric ratio (%)</i>	<i>Compound</i>	<i>Yield (%)</i>	<i>Isomeric ratio (%)</i>
<b>39ab</b>	10	56/44	<b>39cd</b>	26	48/52
<b>40ab</b>	15	60/40	<b>40cd</b>	21	52/48
<b>41ab</b>	7	56/44	<b>41cd</b>	16	61/39
<b>37ab</b>	47	63/34	<b>37cd</b>	10	55/45
<b>42ab</b>	36	58/42	<b>42cd</b>	13	69/31
<b>43ab</b>	27	52/48	<b>43cd</b>	14	53/47
<b>44ab</b>	40	62/38	<b>44cd</b>	7	59/41
<b>45ab</b>	38	60/40	<b>45cd</b>	14	60/40

## 5.8.9 Characterization of ethyl 6-O-palmitoyl-D-glucopyranosides (39ab)



$R_f$  (eluent: *n*-hexane/EtOAc; 2:8): 0.12.

Isomeric ratio a/b: 53/37.

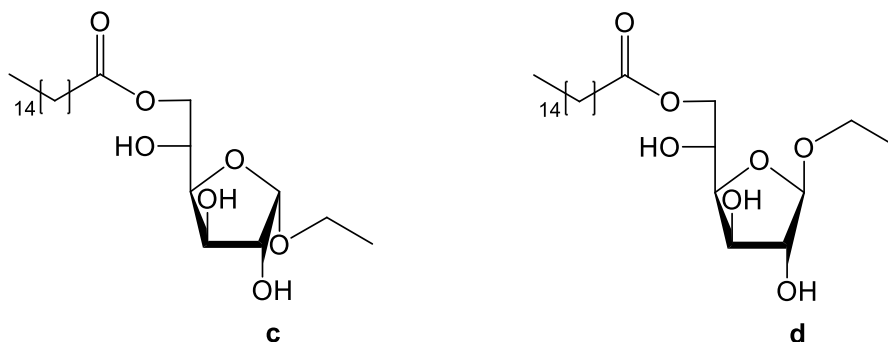
$^1\text{H NMR}$  (DMSO-*d*<sub>6</sub>, 400 MHz):  $\delta$  (ppm) 5.20 – 4.99 (br s, OH), 4.96 – 4.92 (m, OH), 4.82 (s, OH), 4.64 (d,  $J = 3.7$  Hz,  $\text{CH}^1_\alpha$ ), 4.29 (ddd,  $J = 11.5, 7.3, 1.7$  Hz,  $\text{CH}^2_{6^{\beta}}$ ), 4.14 (d,  $J = 7.8$  Hz,  $\text{CH}^1_\beta$ ), 4.03 (ddd,  $J = 16.7, 11.7, 6.9$  Hz,  $\text{CH}^2_{6^{\alpha}}$ ), 3.74 (dd,  $J = 9.7, 7.1$  Hz,  $\text{OCH}^2'_\beta$ ), 3.68 – 3.54 (m,  $\text{CH}^5_\alpha, \text{OCH}^2'_\alpha$ ), 3.54 – 3.45 (m,  $\text{OCH}^2''_\beta$ ), 3.45 – 3.37 (m,  $\text{CH}^3_\alpha, \text{OCH}^2''_\alpha$ ), 3.36 – 3.30 (m,  $\text{CH}^5_\beta$ ), 3.22 – 3.17 (m,  $\text{CH}^2_\alpha$ ), 3.17 – 3.11 (m,  $\text{CH}^3_\beta$ ), 3.05 (t,  $J = 9.6$  Hz,  $\text{CH}^4_\alpha, \text{CH}^4_\beta$ ), 2.95 (t,  $J = 8.4$  Hz,  $\text{CH}^2_\beta$ ), 2.28 (td,  $J = 7.3, 4.9$  Hz,  $\text{COOCH}_2$ ), 2.15 (t,  $J = 7.4$  Hz,  $\text{HCOOCH}_2$ ), 1.56 – 1.46 (br t,  $\text{COOCH}_2\text{CH}_2$ ), 1.32 – 1.20 (m,  $(\text{CH}_2)_{12}$ ), 1.18 – 1.10 (m,  $\text{OCH}_2\text{CH}_3$ ), 0.86 (t,  $J = 6.8$  Hz,  $\text{CH}_3$ ).

$^{13}\text{C NMR}$  (DMSO-*d*<sub>6</sub>, 101 MHz):  $\delta$  (ppm) 175.16 (HCOO), 173.28 (COO), 173.23 (COO), 103.12 ( $\text{CH}^1_\beta$ ), 98.92 ( $\text{CH}^1_\alpha$ ), 76.90 ( $\text{CH}^3_\beta$ ), 74.05 ( $\text{CH}^5_\beta$ ), 73.76 ( $\text{CH}^2_\beta$ ), 73.58 ( $\text{CH}^3_\alpha$ ), 72.22 ( $\text{CH}^2_\alpha$ ), 70.97 ( $\text{CH}^4_\beta$ ), 70.59 ( $\text{CH}^4_\alpha$ ), 70.16 ( $\text{CH}^5_\alpha$ ), 64.42 ( $\text{OCH}_2_\beta$ ), 64.11 ( $\text{CH}^2_{6_\beta}$ ), 64.04 ( $\text{CH}^2_{6_\alpha}$ ), 63.00 ( $\text{OCH}_2_\alpha$ ), 34.58 ( $\text{HCOOCH}_2$ ), 33.99 ( $\text{COOCH}_2$ ), 29.48, 29.33, 29.17, 28.88 ( $(\text{CH}_2)_{12}$ ), 24.94 ( $\text{COOCH}_2\text{CH}_2$ ), 15.65, 15.50 (2  $\text{OCH}_2\text{CH}_3$ ), 14.41 ( $\text{CH}_3$ ).

**MS (ESI<sup>+</sup>):**  $m/z$  calcd for  $[\text{C}_{24}\text{H}_{46}\text{O}_7]$ : 446.32; found: 469.51  $[\text{M}+\text{Na}]^+$ ; 915.44  $[2\text{M}+\text{Na}]^+$ .

**MS (ESI<sup>-</sup>):**  $m/z$  calcd for  $[\text{C}_{24}\text{H}_{46}\text{O}_7]$ : 446.32; found: 445.47  $[\text{M}-\text{H}]^-$ ; 891.46  $[2\text{M}-\text{H}]^-$ .

## 5.8.10 Characterization of ethyl 6-O-palmitoyl-D-glucofuranosides (39cd)



$R_f$  (eluent: *n*-hexane/EtOAc; 2:8): 0.30.

Isomeric ratio **c/d**: 48/52.

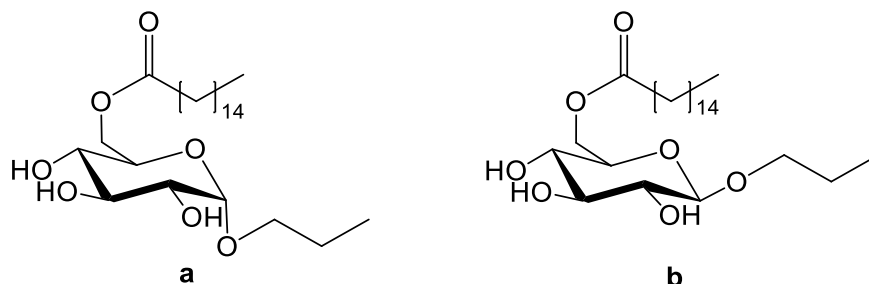
**$^1\text{H NMR}$  (DMSO- $d_6$ , 400 MHz):**  $\delta$  (ppm) 5.31 (br s, OH), 5.11 (br s, OH), 4.94 (d,  $J = 4.0$  Hz,  $\text{CH}^{1\alpha}$ ), 4.85 – 4.76 (m, OH), 4.72 (br s,  $\text{CH}^{1\beta}$ ), 4.67 (br d, OH), 4.25 (q,  $J = 5.6$  Hz,  $\text{CH}_2^{6\alpha}$ ), 4.22 – 4.16 (m,  $\text{CH}_2^{6\beta}$ ), 4.07 – 3.90 (m, CH, CH, CH,  $\text{CH}_2^{6\gamma}$ ), 3.90 – 3.78 (m, 5 CH), 3.71 – 3.55 (m,  $\text{OCH}_2'$ ), 3.48 (dq,  $J = 9.8, 7.0$  Hz, 1H,  $\text{OCH}_2''\alpha$ ), 3.42 – 3.34 (m,  $\text{OCH}_2''\beta$ ), 2.29 (td,  $J = 7.4, 2.4$  Hz,  $\text{COOCH}_2$ ), 2.15 (t,  $J = 7.3$  Hz,  $\text{HCOOCH}_2$ ), 1.58 – 1.45 (m,  $\text{COOCH}_2\text{CH}_2$ ), 1.33 – 1.19 (m,  $(\text{CH}_2)_{12}$ ), 1.19 – 1.06 (m,  $\text{OCH}_2\text{CH}_3$ ), 0.86 (t,  $J = 6.8$  Hz,  $\text{CH}_3$ ).

**$^{13}\text{C NMR}$  (DMSO- $d_6$ , 101 MHz):**  $\delta$  (ppm) 174.16 (HCOO), 173.44 (COO), 109.17 ( $\text{CH}^{1\beta}$ ), 102.48 ( $\text{CH}^{1\alpha}$ ), 81.92, 81.04, 78.84, 77.62, 75.71, 75.56, 67.13 (7 CH), 67.06 ( $\text{CH}_2^{6\alpha}$ ), 66.91 (CH), 66.80 ( $\text{CH}_2^{6\beta}$ ), 63.79 ( $\text{OCH}_2 \alpha$ ), 63.16 ( $\text{OCH}_2 \beta$ ), 34.67 ( $\text{HCOOCH}_2$ ), 34.00 ( $\text{COOCH}_2$ ), 29.50, 29.37, 29.18, 28.94 ( $(\text{CH}_2)_{12}$ ), 24.93 ( $\text{COOCH}_2\text{CH}_2$ ), 15.68, 15.55 (2  $\text{OCH}_2\text{CH}_3$ ), 14.41 ( $\text{CH}_3$ ).

**MS (ESI<sup>+</sup>):**  $m/z$  calcd for  $[\text{C}_{24}\text{H}_{46}\text{O}_7]$ : 446.32; found: 469.55  $[\text{M}+\text{Na}]^+$ ; 915.16  $[2\text{M}+\text{Na}]^+$ ; 937.38  $[2\text{M}+2\text{Na}]^+$ .

**MS (ESI<sup>-</sup>):**  $m/z$  calcd for  $[\text{C}_{24}\text{H}_{46}\text{O}_7]$ : 446.32; found: 445.41  $[\text{M}-\text{H}]^-$ ; 891.55  $[2\text{M}-\text{H}]^-$ .

## 5.8.11 Characterization of 1-propyl 6-O-palmitoyl-D-glucopyranosides (40ab)



$R_f$  (eluent: *n*-hexane/EtOAc; 2:8): 0.23.

Isomeric ratio a/b: 60/40.

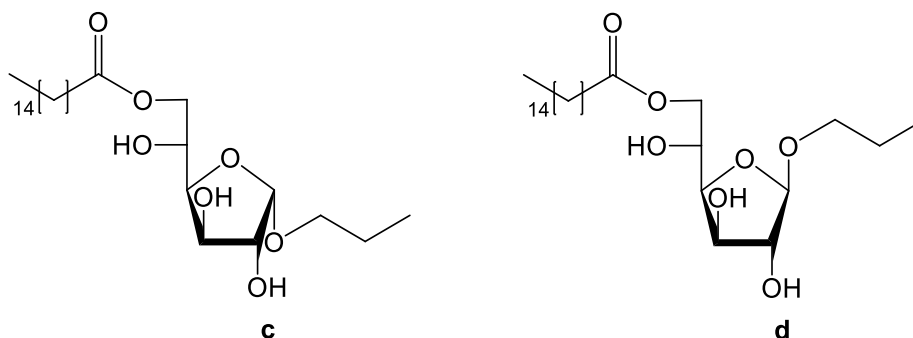
$^1\text{H NMR}$  (DMSO- $d_6$ , 400 MHz):  $\delta$  (ppm) 5.12 (br d,  $J = 5.8$  Hz, OH), 5.03 (br d,  $J = 4.8$  Hz, OH), 4.84 (br s, OH), 4.72 – 4.66 (m, OH), 4.62 (d,  $J = 3.6$  Hz,  $\text{CH}^1_\alpha$ ), 4.29 (td,  $J = 11.8, 1.6$  Hz,  $\text{CH}_2^{6'}$ ), 4.13 (d,  $J = 7.8$  Hz,  $\text{CH}^1_\beta$ ), 4.08 – 3.96 (m,  $\text{CH}_2^{6''}$ ), 3.67 – 3.55 (m,  $\text{CH}^5_\alpha$ ,  $\text{OCH}_2^{2'\beta}$ ), 3.51 (dt,  $J = 9.6, 6.9$  Hz,  $\text{OCH}_2^{2'\alpha}$ ), 3.45 – 3.36 (m,  $\text{CH}^3_\alpha$ ,  $\text{OCH}_2^{2'\beta}$ ), 3.36 – 3.29 (m,  $\text{CH}^5_\beta$ ,  $\text{OCH}_2^{2''\alpha}$ ), 3.23 – 3.18 (m,  $\text{CH}^2_\alpha$ ), 3.18 – 3.12 (m,  $\text{CH}^3_\beta$ ), 3.09 – 3.00 (m,  $\text{CH}^4_\alpha$ ,  $\text{CH}^4_\beta$ ), 2.96 (d,  $J = 4.4$  Hz,  $\text{CH}^2_\beta$ ), 2.28 (td,  $J = 7.3, 4.2$  Hz,  $\text{COOCH}_2$ ), 1.58 – 1.47 (m,  $\text{COOCH}_2\text{CH}_2$ ,  $\text{OCH}_2\text{CH}_2$ ), 1.26 (br s,  $(\text{CH}_2)_{12}$ ), 0.87 (ddd,  $J = 9.1, 8.7, 4.5$  Hz,  $\text{CH}_3$ ).

$^{13}\text{C NMR}$  (DMSO- $d_6$ , 101 MHz):  $\delta$  (ppm) 173.25 ( $\text{COO}_\beta$ ), 173.18 ( $\text{COO}_\alpha$ ), 103.33 ( $\text{CH}^1_\beta$ ), 99.01 ( $\text{CH}^1_\alpha$ ), 76.92 ( $\text{CH}^3_\beta$ ), 74.05 ( $\text{CH}^5_\beta$ ), 73.78 ( $\text{CH}^2_\beta$ ), 73.58 ( $\text{CH}^3_\alpha$ ), 72.28 ( $\text{CH}^2_\alpha$ ), 70.99 ( $\text{CH}^4_\beta$ ), 70.75 ( $\text{OCH}_2 \beta$ ), 70.64 ( $\text{CH}^4_\alpha$ ), 70.22 ( $\text{CH}^5_\alpha$ ), 69.15 ( $\text{OCH}_2 \alpha$ ), 64.16 ( $\text{CH}_2^{6\beta}$ ), 64.03 ( $\text{CH}_2^{6\alpha}$ ), 34.03 ( $\text{COOCH}_2 \beta$ ), 33.99 ( $\text{COOCH}_2 \alpha$ ), 29.50, 29.49, 29.47, 29.44, 29.32, 29.17, 28.90, 28.89 ( $(\text{CH}_2)_{12}$ ), 24.98, 24.95 (2  $\text{COOCH}_2\text{CH}_2$ ), 23.02, 22.87 (2  $\text{OCH}_2\text{CH}_2$ ), 14.41 ( $\text{CH}_3$ ), 11.10, 10.87 (2  $\text{OCH}_2\text{CH}_2\text{CH}_3$ ).

**MS (ESI $^+$ ):**  $m/z$  calcd for  $[\text{C}_{25}\text{H}_{48}\text{O}_7]$ : 460.34; found: 483.59  $[\text{M}+\text{Na}]^+$ ; 943.21  $[2\text{M}+\text{Na}]^+$ .

**MS (ESI $^-$ ):**  $m/z$  calcd for  $[\text{C}_{25}\text{H}_{48}\text{O}_7]$ : 460.34; found: 459.46  $[\text{M}-\text{H}]^-$ ; 919.71  $[2\text{M}-\text{H}]^-$ .

## 5.8.12 Characterization of 1-propyl 6-O-palmitoyl-D-glucofuranosides (40cd)



$R_f$  (eluent: *n*-hexane/EtOAc; 2:8): 0.44.

Isomeric ratio c/d: 52/48.

**$^1\text{H NMR}$  (DMSO- $d_6$ , 400 MHz):**  $\delta$  (ppm) 5.30 (br d,  $J = 3.0$  Hz, OH), 5.10 (br s, OH), 4.92 (d,  $J = 4.0$  Hz,  $\text{CH}^1_\alpha$ ), 4.79 (br s, OH), 4.71 (br s,  $\text{CH}^1_\beta$ ), 4.68 (d,  $J = 4.7$  Hz, OH), 4.64 (d,  $J = 5.4$  Hz, OH), 4.25 (m,  $\text{CH}_2^{6\alpha}$ ), 4.19 (m,  $\text{CH}_2^{6\beta}$ ), 4.03 – 3.91 (m, CH, CH,  $\text{CH}_2^{6''}$ ), 3.91 – 3.79 (m, 6 CH), 3.57 – 3.48 (m,  $\text{OCH}_2'$ ), 3.42 – 3.35 (dt,  $J = 9.7, 6.8$  Hz,  $\text{OCH}_2''_\alpha$ ), 3.32 – 3.23 (m,  $\text{OCH}_2''_\beta$ ), 2.29 (td,  $J = 7.4, 3.1$  Hz,  $\text{COOCH}_2$ ), 1.51 (qd,  $J = 14.2, 7.0$  Hz,  $\text{COOCH}_2\text{CH}_2$ ,  $\text{OCH}_2\text{CH}_2$ ), 1.22 (br s,  $(\text{CH}_2)_{12}$ ), 0.86 (m,  $\text{CH}_3$ ).

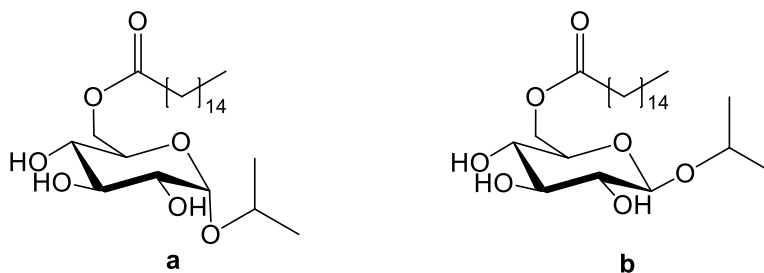
**$^{13}\text{C NMR}$  (DMSO- $d_6$ , 101 MHz):**  $\delta$  (ppm) 173.44 ( $\text{COO}_\beta$ ), 173.42 ( $\text{COO}_\alpha$ ), 109.28 ( $\text{CH}^1_\beta$ ), 102.49 ( $\text{CH}^1_\alpha$ ), 81.94, 80.97, 78.73, 77.75, 75.72, 75.58 (6 CH) 69.97 ( $\text{OCH}_2_\alpha$ ), 69.33 ( $\text{OCH}_2_\beta$ ), 67.16 ( $\text{CH}_2^{6\alpha}$ ), 67.09 (CH), 66.93 ( $\text{CH}_2^{6\beta}$ ), 66.76 (CH), 34.01 ( $\text{COOCH}_2_\alpha$ ), 33.73 ( $\text{COOCH}_2_\beta$ ), 29.50, 29.49, 29.47, 29.45, 29.37, 29.35, 29.17, 28.95, 28.93, 28.91 ( $(\text{CH}_2)_{12}$ ), 24.95, 24.92 (2  $\text{COOCH}_2\text{CH}_2$ ), 23.02, 22.87 (2  $\text{OCH}_2\text{CH}_2$ ), 14.41 ( $\text{CH}_3$ ), 10.99, 10.95 (2  $\text{OCH}_2\text{CH}_2\text{CH}_3$ ).

**MS (ESI $^+$ ):**  $m/z$  calcd for  $[\text{C}_{25}\text{H}_{48}\text{O}_7]$ : 460.34; found: 484.30  $[\text{M}+\text{Na}]^+$ ; 943.78  $[2\text{M}+\text{Na}]^+$ .

**MS (ESI $^-$ ):**  $m/z$  calcd for  $[\text{C}_{25}\text{H}_{48}\text{O}_7]$ : 460.34; found: 459.65  $[\text{M}-\text{H}]^-$ ; 919.98  $[2\text{M}-\text{H}]^-$ .



## 5.8.13 Characterization of 2-propyl 6-O-palmitoyl-D-glucopyranosides (41ab)



$R_f$  (eluent: *n*-hexane/EtOAc; 2:8): 0.18.

Isomeric ratio a/b: 66/44.

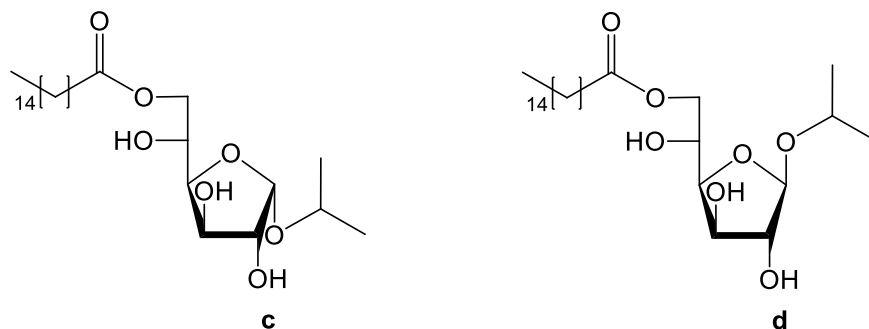
$^1\text{H NMR}$  (DMSO- $d_6$ , 400 MHz):  $\delta$  (ppm) 5.13 – 5.06 (m, OH), 4.99 (br d,  $J = 4.2$  Hz, OH), 4.93 (br d,  $J = 4.4$  Hz, OH), 4.80 (br d,  $J = 4.1$  Hz, OH), 4.72 (br s,  $\text{CH}^1_\alpha$ ), 4.54 (br d,  $J = 6.4$  Hz, OH), 4.29 (t,  $J = 10.2$  Hz,  $\text{CH}_2^{6\prime}$ ), 4.20 (d,  $J = 7.6$  Hz,  $\text{CH}^1_\beta$ ), 4.08 – 3.94 (m,  $\text{CH}_2^{6''}$ ), 3.90 – 3.81 (m,  $\text{OCH}_\beta$ ), 3.82 – 3.72 (m,  $\text{OCH}_\alpha$ ), 3.71 – 3.63 (m,  $\text{CH}^5_\alpha$ ), 3.42 – 3.29 (m,  $\text{CH}^3_\alpha$ ,  $\text{CH}^5_\beta$ ), 3.22 – 3.11 (m,  $\text{CH}^2_\alpha$ ,  $\text{CH}^3_\beta$ ), 3.07 – 2.99 (m,  $\text{CH}^4_\alpha$ ,  $\text{CH}^4_\beta$ ), 2.92 (m,  $\text{CH}^2_\beta$ ), 2.27 (br d,  $J = 6.0$  Hz,  $\text{COOCH}_2$ ), 1.51 (br s,  $\text{COOCH}_2\text{CH}_2$ ), 1.24 (br s,  $(\text{CH}_2)_{12}$ ), 1.18 – 1.13 (m,  $\text{OCH}(\text{CH}_3)_2'$ ), 1.13 – 1.07 (br s,  $\text{OCH}(\text{CH}_3)_2''$ ), 0.85 (br d,  $J = 6.3$  Hz,  $\text{CH}_3$ ).

$^{13}\text{C NMR}$  (DMSO- $d_6$ , 101 MHz):  $\delta$  (ppm) 173.22 ( $\text{COO}_\beta$ ), 173.19 ( $\text{COO}_\alpha$ ), 101.84 ( $\text{CH}^1_\beta$ ), 97.64 ( $\text{CH}^1_\alpha$ ), 77.00 ( $\text{CH}^3_\beta$ ), 73.95 ( $\text{CH}^5_\beta$ ), 73.83 ( $\text{CH}^2_\beta$ ), 73.55 ( $\text{CH}^3_\alpha$ ), 72.15 ( $\text{CH}^2_\alpha$ ), 71.10 ( $\text{CH}^4_\beta$ ), 71.04 ( $\text{CH}^4_\alpha$ ), 70.71 ( $\text{OCH}_2 \beta$ ), 70.25 ( $\text{CH}^5_\alpha$ ), 69.82 ( $\text{OCH}_2 \alpha$ ), 64.26 ( $\text{CH}_2^{6\alpha}$ ), 64.09 ( $\text{CH}_2^{6\beta}$ ), 34.01 ( $\text{COOCH}_2$ ), 29.49, 29.47, 29.31, 29.17, 28.89 ( $(\text{CH}_2)_{12}$ ), 24.95, 24.90 (2  $\text{COOCH}_2\text{CH}_2$ ), 23.91, 23.63 ( $\text{OCH}(\text{CH}_3)_2$ ), 22.41, 22.05 ( $\text{OCH}(\text{CH}_3)_2$ ), 14.40 ( $\text{CH}_3$ ).

**MS (ESI $^+$ ):**  $m/z$  calcd for  $[\text{C}_{25}\text{H}_{48}\text{O}_7]$ : 460.34; found: 483.60  $[\text{M}+\text{Na}]^+$ ; 943.21  $[2\text{M}+\text{Na}]^+$ .

**MS (ESI $^-$ ):**  $m/z$  calcd for  $[\text{C}_{25}\text{H}_{48}\text{O}_7]$ : 460.34; found: 459.86  $[\text{M}-\text{H}]^-$ ; 919.96  $[2\text{M}-\text{H}]^-$ .

## 5.8.14 Characterization of 2-propyl 6-O-palmitoyl-D-glucofuranosides (41cd)



$R_f$  (eluent: *n*-hexane/EtOAc; 2:8): 0.40.

Isomeric ratio c/d: 61/39.

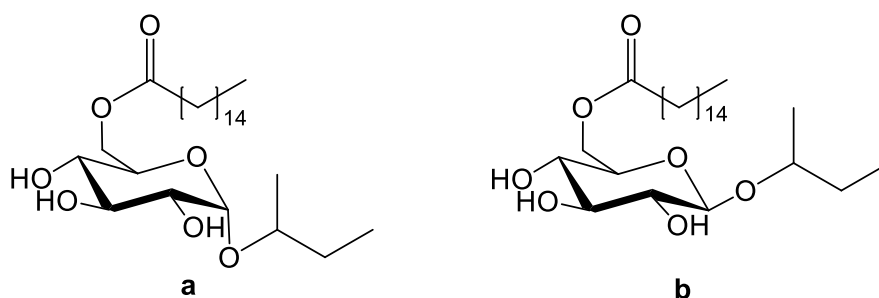
**$^1\text{H NMR}$  (DMSO- $d_6$ , 400 MHz):**  $\delta$  (ppm) 5.34 (d,  $J = 3.9$  Hz, OH), 5.13 (d,  $J = 4.7$  Hz, OH), 5.09 (d,  $J = 4.0$  Hz,  $\text{CH}^{1\alpha}$ ), 4.86 (br s,  $\text{CH}^{1\beta}$ ), 4.83 (d,  $J = 5.1$  Hz, OH), 4.65 (d,  $J = 5.3$  Hz, OH), 4.54 (d,  $J = 5.3$  Hz, OH), 4.30 (q,  $J = 8.8$  Hz,  $\text{CH}_2^{6\prime\alpha}$ ), 4.27 – 4.20 (m,  $\text{CH}_2^{6\prime\beta}$ ), 4.07 – 3.95 (m, CH, CH,  $\text{CH}_2^{6\prime\gamma}$ ), 3.94 – 3.87 (m, 4 CH,  $\text{OCH}_\alpha$ ), 3.87 – 3.81 (m, CH, CH,  $\text{OCH}_\beta$ ), 2.35 (td,  $J = 7.4, 3.8$  Hz,  $\text{COOCH}_2$ ), 1.58 (m,  $\text{COOCH}_2\text{CH}_2$ ), 1.29 (br s,  $(\text{CH}_2)_{12}$ ), 1.21 – 1.11 (m,  $\text{OCH}(\text{CH}_3)_2$ ), 0.91 (t,  $J = 6.8$  Hz,  $\text{CH}_3$ ).

**$^{13}\text{C NMR}$  (DMSO- $d_6$ , 101 MHz):**  $\delta$  (ppm) 173.45 (COO), 107.54 ( $\text{CH}^{1\beta}$ ), 101.07 ( $\text{CH}^{1\alpha}$ ), 81.75, 81.29, 78.63, 77.92, 75.68, 75.66 (6 CH), 70.46 ( $\text{OCH}_\alpha$ ), 69.49 ( $\text{OCH}_\alpha$ ), 67.21 (CH), 67.11 ( $\text{CH}_2^{6\prime\alpha}$ ), 66.86 (CH), 66.80 ( $\text{CH}_2^{6\prime\beta}$ ), 34.00 ( $\text{COOCH}_2$ ), 29.50, 29.47, 29.45, 29.34, 29.17, 28.94 ( $(\text{CH}_2)_{12}$ ), 24.95, 24.92 (2  $\text{COOCH}_2\text{CH}_2$ ), 23.87, 23.84, 22.52, 22.11 (2  $\text{OCH}(\text{CH}_3)_2$ ), 14.41 ( $\text{CH}_3$ ).

**MS (ESI $^+$ ):**  $m/z$  calcd for  $[\text{C}_{25}\text{H}_{48}\text{O}_7]$ : 460.34; found: 484.67  $[\text{M}+\text{Na}]^+$ ; 943.32  $[2\text{M}+\text{Na}]^+$ .

**MS (ESI $^-$ ):**  $m/z$  calcd for  $[\text{C}_{25}\text{H}_{48}\text{O}_7]$ : 460.34; found: 460.17  $[\text{M}-\text{H}]^-$ ; 920.03  $[2\text{M}-\text{H}]^-$ .

## 5.8.15 Characterization of 2-butyl 6-O-palmitoyl-D-glucopyranosides (42ab)



$R_f$  (eluent: *n*-hexane/EtOAc; 2:8): 0.12.

Isomeric ratio a/b: 58/42.

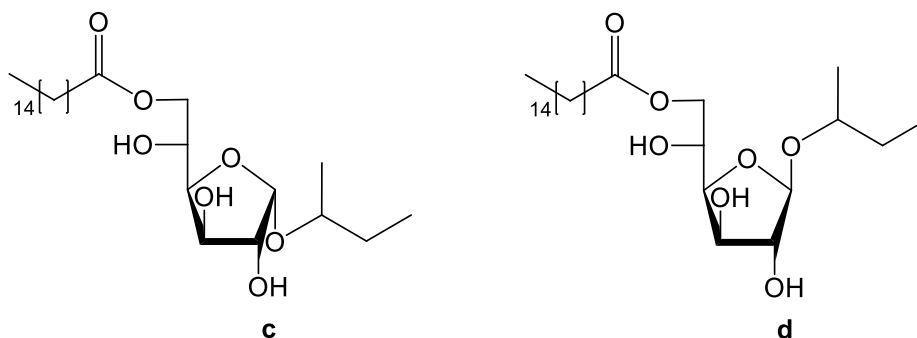
$^1\text{H NMR}$  (DMSO- $d_6$ , 400 MHz):  $\delta$  (ppm) 5.11 (dd,  $J = 6.9, 5.7$  Hz, OH), 4.99 (d,  $J = 4.8$  Hz, OH), 4.94 (dd,  $J = 9.8, 5.0$  Hz, OH), 4.81 (d,  $J = 4.9$  Hz, OH), 4.73 (dd,  $J = 7.1, 3.8$  Hz,  $\text{CH}^1_\alpha$ ), 4.59 (d,  $J = 6.4$  Hz, OH), 4.55 (d,  $J = 6.6$  Hz, OH), 4.34 – 4.25 (m,  $\text{CH}_2^{6'}$ ), 4.18 (dd,  $J = 7.8, 3.1$  Hz,  $\text{CH}^1_\beta$ ), 4.07 – 3.95 (m,  $\text{CH}_2^{6''}$ ), 3.69 (dd,  $J = 9.7, 7.7$  Hz,  $\text{CH}^5_\alpha$ ), 3.63 – 3.51 (m, 2 OCH), 3.44 – 3.36 (m,  $\text{CH}^3_\alpha$ ), 3.34 – 3.29 (m,  $\text{CH}^5_\beta$ ), 3.22 – 3.11 (m,  $\text{CH}^2_\alpha, \text{CH}^3_\beta$ ), 3.08 – 3.98 (m,  $\text{CH}^4_\alpha, \text{CH}^4_\beta$ ), 2.93 (ddd,  $J = 13.9, 8.3, 5.7$  Hz,  $\text{CH}^2_\beta$ ), 2.27 (m,  $\text{COOCH}_2$ ), 1.56 – 1.46 (m,  $\text{COOCH}_2\text{CH}_2, \text{OCHCH}_2$ ), 1.45 – 1.35 (m,  $\text{OCHCH}_2$ ), 1.26 (br s,  $(\text{CH}_2)_{12}$ ), 1.17 – 1.05 (m,  $\text{OCHCH}_3$ ), 0.92 – 0.80 (m,  $\text{OCHCH}_2\text{CH}_3, \text{CH}_3$ ).

$^{13}\text{C NMR}$  (DMSO- $d_6$ , 101 MHz):  $\delta$  (ppm) 173.18 (COO), 103.14, 101.57 ( $\text{CH}^1_\beta$ ), 99.10, 96.73 ( $\text{CH}^1_\alpha$ ), 77.09, 77.06 ( $\text{CH}^3_\beta$ ), 77.01, 76.12, 75.75, (3 OCH), 74.02, 73.99, ( $\text{CH}^5_\beta$ ), 73.93, 73.94 ( $\text{CH}^2_\beta$ ), 73.82 (OCH), 73.53, 73.46 ( $\text{CH}^3_\alpha$ ), 72.37, 72.12 ( $\text{CH}^2_\alpha$ ), 71.14, 71.09 ( $\text{CH}^4_\beta$ ), 70.79, 70.78 ( $\text{CH}^4_\alpha$ ), 70.47, 70.33 ( $\text{CH}^5_\alpha$ ), 64.33 ( $\text{CH}_2^{6_\alpha}$ ), 64.08 ( $\text{CH}_2^{6_\beta}$ ), 34.03 ( $\text{COOCH}_2$ ), 30.07, 29.98 ( $\text{OCHCH}_2$ ), 29.49, 29.46, 29.30, 29.25, 29.16, 28.88 ( $(\text{CH}_2)_{12}$ ), 24.96, 24.91 (2  $\text{COOCH}_2\text{CH}_2$ ), 21.57, 21.14, 19.68, 19.06 (4  $\text{OCHCH}_3$ ), 14.41 ( $\text{CH}_3$ ), 10.61, 10.20, 9.97, 9.88 (4  $\text{OCHCH}_2\text{CH}_3$ ).

$\text{MS (ESI}^+)$ :  $m/z$  calcd for  $[\text{C}_{26}\text{H}_{50}\text{O}_7]$ : 474.36; found: 497.79  $[\text{M}+\text{Na}]^+$ ; 971.82  $[\text{2M}+\text{Na}]^+$ .

$\text{MS (ESI}^-)$ :  $m/z$  calcd for  $[\text{C}_{26}\text{H}_{50}\text{O}_7]$ : 474.36; found: 473.19  $[\text{M}-\text{H}]^-$ ; 947.26  $[\text{2M}-\text{H}]^-$ .

## 5.8.16 Characterization of 2-butyl 6-O-palmitoyl-D-glucofuranosides (42cd)



$R_f$  (eluent: *n*-hexane/EtOAc; 2:8): 0.30.

Isomeric ratio *c/d*: 69/31.

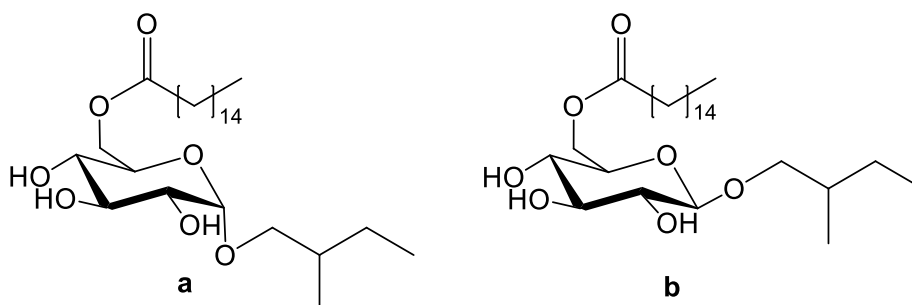
$^1\text{H NMR}$  (DMSO-*d*<sub>6</sub>, 400 MHz):  $\delta$  (ppm) 5.28 (dd,  $J = 3.9, 0.9$  Hz, OH), 5.10 – 5.04 (m, OH), 5.02 (m,  $\text{CH}^{1\alpha}$ ), 4.83 (br s,  $\text{CH}^{1\beta'}$ ), 4.80 – 4.76 (m,  $\text{CH}^{1\beta''}$ , OH), 4.57 (m, OH), 4.46 (dd,  $J = 12.5, 5.5$  Hz, OH), 4.29 – 4.22 (m,  $\text{CH}_2^{6\alpha}$ ), 4.20 – 4.15 (m,  $\text{CH}_2^{6\beta}$ ), 4.04 – 3.89 (m, 6 CH,  $\text{CH}_2^{6''}$ ), 3.89 – 3.77 (m, 10 CH), 3.64 – 3.49 (m, 4 OCH), 2.29 (m,  $\text{COOCH}_2$ ), 1.57 – 1.49 (m,  $\text{COOCH}_2\text{CH}_2$ ), 1.49 – 1.34 (m,  $\text{OCHCH}_2$ ), 1.26 (br s,  $(\text{CH}_2)_{12}$ ), 1.14 – 1.07 (m,  $\text{OCHCH}_3'$ ), 1.07 – 1.03 (m,  $\text{OCHCH}_3''$ ), 0.89 – 0.81 (m,  $\text{CH}_3$ ).

$^{13}\text{C NMR}$  (DMSO-*d*<sub>6</sub>, 101 MHz):  $\delta$  (ppm) 173.44 (COO), 108.87, 106.77 ( $\text{CH}^{1\beta}$ ), 102.21, 100.07 ( $\text{CH}^{1\alpha}$ ), 81.97, 81.76, 81.18, 81.10, 78.53, 78.44, 78.09, 78.06 (8 CH), 76.47 (OCH), 75.82, 75.64, 75.59, 75.54 (4 CH), 75.47, 74.54, 73.47 (3 OCH), 67.17, 67.12 (2  $\text{CH}_2^{6'}$ ), 67.09, 67.07, 66.93, 66.88, (4 CH), 66.77, 66.69 (2  $\text{CH}_2^{6''}$ ), 34.00 ( $\text{COOCH}_2$ ), 30.04, 29.96 (2  $\text{OCHCH}_2$ ), 29.50, 29.33, 29.17, 29.08, 28.94 ( $(\text{CH}_2)_{12}$ ), 24.96, 24.91 ( $\text{COOCH}_2\text{CH}_2$ ), 21.45, 21.27 ( $\text{OCHCH}_3'$ ), 19.63, 19.26 ( $\text{OCHCH}_3''$ ), 14.41 ( $\text{CH}_3$ ), 10.24, 10.23, 10.11, 9.98 ( $\text{OCHCH}_2\text{CH}_3$ ).

$\text{MS (ESI}^+)$ :  $m/z$  calcd for  $[\text{C}_{26}\text{H}_{50}\text{O}_7]$ : 474.36; found: 497.83  $[\text{M}+\text{Na}]^+$ ; 971.36  $[\text{2M}+\text{Na}]^+$ .

$\text{MS (ESI}^-)$ :  $m/z$  calcd for  $[\text{C}_{26}\text{H}_{50}\text{O}_7]$ : 474.36; found: 473.39  $[\text{M}-\text{H}]^-$ ; 947.44  $[\text{2M}-\text{H}]^-$ .

### 5.8.17 Characterization of 2-methyl-1-butyl 6-O-palmitoyl-D-glucopyranosides (43ab)



$R_f$  (eluent: *n*-hexane/EtOAc; 2:8): 0.19.

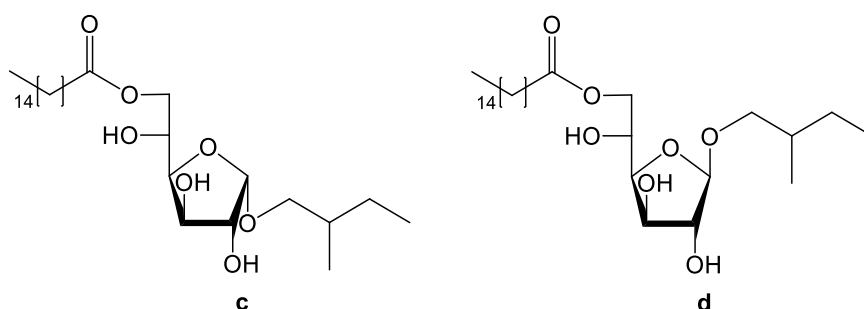
Isomeric ratio a/b: 52/48.

**$^1\text{H}$  NMR (DMSO-*d*<sub>6</sub>, 400 MHz):**  $\delta$  (ppm) 5.12 (m, OH), 4.99 (m, OH), 4.84 (d,  $J = 4.9$  Hz, OH), 4.67 (d,  $J = 5.6$  Hz, OH), 4.61 (d,  $J = 3.6$  Hz,  $\text{CH}^1_\alpha$ ), 4.30 (dd,  $J = 19.0, 7.0$  Hz,  $\text{CH}_2^{6\prime}$ ), 4.12 (d,  $J = 7.8$  Hz,  $\text{CH}^1_\beta$ ), 4.02 (ddd,  $J = 28.5, 11.7, 7.2$  Hz,  $\text{CH}_2^{6''}$ ), 3.58 (m,  $\text{CH}^5_\alpha$ ,  $\text{OCH}_2'^\alpha$ ), 3.51 – 3.39 (m,  $\text{CH}^3_\alpha$ ,  $\text{OCH}_2''_\alpha$ ,  $\text{OCH}_2''_\beta$ ), 3.39 – 3.27 (m,  $\text{CH}^5_\beta$ ,  $\text{OCH}_2'_\alpha$ ,  $\text{OCH}_2''_\beta$ ), 3.25 – 3.17 (m,  $\text{CH}^2_\alpha$ ,  $\text{OCH}_2''_\alpha$ ), 3.17 – 3.10 (m,  $\text{CH}^3_\beta$ ,  $\text{OCH}_2''_\beta$ ), 3.10 – 3.00 (m,  $\text{CH}^4_\alpha$ ,  $\text{CH}^4_\beta$ ), 3.00 – 2.94 (m,  $\text{CH}^2_\beta$ ), 2.28 (td,  $J = 7.3, 4.1$  Hz,  $\text{COOCH}_2$ ), 1.68 – 1.57 (m,  $\text{OCH}_2\text{CH}$ ), 1.57 – 1.47 (m,  $\text{COOCH}_2\text{CH}_2$ ), 1.48 – 1.36 (m,  $\text{OCH}_2'$ ), 1.31 – 1.21 (br s,  $(\text{CH}_2)_{12}$ ,  $\text{OCH}_2\text{CHCH}_2$ ), 1.20 – 1.04 (m,  $\text{OCH}_2''$ ), 0.91 – 0.82 (m,  $\text{CH}_3$ ).

**$^{13}\text{C}$  NMR (DMSO-*d*<sub>6</sub>, 101 MHz):**  $\delta$  (ppm) 173.19 ( $\text{COO}_\beta$ ), 173.13 ( $\text{COO}_\alpha$ ), 103.65, 103.51 ( $\text{CH}^1_\beta$ ), 99.21, 99.05 ( $\text{CH}^1_\alpha$ ), 77.01 ( $\text{CH}^3_\beta$ ), 74.22, 74.15, ( $\text{OCH}_2_\beta$ ), 74.08 ( $\text{CH}^5_\beta$ ), 73.83 ( $\text{CH}^2_\beta$ ), 73.59 ( $\text{CH}^3_\alpha$ ), 72.56 72.45, ( $\text{OCH}_2_\alpha$ ), 72.33 ( $\text{CH}^2_\alpha$ ), 71.06 ( $\text{CH}^4_\beta$ ), 70.74 ( $\text{CH}^4_\alpha$ ), 70.34 ( $\text{CH}^5_\alpha$ ), 64.27 ( $\text{CH}_2^{6\alpha}$ ), 64.04 ( $\text{CH}_2^{6\beta}$ ), 34.84 ( $\text{OCH}_2\text{CH}$ ), 34.10 ( $\text{COOCH}_2$ ), 29.46, 29.32, 29.15, 28.93 ( $(\text{CH}_2)_{12}$ ), 26.25, 26.13, 26.00 (3  $\text{OCH}_2$ ), 24.97 ( $\text{COOCH}_2\text{CH}_2$ ), 22.55 ( $\text{OCH}_2\text{CHCH}_2$ ), 17.13, 16.82 (2  $\text{OCH}_2\text{CHCH}_3$ ), 14.39 ( $\text{CH}_3$ ), 11.66, 11.47, 11.43 (3  $\text{OCH}_2\text{CHCH}_2\text{CH}_3$ ).

**MS (ESI<sup>+</sup>):**  $m/z$  calcd for  $[\text{C}_{27}\text{H}_{52}\text{O}_7]$ : 488.37; found: 511.70  $[\text{M}+\text{Na}]^+$ ; 999.12  $[2\text{M}+\text{Na}]^+$ .

**MS (ESI<sup>-</sup>):**  $m/z$  calcd for  $[\text{C}_{27}\text{H}_{52}\text{O}_7]$ : 488.37; found: 487.45  $[\text{M}-\text{H}]^-$ ; 975.50  $[2\text{M}-\text{H}]^-$ .

5.8.18 Characterization of 2-methyl-1-butyl 6-*O*-palmitoyl-D-glucofuranosides (43cd)

$R_f$  (eluent: *n*-hexane/EtOAc; 2:8): 0.40.

Isomeric ratio c/d: 53/47.

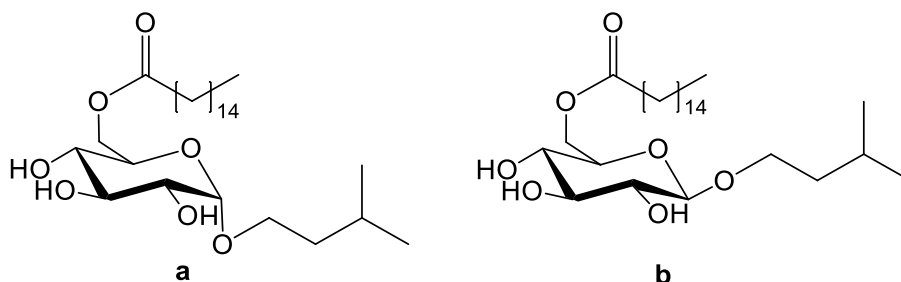
$^1\text{H NMR}$  (DMSO- $d_6$ , 400 MHz):  $\delta$  (ppm) 5.30 (d,  $J = 3.9$  Hz, OH), 5.10 (d,  $J = 4.8$  Hz, OH), 4.89 (d,  $J = 4.1$  Hz,  $\text{CH}^{1\alpha}$ ), 4.78 (dd,  $J = 5.0, 2.8$  Hz, OH), 4.70 (br s,  $\text{CH}^{1\beta}$ ), 4.64 (dd,  $J = 5.0, 3.6$  Hz, OH), 4.58 (d,  $J = 5.5$  Hz, OH), 4.26 (q,  $J = 5.5$  Hz,  $\text{CH}_2^{6\alpha}$ ), 4.18 (m,  $\text{CH}_2^{6\beta}$ ), 4.04 – 3.92 (m, CH, CH, CH,  $\text{CH}_2^{6\gamma}$ ), 3.91 – 3.80 (m, 5 CH), 3.49 – 3.07 (m,  $\text{OCH}_2$ ), 2.29 (ddd,  $J = 11.0, 7.4, 3.4$  Hz,  $\text{COOCH}_2$ ), 1.64 – 1.57 (m,  $\text{OCH}_2\text{CH}$ ), 1.57 – 1.48 (m,  $\text{COOCH}_2\text{CH}_2$ ), 1.46 – 1.35 (m,  $\text{OCH}_2\text{CHCH}_2'$ ), 1.24 (br s,  $(\text{CH}_2)_{12}$ ), 1.15 – 1.05 (m,  $\text{OCH}_2\text{CHCH}_2'$ ), 0.85 (m,  $\text{CH}_3$ ).

$^{13}\text{C NMR}$  (DMSO- $d_6$ , 101 MHz):  $\delta$  (ppm) 173.43 (COO), 109.38, 109.32 ( $\text{CH}^{1\beta}$ ), 102.45, 102.35 ( $\text{CH}^{1\alpha}$ ), 82.00, 80.90, 78.59, 77.91, 75.74, 75.59 (6 CH), 73.26, 73.14, 72.67, 72.63 (4  $\text{OCH}_2$ ), 67.20 (CH), 67.14 ( $\text{CH}_2^{6\alpha}$ ), 66.93 (CH), 66.69 ( $\text{CH}_2^{6\beta}$ ), 34.90, 34.79 (2  $\text{OCH}_2\text{CH}$ ), 34.01 ( $\text{COOCH}_2$ ), 29.49, 29.47, 29.44, 29.34, 29.16, 28.94, 28.92 ( $(\text{CH}_2)_{12}$ ), 26.06 ( $\text{OCH}_2\text{CHCH}_2$ ), 24.95, 24.92 (2  $\text{COOCH}_2\text{CH}_2$ ), 16.92, 16.81 (2  $\text{OCH}_2\text{CHCH}_3$ ), 14.41 ( $\text{CH}_3$ ), 11.61, 11.49 (2  $\text{OCH}_2\text{CHCH}_2\text{CH}_3$ ).

**MS (ESI<sup>+</sup>):**  $m/z$  calcd for  $[\text{C}_{27}\text{H}_{52}\text{O}_7]$ : 488.37; found: 511.72  $[\text{M}+\text{Na}]^+$ ; 998.93  $[2\text{M}+\text{Na}]^+$ .

**MS (ESI<sup>-</sup>):**  $m/z$  calcd for  $[\text{C}_{27}\text{H}_{52}\text{O}_7]$ : 488.37; found: 487.78  $[\text{M}-\text{H}]^-$ ; 975.86  $[2\text{M}-\text{H}]^-$ .

### 5.8.19 Characterization of 3-methyl-1-butyl 6-O-palmitoyl-D-glucopyranosides (44ab)



$R_f$  (eluent: *n*-hexane/EtOAc; 2:8): 0.18.

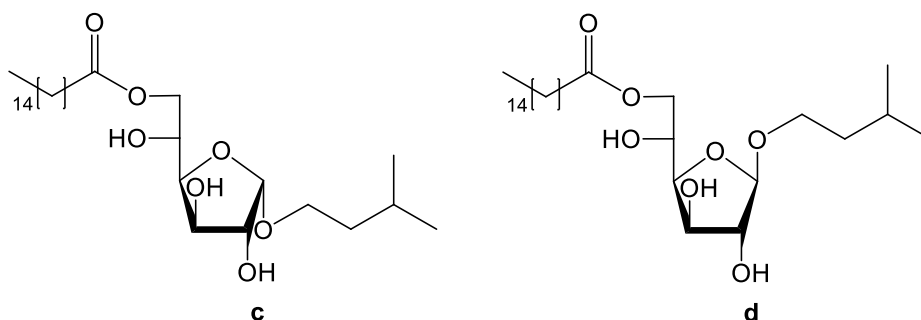
Isomeric ratio a/b: 62/38.

**$^1\text{H NMR}$  (DMSO- $d_6$ , 400 MHz):**  $\delta$  (ppm) 5.13 (m, OH), 5.01 (d,  $J = 4.9$  Hz, OH), 4.85 (d,  $J = 4.9$  Hz, OH), 4.69 (d,  $J = 6.2$  Hz, OH), 4.62 (d,  $J = 3.6$  Hz,  $\text{CH}^1_\alpha$ ), 4.30 (ddd,  $J = 11.5, 7.0, 1.7$  Hz,  $\text{CH}_2^{6\alpha}$ ), 4.13 (d,  $J = 7.8$  Hz,  $\text{CH}^1_\beta$ ), 4.02 (ddd,  $J = 22.3, 11.7, 7.2$  Hz, 2H,  $\text{CH}_2^{6\beta}$ ), 3.72 (dt,  $J = 9.7, 6.9$  Hz,  $\text{OCH}_2^\beta$ ), 3.66 – 3.55 (m,  $\text{CH}^5_\alpha$ ,  $\text{OCH}_2^\alpha$ ), 3.49 – 3.44 (m,  $\text{OCH}_2^\beta$ ), 3.44 – 3.30 (m,  $\text{CH}^3_\alpha$ ,  $\text{CH}^5_\beta$ ,  $\text{OCH}_2^\alpha$ ), 3.19 (ddd,  $J = 9.7, 6.2, 3.7$  Hz,  $\text{CH}^2_\alpha$ ), 3.16 – 3.11 (m,  $\text{CH}^3_\beta$ ), 3.03 (m,  $\text{CH}^4_\alpha$ ,  $\text{CH}^4_\beta$ ), 2.95 (td,  $J = 8.3, 5.0$  Hz,  $\text{CH}^2_\beta$ ), 2.28 (m,  $\text{COOCH}_2$ ), 1.75 – 1.62 (m,  $\text{OCH}_2\text{CH}_2\text{CH}$ ), 1.56 – 1.47 (m,  $\text{COOCH}_2\text{CH}_2$ ), 1.47 – 1.35 (m,  $\text{OCH}_2\text{CH}_2$ ), 1.26 (br s,  $(\text{CH}_2)_{12}$ ), 0.92 – 0.82 (m,  $\text{CH}_3$ ).

**$^{13}\text{C NMR}$  (DMSO- $d_6$ , 101 MHz):**  $\delta$  (ppm) 173.24 ( $\text{COO}_\beta$ ), 173.20 ( $\text{COO}_\alpha$ ), 103.29 ( $\text{CH}^1_\beta$ ), 99.08 ( $\text{CH}^1_\alpha$ ), 76.95 ( $\text{CH}^3_\beta$ ), 74.05 ( $\text{CH}^5_\beta$ ), 73.76 ( $\text{CH}^2_\beta$ ), 73.53 ( $\text{CH}^3_\alpha$ ), 72.22 ( $\text{CH}^2_\alpha$ ), 71.02 ( $\text{CH}^4_\beta$ ), 70.68 ( $\text{CH}^4_\alpha$ ), 70.32 ( $\text{CH}^5_\alpha$ ), 67.36 ( $\text{OCH}_2_\beta$ ), 65.85 ( $\text{OCH}_2_\alpha$ ), 64.29 ( $\text{CH}_2^{6\alpha}$ ), 64.04 ( $\text{CH}_2^{6\beta}$ ), 38.60, 38.49 (2  $\text{OCH}_2\text{CH}_2$ ), 34.03 ( $\text{COOCH}_2$ ), 29.49, 29.46, 29.31, 29.16, 29.12, 28.90 ( $(\text{CH}_2)_{12}$ ), 24.99 ( $\text{COOCH}_2\text{CH}_2$ ), 24.98 ( $\text{OCH}_2\text{CH}_2\text{CH}$ ), 24.93 ( $\text{COOCH}_2\text{CH}_2$ ), 24.76 ( $\text{OCH}_2\text{CH}_2\text{CH}$ ), 23.16, 22.96, 22.79, 22.65 (4  $\text{OCH}_2\text{CH}_2\text{CH}(\text{CH}_3)_2$ ), 14.41 ( $\text{CH}_3$ ).

**MS (ESI $^+$ ):**  $m/z$  calcd for  $[\text{C}_{27}\text{H}_{52}\text{O}_7]^+$ : 488.37; found: 511.72  $[\text{M}+\text{Na}]^+$ ; 999.61  $[\text{2M}+\text{Na}]^+$ .

**MS (ESI $^-$ ):**  $m/z$  calcd for  $[\text{C}_{27}\text{H}_{52}\text{O}_7]^-$ : 488.37; found: 487.82  $[\text{M}-\text{H}]^-$ ; 976.17  $[\text{2M}-\text{H}]^-$ .

5.8.20 Characterization of 3-methyl-1-butyl 6-*O*-palmitoyl-D-glucofuranosides (44cd)

$R_f$  (eluent: *n*-hexane/EtOAc; 2:8): 0.32.

Isomeric ratio *c/d*: 59/41.

$^1\text{H NMR}$  (DMSO- $d_6$ , 400 MHz):  $\delta$  (ppm) 5.35 (d,  $J = 3.9$  Hz, OH), 5.15 (d,  $J = 4.7$  Hz, OH), 4.97 (d,  $J = 4.0$  Hz,  $\text{CH}^{1\alpha}$ ), 4.84 (d,  $J = 3.4$  Hz, OH), 4.76 (br s,  $\text{CH}^{1\beta}$ ), 4.70 (d,  $J = 5.0$  Hz, OH), 4.66 (d,  $J = 5.4$  Hz, OH), 4.31 (dd,  $J = 14.4, 5.5$  Hz,  $\text{CH}_2^{6\prime\alpha}$ ), 4.24 (d,  $J = 12.1$  Hz,  $\text{CH}_2^{6\prime\beta}$ ), 4.08 – 3.97 (m, CH, CH,  $\text{CH}_2^{6''}$ ), 3.96 – 3.85 (m, 6 CH), 3.72 – 3.60 (m,  $\text{OCH}_2'$ ), 3.50 (dt,  $J = 9.9, 6.7$  Hz,  $\text{OCH}_2''\alpha$ ), 3.42 – 3.37 (m,  $\text{OCH}_2''\beta$ ), 2.35 (td,  $J = 7.4, 3.0$  Hz,  $\text{COOCH}_2$ ), 1.72 (dq,  $J = 20.1, 6.7$  Hz,  $\text{OCH}_2\text{CH}_2\text{CH}$ ), 1.62 – 1.53 (m,  $\text{COOCH}_2\text{CH}_2$ ), 1.51 – 1.39 (m,  $\text{OCH}_2\text{CH}_2$ ), 1.30 (br s,  $(\text{CH}_2)_{12}$ ), 0.96 – 0.88 (m,  $\text{CH}_3$ ).

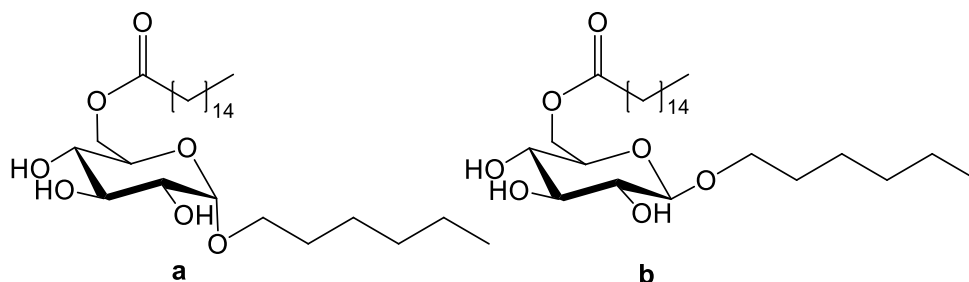
$^{13}\text{C NMR}$  (DMSO- $d_6$ , 101 MHz):  $\delta$  (ppm) 173.44 (COO), 109.29 ( $\text{CH}^{1\beta}$ ), 102.41 ( $\text{CH}^{1\alpha}$ ), 81.96, 80.94, 78.69, 77.77, 75.76, 75.56, 67.20 (7 CH), 67.13 ( $\text{CH}_2^{6\alpha}$ ), 66.92 (CH), 66.72 ( $\text{CH}_2^{6\beta}$ ), 66.58, 65.96 (2  $\text{OCH}_2$ ), 38.58 ( $\text{OCH}_2\text{CH}_2$ ), 34.02 ( $\text{COOCH}_2$ ), 29.48, 29.35, 29.16, 28.93 ( $(\text{CH}_2)_{12}$ ), 24.93 ( $\text{COOCH}_2\text{CH}_2$ ), 24.85 ( $\text{OCH}_2\text{CH}_2\text{CH}$ ), 22.98, 22.80 ( $\text{OCH}_2\text{CH}_2\text{CH}(\text{CH}_3)_2$ ), 14.41 ( $\text{CH}_3$ ).

$\text{MS (ESI}^+)$ :  $m/z$  calcd for  $[\text{C}_{27}\text{H}_{52}\text{O}_7]$ : 488.37; found: 511.88  $[\text{M}+\text{Na}]^+$ ; 998.71  $[2\text{M}+\text{Na}]^+$ .

$\text{MS (ESI}^-)$ :  $m/z$  calcd for  $[\text{C}_{27}\text{H}_{52}\text{O}_7]$ : 488.37; found: 487.54  $[\text{M}-\text{H}]^-$ ; 975.69  $[2\text{M}-\text{H}]^-$ .



## 5.8.21 Characterization of 1-hexyl 6-O-palmitoyl-D-glucopyranosides (45ab)



$R_f$  (eluent: *n*-hexane/EtOAc; 2:8): 0.20.

Isomeric ratio a/b: 60/40.

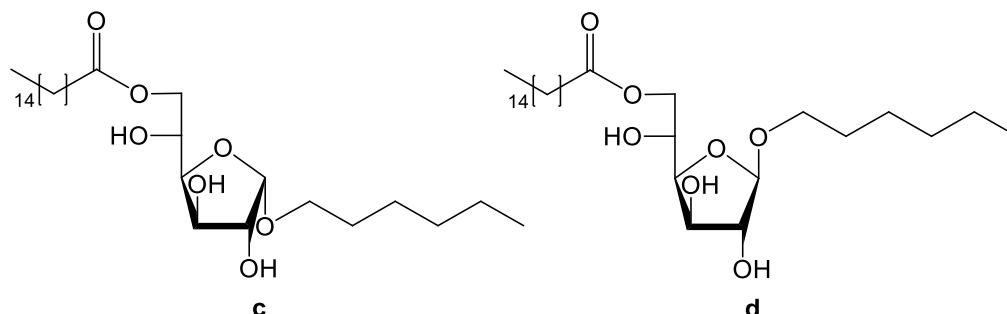
**<sup>1</sup>H NMR (DMSO-*d*<sub>6</sub>, 400 MHz):** δ (ppm) 5.13 (d, *J* = 5.7 Hz, OH), 5.02 (m, OH), 4.85 (d, *J* = 4.9 Hz, OH), 4.69 (d, *J* = 6.3 Hz, OH), 4.62 (d, *J* = 3.7 Hz, CH<sup>1</sup><sub>α</sub>), 4.30 (td, *J* = 12.0, 1.6 Hz, CH<sub>2</sub><sup>6'</sup><sub>α</sub>, CH<sub>2</sub><sup>6'</sup><sub>β</sub>), 4.12 (d, *J* = 7.8 Hz, CH<sup>1</sup><sub>β</sub>), 4.01 (ddd, *J* = 25.7, 11.7, 7.3 Hz, CH<sub>2</sub><sup>6''</sup><sub>α</sub>, CH<sub>2</sub><sup>6''</sup><sub>β</sub>), 3.67 (dt, *J* = 9.6, 6.8 Hz, OCH<sub>2</sub>'<sub>β</sub>), 3.57 (ddd, *J* = 18.8, 10.6, 6.3 Hz, CH<sup>5</sup><sub>α</sub>, OCH<sub>2</sub>'<sub>α</sub>), 3.45 – 3.38 (m, CH<sup>3</sup><sub>α</sub>, OCH<sub>2</sub>'<sub>β</sub>), 3.37 – 3.29 (m, CH<sup>5</sup><sub>β</sub>, OCH<sub>2</sub>'<sub>α</sub>), 3.20 (ddd, *J* = 9.6, 6.2, 3.6 Hz, CH<sup>2</sup><sub>α</sub>), 3.17 – 3.11 (m, CH<sup>3</sup><sub>β</sub>), 3.03 (ddd, *J* = 16.0, 8.9, 6.5 Hz, CH<sup>4</sup><sub>α</sub>, CH<sup>4</sup><sub>β</sub>), 2.95 (td, *J* = 8.4, 5.0 Hz, CH<sup>2</sup><sub>β</sub>), 2.28 (td, *J* = 7.2, 4.0 Hz, COOCH<sub>2</sub>), 1.52 (m, COOCH<sub>2</sub>CH<sub>2</sub>, OCH<sub>2</sub>CH<sub>2</sub>), 1.26 (br s, OCH<sub>2</sub>CH<sub>2</sub>(CH<sub>2</sub>)<sub>3</sub>, (CH<sub>2</sub>)<sub>12</sub>), 0.86 (t, *J* = 5.8 Hz, CH<sub>3</sub>).

**<sup>13</sup>C NMR (DMSO-*d*<sub>6</sub>, 101 MHz):** δ (ppm) 173.22 (COO<sub>β</sub>), 173.15 (COO<sub>α</sub>), 103.33 (CH<sup>1</sup><sub>β</sub>), 99.01 (CH<sup>3</sup><sub>β</sub>), 76.94 (CH<sup>3</sup><sub>β</sub>), 74.05 (CH<sup>5</sup><sub>β</sub>), 73.77 (CH<sup>2</sup><sub>β</sub>), 73.56 (CH<sup>3</sup><sub>α</sub>), 72.25 (CH<sup>2</sup><sub>α</sub>), 71.04 (CH<sup>4</sup><sub>α</sub>), 70.69 (CH<sup>4</sup><sub>β</sub>), 70.26 (CH<sup>5</sup><sub>α</sub>), 69.13 (OCH<sub>2</sub> β), 67.49 (OCH<sub>2</sub> α), 64.28 (CH<sub>2</sub><sup>6</sup><sub>α</sub>), 64.06 (CH<sub>2</sub><sup>6</sup><sub>β</sub>), 34.06, 34.02 (2 COOCH<sub>2</sub>), 31.58, 31.54 (2 OCH<sub>2</sub>CH<sub>2</sub>CH<sub>2</sub>), 29.77, 29.55 ((CH<sub>2</sub>)<sub>12</sub>), 29.50, 29.47 (2 OCH<sub>2</sub>CH<sub>2</sub>CH<sub>2</sub>), 29.34, 29.16, 28.93, 28.90 ((CH<sub>2</sub>)<sub>12</sub>), 25.85, 25.65 (OCH<sub>2</sub>CH<sub>2</sub>(CH<sub>2</sub>)<sub>3</sub>), 25.01, 24.96 (COOCH<sub>2</sub>CH<sub>2</sub>), 14.40, 14.35 (CH<sub>3</sub>).

**MS (ESI<sup>+</sup>):** *m/z* calcd for [C<sub>28</sub>H<sub>54</sub>O<sub>7</sub>]: 502.39; found: 525.72 [M+Na]<sup>+</sup>; 1027.05 [2M+Na]<sup>+</sup>.

**MS (ESI<sup>-</sup>):** *m/z* calcd for [C<sub>28</sub>H<sub>54</sub>O<sub>7</sub>]: 502.39; found: 501.88 [M-H]<sup>-</sup>; 1004.20 [2M-H]<sup>-</sup>.

## 5.8.22 Characterization of 1-hexyl 6-O-palmitoyl-D-glucofuranosides (45cd)



$R_f$  (eluent: *n*-hexane/EtOAc; 2:8): 0.45.

Isomeric ratio c/d: 60/40.

**$^1\text{H NMR}$  (DMSO- $d_6$ , 400 MHz):**  $\delta$  (ppm) 5.35 (d,  $J = 3.9$  Hz, OH), 5.15 (d,  $J = 4.7$  Hz, OH), 4.96 (d,  $J = 4.0$  Hz,  $\text{CH}^{1\alpha}$ ), 4.84 (dd,  $J = 5.0, 2.8$  Hz, OH), 4.76 (br s,  $\text{CH}^{1\beta}$ ), 4.71 (d,  $J = 5.0$  Hz, OH), 4.68 (d,  $J = 5.4$  Hz, OH), 4.30 (dd,  $J = 14.4, 5.5$  Hz,  $\text{CH}_2^{6\alpha}$ ), 4.23 (d,  $J = 11.9$  Hz,  $\text{CH}_2^{6\beta}$ ), 4.08 – 3.97 (m, CH, CH,  $\text{CH}_2^{6''}$ ), 3.95 – 3.84 (m, 6 CH), 3.67 – 3.57 (m,  $\text{OCH}_2'$ ), 3.47 (dt,  $J = 9.6, 6.6$  Hz,  $\text{OCH}_2''\alpha$ ), 3.39 – 3.34 (m,  $\text{OCH}_2''\beta$ ), 2.34 (m,  $\text{COOCH}_2$ ), 1.63 – 1.48 (m,  $\text{COOCH}_2\text{CH}_2$ ,  $\text{OCH}_2\text{CH}_2$ ), 1.30 (br s,  $\text{OCH}_2\text{CH}_2(\text{CH}_2)_3$ ,  $(\text{CH}_2)_{12}$ ), 0.92 (m,  $\text{CH}_3$ ).

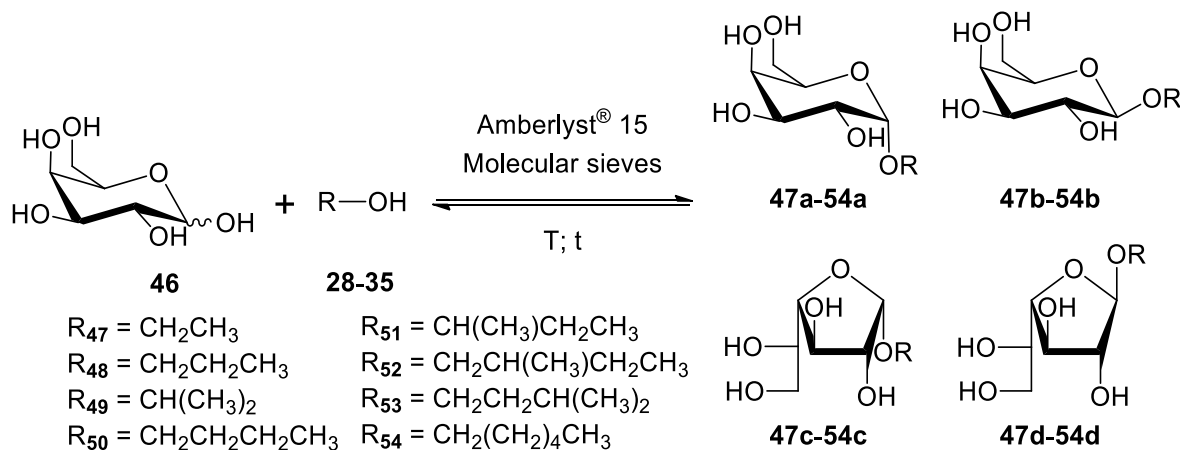
**$^{13}\text{C NMR}$  (DMSO- $d_6$ , 101 MHz):**  $\delta$  (ppm) 173.41 (COO), 109.29 ( $\text{CH}^{1\beta}$ ), 102.43 ( $\text{CH}^{1\alpha}$ ), 81.98, 80.97, 78.67, 77.82, 75.78, 75.63 (6 CH), 68.32, 67.72 (2  $\text{OCH}_2$ ), 67.24 (CH), 67.14 ( $\text{CH}_2^{6\alpha}$ ), 66.94 (CH), 66.72 ( $\text{CH}_2^{6\beta}$ ), 34.04 ( $\text{COOCH}_2$ ), 31.51 ( $\text{OCH}_2\text{CH}_2\text{CH}_2$ ), 29.75 ( $(\text{CH}_2)_{12}$ ), 29.49 ( $\text{OCH}_2\text{CH}_2\text{CH}_2$ ), 29.49, 29.35, 29.17, 28.95 ( $(\text{CH}_2)_{12}$ ), 25.75 ( $\text{OCH}_2\text{CH}_2(\text{CH}_2)_3$ ), 24.95 ( $\text{COOCH}_2\text{CH}_2$ ), 14.41, 13.44 ( $\text{CH}_3$ ).

**MS (ESI $^+$ ):**  $m/z$  calcd for  $[\text{C}_{28}\text{H}_{54}\text{O}_7]$ : 502.39; found: 525.99  $[\text{M}+\text{Na}]^+$ ; 1027.70  $[2\text{M}+\text{Na}]^+$ .

**MS (ESI $^-$ ):**  $m/z$  calcd for  $[\text{C}_{28}\text{H}_{54}\text{O}_7]$ : 502.39; found: 501.74  $[\text{M}-\text{H}]^-$ ; 1003.45  $[2\text{M}-\text{H}]^-$ .

## 5.9 Alkyl D-galactoside isomeric mixtures

### 5.9.1 Sustainable synthesis of alkyl D-galactosides (47ad-54ad)



D-(+)-Galactose (**46**) was suspended in dry naturally occurring alcohols (**28-35**) (1.8% w/v) in the presence of the strongly acidic cation exchange resin Amberlyst<sup>®</sup> 15 (10 %, w/w) and 3 Å molecular sieves (25 %, w/w), under reflux or at 120 °C, according to the alcohol boiling points.

After reaction times reported in **Table 5.6**, the reactions were stopped by filtration of the solid catalyst, the alcohols were removed under reduced pressure and the reaction mixtures were submitted to flash chromatography (DCM/MeOH; 9:1) to give **alkyl D-galactosides isomeric mixtures (47ad-54ad)** as viscous syrups. All products were fully characterized by TLC, ESI-MS and NMR analysis. Some <sup>1</sup>H and <sup>13</sup>C peaks are not completely resolved because of the instrument resolution.

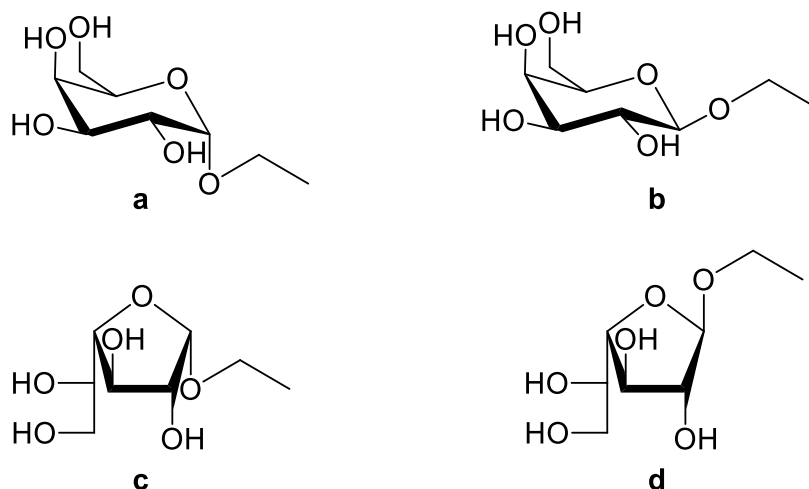
Isomeric ratios of each alkyl D-galactoside isomeric mixture were estimated by <sup>1</sup>H NMR analysis, carried out in D<sub>2</sub>O and in DMSO-*d*<sub>6</sub>, as the ratio of the areas of anomeric proton signals of each isomer present in the reaction mixture.

## 5 | Experimental section

**Table 5.6.** Experimental conditions for the synthesis of alkyl D-galactoside isomeric mixtures.

<i>R-OH</i>	<i>Temperature</i> (°C)	<i>Time</i> (h)	<i>Yield</i> (%)	<i>Isomeric ratio</i> <i>a/b/c/d</i> (%)
EtOH ( <b>28</b> )	90	4	73	13/6/31/50
1-PrOH ( <b>29</b> )	100	3	78	25/10/16/49
2-PrOH ( <b>30</b> )	90	6	36	24/12/21/43
1-BuOH ( <b>31</b> )	120	2.5	81	40/15/34/11
2-BuOH ( <b>32</b> )	120	6	88	36/12/16/36
2-Me-1-BuOH ( <b>33</b> )	120	1.5	95	29/12/17/42
3-Me-1-BuOH ( <b>34</b> )	120	2	88	38/15/11/36
1-HexOH ( <b>35</b> )	120	1.5	32	31/13/14/42

## 5.9.2 Characterization of ethyl D-galactoside isomeric mixture (47ad)



$R_f$  (eluent: DCM/MeOH; 9:1): 0.18; 0.26.

Isomeric ratio a/b/c/d: 13/6/31/50.

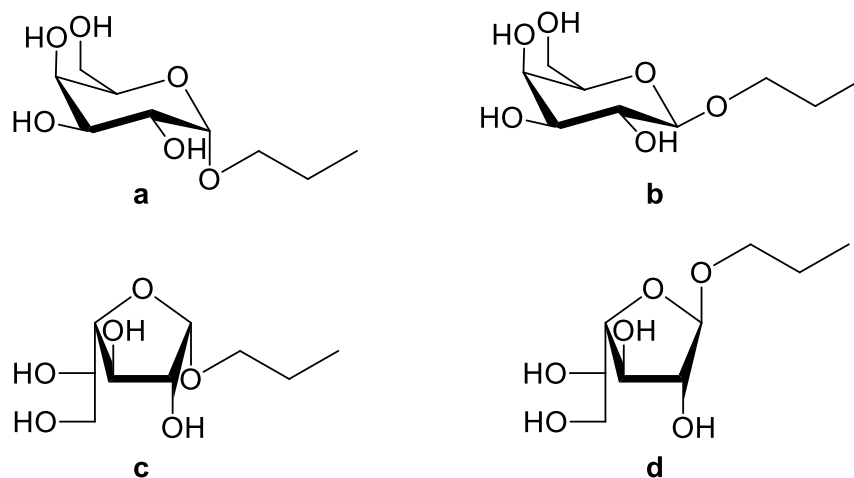
$^1\text{H NMR}$  (DMSO- $d_6$ , 400 MHz):  $\delta$  (ppm) 5.26 (d,  $J = 5.6$  Hz, OH), 5.10 (d,  $J = 5.9$  Hz, OH), 5.05 (d,  $J = 5.7$  Hz, OH), 4.80 (d,  $J = 7.2$  Hz, OH), 4.72 (d,  $J = 4.5$  Hz,  $\text{CH}^1_{\alpha\text{-Fu}}$ ), 4.70 (d,  $J = 2.4$  Hz,  $\text{CH}^1_{\beta\text{-Fu}}$ ), 4.64 (d,  $J = 3.5$  Hz,  $\text{CH}^1_{\alpha\text{-Py}}$ ), 4.51 (m, OH), 4.39 (d,  $J = 6.3$  Hz, OH), 4.32 (d,  $J = 4.2$  Hz, OH), 4.09 (m,  $\text{CH}^1_{\beta\text{-Py}}$ ), 3.90 (dd,  $J = 13.6, 6.9$  Hz, CH), 3.85 – 3.79 (m, CH, CH), 3.78 – 3.68 (m, CH, CH, CH,  $\text{OCH}_2$ ), 3.67 – 3.59 (m, CH,  $\text{OCH}_2$ ), 3.59 – 3.58 (br s, CH), 3.57 – 3.50 (m, CH, CH), 3.50 – 3.45 (m, CH,  $\text{CH}_2^{\delta'}$ ), 3.44 – 3.34 (m, CH, CH,  $\text{CH}_2^{\delta''}$ ,  $\text{OCH}_2$ ), 3.34 – 3.28 (m, CH,  $\text{OCH}_2$ ), 3.28 – 3.24 (m, CH, CH), 1.12 (t,  $J = 7.1$  Hz,  $\text{CH}_3$ ).

$^{13}\text{C NMR}$  (DMSO- $d_6$ , 101 MHz):  $\delta$  (ppm) 107.95 ( $\text{CH}^1_{\beta\text{-Fu}}$ ), 103.67 ( $\text{CH}^1_{\beta\text{-Py}}$ ), 101.15 ( $\text{CH}^1_{\alpha\text{-Fu}}$ ), 99.16 ( $\text{CH}^1_{\alpha\text{-Py}}$ ), 82.46, 82.38, 82.30, 77.70, 76.98, 75.56, 74.73, 73.93, 72.70, 71.59, 71.00, 70.85, 70.08, 69.32, 68.84, 68.62 (16 CH), 64.18, 63.25, 62.98, 62.79 (4  $\text{OCH}_2$ ), 61.08, 60.91 (2  $\text{CH}_2^{\delta}$ ), 15.62 ( $\text{CH}_3$ ).

$\text{MS (ESI}^+)$ :  $m/z$  calcd for  $[\text{C}_8\text{H}_{16}\text{O}_6]$ : 208.09; found: 231.28  $[\text{M}+\text{Na}]^+$ , 439.13  $[\text{2M}+\text{Na}]^+$ .

$\text{MS (ESI}^-)$ :  $m/z$  calcd for  $[\text{C}_8\text{H}_{16}\text{O}_6]$ : 208.09; found: 207.85  $[\text{M}-\text{H}]^-$ .

## 5.9.3 Characterization of 1-propyl D-galactoside isomeric mixture (48ad)



$R_f$  (eluent: DCM/MeOH; 9:1): 0.23; 0.30.

Isomeric ratio a/b/c/d: 25/10/16/49.

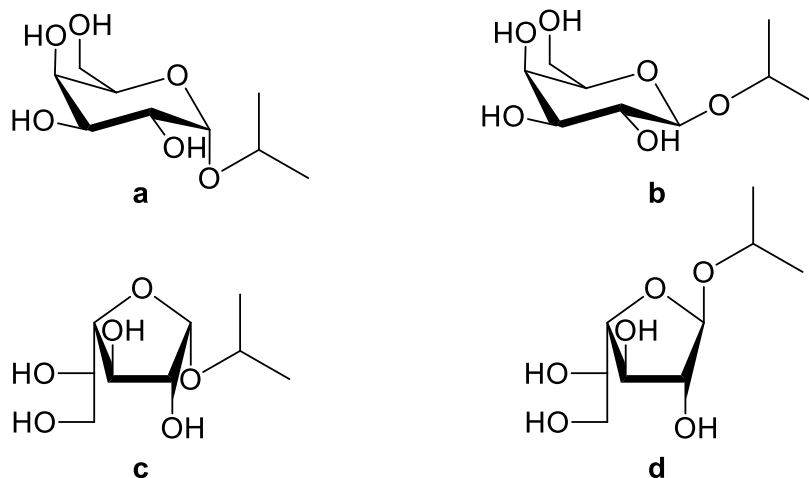
$^1\text{H NMR}$  (DMSO- $d_6$ , 400 MHz):  $\delta$  (ppm) 5.26 (d,  $J = 5.6$  Hz, OH), 5.10 (d,  $J = 5.9$  Hz, OH), 5.04 (d,  $J = 5.6$  Hz, OH), 4.80 – 4.74 (m, OH), 4.71 (d,  $J = 4.5$  Hz,  $\text{CH}^1_{\alpha\text{-Fu}}$ ), 4.69 (d,  $J = 2.3$  Hz,  $\text{CH}^1_{\beta\text{-Fu}}$ ), 4.65 (d,  $J = 5.1$  Hz, OH), 4.63 (d,  $J = 3.3$  Hz,  $\text{CH}^1_{\alpha\text{-Py}}$ ), 4.57 – 4.47 (m, OH), 4.38 (d,  $J = 6.2$  Hz, OH), 4.32 (d,  $J = 4.2$  Hz, OH), 4.09 (m,  $\text{CH}^1_{\beta\text{-Py}}$ ), 3.90 (dd,  $J = 13.6, 7.0$  Hz, CH), 3.82 (dd,  $J = 8.8, 3.7$  Hz, CH), 3.76 (m, CH, CH), 3.71 (m, CH, CH,  $\text{OCH}_2$ ), 3.65 – 3.61 (m, CH,  $\text{OCH}_2$ ), 3.61 – 3.54 (m, CH, CH, CH), 3.53 – 3.46 (m, CH,  $\text{CH}_2^{6'}$ ,  $\text{OCH}_2$ ), 3.46 – 3.43 (m,  $\text{CH}_2^{6'}$ ), 3.42 – 3.26 (m, CH, CH,  $\text{CH}_2^{6''}$ ,  $\text{OCH}_2$ ), 3.34 – 3.14 (m, CH, CH, CH,  $\text{CH}_2^{6''}$ ,  $\text{OCH}_2$ ), 1.52 (dt,  $J = 14.3, 7.2$  Hz,  $\text{OCH}_2\text{CH}_2$ ), 0.88 (m,  $\text{CH}_3$ ).

$^{13}\text{C NMR}$  (DMSO- $d_6$ , 101 MHz):  $\delta$  (ppm) 108.12 ( $\text{CH}^1_{\beta\text{-Fu}}$ ), 103.89 ( $\text{CH}^1_{\beta\text{-Py}}$ ), 101.37 ( $\text{CH}^1_{\alpha\text{-Fu}}$ ), 99.27 ( $\text{CH}^1_{\alpha\text{-Py}}$ ), 82.46, 82.39, 82.38, 77.74, 77.07, 75.55, 74.73, 73.94, 72.82, 71.60, 71.03, 70.89 (12 CH), 70.52 ( $\text{OCH}_2$ ), 70.07, 69.33 (2 CH), 69.28, 69.00, 68.96 (3  $\text{OCH}_2$ ), 68.89, 68.61 (2 CH), 63.29, 62.99, 61.06, 60.89 (4  $\text{CH}_2^6$ ), 22.95, 22.84 (2  $\text{OCH}_2\text{CH}_2$ ), 11.10, 10.99 (2  $\text{CH}_3$ ).

$\text{MS (ESI}^+)$ :  $m/z$  calcd for  $[\text{C}_9\text{H}_{18}\text{O}_6]$ : 222.11; found: 245.50  $[\text{M}+\text{Na}]^+$ .

$\text{MS (ESI}^-)$ :  $m/z$  calcd for  $[\text{C}_9\text{H}_{18}\text{O}_6]$ : 222.11; found: 221.11  $[\text{M}-\text{H}]^-$ .

## 5.9.4 Characterization of 2-propyl D-galactoside isomeric mixture (49ad)



$R_f$  (eluent: DCM/MeOH; 9:1). 0.23; 0.30.

Isomeric ratio a/b/c/d: 24/12/21/43.

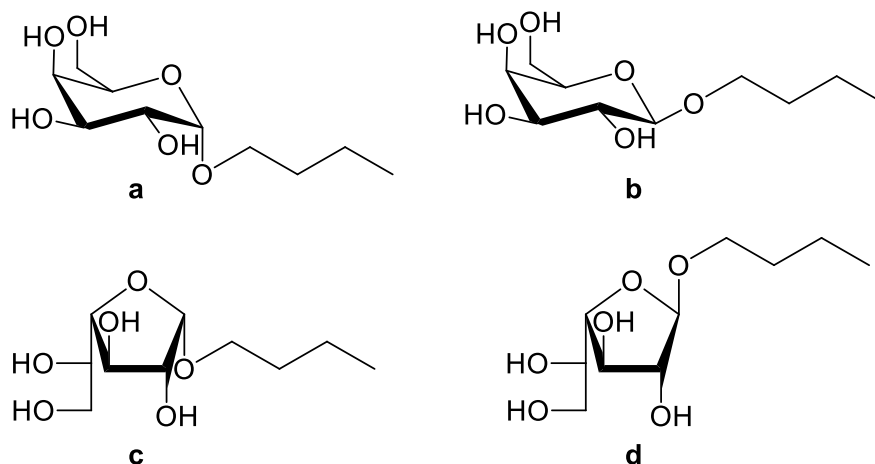
**$^1\text{H NMR}$  (DMSO- $d_6$ , 400 MHz):**  $\delta$  (ppm) 5.23 (d,  $J = 5.7$  Hz, OH), 5.11 (d,  $J = 5.9$  Hz, OH), 5.02 (d,  $J = 5.7$  Hz, OH), 4.84 (d,  $J = 4.6$  Hz,  $\text{CH}^1_{\alpha\text{-Fu}}$ ), 4.79 (d,  $J = 2.4$  Hz,  $\text{CH}^1_{\beta\text{-Fu}}$ ), 4.73 (d,  $J = 3.5$  Hz,  $\text{CH}^1_{\alpha\text{-Py}}$ ), 4.70 (d,  $J = 4.4$  Hz, OH), 4.65 (d,  $J = 7.5$  Hz, OH), 4.52 (m, OH), 4.46 (d,  $J = 5.4$  Hz, OH), 4.30 (d,  $J = 4.0$  Hz, OH), 4.22 (d,  $J = 6.6$  Hz, OH), 4.11 (m,  $\text{CH}^1_{\beta\text{-Py}}$ ), 3.92 – 3.85 (m, CH, OCH), 3.84 – 3.74 (m, CH, CH, OCH, OCH), 3.74 – 3.68 (m, CH, CH, OCH), 3.68 – 3.60 (m, CH, CH), 3.58 – 3.52 (m, CH, CH), 3.52 – 3.45 (m, CH,  $\text{CH}_2^{6'}$ ), 3.45 – 3.36 (m, CH, CH,  $\text{CH}_2^{6''}$ ), 3.34 – 3.28 (m, CH,  $\text{CH}_2^{6'}$ ), 3.27 – 3.20 (m, CH, CH), 1.17 – 1.05 (m,  $\text{CH}_3$ ).

**$^{13}\text{C NMR}$  (DMSO- $d_6$ , 101 MHz):**  $\delta$  (ppm) 106.42 ( $\text{CH}^1_{\beta\text{-Fu}}$ ), 102.12 ( $\text{CH}^1_{\beta\text{-Py}}$ ), 99.73 ( $\text{CH}^1_{\alpha\text{-Fu}}$ ), 97.67 ( $\text{CH}^1_{\alpha\text{-Py}}$ ), 82.77, 82.29, 82.14, 77.52, 77.07, 75.45, 74.80, 74.00, 72.60, 71.58, 71.08, 70.86, 70.26 (13 CH), 70.08, 69.69, 69.33, 69.02 (4 OCH), 68.97, 68.75, 68.59 (3 CH), 63.36, 63.03, 61.04, 60.88 (4  $\text{CH}_2^6$ ), 24.07, 24.01, 23.82, 23.75, 22.26, 22.23, 22.14, 21.90 (8  $\text{CH}_3$ ).

**MS (ESI $^+$ ):**  $m/z$  calcd for  $[\text{C}_9\text{H}_{18}\text{O}_6]$ : 222.11; found: 245.26  $[\text{M}+\text{Na}]^+$ , 467.11  $[2\text{M}+\text{Na}]^+$ .

**MS (ESI $^-$ ):**  $m/z$  calcd for  $[\text{C}_9\text{H}_{18}\text{O}_6]$ : 222.11; found: 221.37  $[\text{M}-\text{H}]^-$ .

## 5.9.5 Characterization of 1-butyl D-galactoside isomeric mixture (50ad)



$R_f$  (eluent: DCM/MeOH; 9:1): 0.26; 0.37.

Isomeric ratio a/b/c/d: 40/15/34/11.

$^1\text{H NMR}$  (DMSO- $d_6$ , 400 MHz):  $\delta$  (ppm) 5.26 (d,  $J = 5.6$  Hz, OH), 5.10 (d,  $J = 5.9$  Hz, OH), 5.04 (d,  $J = 5.6$  Hz, OH), 4.77 (m, OH), 4.71 (d,  $J = 4.5$  Hz,  $\text{CH}^1_{\alpha\text{-Fu}}$ ), 4.68 (d,  $J = 2.3$  Hz,  $\text{CH}^1_{\beta\text{-Fu}}$ ), 4.65 (d,  $J = 5.0$  Hz, OH), 4.62 (d,  $J = 3.4$  Hz,  $\text{CH}^1_{\alpha\text{-Py}}$ ), 4.57 – 4.46 (m, OH), 4.37 (d,  $J = 6.3$  Hz, OH), 4.31 (d,  $J = 4.2$  Hz, OH), 4.08 (d,  $J = 5.3$  Hz, OH), 4.05 (d,  $J = 7.3$  Hz,  $\text{CH}^1_{\beta\text{-Py}}$ ), 3.90 (dd,  $J = 13.5, 6.9$  Hz, CH), 3.82 (m, CH), 3.78 – 3.73 (m, CH, CH,  $\text{CH}_2^{6'}$ ), 3.73 – 3.68 (m, CH, CH,  $\text{OCH}_2$ ), 3.64 – 3.61 (m, CH), 3.60 – 3.54 (m, CH, CH,  $\text{OCH}_2$ ), 3.54 – 3.46 (m, CH,  $\text{CH}_2^{6'}$ ), 3.46 – 3.42 (m,  $\text{CH}_2^{6''}$ ), 3.42 – 3.36 (m, CH,  $\text{CH}_2^{6''}$ ,  $\text{OCH}_2$ ), 3.36 – 3.28 (m, CH, CH,  $\text{OCH}_2$ ), 3.28 – 3.24 (m, CH, CH), 1.50 (m,  $\text{OCH}_2\text{CH}_2$ ), 1.34 (m,  $\text{OCH}_2\text{CH}_2\text{CH}_2$ ), 0.89 (m,  $\text{CH}_3$ ).

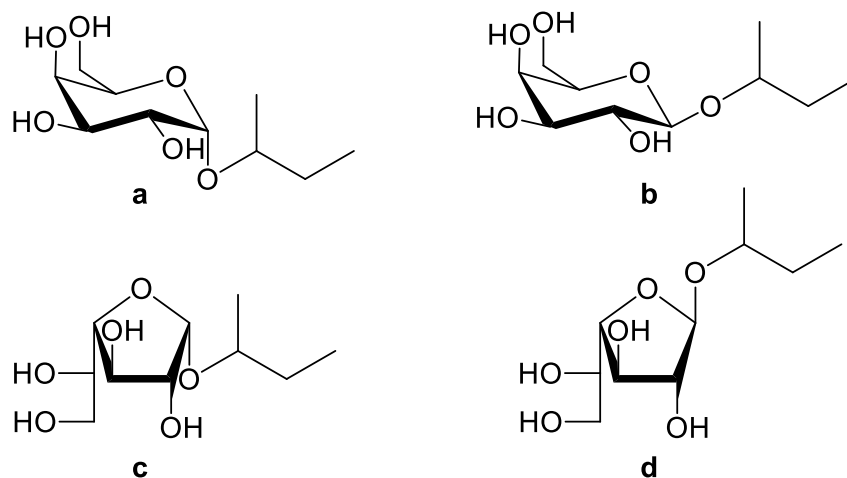
$^{13}\text{C NMR}$  (DMSO- $d_6$ , 101 MHz):  $\delta$  (ppm) 108.13 ( $\text{CH}^1_{\beta\text{-Fu}}$ ), 103.93 ( $\text{CH}^1_{\beta\text{-Py}}$ ), 101.38 ( $\text{CH}^1_{\alpha\text{-Fu}}$ ), 99.32 ( $\text{CH}^1_{\alpha\text{-Py}}$ ), 82.50, 82.49, 82.39, 77.74, 77.06, 75.57, 74.73, 73.96, 72.82, 71.64, 71.02, 70.87, 70.07, 69.33, 68.87, 68.61 (16 CH), 68.57, 67.36, 67.03, 66.98 (4  $\text{OCH}_2$ ), 63.32, 62.99, 61.06, 60.88 (4  $\text{CH}_2^6$ ), 31.89, 31.80, 31.77, 31.70 (4  $\text{OCH}_2\text{CH}_2$ ), 19.41, 19.28, 19.26, 19.19 (4  $\text{OCH}_2\text{CH}_2\text{CH}_2$ ), 14.27, 14.26, 14.19 (3  $\text{CH}_3$ ).

$\text{MS (ESI}^+)$ :  $m/z$  calcd for  $[\text{C}_{10}\text{H}_{20}\text{O}_6]$ : 236.13; found: 259.39  $[\text{M}+\text{Na}]^+$ , 495.26  $[\text{2M}+\text{Na}]^+$ .

$\text{MS (ESI}^-)$ :  $m/z$  calcd for  $[\text{C}_{10}\text{H}_{20}\text{O}_6]$ : 236.13; found: 235.41  $[\text{M}-\text{H}]^-$ , 471.69  $[\text{2M}-\text{H}]^-$ .



## 5.9.6 Characterization of 2-butyl D-galactoside isomeric mixture (51ad)



$R_f$  (eluent: DCM/MeOH; 9:1): 0.29; 0.35; 0.39.

Isomeric ratio a/b/c/d: 36/12/16/36.

$^1\text{H NMR}$  (DMSO- $d_6$ , 400 MHz):  $\delta$  (ppm) 5.31 (d,  $J = 4.3$  Hz, OH), 5.26 – 5.23 (m, OH), 5.21 (d,  $J = 5.6$  Hz, OH), 4.99 (m, OH), 4.85 (d,  $J = 4.7$  Hz,  $\text{CH}^1_{\alpha\text{-Fu}}$ ), 4.83 (d,  $J = 4.6$  Hz,  $\text{CH}^1_{\alpha\text{-Fu}}$ ), 4.78 (d,  $J = 2.1$  Hz,  $\text{CH}^1_{\beta\text{-Fu}}$ ), 4.77 (d,  $J = 2.4$  Hz,  $\text{CH}^1_{\beta\text{-Fu}}$ ), 4.75 (d,  $J = 3.6$  Hz,  $\text{CH}^1_{\alpha\text{-Py}}$ ), 4.72 (d,  $J = 3.5$  Hz,  $\text{CH}^1_{\alpha\text{-Py}}$ ), 4.71 (d,  $J = 4.5$  Hz, OH), 4.68 (d,  $J = 4.4$  Hz, OH), 4.66 – 4.57 (m, OH), 4.49 (m, OH), 4.34 (m, OH), 4.29 (m, OH), 4.24 (d,  $J = 6.3$  Hz, OH), 4.20 (d,  $J = 6.7$  Hz, CH,  $\text{CH}_2^{6'}$ ), 4.12 (dd,  $J = 7.3, 2.1$  Hz,  $\text{CH}^1_{\beta\text{-Py}}$ ), 4.09 (d,  $J = 5.3$  Hz, OH), 4.00 (d,  $J = 5.7$  Hz, OH), 3.98 (dd,  $J = 4.8, 2.3$  Hz, CH), 3.93 – 3.85 (m, CH, CH, CH), 3.84 – 3.77 (m, CH, CH, CH), 3.77 – 3.79 (m, 4 CH,  $\text{CH}_2^{6'}$ ), 3.69 – 3.60 (m, 4 CH, OCH), 3.60 – 3.46 (m, 12 CH,  $\text{CH}_2^{6'}$ , OCH, OCH), 3.46 – 3.41 (m,  $\text{CH}_2$ , OCH), 3.41 – 3.35 (m, CH,  $\text{CH}_2^{6''}$ ), 3.33 – 3.27 (m, CH,  $\text{CH}_2^{6''}$ ), 3.27 – 3.22 (m, CH, CH), 1.59 – 1.32 (m, OCH $\text{CH}_2$ ), 1.16 – 1.02 (m, OCH $\text{CH}_3$ ), 0.91 – 0.80 (m,  $\text{CH}_3$ ).

$^{13}\text{C NMR}$  (DMSO- $d_6$ , 101 MHz):  $\delta$  (ppm) 107.78 ( $\text{CH}^1_{\beta\text{-Fu}}$ ), 105.76 ( $\text{CH}^1_{\beta\text{-Fu}}$ ), 103.45 ( $\text{CH}^1_{\beta\text{-Py}}$ ), 101.92 ( $\text{CH}^1_{\beta\text{-Py}}$ ), 101.07 ( $\text{CH}^1_{\alpha\text{-Fu}}$ ), 99.41 ( $\text{CH}^1_{\alpha\text{-Fu}}$ ), 98.40 ( $\text{CH}^1_{\alpha\text{-Py}}$ ), 96.78 ( $\text{CH}^1_{\alpha\text{-Py}}$ ), 85.39, 82.85, 82.76, 82.47, 82.24, 82.23, 82.16, 81.45, 77.60, 77.47, 77.25, 77.09, 76.28, 75.92, 75.39, 75.01, 74.82, 74.71, 74.54, 74.32, 74.04, 73.05, 72.97, 72.83, 72.54, 72.41, 71.72, 71.57, 71.26, 71.08, 70.88, 70.85, 70.13, 70.03, 69.35, 69.00, 68.72, 68.55. (30 CH, 8 OCH), 64.84 (CH), 63.51, 63.41, 63.23, 63.05 (4  $\text{CH}_2^6$ ), 62.84 (CH), 61.03, 61.01, 60.84, 60.82 (4  $\text{CH}_2^6$ ), 30.09, 29.99, 29.25,

## 5 | Experimental section

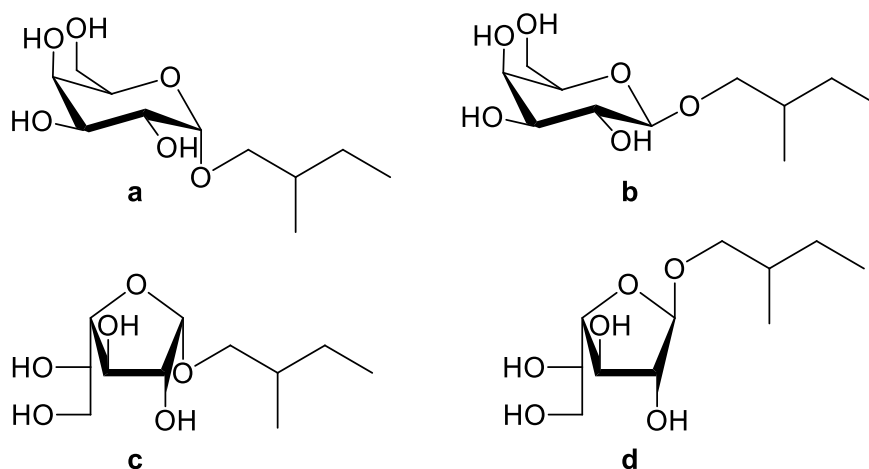
---

29.11, 29.10, 29.08 (6 OCHCH<sub>2</sub>), 21.56, 21.54, 21.28, 21.21, 19.43, 19.37, 19.27, 18.93 (8 OCHCH<sub>3</sub>), 10.56, 10.36, 10.26, 10.23, 10.02, 9.88, 9.87, 9.83 (8 CH<sub>3</sub>).

**MS (ESI<sup>+</sup>):** *m/z* calcd for [C<sub>10</sub>H<sub>20</sub>O<sub>6</sub>]: 236.13; found: 259.37 [M+Na]<sup>+</sup>, 495.24 [2M+Na]<sup>+</sup>.

**MS (ESI<sup>-</sup>):** *m/z* calcd for [C<sub>10</sub>H<sub>20</sub>O<sub>6</sub>]: 236.13; found: 235.99 [M-H]<sup>-</sup>, 471.73 [2M-H]<sup>-</sup>

## 5.9.7 Characterization of 2-methyl-1-butyl D-galactoside isomeric mixture (52ad)



$R_f$  (eluent: DCM/MeOH; 9:1): 0.29; 0.35; 0.39.

Isomeric ratio a/b/c/d: 29/12/17/42.

$^1\text{H NMR}$  (DMSO- $d_6$ , 400 MHz):  $\delta$  (ppm) 5.31 (d,  $J = 5.6$  Hz, OH), 5.16 (d,  $J = 5.9$  Hz, OH), 5.09 (d,  $J = 5.5$  Hz, OH), 4.83 – 4.77 (m, OH), 4.75 (d,  $J = 4.5$  Hz,  $\text{CH}^1_{\alpha\text{-Fu}}$ ), 4.73 (d,  $J = 2.2$  Hz,  $\text{CH}^1_{\beta\text{-Fu}}$ ), 4.71 (d,  $J = 5.0$  Hz, OH), 4.67 (d,  $J = 3.3$  Hz,  $\text{CH}^1_{\beta\text{-Fu}}$ ), 4.63 – 4.53 (m, OH), 4.43 (m, OH), 4.38 (d,  $J = 4.3$  Hz, OH), 4.14 (d,  $J = 5.2$  Hz, OH), 4.10 (d,  $J = 7.1$  Hz,  $\text{CH}^1_{\beta\text{-Py}}$ ), 4.04 (dd,  $J = 4.8, 2.3$  Hz, CH), 3.99 – 3.92 (m, CH, CH), 3.91 – 3.85 (m, CH, CH), 3.85 – 3.79 (m, CH, CH, CH), 3.79 – 3.72 (m, CH, CH, CH), 3.70 – 3.66 (m, CH, CH,  $\text{OCH}_2$ ), 3.66 – 3.47 (m, 6 CH,  $\text{CH}_2^{6'}$ ,  $\text{OCH}_2$ ), 3.47 – 3.41 (m, 4 CH,  $\text{CH}_2^{6'}$ ,  $\text{OCH}_2$ ), 3.39 – 3.34 (m, CH, CH,  $\text{CH}_2^{6''}$ ), 3.34 – 3.30 (m, CH, CH), 3.32 – 3.20 (m,  $\text{OCH}_2$ ), 3.19 – 3.13 (m,  $\text{OCH}_2$ ), 1.73 – 1.58 (m,  $\text{OCH}_2\text{CH}$ ), 1.56 – 1.40 (m,  $\text{OCH}_2\text{CHCH}_2$ ), 1.23 – 1.09 (m,  $\text{OCH}_2\text{CHCH}_2$ ), 0.98 – 0.86 (m,  $\text{CH}_3$ ).

$^{13}\text{C NMR}$  (DMSO- $d_6$ , 101 MHz):  $\delta$  (ppm) 108.31 ( $\text{CH}^1_{\beta\text{-Fu}}$ ), 108.23 ( $\text{CH}^1_{\beta\text{-Fu}}$ ), 104.28 ( $\text{CH}^1_{\beta\text{-Py}}$ ), 104.15 ( $\text{CH}^1_{\beta\text{-Py}}$ ), 101.63 ( $\text{CH}^1_{\alpha\text{-Fu}}$ ), 101.54 ( $\text{CH}^1_{\alpha\text{-Fu}}$ ), 99.52 ( $\text{CH}^1_{\alpha\text{-Py}}$ ), 99.42 ( $\text{CH}^1_{\alpha\text{-Py}}$ ), 85.41, 82.52, 82.52, 82.49, 82.48, 82.39, 81.46, 77.77, 77.76, 77.15, 75.56, 75.01, 74.73, 74.54 (14 CH), 74.09, 74.06 (2  $\text{OCH}_2$ ), 73.98, 73.97, 72.96, 72.94 (4 CH), 72.82, 72.76 (2  $\text{OCH}_2$ ), 72.42 (CH), 72.39, 72.31, 72.22, 71.69 (4  $\text{OCH}_2$ ), 71.68, 71.25, 71.07, 70.90, 70.06, 69.33, 68.91, 68.90, 68.60 (9 CH), 63.37, 62.99, 61.03, 60.85 (4  $\text{CH}_2^6$ ), 35.00, 34.94, 34.87, 34.86, 34.83, 34.82, 34.80

## 5 | Experimental section

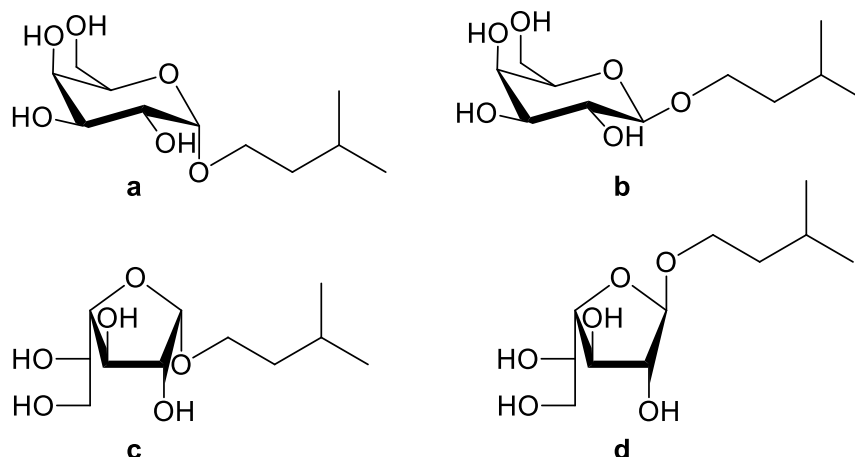
---

(7 OCH<sub>2</sub>CH), 26.25, 26.13, 26.10, 26.05, 26.02, 25.92 (6 OCH<sub>2</sub>CHCH<sub>2</sub>), 17.13, 17.01, 16.92, 16.88, 16.86, 16.84 (6 OCH<sub>2</sub>CHCH<sub>3</sub>), 11.76, 11.66, 11.63, 11.62, 11.58, 11.57, 11.50 (7 CH<sub>3</sub>).

**MS (ESI<sup>+</sup>):** *m/z* calcd for [C<sub>11</sub>H<sub>22</sub>O<sub>6</sub>]: 250.14; found: 273.42 [M+Na]<sup>+</sup>, 523.12 [2M+Na]<sup>+</sup>.

**MS (ESI<sup>-</sup>):** *m/z* calcd for [C<sub>11</sub>H<sub>22</sub>O<sub>6</sub>]: 250.14; found: 249.24 [M-H]<sup>-</sup>, 499.30 [2M-H]<sup>-</sup>.

### 5.9.8 Characterization of 3-methyl-1-butyl D-galactoside isomeric mixture (53ad)



$R_f$  (eluent: DCM/MeOH; 9:1): 0.27; 0.31; 0.35.

Isomeric ratio a/b/c/d: 38/15/11/36.

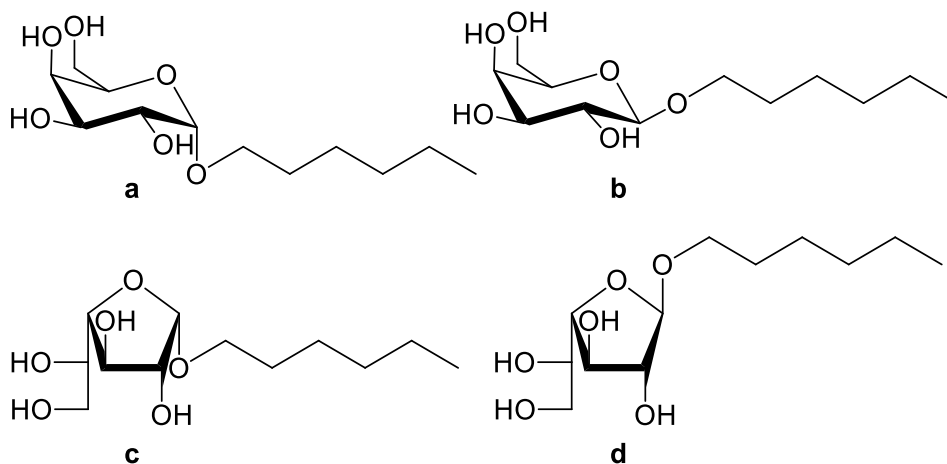
$^1\text{H NMR}$  (DMSO- $d_6$ , 400 MHz):  $\delta$  (ppm) 5.25 (d,  $J = 5.6$  Hz, OH), 5.10 (d,  $J = 5.9$  Hz, OH), 5.03 (br d,  $J = 5.6$  Hz, OH), 4.75 (d,  $J = 7.1$  Hz, OH), 4.71 (d,  $J = 4.5$  Hz,  $\text{CH}^1_{\alpha\text{-Fu}}$ ), 4.68 (d,  $J = 2.2$  Hz,  $\text{CH}^1_{\beta\text{-Fu}}$ ), 4.65 (d,  $J = 4.7$  Hz, OH), 4.62 (d,  $J = 3.5$  Hz,  $\text{CH}^1_{\alpha\text{-Py}}$ ), 4.57 – 4.47 (m, OH), 4.36 (t,  $J = 6.2$  Hz, OH), 4.32 (d,  $J = 4.3$  Hz, OH), 4.10 (m, OH), 4.04 (m,  $\text{CH}^1_{\beta\text{-Py}}$ ), 3.89 (dd,  $J = 13.6, 6.9$  Hz, CH), 3.85 – 3.79 (m, CH), 3.79 – 3.72 (m, CH, CH,  $\text{OCH}_2$ ), 3.72 – 3.67 (m, CH, CH,  $\text{OCH}_2$ ), 3.67 – 3.55 (m, CH, CH,  $\text{OCH}_2$ ), 3.55 – 3.47 (m, 3 CH,  $\text{CH}_2^{6'}$ ), 3.47 – 3.41 (m,  $\text{CH}_2^{6'}$ ,  $\text{OCH}_2$ ), 3.41 – 3.36 (m, CH,  $\text{CH}_2^{6''}$ ,  $\text{OCH}_2$ ), 3.36 – 3.28 (m, CH,  $\text{CH}_2^{6''}$ ,  $\text{OCH}_2$ ), 3.28 – 3.24 (m, CH, CH), 1.75 – 1.60 (m, 4H,  $\text{OCH}_2\text{CH}_2\text{CH}$ ), 1.50 – 1.33 (m, 8H,  $\text{OCH}_2\text{CH}_2$ ), 0.87 (m, 24H,  $(\text{CH}_3)_2$ ).

$^{13}\text{C NMR}$  (DMSO- $d_6$ , 101 MHz):  $\delta$  (ppm) 108.13 ( $\text{CH}^1_{\beta\text{-Fu}}$ ), 103.91 ( $\text{CH}^1_{\beta\text{-Py}}$ ), 101.41 ( $\text{CH}^1_{\alpha\text{-Fu}}$ ), 99.40 ( $\text{CH}^1_{\alpha\text{-Py}}$ ), 82.50, 82.45, 82.38, 77.70, 77.10, 75.53, 74.72, 73.97, 72.83, 71.65, 71.02, 70.88, 70.06, 69.32, 68.84, 68.59 (16 CH), 67.24, 66.06, 65.77, 65.60 (4  $\text{OCH}_2$ ), 63.36, 62.98, 61.05, 60.86 (4  $\text{CH}_2^6$ ), 38.64, 38.56, 38.54, 38.50 (4  $\text{OCH}_2\text{CH}_2$ ), 25.01, 24.93, 24.89, 24.81 (4  $\text{OCH}_2\text{CH}_2\text{CH}$ ), 23.18, 23.02, 23.00, 22.92, 22.77, 22.76 (6  $(\text{CH}_3)_2$ ).

$\text{MS (ESI}^+)$ :  $m/z$  calcd for  $[\text{C}_{11}\text{H}_{22}\text{O}_6]$ : 250.14; found: 273.34  $[\text{M}+\text{Na}]^+$ .

$\text{MS (ESI}^-)$ :  $m/z$  calcd for  $[\text{C}_{11}\text{H}_{22}\text{O}_6]$ : 250.14; found: 249.37  $[\text{M}-\text{H}]^-$ .

## 5.9.9 Characterization of 1-hexyl D-galactoside isomeric mixture (54ad)



$R_f$  (eluent: DCM/MeOH; 9:1): 0.31; 0.35; 0.39.

Isomeric ratio a/b/c/d:31/13/14/42.

**$^1\text{H NMR}$  (DMSO- $d_6$ , 400 MHz):**  $\delta$  (ppm) 5.25 (d,  $J = 5.6$  Hz, OH), 5.10 (d,  $J = 5.9$  Hz, OH), 5.04 (d,  $J = 5.6$  Hz, OH), 4.79 – 4.74 (m, OH), 4.70 (d,  $J = 4.5$  Hz,  $\text{CH}^1_{\alpha\text{-Fu}}$ ), 4.68 (d,  $J = 2.3$  Hz,  $\text{CH}^1_{\beta\text{-Fu}}$ ), 4.65 (d,  $J = 4.9$  Hz, OH), 4.62 (d,  $J = 3.4$  Hz,  $\text{CH}^1_{\alpha\text{-Py}}$ ), 4.52 (m, OH), 4.37 (d,  $J = 6.3$  Hz, OH), 4.31 (d,  $J = 4.4$  Hz, OH), 4.09 (m, OH), 4.05 (d,  $J = 8.4$  Hz,  $\text{CH}^1_{\beta\text{-Py}}$ ), 3.90 (dd,  $J = 13.5, 6.9$  Hz, CH), 3.82 (dt,  $J = 7.2, 5.3$  Hz, CH), 3.75 (ddd,  $J = 7.4, 4.9, 2.6$  Hz, CH, CH), 3.68 – 3.61 (m, CH,  $\text{OCH}_2$ ), 3.61 – 3.52 (m, 4 CH,  $\text{OCH}_2$ ), 3.52 – 3.47 (m, CH,  $\text{CH}_2^{6'}$ ), 3.47 – 3.42 (m,  $\text{CH}_2^{6''}$ ), 3.41 – 3.36 (m, CH, CH,  $\text{CH}_2^{6'}$ ,  $\text{OCH}_2$ ), 3.36 – 3.29 (m, CH, CH,  $\text{OCH}_2$ ), 3.28 – 3.24 (m, CH, CH), 1.57 – 1.45 (m,  $\text{OCH}_2\text{CH}_2$ ), 1.37 – 1.21 (br s,  $(\text{CH}_2)_3$ ), 0.87 (t,  $J = 6.6$  Hz,  $\text{CH}_3$ ).

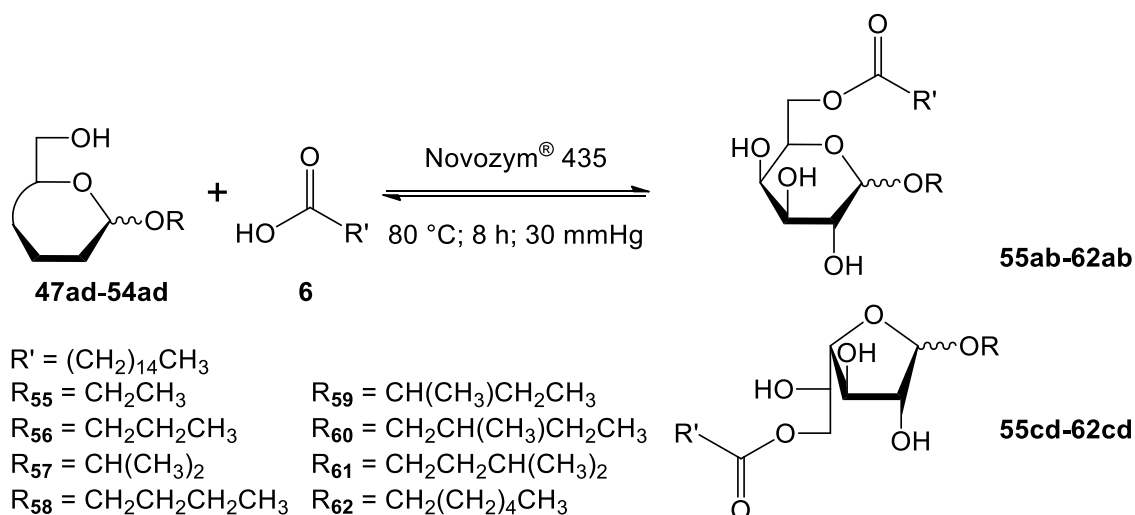
**$^{13}\text{C NMR}$  (DMSO- $d_6$ , 101 MHz):**  $\delta$  (ppm) 108.14 ( $\text{CH}^1_{\beta\text{-Fu}}$ ), 103.93 ( $\text{CH}^1_{\beta\text{-Py}}$ ), 101.39 ( $\text{CH}^1_{\alpha\text{-Fu}}$ ), 99.33 ( $\text{CH}^1_{\alpha\text{-Py}}$ ), 82.49, 82.42, 82.38, 77.73, 77.08, 75.57, 74.72, 73.97, 72.78, 71.63, 71.02, 70.89, 70.07, 69.33 (14 CH), 68.93 ( $\text{OCH}_2$ ), 68.87, 68.61 (2 CH), 67.72, 67.38, 67.34 (3  $\text{OCH}_2$ ), 63.34, 62.99, 61.06, 60.88 (4  $\text{CH}_2^6$ ), 31.62, 31.60, 31.58, 31.54 (4  $\text{OCH}_2\text{CH}_2\text{CH}_2$ ), 29.77, 29.66, 29.56 (3  $\text{OCH}_2\text{CH}_2$ ), 25.84, 25.78, 25.71, 25.68 (4  $\text{OCH}_2\text{CH}_2\text{CH}_2\text{CH}_2$ ), 22.55, 22.53 (2  $\text{OCH}_2\text{CH}_2\text{CH}_2\text{CH}_2\text{CH}_2$ ), 14.39 ( $\text{CH}_3$ ).

**MS (ESI $^+$ ):**  $m/z$  calcd for  $[\text{C}_{12}\text{H}_{24}\text{O}_6]$ : 264.16; found: 287.54  $[\text{M}+\text{Na}]^+$ .

**MS (ESI $^-$ ):**  $m/z$  calcd for  $[\text{C}_{12}\text{H}_{24}\text{O}_6]$ : 264.16; found: 263.58  $[\text{M}-\text{H}]^-$ , 527.82  $[2\text{M}-\text{H}]^-$ .

## 5.10 Alkyl 6-O-acyl-D-galactoside isomeric mixtures

### 5.10.1 Enzymatic synthesis of alkyl 6-O-palmitoyl-D-galactoside isomeric mixtures (55ad-62ad)



Isomeric mixtures of alkyl D-galactosides (**47ad-54ad**), palmitic acid (**6**), in molar ratio 1:1, and Novozym<sup>®</sup> 435 (10 %, w/w) were mixed together and charged into a round-bottom flask. The mixtures were heated to 80 °C while rotating the flask by means of a glass oven B-585 Kugelrohr. After palmitic acid melted, the reactions were performed under reduced pressure (30 mmHg).

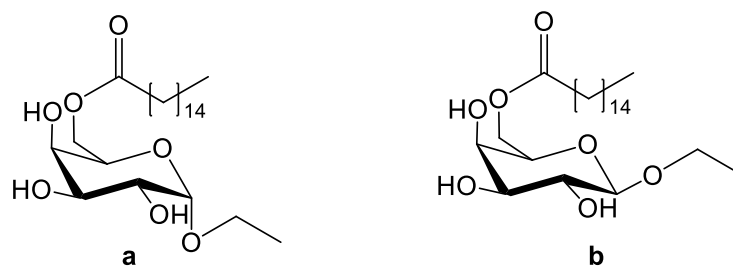
After 8 h, reaction mixtures were taken up in EtOAc and the immobilized enzyme was removed by filtration. Then, the esters were extracted in EtOAc (2 times) from 1 M NaOH, the organic phases were collected, dried over Na<sub>2</sub>SO<sub>4</sub> and the solvent was removed under reduced pressure. Couple of isomers were isolated by flash chromatography (*n*-hexane/EtOAc; 2:8), thus affording **alkyl 6-O-palmitoyl-D-galactopyranosides (55ab-62ab)** and **alkyl 6-O-palmitoyl-D-galactofuranosides (55cd-62cd)**. All products were fully characterized by TLC, ESI-MS and NMR analysis. Some <sup>1</sup>H and <sup>13</sup>C peaks are not completely resolved because of the instrument resolution. Yields and isomeric ratios of each isomeric couple, estimated by <sup>1</sup>H NMR analysis, carried out in DMSO-*d*<sub>6</sub>, as the ratio of the areas of the two anomeric proton signals, are reported in **Table 5.7**. Due to anomeric proton signals overlapping, some isomeric ratios were assessed by quantitative TLC and image analysis, see **Section 5.12**.

*Table 5.7. Yields and isomeric ratios of alkyl 6-O-acyl-D-galactosides.*

<b>Compound</b>	<b>Yield (%)</b>	<b>Isomeric ratio (%)</b>	<b>Compound</b>	<b>Yield (%)</b>	<b>Isomeric ratio (%)</b>
<b>55ab</b>	7	76/24	<b>55cd</b>	28	40/60
<b>56ab</b>	9	93/7	<b>56cd</b>	20	43/57
<b>57ab</b>	5	57/43	<b>57cd</b>	27	41/59
<b>58ab</b>	21	94/6	<b>58cd</b>	14	20/80
<b>59ab</b>	14	97/3	<b>59cd</b>	20	45/55
<b>60ab</b>	4	85/15	<b>60cd</b>	6	8/92
<b>61ab</b>	16	83/17	<b>61cd</b>	14	38/62
<b>62ab</b>	16	88/12	<b>62cd</b>	18	28/72



## 5.10.2 Characterization of ethyl 6-O-palmitoyl-D-galactopyranosides (55ab)



$R_f$  (eluent: *n*-hexane/EtOAc; 2:8): 0.12.

Isomeric ratio a/b: 76/24.

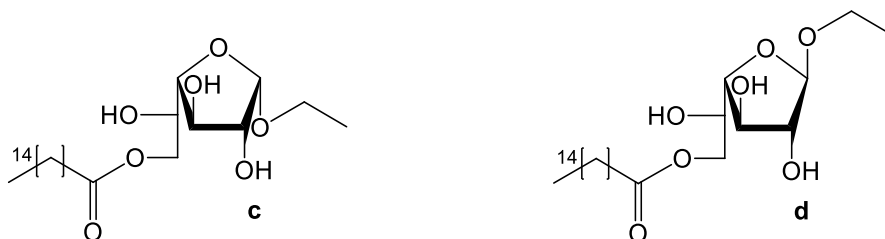
$^1\text{H NMR}$  (DMSO-*d*<sub>6</sub>, 400 MHz):  $\delta$  (ppm) 4.89 – 4.84 (m, OH), 4.80 (m, OH), 4.74 – 4.71 (m, OH), 4.68 (d,  $J = 3.3$  Hz,  $\text{CH}^1_\alpha$ ), 4.60 – 4.55 (m, OH), 4.44 (d,  $J = 6.2$  Hz, OH), 4.19 – 4.03 (m,  $\text{CH}^1_\beta$ ,  $\text{CH}_2^6$ ), 3.82 (dd,  $J = 8.3, 4.6$  Hz,  $\text{CH}^5_\alpha$ ), 3.71 – 3.68 (m,  $\text{CH}^4_\alpha$ ), 3.65 – 3.49 (m,  $\text{CH}^2_\alpha$ ,  $\text{CH}^3_\alpha$ ,  $\text{CH}^4_\beta$ ,  $\text{CH}^5_\beta$ ,  $\text{OCH}_2'$ ), 3.46 – 3.33 (m,  $\text{OCH}_2''$ ), 3.31 – 3.27 (m,  $\text{CH}^2_\beta$ ,  $\text{CH}^3_\beta$ ), 2.33 – 2.26 (m,  $\text{COOCH}_2$ ), 1.53 (m,  $\text{COOCH}_2\text{CH}_2$ ), 1.27 (br s,  $(\text{CH}_2)_{12}$ ), 1.14 (q,  $J = 7.1$  Hz,  $\text{OCH}_2\text{CH}_3$ ), 0.87 (t,  $J = 6.8$  Hz,  $\text{CH}_3$ ).

$^{13}\text{C NMR}$  (DMSO-*d*<sub>6</sub>, 101 MHz):  $\delta$  (ppm) 173.24 (COO), 103.61 ( $\text{CH}^1_\beta$ ), 99.31 ( $\text{CH}^1_\alpha$ ), 73.54 ( $\text{CH}^2_\beta$ ), 72.56 ( $\text{CH}^5_\beta$ ), 70.74 ( $\text{CH}^3_\beta$ ), 69.70 ( $\text{CH}^4_\beta$ ), 69.61 ( $\text{CH}^4_\alpha$ ), 68.95 ( $\text{CH}^3_\alpha$ ), 68.81 ( $\text{CH}^5_\alpha$ ), 68.57 ( $\text{CH}^2_\alpha$ ), 64.44 ( $\text{CH}_2^6_\alpha$ ), 64.31 ( $\text{CH}_2^6_\beta$ ), 62.99 ( $\text{OCH}_2 \alpha$ ), 62.50 ( $\text{OCH}_2 \beta$ ), 33.99 ( $\text{COOCH}_2$ ), 29.47, 29.15, 28.87 ( $(\text{CH}_2)_{12}$ ), 24.89 ( $\text{COOCH}_2\text{CH}_2$ ), 15.50 ( $\text{OCH}_2\text{CH}_3$ ), 14.41 ( $\text{CH}_3$ ).

**MS (ESI<sup>+</sup>):**  $m/z$  calcd for  $[\text{C}_{24}\text{H}_{46}\text{O}_7]$ : 446.32; found: 469.95  $[\text{M}+\text{Na}]^+$ ; 915.48  $[2\text{M}+\text{Na}]^+$ .

**MS (ESI<sup>-</sup>):**  $m/z$  calcd for  $[\text{C}_{24}\text{H}_{46}\text{O}_7]$ : 446.32; found: 445.36  $[\text{M}-\text{H}]^-$ ; 891.41  $[2\text{M}-\text{H}]^-$ .

## 5.10.3 Characterization of ethyl 6-O-palmitoyl-D-galactofuranosides (55cd)



$R_f$  (eluent: *n*-hexane/EtOAc; 2:8): 0.30.

Isomeric ratio **c/d**: 40/60.

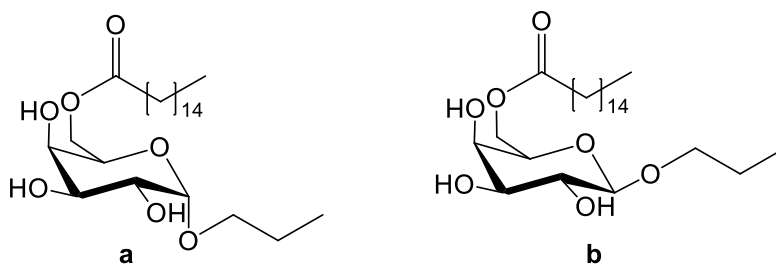
**$^1\text{H NMR}$  (DMSO-*d*<sub>6</sub>, 400 MHz):**  $\delta$  (ppm) 5.34 (d,  $J = 5.4$  Hz, OH), 5.21 (d,  $J = 6.0$  Hz, OH), 5.17 (d,  $J = 5.8$  Hz, OH), 5.01 (d,  $J = 6.7$  Hz, OH), 4.86 (d,  $J = 7.2$  Hz, OH), 4.77 (m,  $\text{CH}^1_\alpha$ ,  $\text{CH}^1_\beta$ ), 4.66 (d,  $J = 5.9$  Hz, OH), 4.12 – 4.01 (m,  $\text{CH}_2'^6$ ,  $\text{CH}_2''6$ ), 3.99 – 3.92 (dt,  $J = 10.9, 5.2$  Hz, CH,  $\text{CH}_2''6$ ), 3.92 – 3.86 (dd,  $J = 12.8, 5.4$  Hz, CH), 3.84 – 3.74 (m, CH, CH, CH,  $\text{OCH}_2'\alpha$ ), 3.73 – 3.64 (m, CH, CH,  $\text{OCH}_2'\beta$ ), 3.55 (dd,  $J = 6.8, 5.4$  Hz, CH), 3.49 – 3.41 (m,  $\text{OCH}_2''$ ), 2.34 (t,  $J = 7.3$  Hz,  $\text{COOCH}_2$ ), 1.57 (m,  $\text{COOCH}_2\text{CH}_2$ ), 1.31 (d,  $J = 14.1$  Hz,  $(\text{CH}_2)_{12}$ ), 1.17 (t,  $J = 7.1$  Hz,  $\text{OCH}_2\text{CH}_3$ ), 0.91 (t,  $J = 6.8$  Hz,  $\text{CH}_3$ ).

**$^{13}\text{C NMR}$  (DMSO-*d*<sub>6</sub>, 101 MHz):**  $\delta$  (ppm) 173.35 ( $\text{COO}_\beta$ ), 173.27 ( $\text{COO}_\alpha$ ), 108.04 ( $\text{CH}^1_\beta$ ), 101.22 ( $\text{CH}^1_\alpha$ ), 82.62, 82.43, 82.27, 77.72, 76.84, 74.65, 69.91, 67.53 (8 CH), 65.64 ( $\text{CH}_2^6_\beta$ ), 65.53 ( $\text{CH}_2^6_\alpha$ ), 62.93 ( $\text{OCH}_2 \alpha$ ), 62.79 ( $\text{OCH}_2 \beta$ ), 33.96 ( $\text{COOCH}_2$ ), 29.50, 29.48, 29.46, 29.45, 29.36, 29.33, 29.17, 29.16, 28.92 ( $(\text{CH}_2)_{12}$ ), 24.91 ( $\text{COOCH}_2\text{CH}_2$ ), 15.63 ( $\text{OCH}_2\text{CH}_3 \beta$ ), 15.58 ( $\text{OCH}_2\text{CH}_3 \alpha$ ), 14.39 ( $\text{CH}_3$ ).

**MS (ESI<sup>+</sup>):**  $m/z$  calcd for  $[\text{C}_{24}\text{H}_{46}\text{O}_7]$ : 446.32; found: 469.53  $[\text{M}+\text{Na}]^+$ ; 915.15  $[\text{2M}+\text{Na}]^+$ .

**MS (ESI<sup>-</sup>):**  $m/z$  calcd for  $[\text{C}_{24}\text{H}_{46}\text{O}_7]$ : 446.32; found: 445.44  $[\text{M}-\text{H}]^-$ ; 891.45  $[\text{2M}-\text{H}]^-$ .

## 5.10.4 Characterization of 1-propyl 6-O-palmitoyl-D-galactopyranosides (56ab)



$R_f$  (eluent: *n*-hexane/EtOAc; 2:8): 0.23.

Isomeric ratio a/b: 93/7.

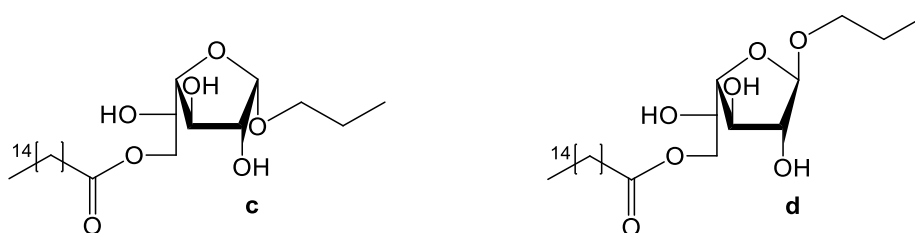
$^1\text{H NMR}$  (DMSO- $d_6$ , 400 MHz):  $\delta$  (ppm) 4.98 – 4.91 (m, OH), 4.88 – 4.78 (m, OH), 4.76 (br d,  $J = 5.0$  Hz, OH), 4.72 (m, OH), 4.66 (d,  $J = 3.1$  Hz,  $\text{CH}^1_\alpha$ ), 4.61 (m, OH), 4.48 (d,  $J = 6.0$  Hz, OH), 4.22 – 3.97 (m,  $\text{CH}^1_\beta$ ,  $\text{CH}_2^6$ ), 3.81 (dd,  $J = 8.1, 4.0$  Hz,  $\text{CH}^5_\alpha$ ), 3.69 (m,  $\text{CH}^4_\alpha$ ), 3.68 – 3.63 (m,  $\text{OCH}_2'\beta$ ), 3.61 – 3.53 (m,  $\text{CH}^2_\alpha$ ,  $\text{CH}^3_\alpha$ ,  $\text{CH}^4_\beta$ ,  $\text{CH}^5_\beta$ ), 3.53 – 3.46 (m,  $\text{OCH}_2'\alpha$ ), 3.42 – 3.36 (m,  $\text{OCH}_2''\beta$ ), 3.36 – 3.27 (m,  $\text{CH}^2_\beta$ ,  $\text{CH}^3_\beta$ ,  $\text{OCH}_2''\alpha$ ), 2.28 (br td,  $J = 7.4, 3.7$  Hz,  $\text{COOCH}_2$ ), 1.54 (br dd,  $J = 13.9, 6.8$  Hz,  $\text{COOCH}_2\text{CH}_2$ ,  $\text{OCH}_2\text{CH}_2$ ), 1.24 (br s,  $(\text{CH}_2)_{12}$ ), 0.91 – 0.83 (m,  $\text{CH}_3$ ).

$^{13}\text{C NMR}$  (DMSO- $d_6$ , 101 MHz):  $\delta$  (ppm) 173.20 (COO), 103.84 ( $\text{CH}^1_\beta$ ), 99.38 ( $\text{CH}^1_\alpha$ ), 73.55 ( $\text{CH}^2_\beta$ ), 72.56 ( $\text{CH}^5_\beta$ ), 71.21 ( $\text{CH}^4_\beta$ ), 70.77 ( $\text{CH}^3_\beta$ ), 70.69 ( $\text{OCH}_2 \beta$ ), 69.70 ( $\text{CH}^3_\alpha$ ), 69.66 ( $\text{CH}^4_\alpha$ ), 69.15 ( $\text{OCH}_2 \alpha$ ), 68.87 ( $\text{CH}^5_\alpha$ ), 68.61 ( $\text{CH}^2_\alpha$ ), 64.53 ( $\text{CH}_2^6$ ), 34.02 ( $\text{COOCH}_2$ ), 29.49, 29.42, 29.29, 29.16, 29.13, 28.89 ( $(\text{CH}_2)_{12}$ ), 24.91 ( $\text{COOCH}_2\text{CH}_2$ ), 23.06, 22.87 (2  $\text{COOCH}_2\text{CH}_2$ ), 14.41 ( $\text{CH}_3$ ), 11.12, 11.00 (2  $\text{OCH}_2\text{CH}_2\text{CH}_3$ ).

$\text{MS}$  (ESI $^+$ ):  $m/z$  calcd for  $[\text{C}_{25}\text{H}_{48}\text{O}_7]$ : 460.34; found: 483.69  $[\text{M}+\text{Na}]^+$ ; 943.27  $[2\text{M}+\text{Na}]^+$ .

$\text{MS}$  (ESI $^-$ ):  $m/z$  calcd for  $[\text{C}_{25}\text{H}_{48}\text{O}_7]$ : 460.34; found: 459.20  $[\text{M}-\text{H}]^-$ ; 919.24  $[2\text{M}-\text{H}]^-$ .

## 5.10.5 Characterization of 1-propyl 6-O-palmitoyl-D-galactofuranosides (56cd)



$R_f$  (eluent: *n*-hexane/EtOAc; 2:8): 0.44.

Isomeric ratio c/d: 43/57.

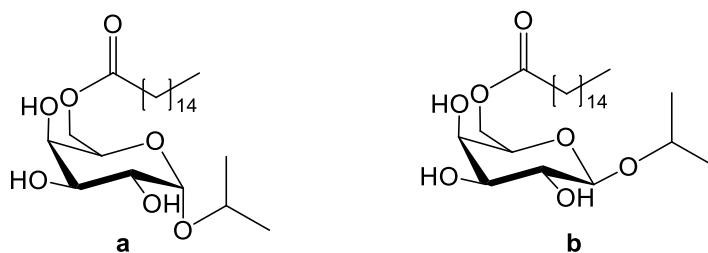
$^1\text{H NMR}$  (DMSO- $d_6$ , 400 MHz):  $\delta$  (ppm) 5.29 (d,  $J = 5.4$  Hz, OH), 5.17 (d,  $J = 6.1$  Hz, OH), 5.12 (d,  $J = 5.7$  Hz, OH), 4.96 (d,  $J = 6.7$  Hz, OH), 4.79 (d,  $J = 7.2$  Hz, OH), 4.71 (m,  $\text{CH}^1_\alpha$ ,  $\text{CH}^1_\beta$ ), 4.60 (d,  $J = 5.9$  Hz, OH), 4.08 – 3.95 (m,  $\text{CH}_2'^6$ ,  $\text{CH}_2''^6$ ), 3.92 – 3.88 (m, CH,  $\text{CH}_2''^6$ ), 3.86 – 3.81 (m, CH), 3.80 – 3.74 (m, CH, CH), 3.74 – 3.70 (m, CH), 3.68 – 3.59 (m, CH, CH,  $\text{OCH}_2'_\alpha$ ), 3.55 – 3.48 (m, CH,  $\text{OCH}_2'_\beta$ ), 3.34 – 3.26 (m,  $\text{OCH}_2''$ ), 2.28 (t,  $J = 7.4$  Hz,  $\text{COOCH}_2$ ), 1.57 – 1.47 (m,  $\text{COOCH}_2\text{CH}_2$ ,  $\text{OCH}_2\text{CH}_2$ ), 1.26 (br s,  $(\text{CH}_2)_{12}$ ), 0.90 – 0.83 (m,  $\text{CH}_3$ ).

$^{13}\text{C NMR}$  (DMSO- $d_6$ , 101 MHz):  $\delta$  (ppm) 173.33 ( $\text{COO}_\beta$ ), 173.23 ( $\text{COO}_\alpha$ ), 108.20 ( $\text{CH}^1_\beta$ ), 101.43 ( $\text{CH}^1_\alpha$ ), 82.66, 82.42, 82.22, 77.76, 76.86, 74.64, 70.07 (7 CH), 69.21 ( $\text{OCH}_2_\alpha$ ), 68.98 ( $\text{OCH}_2_\beta$ ), 67.41 (CH), 65.59 ( $\text{CH}_2^6_\beta$ ), 65.52 ( $\text{CH}_2^6_\alpha$ ), 33.95 ( $\text{COOCH}_2$ ), 29.51, 29.49, 29.48, 29.46, 29.37, 29.35, 29.18, 28.93 ( $(\text{CH}_2)_{12}$ ), 24.90 ( $\text{COOCH}_2\text{CH}_2$ ), 22.98 ( $\text{OCH}_2\text{CH}_2_\beta$ ), 22.89 ( $\text{OCH}_2\text{CH}_2_\alpha$ ), 14.39 ( $\text{CH}_3$ ), 10.99 ( $\text{OCH}_2\text{CH}_2\text{CH}_3_\beta$ ), 10.96 ( $\text{OCH}_2\text{CH}_2\text{CH}_3_\alpha$ ).

$\text{MS (ESI}^+)$ :  $m/z$  calcd for  $[\text{C}_{25}\text{H}_{48}\text{O}_7]$ : 460.34; found: 484.90  $[\text{M}+\text{Na}]^+$ .

$\text{MS (ESI}^-)$ :  $m/z$  calcd for  $[\text{C}_{25}\text{H}_{48}\text{O}_7]$ : 460.34; found: 459.33  $[\text{M}-\text{H}]^-$ ; 919.43  $[2\text{M}-\text{H}]^-$ .

## 5.10.6 Characterization of 2-propyl 6-O-palmitoyl-D-galactopyranosides (57ab)



$R_f$  (eluent: *n*-hexane/EtOAc; 2:8): 0.18.

Isomeric ratio a/b: 57/43.

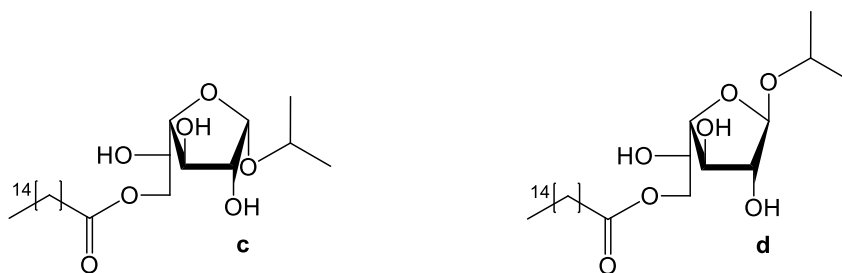
**$^1\text{H NMR}$  (DMSO- $d_6$ , 400 MHz):**  $\delta$  (ppm) 5.35 (d,  $J = 6.1$  Hz, OH), 5.21 (d,  $J = 5.8$  Hz, OH), 4.75 (d,  $J = 3.9$  Hz,  $\text{CH}^1_\alpha$ ), 4.66 (d,  $J = 6.9$  Hz, OH), 4.59 (m, OH), 4.33 (d,  $J = 6.2$  Hz, OH), 4.20 – 4.01 (m,  $\text{CH}^1_\beta$ ,  $\text{CH}_2^6$ ), 3.88 (dd,  $J = 7.9, 4.2$  Hz,  $\text{CH}^5_\alpha$ ), 3.80 – 3.73 (m,  $\text{CH}^4_\alpha$ ), 3.68 (m,  $\text{CH}^3_\alpha$ ), 3.60 – 3.48 (m,  $\text{CH}^2_\alpha$ ,  $\text{CH}^4_\beta$ ,  $\text{CH}^5_\beta$ , 2 OCH), 3.32 – 3.26 (m,  $\text{CH}^3_\beta$ ), 3.26 – 3.20 (m,  $\text{CH}^2_\beta$ ), 2.27 (m,  $\text{COOCH}_2$ ), 1.51 (br s,  $\text{COOCH}_2\text{CH}_2$ ), 1.24 (br s,  $(\text{CH}_2)_{12}$ ), 1.16 – 1.04 (m,  $\text{OCH}(\text{CH}_3)_2$ ), 0.86 (t,  $J = 6.6$  Hz,  $\text{CH}_3$ ).

**$^{13}\text{C NMR}$  (DMSO- $d_6$ , 101 MHz):**  $\delta$  (ppm) 173.21 ( $\text{COO}_\alpha$ ), 172.89 ( $\text{COO}_\beta$ ), 102.30 ( $\text{CH}^1_\beta$ ), 98.06 ( $\text{CH}^1_\alpha$ ), 73.60 ( $\text{CH}^3_\beta$ ), 72.47 ( $\text{CH}^4_\beta$ ), 70.81 ( $\text{CH}^2_\beta$ ), 69.72 ( $\text{CH}^5_\beta$ ), 69.69 ( $\text{OCH}_\alpha$ ), 69.55 ( $\text{CH}^3_\alpha$ ), 69.03 ( $\text{CH}^4_\alpha$ ), 68.97 ( $\text{OCH}_\beta$ ), 68.86 ( $\text{CH}^5_\alpha$ ), 68.48 ( $\text{CH}^2_\alpha$ ), 64.59 ( $\text{CH}_2^6_\alpha$ ), 64.05 ( $\text{CH}_2^6_\beta$ ), 34.25 ( $\text{COOCH}_2_\beta$ ), 33.99 ( $\text{COOCH}_2_\alpha$ ), 29.48, 29.30, 29.16, 28.88 ( $(\text{CH}_2)_{12}$ ), 24.94, 24.85 (2  $\text{COOCH}_2\text{CH}_2$ ), 23.82, 23.61 ( $\text{OCH}(\text{CH}_3)'$ ), 22.08, 21.90 ( $\text{OCH}(\text{CH}_3)''$ ), 14.42 ( $\text{CH}_3$ ).

**MS (ESI $^+$ ):**  $m/z$  calcd for  $[\text{C}_{25}\text{H}_{48}\text{O}_7]$ : 460.34; found: 483.87  $[\text{M}+\text{Na}]^+$ ; 943.42  $[2\text{M}+\text{Na}]^+$ .

**MS (ESI $-$ ):**  $m/z$  calcd for  $[\text{C}_{25}\text{H}_{48}\text{O}_7]$ : 460.34; found: 459.45  $[\text{M}-\text{H}]^-$ ; 919.42  $[2\text{M}-\text{H}]^-$ .

## 5.10.7 Characterization of 2-propyl 6-O-palmitoyl-D-galactofuranosides (57cd)



$R_f$  (eluent: *n*-hexane/EtOAc; 2:8): 0.40.

Isomeric ratio c/d: 41/59.

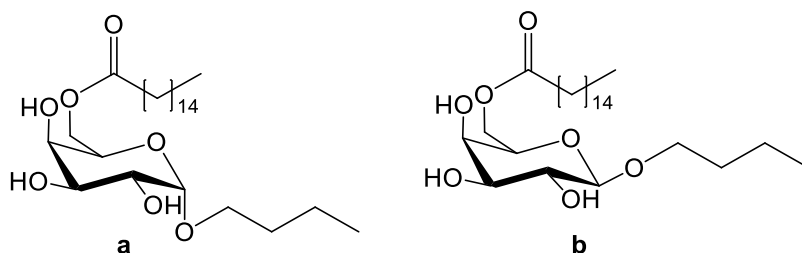
$^1\text{H NMR}$  (DMSO- $d_6$ , 400 MHz):  $\delta$  (ppm) 5.17 (d,  $J = 6.0$  Hz, OH), 5.09 (d,  $J = 5.8$  Hz, OH), 4.93 (d,  $J = 6.7$  Hz, OH), 4.85 (d,  $J = 4.6$  Hz,  $\text{CH}^1_\alpha$ ), 4.81 (d,  $J = 2.3$  Hz,  $\text{CH}^1_\beta$ ), 4.66 (d,  $J = 7.4$  Hz, OH), 4.47 (d,  $J = 6.1$  Hz, OH), 4.07 – 4.02 (m,  $\text{CH}_2^{6\beta}$ ), 4.02 – 3.98 (m,  $\text{CH}_2^{6\alpha}$ ,  $\text{CH}_2^{6''\beta}$ ), 3.93 – 3.85 (m, CH,  $\text{CH}_2^{6''\alpha}$ ,  $\text{OCH}_\alpha$ ), 3.85 – 3.80 (m, CH), 3.79 – 3.70 (m, CH, CH, CH,  $\text{OCH}_\beta$ ), 3.66 (dd,  $J = 7.6, 3.0$  Hz, CH), 3.64 – 3.62 (m, CH), 3.51 (dd,  $J = 6.7, 5.2$  Hz, CH), 2.29 (td,  $J = 7.4, 2.2$  Hz,  $\text{COOCH}_2$ ), 1.52 (m,  $\text{COOCH}_2\text{CH}_2$ ), 1.31 – 1.21 (m,  $(\text{CH}_2)_{12}$ ), 1.16 – 1.06 (m,  $\text{OCHCH}_3$ ), 0.86 (t,  $J = 6.8$  Hz,  $\text{CH}_3$ ).

$^{13}\text{C NMR}$  (DMSO- $d_6$ , 101 MHz):  $\delta$  (ppm) 173.35 ( $\text{COO}_\beta$ ), 173.26 ( $\text{COO}_\alpha$ ), 106.61 ( $\text{CH}^1_\beta$ ), 99.75 ( $\text{CH}^1_\alpha$ ), 82.97, 82.39, 81.97, 77.54, 76.87, 74.73, 69.89 (7 CH), 69.56 ( $\text{OCH}_\alpha$ ), 69.08 ( $\text{OCH}_\beta$ ), 67.37 (CH), 65.61 ( $\text{CH}_2^{6\beta}$ ), 65.58 ( $\text{CH}_2^{6\alpha}$ ), 33.95 ( $\text{COOCH}_2$ ), 29.49, 29.46, 29.44, 29.35, 29.32, 29.16, 28.91 ( $(\text{CH}_2)_{12}$ ), 24.90 ( $\text{COOCH}_2\text{CH}_2$ ), 24.05 ( $\text{OCHCH}_3'_\beta$ ), 23.83 ( $\text{OCHCH}_3'_\alpha$ ), 22.28 ( $\text{OCHCH}_3''_\beta$ ), 22.08 ( $\text{OCHCH}_3'_\alpha$ ), 14.40 ( $\text{CH}_3$ ).

$\text{MS (ESI}^+)$ :  $m/z$  calcd for  $[\text{C}_{25}\text{H}_{48}\text{O}_7]$ : 460.34; found: 484.66  $[\text{M}+\text{Na}]^+$ ; 943.22  $[\text{2M}+\text{Na}]^+$ .

$\text{MS (ESI}^-)$ :  $m/z$  calcd for  $[\text{C}_{25}\text{H}_{48}\text{O}_7]$ : 460.34; found: 459.08  $[\text{M}-\text{H}]^-$ ; 919.14  $[\text{2M}-\text{H}]^-$ .

## 5.10.8 Characterization of 1-butyl 6-O-palmitoyl-D-galactopyranosides (58ab)



$R_f$  (eluent: *n*-hexane/EtOAc; 2:8): 0.23; 0.29.

Isomeric ratio c/d: 94/6.

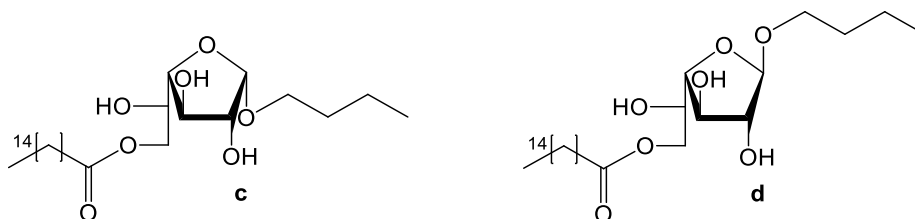
$^1\text{H NMR}$  (DMSO- $d_6$ , 400 MHz):  $\delta$  (ppm) 4.65 (d,  $J = 3.2$  Hz, 1H,  $\text{CH}^1_a$ ), 4.61 (m, 2H,  $\text{OH}^3$ ,  $\text{OH}^4$ ), 4.48 (d,  $J = 6.0$  Hz, 1H,  $\text{OH}^2$ ), 4.16 – 4.00 (m, 2H,  $\text{CH}_2^6$ ), 3.80 (dd,  $J = 8.0, 3.7$  Hz, 1H,  $\text{CH}^5$ ), 3.68 (d,  $J = 2.8$  Hz, 1H,  $\text{CH}^4$ ), 3.61 – 3.51 (m, 3H,  $\text{CH}^2$ ,  $\text{CH}^3$ ,  $\text{OCH}_2'$ ), 3.38 – 3.32 (m, 1H,  $\text{OCH}_2''$ ), 2.27 (t,  $J = 7.1$  Hz, 2H,  $\text{COOCH}_2$ ), 1.56 – 1.46 (m, 4H,  $\text{OCH}_2\text{CH}_2$ ,  $\text{COOCH}_2\text{CH}_2$ ), 1.39 – 1.30 (m, 2H,  $\text{OCH}_2\text{CH}_2\text{CH}_2$ ), 1.24 (br s, 24H,  $(\text{CH}_2)_{12}$ ), 0.87 (m, 6H,  $\text{CH}_3$ ).

$^{13}\text{C NMR}$  (DMSO- $d_6$ , 101 MHz):  $\delta$  (ppm) 173.19 (COO), 99.40 ( $\text{CH}^1_a$ ), 69.69 ( $\text{CH}^3$ ,  $\text{CH}^4$ ), 68.92 ( $\text{CH}^5$ ), 68.58 ( $\text{CH}^2$ ), 67.15 ( $\text{OCH}_2$ ), 64.60 ( $\text{CH}_2^6$ ), 34.03 ( $\text{COOCH}_2$ ), 31.75 ( $\text{COOCH}_2\text{CH}_2$ ), 29.49, 29.48, 29.46, 29.45, 29.43, 29.30, 29.16, 29.13, 28.90 (9  $(\text{CH}_2)_{12}$ ), 24.92 ( $\text{OCH}_2\text{CH}_2$ ), 19.42 ( $\text{OCH}_2\text{CH}_2\text{CH}_2$ ), 14.41, 14.17 (2  $\text{CH}_3$ ).

**MS (ESI<sup>+</sup>):**  $m/z$  calcd for  $[\text{C}_{26}\text{H}_{50}\text{O}_7]$ : 474.36; found: 497.64  $[\text{M}+\text{Na}]^+$ ; 971.19  $[\text{2M}+\text{Na}]^+$ .

**MS (ESI<sup>-</sup>):**  $m/z$  calcd for  $[\text{C}_{26}\text{H}_{50}\text{O}_7]$  474.36; found: 473.65  $[\text{M}-\text{H}]^-$ .

## 5.10.9 Characterization of 1-butyl 6-O-palmitoyl-D-galactofuranosides (58cd)



$R_f$  (eluent: *n*-hexane/EtOAc; 2:8): 0.45; 0.57.

Isomeric ratio **c/d**: 20/80.

**$^1\text{H NMR}$  (DMSO- $d_6$ , 400 MHz):**  $\delta$  (ppm) 5.36 (d,  $J = 6.3$  Hz, OH), 5.29 (d,  $J = 5.4$  Hz, OH), 5.17 (d,  $J = 6.0$  Hz, OH), 5.13 (d,  $J = 5.7$  Hz, OH), 4.97 (d,  $J = 6.7$  Hz, OH), 4.94 (d,  $J = 4.6$  Hz, OH), 4.87 – 4.77 (m, OH), 4.72 (br s,  $\text{CH}^1_\alpha$ ), 4.70 (d,  $J = 2.2$  Hz,  $\text{CH}^1_\beta$ ), 4.61 (d,  $J = 5.9$  Hz, OH), 4.09 – 4.02 (m,  $\text{CH}_2^{6'}$ ), 4.02 – 3.96 (m, CH,  $\text{CH}_2^{6''}$ ), 3.92 – 3.88 (m, CH), 3.88 – 3.81 (dd,  $J = 12.6, 5.4$  Hz, CH), 3.79 – 3.74 (m, CH), 3.74 – 3.68 (dd,  $J = 10.4, 4.0$  Hz, CH), 3.68 – 3.63 (m, CH,  $\text{OCH}_2$ ), 3.63 – 3.58 (dd,  $J = 10.5, 4.7$  Hz, CH), 3.58 – 3.53 (dd,  $J = 6.7, 3.0$  Hz,  $\text{OCH}_2$ ), 3.52 – 3.47 (dd,  $J = 13.4, 6.7$  Hz, CH), 3.40 – 3.29 (m,  $\text{OCH}_2$ ), 2.28 (t,  $J = 7.4$  Hz,  $\text{COOCH}_2$ ), 1.56 – 1.45 (m,  $\text{OCH}_2\text{CH}_2$ ,  $\text{COOCH}_2\text{CH}_2$ ), 1.38 – 1.29 (m,  $\text{OCH}_2\text{CH}_2\text{CH}_2$ ), 1.26 (br s,  $(\text{CH}_2)_{12}$ ), 0.87 (m,  $\text{CH}_3$ ).

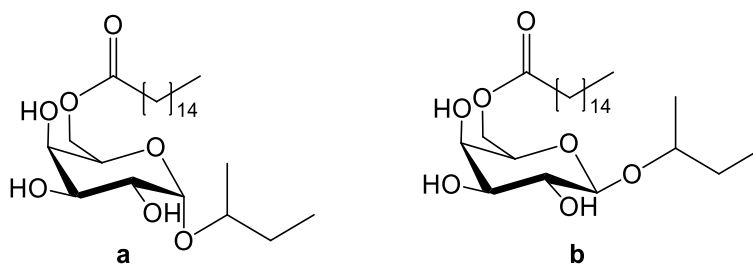
**$^{13}\text{C NMR}$  (DMSO- $d_6$ , 101 MHz):**  $\delta$  (ppm) 173.26 (COO), 108.19 ( $\text{CH}^1_\beta$ ), 101.43 ( $\text{CH}^1_\alpha$ ), 82.70, 82.43, 82.15, 77.75, 76.85, 74.64, 70.14, 67.34 (8 CH), 67.27, 66.96 (2  $\text{OCH}_2$ ), 65.56, 65.55 (2  $\text{CH}_2^6$ ), 33.95 ( $\text{COOCH}_2$ ), 31.76 ( $\text{COOCH}_2\text{CH}_2$ ), 29.50, 29.33, 29.17, 28.92 (4  $(\text{CH}_2)_{12}$ ), 24.90 ( $\text{OCH}_2\text{CH}_2$ ), 19.29 ( $\text{OCH}_2\text{CH}_2\text{CH}_2$ ), 14.42, 14.15 (2  $\text{CH}_3$ ).

**MS (ESI $^+$ ):**  $m/z$  calcd for  $[\text{C}_{26}\text{H}_{50}\text{O}_7]$ : 474.36; found: 497.56  $[\text{M}+\text{Na}]^+$ ; 971.15  $[2\text{M}+\text{Na}]^+$ .

**MS (ESI $^-$ ):**  $m/z$  calcd for  $[\text{C}_{26}\text{H}_{50}\text{O}_7]$ : 474.36; found: 473.39  $[\text{M}-\text{H}]^-$ ; 947.48  $[2\text{M}-\text{H}]^-$ .



## 5.10.10 Characterization of 2-butyl 6-O-palmitoyl-D-galactopyranosides (59ab)



$R_f$  (eluent: *n*-hexane/EtOAc; 2:8): 0.12.

Isomeric ratio a/b: 97/3.

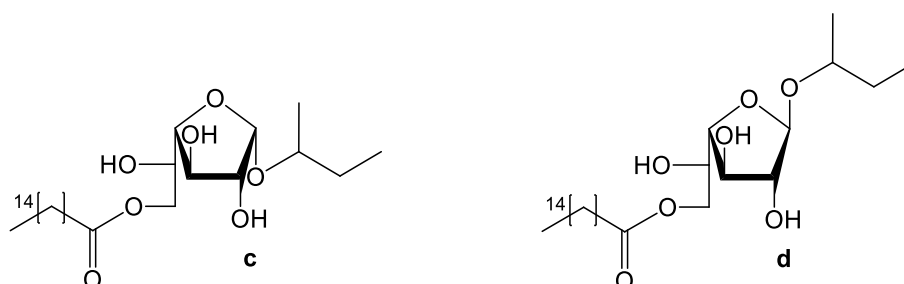
**$^1\text{H NMR}$  (DMSO- $d_6$ , 400 MHz):**  $\delta$  (ppm) 4.81 (dd,  $J = 7.4, 3.5$  Hz, 1H,  $\text{CH}^1_\alpha$ ), 4.63 (m, 2H, OH), 4.40 (d,  $J = 6.1$  Hz, 1H, OH), 4.35 (d,  $J = 6.5$  Hz, 1H, OH), 4.21 – 4.10 (m, 2H,  $\text{CH}_2^6_\alpha$ ), 3.96 (m, 1H,  $\text{CH}^5$ ), 3.74 (br s, 1H,  $\text{CH}^4$ ), 3.66 – 3.55 (m, 3H,  $\text{CH}^2$ ,  $\text{CH}^3$ ,  $\text{OCH}_\alpha$ ), 2.31 (br t,  $J = 6.5$  Hz, 2H,  $\text{COOCH}_2$ ), 1.62 – 1.52 (m, 2H,  $\text{COOCH}_2\text{CH}_2$ ), 1.52 – 1.40 (m, 2H,  $\text{OCHCH}_2$ ), 1.32 (br s, 24H,  $(\text{CH}_2)_{12}$ ), 1.20 – 1.16 (m, 3H,  $\text{OCHCH}_3'$ ), 1.13 – 1.10 (m, 3H,  $\text{OCHCH}_3''$ ), 0.96 – 0.88 (m, 9H,  $\text{CH}_3$ ,  $\text{OCHCH}_2\text{CH}_3$ ).

**$^{13}\text{C NMR}$  (DMSO- $d_6$ , 101 MHz):**  $\delta$  (ppm) 173.20, 173.17 (2  $\text{COO}_\alpha$ ), 99.55, 97.09 (2  $\text{CH}^1_\alpha$ ), 75.91, 73.63 (2  $\text{OCH}_\alpha$ ), 69.78, 69.76 (2  $\text{CH}^4$ ), 69.75, 69.64 (2  $\text{CH}^3$ ), 69.11, 68.94 (2  $\text{CH}^5$ ), 68.73, 68.44 (2  $\text{CH}^2$ ), 64.69, 64.65 (2  $\text{CH}_2^6$ ), 34.02, 34.00 (2  $\text{COOCH}_2$ ), 30.06 ( $\text{OCHCH}_2$ ), 29.48, 29.47, 29.45, 29.40, 29.29, 29.28, 29.15, 29.10, 28.89 ( $(\text{CH}_2)_{12}$ ), 24.87, 24.84 (2  $\text{COOCH}_2\text{CH}_2$ ), 21.08 ( $\text{OCHCH}_3'_\alpha$ ), 19.05 ( $\text{OCHCH}_3''_\alpha$ ), 14.39 ( $\text{CH}_3$ ), 10.56, 9.90 (2  $\text{OCHCH}_2\text{CH}_3$ ).

**MS (ESI $^+$ ):**  $m/z$  calcd for  $[\text{C}_{26}\text{H}_{50}\text{O}_7]$ : 474.36; found: 497.79  $[\text{M}+\text{Na}]^+$ ; 971.82  $[2\text{M}+\text{Na}]^+$ .

**MS (ESI $^-$ ):**  $m/z$  calcd for  $[\text{C}_{26}\text{H}_{50}\text{O}_7]$ : 474.36; found: 473.19  $[\text{M}-\text{H}]^-$ ; 947.26  $[2\text{M}-\text{H}]^-$ .

## 5.10.11 Characterization of 2-butyl 6-O-palmitoyl-D-galactofuranosides (59cd)



$R_f$  (eluent: *n*-hexane/EtOAc; 2:8): 0.30.

Isomeric ratio c/d: 45/55.

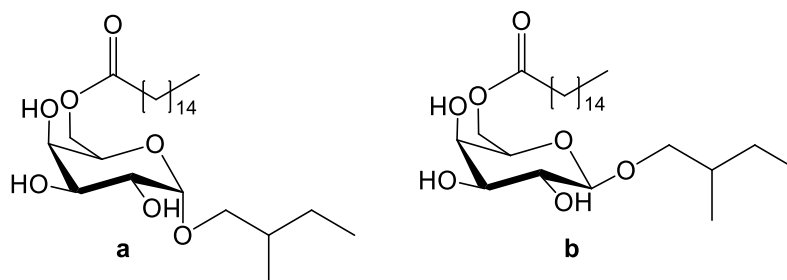
**$^1\text{H NMR}$  (DMSO- $d_6$ , 400 MHz):**  $\delta$  (ppm) 5.25 (d,  $J = 5.5$  Hz, OH), 5.16 (d,  $J = 6.0$  Hz, OH), 5.09 (dd,  $J = 5.7, 2.5$  Hz, OH), 4.93 (d,  $J = 6.7$  Hz, OH), 4.87 (d,  $J = 4.7$  Hz,  $\text{CH}^{1\alpha'}$ ), 4.84 (d,  $J = 4.6$  Hz,  $\text{CH}^{1\alpha''}$ ), 4.80 (dd,  $J = 3.5, 2.4$  Hz,  $\text{CH}^{1\beta}$ ), 4.67 (d,  $J = 7.5$  Hz, OH), 4.63 (d,  $J = 7.5$  Hz, OH), 4.52 (d,  $J = 5.9$  Hz, OH), 4.43 (d,  $J = 6.2$  Hz, OH), 4.08 – 4.02 (m,  $\text{CH}_2^{6\beta}$ ), 3.99 (dd,  $J = 6.3, 1.8$  Hz,  $\text{CH}_2^{6\alpha}$ ,  $\text{CH}_2^{6\beta}$ ), 3.94 – 3.86 (m,  $\text{CH}_2^{6\alpha}$ ,  $\text{OCH}_\beta$ ), 3.86 – 3.81 (m, CH, CH), 3.78 – 3.71 (m, 6 CH), 3.70 – 3.65 (m, CH, CH,  $\text{OCH}_\alpha$ ), 3.65 – 3.60 (m, CH, CH,  $\text{OCH}_\alpha$ ), 3.57 – 3.48 (m, 4 CH,  $\text{OCH}_\beta$ ), 2.28 (m,  $\text{COOCH}_2$ ), 1.51 (br t,  $J = 8.6$  Hz,  $\text{COOCH}_2\text{CH}_2$ ), 1.47 – 1.35 (m,  $\text{OCHCH}_2$ ), 1.31 – 1.20 (m,  $(\text{CH}_2)_{12}$ ), 1.15 – 1.08 (m,  $\text{OCHCH}_3$ ), 1.08 – 1.04 (dd,  $J = 6.1, 2.3$  Hz,  $\text{OCHCH}_3$ ), 0.89 – 0.82 (m,  $\text{CH}_3$ ,  $\text{OCHCH}_2\text{CH}_3$ ).

**$^{13}\text{C NMR}$  (DMSO- $d_6$ , 101 MHz):**  $\delta$  (ppm) 173.26 (COO), 107.96, 105.89 (2  $\text{CH}^{1\beta}$ ), 101.09, 99.37 (2  $\text{CH}^{1\alpha}$ ), 83.08, 82.97, 82.33, 82.27, 82.09, 81.94, 77.62, 77.51, 76.95, 76.84 (10 CH), 75.81 ( $\text{OCH}_\alpha$ ), 75.13 ( $\text{OCH}_\beta$ ), 74.65 (CH), 74.12 ( $\text{OCH}_\alpha$ ), 73.09 ( $\text{OCH}_\beta$ ), 72.11, 70.14, 69.85, 67.30, 67.21 (5 CH), 65.59 ( $\text{CH}_2^{6\alpha}$ ), 65.56 ( $\text{CH}_2^{6\beta}$ ), 33.95 ( $\text{COOCH}_2$ ), 30.08 ( $\text{OCHCH}_2$   $\beta$ ), 30.00 ( $\text{OCHCH}_2$   $\alpha$ ), 29.49, 29.46, 29.35, 29.32, 29.29, 29.15, 29.02, 28.91 ( $(\text{CH}_2)_{12}$ ), 24.91, 24.90, 24.89, 24.87 (4  $\text{COOCH}_2\text{CH}_2$ ), 21.55 ( $\text{OCHCH}_3$   $\beta$ ), 21.27 ( $\text{OCHCH}_3$   $\alpha$ ), 19.41 ( $\text{OCHCH}_3$   $\beta$ ), 19.19 ( $\text{OCHCH}_3$   $\alpha$ ), 14.40 ( $\text{CH}_3$ ), 10.32, 10.21, 10.01, 9.86 (4  $\text{OCHCH}_2\text{CH}_3$ ).

**MS (ESI<sup>+</sup>):**  $m/z$  calcd for  $[\text{C}_{26}\text{H}_{50}\text{O}_7]$ : 474.36; found: 497.83  $[\text{M}+\text{Na}]^+$ ; 971.36  $[2\text{M}+\text{Na}]^+$ .

**MS (ESI<sup>-</sup>):**  $m/z$  calcd for  $[\text{C}_{26}\text{H}_{50}\text{O}_7]$ : 474.36; found: 473.39  $[\text{M}-\text{H}]^-$ ; 947.44  $[2\text{M}-\text{H}]^-$ .

### 5.10.12 Characterization of 2-methyl-1-butyl 6-O-palmitoyl-D-galactopyranosides (60ab)



$R_f$  (eluent: *n*-hexane/EtOAc; 2:8): 0.19.

Isomeric ratio a/b: 85/15.

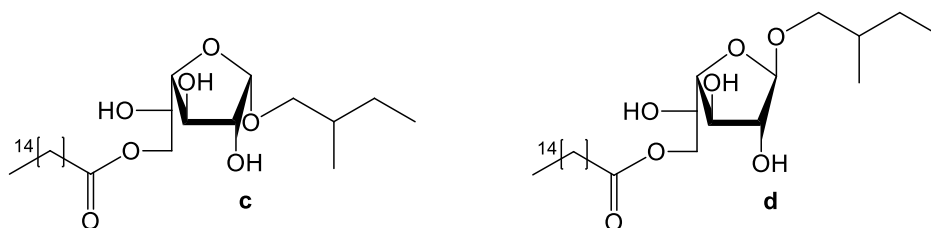
**$^1\text{H NMR}$  (DMSO- $d_6$ , 400 MHz):**  $\delta$  (ppm) 5.29 (d,  $J = 5.4$  Hz, OH), 5.13 (d,  $J = 5.6$  Hz, OH), 4.99 (d,  $J = 6.7$  Hz, OH), 4.69 (d,  $J = 2.0$  Hz,  $\text{CH}^1_\beta$ ), 4.63 (dd,  $J = 6.5, 4.2$  Hz,  $\text{CH}^1_\alpha$ ), 4.47 (dd,  $J = 6.0, 1.4$  Hz, OH), 4.16 – 4.05 (m,  $\text{CH}_2^{6'}$ ,  $\text{CH}_2^{6''}_\beta$ ), 4.01 – 3.97 (m,  $\text{CH}_2^{6''}_\alpha$ ), 3.87 – 3.81 (m,  $\text{CH}^4_\beta$ ), 3.82 – 3.77 (m,  $\text{CH}^5_\alpha$ ,  $\text{CH}^2_\beta$ ), 3.76 – 3.72 (m,  $\text{CH}^5_\beta$ ), 3.72 – 3.69 (br s,  $\text{CH}^4_\alpha$ ), 3.67 – 3.64 (dd,  $J = 7.5, 3.2$  Hz,  $\text{CH}^3_\beta$ ), 3.62 – 3.55 (m,  $\text{CH}^2_\alpha$ ,  $\text{CH}^3_\alpha$ ), 3.44 – 3.38 (m,  $\text{OCH}_2'_\beta$ ), 3.38 – 3.31 (m,  $\text{OCH}_2'_\alpha$ ), 3.21 (dd,  $J = 9.3, 5.5$  Hz,  $\text{OCH}_2''_\beta$ ), 3.12 (m,  $\text{OCH}_2''_\alpha$ ), 2.27 (m,  $\text{COOCH}_2$ ), 1.65 – 1.56 (m,  $\text{OCH}_2\text{CH}$ ), 1.56 – 1.48 (m,  $\text{COOCH}_2\text{CH}_2$ ), 1.48 – 1.37 (m,  $\text{OCH}_2\text{CHCH}_2'$ ), 1.24 (br s,  $(\text{CH}_2)_{12}$ ), 1.15 – 1.06 (m,  $\text{OCH}_2\text{CHCH}_2''$ ), 0.86 (m,  $\text{CH}_3$ ).

**$^{13}\text{C NMR}$  (DMSO- $d_6$ , 101 MHz):**  $\delta$  (ppm) 173.16 (COO), 108.38, 108.29 (2  $\text{CH}^1_\beta$ ), 99.54, 99.37 (2  $\text{CH}^1_\alpha$ ), 82.71 ( $\text{CH}^2_\beta$ ), 82.31 ( $\text{CH}^3_\beta$ ), 76.97 ( $\text{CH}^4_\beta$ ), 72.53, 72.40 (2  $\text{OCH}_2_\alpha$ ), 72.31, 72.21 (2  $\text{OCH}_2_\beta$ ), 69.73 ( $\text{CH}^4_\alpha$ ), 69.00 ( $\text{CH}^3_\alpha$ ), 68.98 ( $\text{CH}^5_\alpha$ ), 68.62 ( $\text{CH}^2_\alpha$ ), 67.42 ( $\text{CH}^4_\beta$ ), 65.88, 65.86 (2  $\text{CH}_2^{6\beta}$ ), 64.65, 64.64 (2  $\text{CH}_2^{6\alpha}$ ), 34.82 ( $\text{OCH}_2\text{CH}$ ), 34.08 ( $\text{COOCH}_2$ ), 29.47, 29.47, 29.41, 29.29, 29.15, 29.12, 28.92 ( $(\text{CH}_2)_{12}$ ), 26.28, 26.15 (2  $\text{OCH}_2\text{CHCH}_2$ ), 24.93 ( $\text{COOCH}_2\text{CH}_2$ ), 17.16, 17.02, 16.83, 16.73 (4  $\text{OCH}_2\text{CHCH}_3$ ), 14.40 ( $\text{CH}_3$ ), 11.67, 11.62, 11.48, 11.46 (4  $\text{OCH}_2\text{CHCH}_2\text{CH}_3$ ).

**MS (ESI $^+$ ):**  $m/z$  calcd for  $[\text{C}_{27}\text{H}_{52}\text{O}_7]$ : 488.37; found: 511.70  $[\text{M}+\text{Na}]^+$ ; 999.12  $[2\text{M}+\text{Na}]^+$ .

**MS (ESI $^-$ ):**  $m/z$  calcd for  $[\text{C}_{27}\text{H}_{52}\text{O}_7]$ : 488.37; found: 487.45  $[\text{M}-\text{H}]^-$ ; 975.50  $[2\text{M}-\text{H}]^-$ .

### 5.10.13 Characterization of 2-methyl-1-butyl 6-O-palmitoyl-D-galactofuranosides (60cd)



$R_f$  (eluent: *n*-hexane/EtOAc; 2:8): 0.40.

Isomeric ratio **c/d**: 8/92.

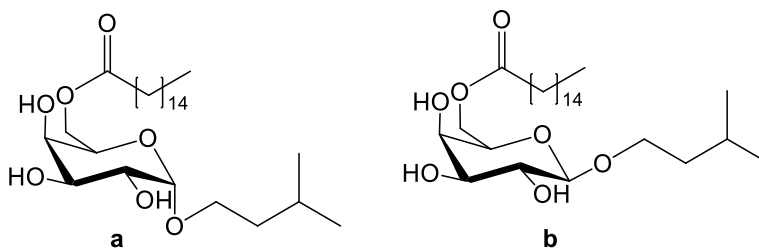
**$^1\text{H NMR}$  (DMSO- $d_6$ , 400 MHz):**  $\delta$  (ppm) 5.29 (d,  $J = 5.4$  Hz, OH), 5.18 (d,  $J = 6.1$  Hz, OH), 5.13 (d,  $J = 5.6$  Hz, OH), 4.97 (d,  $J = 6.8$  Hz, OH), 4.77 (dd,  $J = 7.2, 2.3$  Hz, OH), 4.70 (m,  $\text{CH}^{1\alpha}, \text{CH}^{1\beta}$ ), 4.60 (d,  $J = 5.9$  Hz, OH), 4.10 – 3.98 (m,  $\text{CH}_2^6$ ), 3.93 – 3.88 (m, CH), 3.88 – 3.83 (m, CH), 3.81 – 3.77 (m, CH, CH), 3.77 – 3.70 (m, CH), 3.68 – 3.64 (dd,  $J = 7.6, 3.0$  Hz, CH), 3.64 – 3.60 (dd,  $J = 11.6, 4.7$  Hz, CH), 3.52 – 3.47 (m, CH), 3.47 – 3.34 (m,  $\text{OCH}_2'^\alpha, \text{OCH}_2'^\beta$ ), 3.27 – 3.17 (m,  $\text{OCH}_2''^\alpha$ ), 3.15 – 3.09 (m,  $\text{OCH}_2''^\beta$ ), 2.29 (td,  $J = 7.5, 2.7$  Hz,  $\text{COOCH}_2$ ), 1.64 – 1.48 (m,  $\text{COOCH}_2\text{CH}_2, \text{OCH}_2\text{CH}$ ), 1.47 – 1.36 (m,  $\text{OCH}_2\text{CHCH}_2'$ ), 1.32 – 1.22 (m,  $(\text{CH}_2)_{12}$ ), 1.15 – 1.05 (m,  $\text{OCH}_2\text{CHCH}_2''$ ), 0.86 (m,  $\text{CH}_3$ ).

**$^{13}\text{C NMR}$  (DMSO- $d_6$ , 101 MHz):**  $\delta$  (ppm) 173.34, 173.23 (2 COO), 108.36, 108.27 (2  $\text{CH}^{1\beta}$ ), 101.69, 101.61 (2  $\text{CH}^{1\alpha}$ ), 82.75, 82.45, 82.17, 77.80, 76.91, 74.66 (CH), 72.74, 72.68 (2  $\text{OCH}_2^\alpha$ ), 72.28, 72.17 (2  $\text{OCH}_2^\beta$ ), 70.34, 67.28 (2 CH), 65.54, 65.51 (2  $\text{CH}_2^6$ ), 34.87, 34.84 (2  $\text{OCH}_2\text{CH}$ ), 33.96 ( $\text{COOCH}_2$ ), 29.52, 29.49, 29.47, 29.38, 29.35, 29.20, 29.18, 28.95, 28.93 ( $(\text{CH}_2)_{12}$ ), 26.14, 26.12 (2  $\text{OCH}_2\text{CHCH}_2$ ), 24.93, 24.90 (2  $\text{COOCH}_2\text{CH}_2$ ), 17.02, 16.90, 16.85, 16.83, (4  $\text{OCH}_2\text{CHCH}_3$ ), 14.41 ( $\text{CH}_3$ ), 11.66, 11.62, 11.60, 11.47 (4  $\text{OCH}_2\text{CHCH}_2\text{CH}_3$ ).

**MS (ESI $^+$ ):**  $m/z$  calcd for  $[\text{C}_{27}\text{H}_{52}\text{O}_7]$ : 488.37; found: 511.91  $[\text{M}+\text{Na}]^+$ ; 999.38  $[2\text{M}+\text{Na}]^+$ .

**MS (ESI $^-$ ):**  $m/z$  calcd for  $[\text{C}_{27}\text{H}_{52}\text{O}_7]$ : 488.37; found: 487.40  $[\text{M}-\text{H}]^-$ ; 975.52  $[2\text{M}-\text{H}]^-$ .

### 5.10.14 Characterization of 3-methyl-1-butyl 6-O-palmitoyl-D-galactopyranosides (61ab)



$R_f$  (eluent: *n*-hexane/EtOAc; 2:8): 0.18.

Isomeric ratio a/b: 83/17.

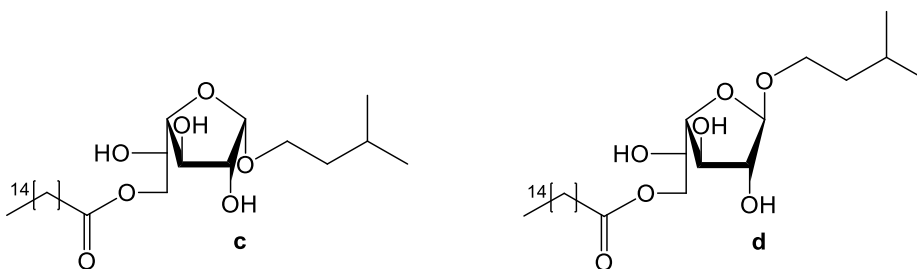
$^1\text{H NMR}$  (DMSO-*d*<sub>6</sub>, 400 MHz):  $\delta$  (ppm) 4.64 (m, 3H, CH<sup>1</sup> <sub>$\alpha$</sub> , OH), 4.49 (d, *J* = 6.1 Hz, 1H, OH), 4.11 (ddd, *J* = 15.0, 11.4, 6.0 Hz, 2H, CH<sup>2</sup> <sub>$\alpha$</sub> ), 3.80 (dd, *J* = 8.2, 3.5 Hz, 1H, CH<sup>5</sup>), 3.69 (d, *J* = 3.1 Hz, 1H, CH<sup>4</sup>), 3.65 – 3.51 (m, 3H, CH<sup>2</sup>, CH<sup>3</sup>, OCH<sup>2</sup>' <sub>$\alpha$</sub> ), 3.38 – 3.32 (m, 1H, OCH<sup>2</sup>'' <sub>$\alpha$</sub> ), 2.28 (m, 2H, COOCH<sub>2</sub>), 1.68 (td, *J* = 13.3, 6.7 Hz, 1H, OCH<sub>2</sub>CH<sub>2</sub>CH), 1.57 – 1.49 (m, 2H, COOCH<sub>2</sub>CH<sub>2</sub>), 1.49 – 1.36 (m, 2H, OCH<sub>2</sub>CH<sub>2</sub>), 1.27 (br s, 24H, (CH<sub>2</sub>)<sub>12</sub>), 0.87 (m, 9H, CH<sub>3</sub>).

$^{13}\text{C NMR}$  (DMSO-*d*<sub>6</sub>, 101 MHz):  $\delta$  (ppm) 173.19 (COO), 99.48 (CH<sup>1</sup> <sub>$\alpha$</sub> ), 69.73 (CH<sup>3</sup> <sub>$\alpha$</sub> ), 69.68 (CH<sup>4</sup> <sub>$\alpha$</sub> ), 69.00 (CH<sup>5</sup> <sub>$\alpha$</sub> ), 68.56 (CH<sup>2</sup> <sub>$\alpha$</sub> ), 65.85 (OCH<sub>2</sub>  $\alpha$ ), 64.68 (CH<sub>2</sub><sup>6</sup>), 38.52 (OCH<sub>2</sub>CH<sub>2</sub>), 34.04 (COOCH<sub>2</sub>), 29.49, 29.31, 29.17, 28.92 ((CH<sub>2</sub>)<sub>12</sub>), 25.04 (OCH<sub>2</sub>CH<sub>2</sub>CH), 24.92 (COOCH<sub>2</sub>CH<sub>2</sub>), 23.18, 22.66 (2 OCH<sub>2</sub>CH<sub>2</sub>CH(CH<sub>3</sub>)<sub>2</sub>), 14.42 (CH<sub>3</sub>).

**MS (ESI<sup>+</sup>):** *m/z* calcd for [C<sub>27</sub>H<sub>52</sub>O<sub>7</sub>]: 488.37; found: 511.62 [M+Na]<sup>+</sup>; 999.19 [2M+Na]<sup>+</sup>.

**MS (ESI<sup>-</sup>):** *m/z* calcd for [C<sub>27</sub>H<sub>52</sub>O<sub>7</sub>]<sup>-</sup>: 488.37; found: 487.25 [M-H]<sup>-</sup>; 975.36 [2M-H]<sup>-</sup>.

## 5.10.15 Characterization of 3-methyl-1-butyl 6-O-palmitoyl-D-galactofuranosides (61cd)



$R_f$  (eluent: *n*-hexane/EtOAc; 2:8): 0.32.

Isomeric ratio c/d: 38/62.

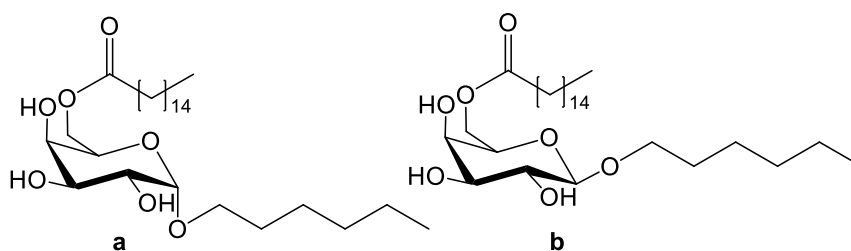
$^1\text{H NMR}$  (DMSO- $d_6$ , 400 MHz):  $\delta$  (ppm) 5.30 (d,  $J = 5.4$  Hz, OH), 5.18 (d,  $J = 6.1$  Hz, OH), 5.14 (d,  $J = 5.7$  Hz, OH), 4.98 (d,  $J = 6.8$  Hz, OH), 4.80 (d,  $J = 7.1$  Hz, OH), 4.72 (d,  $J = 4.5$  Hz,  $\text{CH}^{1\alpha}$ ), 4.70 (d,  $J = 2.2$  Hz,  $\text{CH}^{1\beta}$ ), 4.63 (d,  $J = 5.9$  Hz, OH), 4.09 – 3.97 (m,  $\text{CH}_2^{6'}$ ,  $\text{CH}_2^{6''}$ ), 3.92 – 3.86 (dd,  $J = 6.9, 4.3$  Hz, CH,  $\text{CH}_2^{6''}$ ), 3.86 – 3.80 (m, CH), 3.79 – 3.74 (ddd,  $J = 7.2, 4.7, 2.2$  Hz, CH, CH), 3.74 – 3.69 (m, CH), 3.65 (dd,  $J = 7.6, 3.0$  Hz, CH), 3.63 – 3.59 (ddd,  $J = 11.8, 8.3, 5.0$  Hz, CH,  $\text{OCH}_2$ ), 3.50 (dd,  $J = 6.9, 5.5$  Hz, CH), 3.39 – 3.34 (m,  $\text{OCH}_2$ ), 2.29 (m,  $\text{COOCH}_2$ ), 1.67 (dt,  $J = 13.4, 6.7$  Hz,  $\text{OCH}_2\text{CH}_2\text{CH}$ ), 1.57 – 1.46 (m,  $\text{COOCH}_2\text{CH}_2$ ), 1.45 – 1.34 (m,  $\text{OCH}_2\text{CH}_2$ ), 1.34 – 1.21 (m,  $(\text{CH}_2)_{12}$ ), 0.91 – 0.83 (m,  $\text{CH}_3$ ).

$^{13}\text{C NMR}$  (DMSO- $d_6$ , 101 MHz):  $\delta$  (ppm) 173.24 (COO), 108.22 ( $\text{CH}^{1\beta}$ ), 101.46 ( $\text{CH}^{1\alpha}$ ), 82.73, 82.43, 82.12, 77.73, 76.84, 74.62, 70.15, 67.28 (8 CH), 65.60 ( $\text{OCH}_2$ ), 65.53 ( $\text{CH}_2^6$ ), 38.57 ( $\text{OCH}_2\text{CH}_2$ ), 33.96 ( $\text{COOCH}_2$ ), 29.51, 29.36, 29.18, 28.93 ( $(\text{CH}_2)_{12}$ ), 24.95 ( $\text{OCH}_2\text{CH}_2\text{CH}$ ), 24.91 ( $\text{COOCH}_2\text{CH}_2$ ), 23.02, 22.74 (2  $\text{OCH}_2\text{CH}_2\text{CH}(\text{CH}_3)_2$ ), 14.42 ( $\text{CH}_3$ ).

**MS (ESI $^+$ ):**  $m/z$  calcd for  $[\text{C}_{27}\text{H}_{52}\text{O}_7]$ : 488.37; found: 511.84  $[\text{M}+\text{Na}]^+$ ; 999.40  $[\text{2M}+\text{Na}]^+$ .

**MS (ESI $^-$ ):**  $m/z$  calcd for  $[\text{C}_{27}\text{H}_{52}\text{O}_7]$ : 488.37; found: 488.16  $[\text{M}-\text{H}]^-$ ; 976.05  $[\text{2M}-\text{H}]^-$ .

## 5.10.16 Characterization of 1-hexyl 6-O-palmitoyl-D-galactopyranosides (62ab)



$R_f$  (eluent: *n*-hexane/EtOAc; 2:8): 0.20.

Isomeric ratio a/b: 88/12.

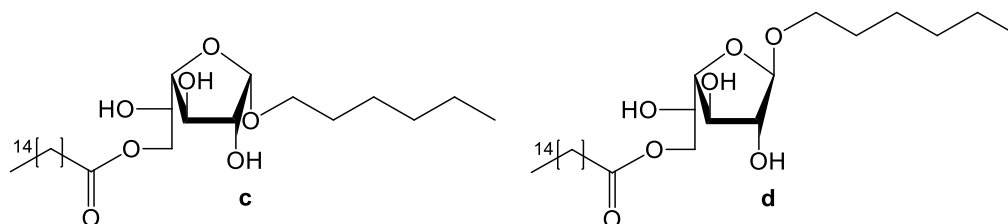
$^1\text{H NMR}$  (DMSO- $d_6$ , 400 MHz):  $\delta$  (ppm) 4.62 (d,  $J = 3.3$  Hz, 1H,  $\text{CH}^1_\alpha$ ), 4.61 – 4.57 (m, 2H, OH), 4.45 (d,  $J = 6.1$  Hz, 1H, OH), 4.14 – 4.01 (ddt,  $J = 11.8, 7.3, 6.0$  Hz, 2H,  $\text{CH}_2^6$ ), 3.80 – 3.74 (m, 1H,  $\text{CH}^5$ ), 3.69 – 3.64 (m, 1H,  $\text{CH}^4$ ), 3.59 – 3.47 (m, 3H,  $\text{CH}^2$ ,  $\text{CH}^3$ ,  $\text{OCH}_2'^\alpha$ ), 3.34 – 3.27 (m, 1H,  $\text{OCH}_2''_\alpha$ ), 2.28 – 2.22 (m, 2H,  $\text{COOCH}_2$ ), 1.48 (m, 4H,  $\text{COOCH}_2\text{CH}_2$ ,  $\text{OCH}_2\text{CH}_2$ ), 1.34 – 1.17 (m, 30H,  $(\text{CH}_2)_{12}$ ,  $(\text{CH}_2)_3$ ), 0.84 (m, 6H,  $\text{CH}_3$ ).

$^{13}\text{C NMR}$  (DMSO- $d_6$ , 101 MHz):  $\delta$  (ppm) 173.15 (COO), 99.40 ( $\text{CH}^1_\alpha$ ), 69.72 ( $\text{CH}^3_\alpha$ ), 69.70 ( $\text{CH}^4_\alpha$ ), 68.95 ( $\text{CH}^5_\alpha$ ), 68.59 ( $\text{CH}^2_\alpha$ ), 67.49 ( $\text{OCH}_2$ ), 64.64 ( $\text{CH}_2^6$ ), 34.07 ( $\text{COOCH}_2$ ), 31.77 ( $\text{OCH}_2\text{CH}_2$ ), 31.57 ( $\text{OCH}_2\text{CH}_2\text{CH}_2$ ), 29.58, 29.50, 29.34, 29.18, 28.94 ( $(\text{CH}_2)_{12}$ ), 25.92 ( $\text{OCH}_2\text{CH}_2\text{CH}_2\text{CH}_2$ ), 24.94 ( $\text{COOCH}_2\text{CH}_2$ ), 22.57 ( $\text{OCH}_2\text{CH}_2\text{CH}_2\text{CH}_2\text{CH}_2$ ), 14.40 ( $\text{CH}_3$ ).

**MS (ESI $^+$ ):**  $m/z$  calcd for  $[\text{C}_{28}\text{H}_{54}\text{O}_7]$ : 502.39; found: 526.04  $[\text{M}+\text{Na}]^+$ ; 1027.13  $[\text{2M}+\text{Na}]^+$ .

**MS (ESI $^-$ ):**  $m/z$  calcd for  $[\text{C}_{28}\text{H}_{54}\text{O}_7]$ : 502.39; found: 502.43  $[\text{M}-\text{H}]^-$ ; 1003.60  $[\text{2M}-\text{H}]^-$ .

## 5.10.17 Characterization of 1-hexyl 6-O-palmitoyl-D-galactofuranosides (62cd)



$R_f$  (eluent: *n*-hexane/EtOAc; 2:8): 0.45.

Isomeric ratio c/d: 28/72.

$^1\text{H NMR}$  (DMSO- $d_6$ , 400 MHz):  $\delta$  (ppm) 5.30 (d,  $J = 5.4$  Hz, OH), 5.18 (d,  $J = 6.1$  Hz, OH), 5.13 (d,  $J = 5.7$  Hz, OH), 4.97 (d,  $J = 6.8$  Hz, OH), 4.81 (d,  $J = 7.1$  Hz, OH), 4.71 (m,  $\text{CH}^1_\alpha$ ,  $\text{CH}^1_\beta$ ), 4.61 (d,  $J = 6.0$  Hz, OH), 4.09 – 3.96 (m,  $\text{CH}_2^6$ ), 3.92 – 3.88 (m, CH), 3.88 – 3.82 (m, CH), 3.79 – 3.75 (m, CH, CH), 3.75 – 3.71 (m, CH), 3.70 – 3.64 (m, CH,  $\text{OCH}_2'\beta$ ), 3.64 – 3.60 (m, CH), 3.59 – 3.52 (m,  $\text{OCH}_2'\alpha$ ), 3.52 – 3.49 (m, CH), 3.38 – 3.30 (m,  $\text{OCH}_2''$ ), 2.29 (t,  $J = 7.4$  Hz,  $\text{COOCH}_2$ ), 1.49 (m,  $\text{COOCH}_2$ ,  $\text{OCH}_2\text{CH}_2$ ), 1.34 – 1.21 (m,  $(\text{CH}_2)_{12}$ ,  $(\text{CH}_2)_3$ ), 0.87 (m,  $\text{CH}_3$ ).

$^{13}\text{C NMR}$  (DMSO- $d_6$ , 101 MHz):  $\delta$  (ppm) 173.21 (COO), 108.21 ( $\text{CH}^1_\beta$ ), 101.45 ( $\text{CH}^1_\alpha$ ), 82.71, 82.48, 82.12, 77.76, 76.85, 74.66, 70.20 (7 CH), 67.60 ( $\text{OCH}_2\beta$ ), 67.32 ( $\text{OCH}_2\alpha$ ), 67.28 (CH), 65.53 ( $\text{CH}_2^6$ ), 33.97 ( $\text{COOCH}_2$ ), 31.78, 31.62 (2  $\text{OCH}_2\text{CH}_2$ ), 31.57 ( $\text{OCH}_2\text{CH}_2\text{CH}_2$ ), 29.71, 29.65, 29.52, 29.49, 29.37, 29.19, 28.95 ( $(\text{CH}_2)_{12}$ ), 25.83, 25.76 (2  $\text{OCH}_2\text{CH}_2\text{CH}_2\text{CH}_2$ ), 24.92 ( $\text{COOCH}_2\text{CH}_2$ ), 22.59, 22.57 (2  $\text{OCH}_2\text{CH}_2\text{CH}_2\text{CH}_2\text{CH}_2$ ), 14.41, 14.38 (2  $\text{CH}_3$ ).

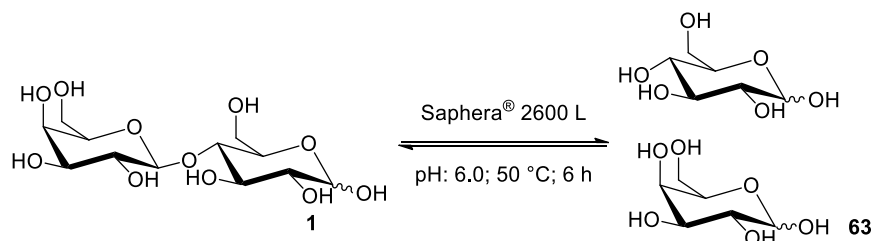
$\text{MS (ESI}^+)$ :  $m/z$  calcd for  $[\text{C}_{28}\text{H}_{54}\text{O}_7]$ : 502.39; found: 526.20  $[\text{M}+\text{Na}]^+$ ; 1027.38  $[\text{2M}+\text{Na}]^+$ .

$\text{MS (ESI}^-)$ :  $m/z$  calcd for  $[\text{C}_{28}\text{H}_{54}\text{O}_7]$ : 502.39; found: 502.04  $[\text{M}-\text{H}]^-$ ; 1004.06  $[\text{2M}-\text{H}]^-$ .



## 5.11 Synthesis of 1-butyl 6-O-palmitoyl-D-glycosides from cheese whey permeate

### 5.11.1 Enzymatic hydrolysis of D-lactose found in cheese whey permeate



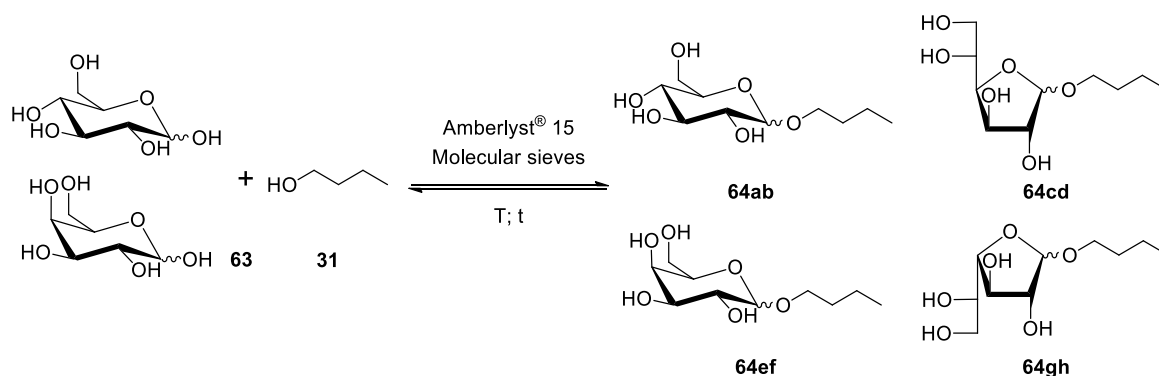
Cheese whey permeate (pH: 6.0), containing D-lactose (**1**, around 50 g L<sup>-1</sup>), was heated to 50 °C. Saphera® 2600 L (1.1 g L<sup>-1</sup>) was added to start the hydrolysis of lactose.

The reaction was monitored as a function of time (CH<sub>3</sub>CN/H<sub>2</sub>O; 8:2).

After 6 h, the enzyme was inactivated by heat treatment at 85 °C for 15 min. The reaction mixture was then filtered and freeze-dried to obtain a mixture 1:1 of **D-glucose / D-galactose (63)**, as corroborated by <sup>1</sup>H NMR analysis carried out in D<sub>2</sub>O.

**Yield:** quantitative

## 5.11.2 Fischer glycosylation of D-glucose and D-galactose mixture



The mixture of D-glucose / D-galactose (**63**) was suspended in dry *n*-butanol (**31**) (1.8% w/v) in the presence of the strongly acidic cation exchange resin Amberlyst® 15 (10 %, w/w) and 3 Å molecular sieves (25 %, w/w), at different temperatures.

After reaction times reported in **Table 5.8**, each reaction was stopped by filtration of the solid catalyst, the alcohol was removed under reduced pressure and the reaction mixture was submitted to flash chromatography (DCM/MeOH; 9:1) to give **1-butyl D-glycoside isomeric mixture (64ah)** as a viscous syrup.

Isomeric ratios of alkyl D-glycoside isomeric mixtures were estimated by <sup>1</sup>H NMR analysis, carried out in D<sub>2</sub>O, as the ratio of the areas of anomeric proton signals of each isomer present in the reaction mixture. NMR anomeric proton signals were identified by comparison with data reported in the literature (Straathof et al., 1987).

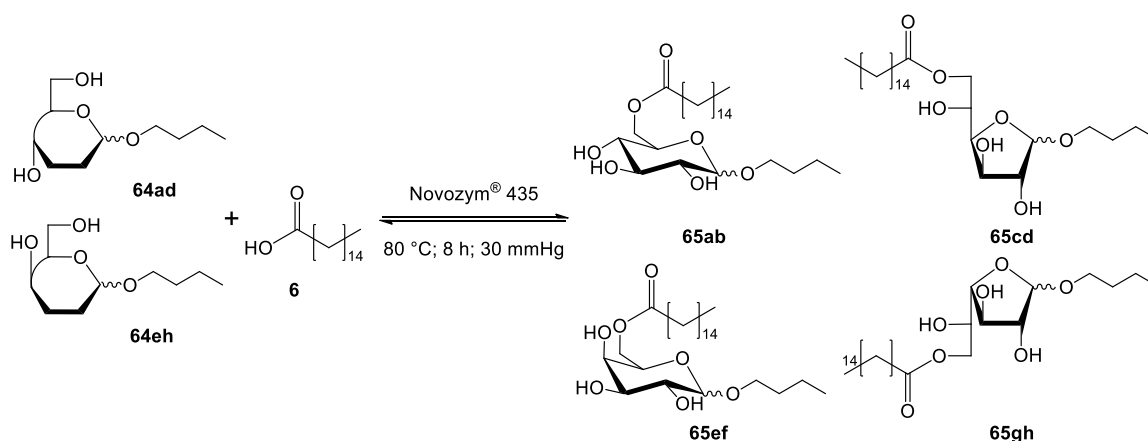
**Isomeric ratio abef/cdgh:** 37/63

**Isomeric ratio a/b/c/e/f/d+g+h:** 10/11/12/10/6/51

**Table 5.8.** Experimental conditions for the synthesis of 1-butyl glycoside isomeric mixture.

<b>Attempt</b>	<b>Temperature (°C)</b>	<b>Time (h)</b>	<b>Yield (%)</b>
64.01	120	3	8
64.02	50	6.5	9
64.03			34
64.04	80	24	15
64.05			22
64.06			24

## 5.11.3 Enzymatic esterification of 1-butyl D-glycosides



Isomeric mixture of 1-butyl D-glycosides (**64ah**), palmitic acid (**6**), in molar ratio 1:1, and Novozym® 435 (10 %, w/w) were mixed together and charged into a round-bottom flask. The mixture was heated to 80 °C while rotating the flask by means of a glass oven B-585 Kugelrohr. After palmitic acid melted, the reaction was performed under reduced pressure (30 mmHg).

After 8 h, reaction mixture was taken up in EtOAc and the immobilized enzyme was removed by filtration. Then, the esters were extracted in EtOAc (2 times) from 1 M NaOH, the organic phases were collected, dried over Na<sub>2</sub>SO<sub>4</sub> and the solvent was removed under reduced pressure. A flash chromatography (*n*-hexane/EtOAc; 2:8), afforded **1-butyl 6-O-palmitoyl-D-glycoside isomeric mixtures (65ah)**. Isomeric ratios were estimated by <sup>1</sup>H NMR analysis, carried out in DMSO-*d*<sub>6</sub> + D<sub>2</sub>O (1 drop), as the ratio of the areas of the anomeric proton signals (**e** and **f** species were present only in traces, thus it was impossible to calculate their amount).

**Yield:** 15%

**Isomeric ratio abef/cdgh:** 32/68

**Isomeric ratio (a/b/c/d/g/h):** 28/4/19/27/14/8

## 5.12 Quantitative TLC and image analysis

The isomeric ratios and the purity of the alkyl 6-*O*-palmitoyl galactoside derivatives were assessed by quantitative TLC and image analysis, as reported elsewhere (Sangiorgio et al., 2022).

Briefly, ethyl, 1-propyl, 2-propyl, 1-butyl, 2-butyl, 2-methyl-1-butyl, 3-methyl-1-butyl, 1-hexyl 6-*O*-palmitoyl-*D*-galactopyranosides (**55ab**, **56ab**, **57ab**, **58ab**, **59ab**, **60ab**, **61ab**, **62ab**) and *D*-galactofuranosides (**55cd**, **56cd**, **57cd**, **58cd**, **59cd**, **60cd**, **61cd**, **62cd**) were solubilized in EtOAc (0.1 % w/v, final concentration). TLCs were performed on Silica gel 60 F<sub>254</sub> precoated aluminum sheets (Merck, Darmstadt, Germany). Plates were 10 cm high; solutions of each compound were spotted 1 cm from the lower edge using Blaubrand intraMark graduated micropipettes (5 ring marks, 1 µL each, Brand GMBH + CO KG, Wertheim, Germany) and eluted in *n*-hexane/AcOEt (2:8). Compounds were detected by spraying with Ce(SO<sub>4</sub>)<sub>2</sub> / (NH<sub>4</sub>)<sub>6</sub>Mo<sub>7</sub>O<sub>24</sub>·4H<sub>2</sub>O solution, followed by heating at ca 150 °C (**Figure 5.1**). The image was acquired with a scanner and subjected to image analysis, then the purity was calculated as the ratio of the product areas with respect to the total area spotted. The results are reported in **Table 5.9**.

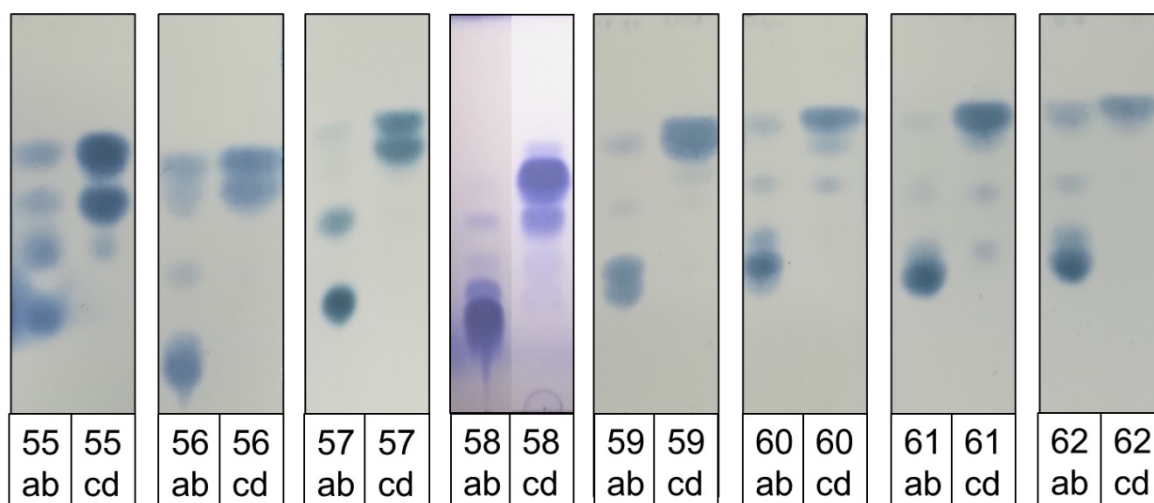


**Figure 5.1.** TLCs of ethyl, 1-propyl, 2-propyl, 1-butyl, 2-butyl, 2-methyl-1-butyl, 3-methyl-1-butyl, 1-hexyl 6-*O*-palmitoyl-*D*-galactopyranosides (**55ab**, **56ab**, **57ab**, **58ab**, **59ab**, **60ab**, **61ab**, **62ab**) and *D*-galactofuranosides (**55cd**, **56cd**, **57cd**, **58cd**, **59cd**, **60cd**, **61cd**, **62cd**).

Eluent: *n*-hexane/AcOEt (2:8:).

*Table 5.9. Purity and isomeric ratio of alkyl 6-O-palmitoyl-D-galactoside isomeric couples.*

<b>Compound</b>	<b>Purity (%)</b>	<b>Isomeric ratio (%)</b>	<b>Compound</b>	<b>Purity (%)</b>	<b>Isomeric ratio (%)</b>
<b>55ab</b>	80	76/24	<b>55cd</b>	97	40/60
<b>56ab</b>	82	93/7	<b>56cd</b>	99	43/57
<b>57ab</b>	91	57/43	<b>57cd</b>	99	41/59
<b>58ab</b>	94	94/6	<b>58cd</b>	94	20/80
<b>59ab</b>	89	97/3	<b>59cd</b>	98	45/55
<b>60ab</b>	79	85/15	<b>60cd</b>	97	8/92
<b>61ab</b>	96	83/17	<b>61cd</b>	95	38/62
<b>62ab</b>	82	88/12	<b>62cd</b>	99	28/72

### 5.13 Fatty acid composition of commercial sunflower oil

The fatty acid composition of commercial sunflower oil was determined by GC/MS analysis carried out after base-catalysed transesterification of triglycerides, according to the ISO 15884:2002 - IDF 182:2002 protocol (Bavaro et al., 2020).

Briefly, a sample of sunflower oil (100 mg), containing methyl nonadecanoate as internal standard (C19Me, 2.5 mL of 10 mg mL<sup>-1</sup> standard stock solution in *n*-heptane), was dissolved in 5 mL of *n*-heptane and submitted to transesterification with KOH/MeOH solution (10%, w/v, 0.2 mL) at room temperature. After 5 minutes, the reaction was quenched by the addition of KHSO<sub>4</sub> (500 mg). Then, the mixture was centrifuged (3000 rpm for 5 min) and the supernatant, containing the methyl esters, was diluted 1:10 with *n*-heptane and analyzed through GC/MS analysis.

GC/MS analyses were carried out on a Thermo Scientific DSQII single quadrupole GC/MS system (TraceDSQII mass spectrometer, Trace GC Ultra gas chromatograph, TriPlus Autosampler - Thermo Scientific®, San Jose, CA, USA). Chromatography was performed on a Rxi-5Sil MS capillary column (30 m length x 0.25 mm ID x 0.25 µm film thickness, Restek, Milan, Italy) with Helium (> 99.99 %) as carrier gas at a constant flow rate of 1.0 mL min<sup>-1</sup>. The injector temperature was set at 250 °C and it was operated in split mode, with a split flow of 10 mL min<sup>-1</sup>. The oven temperature was programmed from 45 °C (isothermal for 4 min) to 175 °C (isothermal for 27 min) at the rate of 13 °C/min and then to 215 °C (isothermal for 35 min) at the rate of 4 °C/min. Mass transfer line temperature was set at 250 °C. Total GC running time was 85 min. All mass spectra were acquired with an electron ionization system (EI, Electron Impact mode) with ionization energy of 70 eV and source temperature of 250 °C, with spectral acquisition in Full Scan mode over a mass range of 35–650 Da. The chromatogram acquisition, detection of mass spectral peaks and their waveform processing were performed using Xcalibur MS Software Version 2.1 (Thermo Scientific Inc.). Assignment of chemical structures to chromatographic peaks was based on the comparison with the databases for GC-MS NIST Mass Spectral Library (NIST 08) and Wiley Registry of Mass Spectral Data (8<sup>th</sup> Edition). The percentage content of each component was directly computed from the peak areas in the GC/MS chromatogram.

### 5.14 Preliminary physico-chemical characterization

#### 5.14.1 Solubility measurements

To assess the solubility of the products, SFAEs (5 mg) were added to water (milli-Q) or sunflower oil (2 mL) and further mixed using a hand-operated laboratory piston-type homogenizer (at 3000 rpm, 30 s; Vortex Mixer, VELP Scientifica, Usmate, Italy). Then, they were also submitted to a heating step (at 80 °C for 30 min) to improve the product solubility.

#### 5.14.2 Hydrophilic-lipophilic balance (HLB) calculation

According to the Griffin method, the HLB values of non-ionic surfactants can be calculated using the following formula:

$$\text{HLB} = 20 \times \frac{M_{\text{H}}}{M}$$

where  $M_{\text{H}}$  is the molecular mass of the hydrophilic moiety of the surfactant, while  $M$  is that of the whole surfactant molecule (Zhang et al., 2014).

#### 5.14.3 Contact angle measurement

Pellets of each of the glucose monoesters (**13**, **14**, **15**) were prepared with powdered pure compound (300 mg). Contact angle measurements were performed on a Krüss Easy instrument. A drop of 5  $\mu\text{L}$  was produced and gently placed on the surface of each pellet. Side view pictures were taken immediately after the water droplet left the syringe tip, using a high-resolution camera. The drop profile was extrapolated using an appropriate fitting function, depending on the curvature radius of the droplet. Measurements were repeated several times to obtain a statistically relevant population.

### 5.15 Surfactant properties study

#### 5.15.1 Interfacial tension measurements

The sunflower oil/water interfacial tension (IFT) values were measured at  $(25 \pm 1)$  °C by means of Gibertini tensiometer following the du Noüy ring method and by varying the concentration (in the range between 0.1 - 4.5 mM in sunflower oil) of alkyl glycoside fatty acid ester compounds. Prior to tensiometric measurements, several parameters were introduced in the relative software to set up the method, such as the liquid density, the platinum ring and radius, required by the Harkins-Jordan correction. Data were reported as average values on three different replicates.

#### 5.15.2 Emulsifying properties

Water (milli-Q) in sunflower oil (W/O) emulsions were prepared using a Thermo Fisher Q700 sonicator equipped with a 3 mm-titanium alloy microtip and optimized surfactant concentration and phase volume (4.5 mM and  $\Phi_V = 0.14$ ). The operative conditions contemplate a frequency of 20 kHz in pulsed mode (3 s on and 3 s off) at 50% amplitude for 45 s. Stability tests were performed by means of turbidimetric measurements and confocal microscopy over time (from 1 h to 1 month).

A turbidimetric method (Song et al., 2000) was adopted, to determine the emulsions stability within 72 h by measuring the absorbance value (Shimadzu UV-Vis spectrophotometer UV-2600) of the prepared samples at a fixed wavelength, in a 1 cm path length optical cell. Since all the investigated systems showed a gradual decrease in the 400–700 nm range, a wavelength of 500 nm was chosen.

Then,  $\tau$  can be easily calculated according to the formula (Aizawa, 2014):

$$\tau = \ln(10) A$$

Then,  $\tau$  was normalized to the value of turbidity obtained at 0 min ( $\tau_0$ ), thus resulting in the normalized turbidity ( $\tau / \tau_0$ ), whose decreasing was studied within time.



Furthermore, the stability index or turbidity ratio (R) was calculated (Song et al., 2000). R is defined as the ratio of turbidity at high and low wavelengths (in the present case 700 and 450 nm,  $R = \tau_{700} / \tau_{450}$ ). Then, the slope of turbidity ratio over time was calculated within 50 min. No samples dilution was performed according to Bai et al. (Bai et al., 2018).

Moreover, droplets size distribution of both fresh and aged emulsions was evaluated by processing (by ImageJ software) the images (droplets number up to 150) acquired by Nikon A1 laser scanning confocal microscope (LSCM) working in oil immersion (NA1.4) equipped with a 60× objective. Before each analysis, emulsions were stained with Rhodamine B (a dye soluble only in the water phase) and samplings in the central part of each vial (where the emulsions showed whitish color typical of well-emulsified systems) were made. Images were acquired with an excitation wavelength of 561 nm and emitted signal was detected between 770 and 620 nm.

## 6 | References

- ACS Chemistry for Life. < <https://www.acs.org/content/acs/en/greenchemistry/what-is-green-chemistry/history-of-green-chemistry.html>> (accessed February 2023).
- Adelhorst, K.; Björkling, F.; Godtfredsen, S. E.; Kirk O. Enzyme Catalysed Preparation of 6-O-Acylglucopyranosides. *Synthesis* **1990**, (2), 112-115. DOI:10.1055/s-1990-26802.
- Aizawa, H. Novel Pragmatic Turbidimetric Data Analysis Method for Evaluating the Stability of Emulsions. *Int. J. Food Prop.* **2014**, 17 (6), 1264-1274. DOI:10.1080/10942912.2012.685674.
- Akkara, J. A.; Ayyagari, M. S. R.; Bruno, F. F. Enzymatic synthesis and modification of polymers in nonaqueous solvents. *Trends Biotechnol.* **1999**, 17 (2), 67-73. DOI:10.1016/S0167-7799(98)01270-0.
- Alabugin, I. V.; Kuhn, L.; Krivoshchapov, N. V.; Mehaffy, P.; Medvedev, M. G. Anomeric effect, hyperconjugation and electrostatics: lessons from complexity in a classic stereoelectronic phenomenon. *Chem. Soc. Rev.* **2021**, 50, 10212. DOI:10.1039/d1cs00564b.
- Anastas, P. T. Green Chemistry and the role of analytical methodology development. *Crit. Rev. Anal. Chem.* **1999**, 29, 167–175. DOI:10.1080/10408349891199356.
- Anastas P. T., Warner J. C. *Green Chemistry: Theory and Practice*. Oxford University Press, Oxford, 1998.
- Anderson, E. M.; Larsson, K. M.; Kirk, O. One Biocatalyst—Many Applications: The Use of *Candida Antarctica* B-Lipase in Organic Synthesis. *Biocatal. Biotransformations* **1998**, 16 (3), 181-204. DOI:10.3109/10242429809003198.
- Ansorge-Schumacher, M. B.; Thum, O. Immobilised lipases in the cosmetics industry. *Chem. Soc. Rev.* **2013**, 42 (15), 6475-6490. DOI:10.1039/c3cs35484a.
- Arifin, D. Y.; Schnupf, U.; Irle, S. Statistical Mechanics-Based Theoretical Investigation of Solvation Effects on Glucose Anomer Preferences. *J. Phys. Chem. B* **2018**, 122 (1), 290-296. DOI:10.1021/acs.jpcc.7b10270.
- Asakura, J.; Matsubara, Y.; Yoshihara, M. Clay catalyzed acetonation: a simple method for the preparation of isopropylidene carbohydrates. *J. Carbohydr. Chem.* **1996**, 15 (2), 231-239. DOI:10.1080/07328309608005441.
- Audic, J. L.; Chaufer, B.; Daufin, G. Non-food applications of milk components and dairy coproducts: a review. *Lait* **2003**, 83 (6), 417–438. DOI:10.1051/lait:2003027.
- Bai, L.; Xiang, W.; Huan, S.; Rojas, O. J. Formulation and stabilization of concentrated edible oil-in-water emulsions based on electrostatic complexes of a food-grade cationic surfactant (ethyl Lauroyl Arginate) and cellulose nanocrystals. *Biomacromolecules* **2018**, 19, 1674-1685. DOI:10.1021/acs.biomac.8b00233.

- Ballash, N. M.; Robertson, E. B. The Mutarotation of Glucose in Dimethylsulfoxide and Water Mixtures. *Can. J. Chem.* **1973**, *51*, 556-564. DOI:10.1139/V73-085.
- Bavaro, T.; Benucci, I.; Pedrali, A.; Marrubini, G.; Esti, M.; Terreni, M.; Massolini, G.; Ubiali, D. Lipase-mediated hydrolysis of hempseed oil in a packed-bed reactor and in-line purification of PUFA as mono- and diacylglycerols. *Food Bioprod. Process.* **2020**, *123*, 345-353. DOI:10.1016/j.fbp.2020.07.009.
- Begum, F.; Xu, L.; Amin, S. Surfactants. In *Kirk-Othmer Encyclopedia of Chemical Technology*, John Wiley & Sons, Inc., USA, 2020.
- Belhaj, A. F.; Elraies, K. A.; Mahmood, S. M.; Zulkifli, N. N.; Akbari, S.; Hussien O. S. The effect of surfactant concentration, salinity, temperature, and pH on surfactant adsorption for chemical enhanced oil recovery: a review. *J. Petrol. Explor. Prod. Technol.* **2020**, *10*, 125-137. DOI:10.1007/s13202-019-0685-y.
- Bhadani, A.; Kafle, A.; Ogura, T.; Akamatsu, M.; Sakai, K.; Sakai, H.; Abe M. Current perspective of sustainable surfactants based on renewable building blocks. *Curr. Opin. Colloid. Interface Sci.* **2020**, *45*, 124-135. DOI:10.1016/j.cocis.2020.01.002.
- Biermann, U.; Bornscheuer, U.; Meier, M. A. R.; Metzger, J. O.; Schäfer, H. J. Oils and fats as renewable raw materials in chemistry. *Angew. Chem., Int. Ed. Engl.* **2011**, *50* (17), 3854-3871. DOI:10.1002/anie.201002767.
- Björkling, F.; Godtfredsen, S. E.; Kirk O. A Highly Selective Enzyme-catalysed Esterification of Simple Glucosides. *J. Chem. Soc., Chem. Commun.* **1989**, (14), 934-935. DOI:10.1039/C39890000934.
- Bock, K.; Thøgersen, H. (1982): Nuclear Magnetic Resonance Spectroscopy in the Study of Mono- and Oligosaccharides. In *Annual Reports on NMR Spectroscopy*, Webb G. A. Ed.; Academic Press, London, Volume 13, 1983, pp 1-57. DOI:10.1016/S0066-4103(08)60307-5.
- Bos, M. A.; van Vliet, T. Interfacial rheological properties of adsorbed protein layers and surfactants: a review. *Adv. Colloid Interface Sci.* **2001**, *91* (3), 437-471. DOI:10.1016/S0001-8686(00)00077-4.
- Boz, N.; Degirmenbasi, N.; Kalyon, D. M. Esterification and transesterification of waste cooking oil over Amberlyst 15 and modified Amberlyst 15 catalysts, *Appl. Catal. B Environ.* **2015**, *165*, 723-730. DOI:10.1016/j.apcatb.2014.10.079.
- Bui, T.; Frampton, H.; Huang, S.; Collins, I. R.; Striolo, A.; Michaelides, A. Water/oil interfacial tension reduction - an interfacial entropy driven process. *Phys. Chem. Chem. Phys.* **2021**, *23* (44), 25075-25085. DOI:10.1039/D1CP03971G.
- Carson, R. *Silent Spring*, Houghton Mifflin Company, Boston, 1962.

- Carteret, C.; Jacoby, J.; Blin, J. L. Using factorial experimental design to optimize biocatalytic biodiesel production from *Mucor miehei* lipase immobilized onto ordered mesoporous materials. *Microporous Mesoporous Mater.* **2018**, *268*, 39-45. DOI:10.1016/j.micromeso.2018.04.004.
- Carvalho, F.; Prazeres, A. R.; Rivas, J. Cheese whey wastewater: characterization and treatment. *Sci. Total Environ.* **2013**, *445-446*, 385–396. DOI:10.1016/j.scitotenv.2012.12.038.
- Chen, J.-W.; Wu, W.-T. Regeneration of immobilized *Candida antarctica* lipase for transesterification. *J. Biosci. Bioeng.* **2003**, *95* (5), 466-469. DOI:10.1016/s1389-1723(03)80046-4.
- Chhatre, S.; Farid, S. S.; Coffman, J.; Bird, P.; Newcombe, A. R.; Titchener-Hooker, N. J. How implementation of Quality by Design and advances in Biochemical Engineering are enabling efficient bioprocess development and manufacture. *J. Chem. Technol. Biotechnol.* **2011**, *86* (9), 1125-1129. DOI:10.1002/jctb.2628.
- Chiocconi, A. A.; Varela, O.; de Lederkremer, R. M. Stereoselective preparation of alkyl 3-deoxy- $\beta$ -D-galactofuranosides. *Carbohydr. Lett.* **1996**, *2*, 115-122.
- Chopineau, J.; McCafferty, F. D.; Therisod, M.; Klibanov A. M. Production of Biosurfactants from Sugar Alcohols and Vegetable Oils Catalyzed by Lipases in a Nonaqueous Medium. *Biotechnol. Bioeng.* **1988**, *31* (3), 208-214. DOI:10.1002/bit.260310305.
- Cinget, F.; Schmidt, R. R. Synthesis of unprotected O-glycosyl trichloroacetimidates and their reactivity towards some glycosyl acceptors. *Synlett.* **1993**, *2*, 168-170. DOI:10.1055/s-1993-22391.
- Cionti, C.; Vavassori, G.; Pargoletti, E.; Meroni, D.; Cappelletti, G. One-step, highly stable Pickering emulsions stabilized by ZnO: tuning emulsion stability by in situ functionalization. *J. Colloid Interface Sci.* **2022**, *628* (A), 82-89. DOI:10.1016/j.jcis.2022.07.129.
- Clariant. < <https://www.clariant.com/en/Company/DiscoverValue/Glucopure>> (accessed February 2023).
- Collins, P. M.; Ferrier, R. J. *Monosaccharides: their chemistry and their roles in natural products*. Wiley & Sons Ed.; Chichester; New York, 1995.
- Croitoru, R.; Fițigău, F.; van den Broek, L. A. M.; Frissen, A. E.; Davidescu, C. M.; Boeriu, C. G.; Peter, F. Biocatalytic acylation of sugar alcohols by 3-(4-hydroxyphenyl)propionic acid. *Process Biochem.* **2012**, *47* (12), 1894-1902. DOI:10.1016/j.procbio.2012.06.015.
- de Belder, A. N. Cyclic acetals of the aldoses and aldoses. *Adv. Carbohydr. Chem. Biochem.* **1965**, *20*, 219-302. DOI:10.1016/s0096-5332(08)60300-8.
- de Marco, B. A.; Rechelo, B. S.; Tótolí, E. G.; Kogawa, A. C.; Salgado, H. R. N. Evolution of green chemistry and its multidimensional impacts: A review. *Saudi Pharm J.* **2019**, *27* (1), 1-8. DOI:10.1016/j.jsps.2018.07.011.

- Degn, P.; Zimmermann, W. Optimization of carbohydrate fatty acid ester synthesis in organic media by a lipase from *Candida antarctica*. *Biotechnol. Bioeng.* **2001**, *74* (6), 483-491. DOI:10.1002/bit.1139.
- du Noüy, P. L. An Interfacial Tensiometer for Universal Use. *J. Gen. Physiol.* **1925**, *7* (5), 625-631. DOI:10.1085/jgp.7.5.625.
- Ducet, A.; Giroux, A.; Trani, M.; Lortie, R. Enzymatic preparation of biosurfactants from sugars or sugar alcohols and fatty acids in organic media under reduced pressure. *Biotechnol. Bioeng.* **1995**, *48* (3), 214-221. DOI:10.1002/bit.260480308.
- Eastoe, J.; Dalton J. S. Dynamic surface tension and adsorption mechanisms of surfactants at the air-water interface. *Adv. Colloid Interface Sci.* **2000**, *85* (2-3), 103-144. DOI:10.1016/s0001-8686(99)00017-2.
- Edward, J. T. Stability of glycosides to acid hydrolysis - A conformational analysis. *Chem. Ind.* **1955**, *36*, 1102-1104.
- El-Laithy, H. M.; Shoukry, O.; Mahran, L. G. Novel sugar esters proniosomes for transdermal delivery of vinpocetine: preclinical and clinical studies. *Eur J Pharm Biopharm.* **2011**, *77* (1), 43-55. DOI:10.1016/j.ejpb.2010.10.011.
- Enayati, M.; Gong, Y.; Goddard, J. M.; Abbaspourrad, A. Synthesis and characterization of lactose fatty acid ester biosurfactants using free and immobilized lipases in organic solvents. *Food Chem.* **2018**, *266*, 508-513. DOI:10.1016/j.foodchem.2018.06.051.
- EPA United States Environmental Protection Agency. <<https://www.epa.gov/greenchemistry/basics-green-chemistry>> (accessed February 2023).
- FAO Food and Agriculture Organization, Dairy Market Review: Overview of global dairy market developments in 2020, **2021**.
- FBI Fortune Business Insights, Surfactant Market Size, Share & COVID-19 Impact Analysis, By Type (Anionic, Nonionic, Cationic, and Amphoteric), By Application (Home Care, Personal Care, Textile, Food & Beverages, Industrial & Institutional Cleaning, Plastics, and Others), and Regional Forecast, 2021-2028. <<https://www.fortunebusinessinsights.com/surfactants-market-102385>> (accessed February 2023).
- Fregapane, G.; Sarney, D. B.; Vulfson, E. N. Facile chemo-enzymatic synthesis of monosaccharide fatty acid esters. *Biocatalysis* **1994**, *11* (1), 9-18. DOI:10.3109/10242429409034373.
- Gänzle, M.G.; Haase, G.; Jelen, P. Lactose: crystallization, hydrolysis and value-added derivatives. *Int. Dairy J.* **2008**, *18* (7), 685-694. DOI:10.1016/j.idairyj.2008.03.003.

- Ghosh, T.; Mukherji, A.; Srivastava, H. K.; Kancharla P. K. Secondary amine salt catalyzed controlled activation of 2-deoxy sugar lactols towards alpha-selective dehydrative glycosylation. *Org. Biomol. Chem.* **2018**, *16*, 2870-2875. DOI:10.1039/C8OB00423D.
- Goi, A.; Bruzzese, T.; Notarianni, A. F.; Riva, M.; Ronchini, A. Synthesis and pharmacological properties of 3-O-derivatives of 1,2,5,6-di-O-isopropylidene-alpha-D-glucofuranose. *Arzneimittelforschung* **1979**, *29* (7), 986-990. DOI:10.1002/chin.197944341.
- Gonçalves, M. C. P.; Romanelli, J. P.; Guimarães, J. R.; Vieira, A. C.; Pereira de Azevedo, B.; Tardioli, P. W. Reviewing research on the synthesis of CALB-catalyzed sugar esters incorporating systematic mapping principles. *Crit. Rev. Biotechnol.* **2021**, *41* (6), 865-878. DOI:10.1080/07388551.2021.1888071.
- Goulden, J. D. S. Light transmission by dilute emulsions. *Trans. Faraday Soc.* **1958**, *54*, 941-945. DOI:10.1039/TF9585400941.
- Guimarães, P. M. R.; Teixeira, J. A.; Domingues, L. Fermentation of lactose to bio-ethanol by yeasts as part of integrated solutions for the valorisation of cheese whey. *Biotechnol. Adv.* **2010**, *28* (3), 375-384. DOI:10.1016/j.biotechadv.2010.02.002.
- Gumel, A. M.; Annuar, M. S. M.; Heidelberg, T.; Chisti, Y. (2011): Lipase mediated synthesis of sugar fatty acid esters. *Process Biochem.* **2011**, *46* (11), 2079-2090. DOI:10.1016/j.procbio.2011.07.021.
- GVR Grand View Research, Surfactants Market Size, Share & Trends Report Surfactants Market Size, Share & Trends Analysis Report By Product, By Application, By Region (North America, Europe, Asia Pacific, RoW), And Segment Forecasts, 2016 - 2022. <<https://www.grandviewresearch.com/industry-analysis/surfactants-market>> (accessed February 2023).
- Harkins, W. D.; Jordan, H. F. A Method for the Determination of Surface and Interfacial Tension from the Maximum Pull on a Ring. *J. Am. Chem. Soc.* **1930**, *52* (5), 1751-1772. DOI:10.1021/ja01368a004.
- Hasan, F.; Shah, A. A.; Hameed, A. Industrial applications of microbial lipases. *Enzyme Microb. Technol.* **2006**, *39* (2), 235-251. DOI:10.1016/j.enzmictec.2005.10.016.
- Hering, K. W.; Karaveg, K.; Moremen, K. W.; Pearson, W. H. A Practical Synthesis of Kifunensine Analogues as Inhibitors of Endoplasmic Reticulum  $\alpha$ -Mannosidase I. *J. Org. Chem.* **2005**, *70* (24), 9892-904. DOI:10.1021/jo0516382.
- Hill, K.; Rhode, O. Sugar-based surfactants for consumer products and technical applications, *Lipid - Fett.* **1999**, *101* (1), 25-33. DOI:10.1002/(SICI)1521-4133(19991)101:1<25::AID-LIPI25>3.0.CO;2-N.

- Hill, K. Fats and oils as oleochemical raw materials. *Pure Appl. Chem.* **2000**, 72 (7), 1255–1264. DOI:10.1351/pac200072071255.
- Holmberg, K. Natural surfactants. *Curr. Opin. Colloid. Interface Sci.* **2001**, 6 (2), 148-159. DOI:10.1016/S1359-0294(01)00074-7.
- Ikeda, I. Klibanov, A. M. Lipase-catalyzed acylation of sugars solubilized in hydrophobic solvents by complexation. *Biotechnol. Bioeng.* **1993**, 42 (6), 788-791. DOI:10.1002/bit.260420616.
- ISO 15884:2002 - IDF 182:2002. Milk fat - Preparation of fatty acid methyl esters, IDF, Brussels, Belgium, 2002.
- Ivanković, A. Review of 12 Principles of Green Chemistry in Practice. *IJSGE* **2017**, 6 (3), 39-48. DOI:10.11648/j.ijrse.20170603.12.
- Jia, C.; Zhao, J.; Feng, B.; Zhang, X.; Xia, W. A simple approach for the selective enzymatic synthesis of dilauroyl maltose in organic media. *J. Mol. Catal., B Enzym.* **2010**, 62 (3), 265-269. DOI:10.1016/j.molcatb.2009.11.003.
- Juhl, P. B.; Doderer, K.; Hollmann, F.; Thum, O.; Pleiss, J. Engineering of *Candida antarctica* lipase B for hydrolysis of bulky carboxylic acid esters. *J. Biotechnol.* **2010**, 150 (4), 474-480. DOI:10.1016/j.jbiotec.2010.09.951.
- Kartha k. P. R. Iodine, a novel catalyst in carbohydrate reactions I. O-isopropylidination of carbohydrates. *Tetrahedron Lett.* **1986**, 27 (29), 3415-3416. DOI:10.1016/S0040-4039(00)84810-8.
- Kennedy, J. F.; Kumar, H.; Panesar, P. S.; Marwaha, S. S.; Goyal, R.; Parmar, A.; Kaur, S. Enzyme-catalyzed regioselective synthesis of sugar esters and related compounds. *J. Chem. Technol. Biotechnol.* **2006**, 81 (6), 866-876. DOI:10.1002/jctb.1473.
- Khaled, N.; Montet, D.; Pina, M.; Graille, J. Fructose oleate synthesis in a fixed catalyst bed reactor. *Biotechnol. Lett.* **1991**, 13, 167-172. DOI:10.1007/BF01025812.
- Khan, A. T.; Khan, Md. M. A simple and convenient synthetic protocol for O-isopropylidination of sugars using bromodimethylsulfonium bromide (BDMS) as a catalyst. *Carbohydr. Res.* **2010**, 345 (1), 154-159. DOI:10.1016/j.carres.2009.09.017.
- Khan, N. R.; Rathod, V. K. Enzyme catalyzed synthesis of cosmetic esters and its intensification: A review. *Process Biochem.* **2015**, 50 (11), 1793-1806. DOI:10.1016/j.procbio.2015.07.014.
- Kinanti, F. P. A.; Rahayu, D. U. C.; Gustianthy, A. P.; Krisnandi, Y. K. Optimization study of alkyl polyglycoside C12 synthesis using indirect method. *AIP Conference Proceedings* **2021**, 2349, 020018. DOI:10.1063/5.0051813.
- Kosikowski, F. V. Whey Utilization and Whey Products. *J. Dairy Sci.* **1979**, 62 (7), 1149-1160. DOI:10.3168/jds.S0022-0302(79)83389-5.



- Krishna, N. V.; Anuradha, S.; Ganesh, R.; Kumar, V. V.; Selvam, P. Sulfonic Acid Functionalized Ordered Mesoporous Silica and their Application as Highly Efficient and Selective Heterogeneous Catalysts in the Formation of 1,2-Monoacetone-D-glucose. *ChemCatChem* **2018**, *10* (24), 5610-5618. DOI:10.1002/cctc.201801462.
- Kumar, R.; Modak, J.; Madras, G. Effect of the chain length of the acid on the enzymatic synthesis of flavors in supercritical carbon dioxide. *Biochem. Eng. J.* **2005**, *23* (3), 199-202. DOI:10.1016/j.bej.2005.01.007.
- Kumar, A.; Dhar, K.; Kanwar, S. S.; Arora, P. K. Lipase catalysis in organic solvents: advantages and applications. *Biol. Proced. Online* **2016**, *18*, 2. DOI:10.1186/s12575-016-0033-2.
- Lal, B.; Gidwani, R. M.; Rupp, R. H. Aluminium Chloride as a Powerful Catalyst for the Preparation of *O*-Isopropylidene and *O*-Benzylidene Derivatives of Labdanes. *Synthesis* **1989**, *9*, 711-713. DOI:10.1055/s-1989-27370.
- Lemieux, R.U.; Chü P. Conformations and relative stabilities of acetylated sugars as determined by nuclear magnetic resonance spectroscopy and anomerization equilibria. *Abst. Pap. Am. Chem. Soc.* **1958**, *133*, 31N.
- Liang, M.-Y.; Banwell, M. G.; Wang, Y.; Lan, P. Effect of Variations in the Fatty Acid Residue of Lactose Monoesters on Their Emulsifying Properties and Biological Activities. *J. Agric. Food Chem.*, **2018**, *66* (47), 12594-12603. DOI:10.1021/acs.jafc.8b05794.
- Lin, C.-C.; Jan, M.-D.; Weng, S.-S.; Lina, C.-C.; Chen, C.-T. *O*-Isopropylideneation of carbohydrates catalyzed by vanadyl triflate. *Carbohydr. Res.* **2006**, *341* (11), 1948-1953. DOI:10.1016/j.carres.2006.04.001.
- Lin, C. S. K.; Koutinas, A. A.; Stamatelatos, K.; Mubofu, E. B.; Matharu, A. S.; Kopsahelis, N.; Pfaltzgraff, L. A.; Clark, J. H.; Papanikolaou, S.; Kwan, T. H.; Luque, R. Current and future trends in food waste valorization for the production of chemicals, materials and fuels: a global perspective. *Biofuels Bioprod. Bioref.* **2014**, *8* (5), 686-715. DOI:10.1002/bbb.1506.
- Linthorst, J. A. An overview: origins and development of green chemistry. *Found. Chem.* **2010**, *12*, 55-68. DOI:10.1007/s10698-009-9079-4.
- Liu, X.; Gong, L.; Xin, M.; Liu, J. The synthesis of sucrose ester and selection of its catalyst. *J. Mol. Catal. A Chem.* **1999**, *147* (1-2), 37-40. DOI:10.1016/S1381-1169(99)00125-9.
- Lotierzo, A.; Pifferia, V.; Ardizzone, S.; Pasqualin, P.; Cappelletti, G. Insight into the role of amines in Metal Working Fluids. *Corros. Sci.* **2016**, *110*, 192-199. DOI:10.1016/j.corsci.2016.04.028.
- Lotti, M.; Pleiss, J.; Valero, F.; Ferre, P. Effects of methanol on lipases: Molecular, kinetic and process issues in the production of biodiesel. *Biotechnol. J.* **2014**, *10* (1), 22-30. DOI:10.1002/biot.201400158.

- Lou X.; Ge, X.-T.; Zhao, J.; Cassidy, S. Regioselectivity of Esterification of Lactose with Fatty Acid via the Stannylene Acetal. *Method. Asian J. Chem.* **2011**, *23* (8), 3667-3669.
- Maindarkar, S. N.; Hoogland, H.; Henson, M. A. Predicting the combined effects of oil and surfactant concentrations on the drop size distributions of homogenized emulsions. *Colloids Surf. A Physicochem. Eng. Asp.* **2015**, *467*, 18-30. DOI:10.1016/j.colsurfa.2014.11.032.
- Marchant, R.; Banat, I. M. Biosurfactants: a sustainable replacement for chemical surfactants? *Biotechnol. Lett.* **2012**, *34* (9), 1597-1605. DOI: 10.1007/s10529-012-0956-x.
- Markets and Markets, Surfactants Markets by Type (Anionic, Non-ionic, Cationic, and Amphoteric), Application (Home Care, Personal Care, Industrial & Institutional Cleaning, Textile, Elastomers & Plastics, Agrochemicals, and Food & Beverage), Region – Global Forecast to 2025. <[https://www.marketsandmarkets.com/Market-Reports/biosurfactants-market-493.html?gclid=CjwKCAiAuOieBhAIEiwAgjCvcv5VtKqJW4P02hcHrq8lr\\_YiSuYBhJxEDPkGH1JJK6S4L19S3p-HFxoC4ncQAvD\\_BwE](https://www.marketsandmarkets.com/Market-Reports/biosurfactants-market-493.html?gclid=CjwKCAiAuOieBhAIEiwAgjCvcv5VtKqJW4P02hcHrq8lr_YiSuYBhJxEDPkGH1JJK6S4L19S3p-HFxoC4ncQAvD_BwE)> (accessed February 2023).
- McClements, D. J. Edible nanoemulsions: fabrication, properties, and functional performance. *Soft Matter* **2011**, *7* (6), 2297-2316. DOI:10.1039/C0SM00549E
- McClements, D. J.; Jafari, S. M. Improving emulsion formation, stability and performance using mixed emulsifiers: A review. *Adv. Colloid Interface Sci.* **2018**, *251*, 55-79. DOI:10.1016/j.cis.2017.12.001.
- Montgomery, D.C. Design and Analysis of experiments, John Wiley & Sons, Inc., New York, 2004.
- Mowery, D. F. Chromatographic Adsorption. IV. Cation Exchange Resins as Catalysts in Glycoside Formation. *J. Am. Chem. Soc.* **1955**, *77* (6), 1667-1669. DOI:10.1021/ja01611a075.
- MPOC Malaysian Palm Oil Council, < <https://mpoc.org.my/palm-oil-fact/>> (accessed February 2023).
- Mungray, A. K.; Kumar, P. Fate of linear alkylbenzene sulfonates in the environment: A review. *Int. Biodeterior. Biodegradation* **2009**, *63* (8), 981-987. DOI:10.1016/j.ibiod.2009.03.012.
- Nair, P. R. M.; Shah, P. M.; Sreenivasan, B. A Study on the Condensation of Sorbose with Acetone: Catalysis by Macroporous Ion Exchange. *Starch - Stärke*, **1981**, *33* (11), 384-387. DOI:10.1002/star.19810331107.
- Neta, N. S.; Teixeira, J. A.; Rodrigues, L. R. Sugar ester surfactants: enzymatic synthesis and applications in food industry. *Crit. Rev. Food Sci. Nutr.* **2015**, *55* (5), 595-610. DOI:10.1080/10408398.2012.667461.
- Novozymes, Lactose reduction in milk with Novozymes Saphera® 2600 L & 900 L S, Dairy Application Sheet, **2023**.
- Opawale, F. O.; Burgess, D. J. Influence of interfacial properties of lipophilic surfactants on water-in-oil emulsion stability. *J. Colloid Interface Sci.* **1998**, *197*, 142-150. DOI:10.1006/jcis.1997.5222.

- Orsavova, J.; Misurcova, L.; Ambrozova, J.; Vicha, R.; Mlcek, J. Fatty acids composition of vegetable oils and its contribution to dietary energy intake and dependence of cardiovascular mortality on dietary intake of fatty acids. *Int. J. Mol. Sci.* **2015**, *16*, 12871-12890. DOI:10.3390/ijms160612871.
- Pappalardo, V. M.; Boeriu, C. G.; Zaccheria, F.; Ravasio N. Synthesis and characterization of arabinose-palmitic acid esters by enzymatic esterification. *Mol. Catal.* **2017**, *433*, 383-390. DOI:10.1016/j.mcat.2017.02.029.
- Penkov, N. V. Relationships between Molecular Structure of Carbohydrates and Their Dynamic Hydration Shells Revealed by Terahertz Time-Domain Spectroscopy. *Int. J. Mol. Sci.* **2021**, *22* (21), 11969. DOI:10.3390/ijms222111969.
- Pérez, B.; Anankanbil, S.; Guo, Z. Synthesis of Sugar Fatty Acid Esters and their Industrial Utilizations. In *Fatty Acids: Chemistry, Synthesis, and Applications*. M Ahmad Ed.; Academic Press, 2017, pp. 329-354. DOI:10.1016/B978-0-12-809521-8.00010-6.
- Pires, A. F.; Marnotes, N. G.; Rubio, O. D.; Garcia, A. C.; Pereira, C. D. Dairy By-Products: A Review on the Valorization of Whey and Second Cheese Whey. *Foods*, **2021**, *10* (5), 1067. DOI:10.3390/foods10051067.
- Prado, A. G. S. Green chemistry, the chemical challenges of the new millennium. *Química Nova*, **2003**, *26* (5), 738-744. DOI:10.1590/S0100-40422003000500018.
- Prat, D., Hayler, J., Wells, A., A Survey of Solvent Selection Guides. *Green Chem.* **2014**, *16* (10), 4546-4551. DOI:10.1039/C4GC01149J.
- Prazeres, A. R.; Carvalho, F.; Rivas, J. Cheese whey management: a review. *J. Environ. Manag.* **2012**, *110*, 48-68. DOI:10.1016/j.jenvman.2012.05.018.
- Rabail, R.; Shabbir, M.A.; Sahar, A.; Miecznikowski, A.; Kieliszek, M.; Aadil, R. M. An intricate review on nutritional and analytical profiling of coconut, flaxseed, olive, and sunflower oil blends. *Molecules* **2021**, *26*, 7187. DOI:10.3390/molecules26237187.
- Reichardt, C. Solvents and Solvent Effects: An Introduction. *Org. Process Res. Dev.* **2007**, *11* (1), 105-113. DOI:10.1021/op0680082.
- Reis, P.; Holmberg, K.; Watzke, H.; Leser, M. E.; Miller, R. Lipases at interfaces: a review. *Adv. Colloid Interface Sci.* **2009**, *147-148*, 237-250. DOI:10.1016/j.cis.2008.06.001.
- Ren, K.; Lamsal, B. P. Synthesis of some glucose-fatty acid esters by lipase from *Candida antarctica* and their emulsion functions. *Food Chem.* **2017**, *214*, 556-563. DOI:10.1016/j.foodchem.2016.07.031.

- Riva, S.; Chopineau, J.; Kieboom, A. P. G.; Klibanov, A. M. Protease-Catalyzed Regioselective Esterification of Sugars and Related Compounds in Anhydrous Dimethylformamide. *J. Am. Chem. Soc.* **1988**, *110* (2), 584-589. DOI:10.1021/ja00210a045.
- Rokade, S. M.; Bhate, P. M. Practical preparation of mono- and di-O-isopropylidene derivatives of monosaccharides and methyl 4,6-O-benzylidene glycosides from free sugars in a deep eutectic solvent. *J. Carbohydr. Chem.* **2017**, *36* (1), 20-30. DOI:10.1080/07328303.2017.1347262.
- Šabeder, S.; Habulin, M.; Knez, Ž. Lipase-catalyzed synthesis of fatty acid fructose esters. *J. Food Eng.* **2006**, *77* (4), 880-886. DOI:10.1016/j.jfoodeng.2005.08.016.
- Sangiorgio, S.; Pargoletti, E.; Rabuffetti, M.; Robescu, M.S.; Semproli, R.; Ubiali, D.; Cappelletti, G.; Speranza, G. Emulsifying properties of sugar-based surfactants prepared by chemoenzymatic synthesis. *Colloid Interface Sci. Commun.* **2022**, *48*, 100630. DOI:10.1016/j.colcom.2022.100630.
- Sarkar, R.; Pal, A.; Rakshit, A.; Saha B. Properties and applications of amphoteric surfactant: A concise review. *J. Surfactants Deterg.* **2021**, *24* (5), 709-730. DOI:10.1002/jsde.12542.
- Sarmah, N.; Revathi, D.; Sheelu, G.; Yamuna Rani, K.; Sridhar, S.; Mehtab, V.; Sumana, C. Recent advances on sources and industrial applications of lipases, *Biotechnol. Prog.* **2018**, *34*, 5-28. DOI:10.1002/btpr.2581.
- Sarney, D.; Vulfson, E. Application of enzymes to the synthesis of surfactants. *Trends Biotechnol.* **1995**, *13* (5), 164-172. DOI:10.1016/S0167-7799(00)88933-7.
- Schramm, L. L. *Emulsions, Foams, and Suspensions: Fundamentals and Applications*. Wiley-VCH Verlag GmbH & Co. KGaA, Weinheim, Germany, 2005. DOI:10.1002/3527606750.
- Secundo, F.; Carrea, G.; Tarabiono, C.; Gatti-Lafranconi, P.; Brocca, S.; Lotti, M. Karl-Erich Jaeger, K.-E.; Puls, M.; Eggert, T. The lid is a structural and functional determinant of lipase activity and selectivity. *J. Mol. Catal., B Enzym.* **2006**, *39* (1-4), 166-170. DOI:10.1016/j.molcatb.2006.01.018.
- Semproli, R.; Robescu, M.S.; Sangiorgio, S.; Pargoletti, E.; Bavaro, T.; Rabuffetti, M.; Cappelletti, G.; Speranza, G.; Ubiali, D. From Lactose to Alkyl Galactoside Fatty Acid Esters as Non-Ionic Biosurfactants: A Two-Step Enzymatic Approach to Cheese Whey Valorization. *ChemPlusChem* **2023**, *88* (1), e202200331. DOI:10.1002/cplu.202200331.
- Sen, R.; Swaminathan, T. Application of response-surface methodology to evaluate the optimum environmental conditions for the enhanced production of surfactin. *Appl. Microbiol. Biotechnol.* **1997**, *47* (4), 358-363. DOI:10.1007/s002530050940.
- Sheldon, R. A. Utilisation of biomass for sustainable fuels and chemicals: Molecules, methods and metrics. *Catalysis Today* **2011**, *167* (1), 3-13. DOI:10.1016/j.cattod.2010.10.100.

Sheldon, R. A. Green chemistry and resource efficiency: towards a green economy. *Green Chem.* **2016**, *18*, 3180-3183. DOI:10.1039/C6GC90040B.

Shintani, T. Food Industrial Production of Monosaccharides Using Microbial, Enzymatic, and Chemical Methods. *Fermentation* **2019**, *5* (2), 47. DOI:10.3390/fermentation5020047.

Silva, S.; Sánchez-Fernández, E. M.; Mellet, C. O.; Tatibouët, A.; Rauter, A. P.; Rollin, P. *N*-Thiocarbonyl Iminosugars: Synthesis and Evaluation of Castanospermine Analogues Bearing Oxazole-2(3H)-thione Moieties. *EurJOC* **2013**, *2013* (35), 7941-7951. <https://doi.org/10.1002/ejoc.201300720>

Silva, K. C. G.; Sato, A. C. K. Sonication technique to produce emulsions: the impact of ultrasonic power and gelatin concentration. *Ultrason. Sonochem.* **2019**, *52*, 286-293. DOI:10.1016/j.ultsonch.2018.12.001.

Singh, P. P.; Gharia, M. M.; Dasgupta F.; Srivastava H. C. Use of Ferric Chloride in Carbohydrate Chemistry. I. A Quick Method for the Preparation of *O*-Isopropylidene Derivatives of Carbohydrates. *Tetrahedron Lett.* **1977**, *18* (5), 439-440. DOI:10.1016/S0040-4039(01)92659-0.

Siso, M. I. G. The biotechnological utilization of cheese whey: a review. *Bioresour. Technol.* **1996**, *57* (1), 1-11. DOI:10.1016/0960-8524(96)00036-3.

Somasundaran, P.; Huang, L. Adsorption/aggregation of surfactants and their mixtures at solid-liquid interfaces. *Adv. Colloid Interface Sci.* **2000**, *88* (1-2), 179-208. DOI:10.1016/s0001-8686(00)00044-0.

Song, M. G.; Jho, S. H.; Kim, J. Y.; Kim, J. D. Rapid Evaluation of Water-in-Oil (w/o) Emulsion Stability by Turbidity Ratio Measurements. *J. Colloid Interface Sci.* **2000**, *230* (1), 213-215. DOI:10.1006/jcis.2000.7090.

Soultani, S.; Ognier, S.; Engasser, J.-M.; Ghoul, M. Comparative study of some surface active properties of fructose esters and commercial sucrose esters. *Colloids Surf. A Physicochem. Eng. Asp.* **2003**, *227*, (1-3), 35-44. DOI:10.1016/S0927-7757(03)00360-1.

Statista, Annual cheese production worldwide from 2015 to 2022. <<https://www.statista.com/statistics/1120911/cheese-production-worldwide/>> (accessed February 2023).

Staroń, J.; Dąbrowski, J. M.; Cichoń, E.; Guzik, M. Lactose esters: synthesis and biotechnological applications. *Crit. Rev. Biotechnol.* **2018**, *38* (2), 245-258. DOI:10.1080/07388551.2017.1332571.

Staucha, B.; Fisherc, S. J.; Cianci, M. Open and closed states of *Candida antarctica* Lipase B: protonation and the mechanism of interfacial activation. *J. Lipid Res.* **2015**, *56* (12), 2348-2358. DOI:10.1194/jlr.M063388.

- Straathof, A. J. J.; Romein, J.; van Rantwijk, F.; Kieboom, A. P. G.; van Bekkum, H. Preparation of long-chain alkyl D-glucosides by alcoholysis of 1,2:5,6-di-O-Isopropylidene- $\alpha$ -D-Glucopyranose, *Starch - Stärke* **1987**, 39, 362-368. DOI:10.1002/star.19870391007.
- Stubenrauch, C. Sugar surfactants - aggregation, interfacial, and adsorption phenomena. *Curr. Opin. Colloid. Interface Sci.* **2001**, 6 (2), 160-170. DOI:10.1016/S1359-0294(01)00080-2.
- Taddeo, F.; Vitiello, R.; Tesser, R.; Melchiorre, M.; Eränen, K.; Salmi, T.; Russo, V.; Di Serio, M. Nonanoic acid esterification with 2-ethylhexanol: From batch to continuous operation. *Chem. Eng. J.* **2022**, 444, 136572. DOI:10.1016/j.cej.2022.136572.
- Tambe, K.; Bonde, S. A review on: application of pharmaceutical quality by design in product development. *World J. Pharm. Sci.* **2017**, 5 (1), 58-70.
- Tobiszewski, M.; Mechlińska, A.; Zygmunt, B.; Namieśnik J. Green analytical chemistry in sample preparation for determination of trace organic pollutants. *Trends Anal. Chem.* **2009**, 28 (8), 943-951. DOI:10.1016/j.trac.2009.06.001.
- Tokiwa, Y.; Raku, T.; Kitagawa, M.; Kurane, R. Preparation of polymeric biosurfactant containing sugar and fatty acid esters. *Clean Products and Processes* **2000**, 2, 108-111. DOI:10.1007/s100980000062.
- Traverso-Soto, J. M.; Lara-Martín, P. A.; León, V. M.; González-Mazo, E. Analysis of alcohol polyethoxylates and polyethylene glycols in marine sediments. *Talanta*, **2013**, 110: 171-179. DOI:10.1016/j.talanta.2013.02.027.
- Tundo, P.; Anastas, P.; Black, D. StC.; Breen, J.; Collins, T. J.; Memoli, S.; Miyamoto, J.; Polyakoff, M.; Tumas, W. Synthetic pathways and processes in green chemistry. Introductory overview. *Pure Appl. Chem.* **2000**, 72 (7), 1207-1228. DOI:10.1351/pac200072071207.
- Uppenberg, J.; Oehrner, N.; Norin, M.; Hult, K.; Kleywegt, G. J.; Patkar, S.; Waagen, V.; Anthonsen, T.; Jones, T. A. Crystallographic and molecular-modeling studies of lipase B from *Candida antarctica* reveal a stereospecificity pocket for secondary alcohols. *Biochemistry* **1995**, 34 (51), 16838-16851. DOI:10.1021/bi00051a035.
- van Oss, C. J. Development and applications of the interfacial tension between water and organic or biological surfaces. *Colloids Surf. B Biointerfaces.* **2007**, 54 (1), 2-9. DOI:10.1016/j.colsurfb.2006.05.024.
- Vera, C.; Guerrero, C.; Illanes, A. Trends in lactose-derived bioactives: synthesis and purification. *Syst. Microbiol. Biomanuf.* **2022**, 2 (3), 393-412. DOI:10.1007/s43393-021-00068-2.
- Verboni, M.; Lucarini, S.; Duranti, A. 6'-O-Lactose Ester Surfactants as an Innovative Opportunity in the Pharmaceutical Field: From Synthetic Methods to Biological Applications. *Pharmaceuticals*, **2021**, 14 (12), 1306. DOI:10.3390/ph14121306.

- Wafii, N. S. A.; Yunus, R.; Lau, H. L. N.; Yaw, T. C. S.; Aziz, S. A. Immobilized lipase-catalyzed transesterification for synthesis of biolubricant from palm oil methyl ester and trimethylolpropane. *Bioprocess Biosyst. Eng.* **2021**, *44* (11), 2429-2444. DOI:10.1007/s00449-021-02615-6.
- Walsh, M. K.; Bombyk, R. A.; Wagh, A.; Bingham, A.; Berreau, L. M. Synthesis of lactose monolaurate as influenced by various lipases and solvents. *J. Mol. Catal., B Enzym.* **2009**, *60* (3-4), 171-177. DOI:10.1016/j.molcatb.2009.05.003.
- Wang, T.; Demchenko, A. V. Synthesis of carbohydrate building blocks via regioselective uniform protection/deprotection strategies. *Org. Biomol. Chem.* **2019**, *17*, 4934-4950. DOI:10.1039/C9OB00573K.
- Whistler, R. L.; Wolfrom, M. L. *Methods in carbohydrate chemistry. Volume 2: Reactions of carbohydrates*, Academic Press, New York, 1963.
- Xiang, W.; Tardy, B.; Bai, L.; Stubenrauch, C.; Rojas, O. J. Chapter 12 - Measuring the Interfacial Behavior of Sugar-Based Surfactants to Link Molecular Structure and Uses. In *Biobased Surfactants*; 2<sup>nd</sup> ed.; Hayes, D. G.; Solaiman, D. K. J.; Ashby, R. D.; AOCS Press, 2019, pp 387-412. DOI:10.1016/B978-0-12-812705-6.00012-5.
- Yan, Y.; Bornscheuera, U. T.; Caob, L.; Schmid R. D. Lipase-catalyzed solid-phase synthesis of sugar fatty acid esters: Removal of byproducts by azeotropic distillation. *Enzyme Microb. Technol.* **1999**, *25* (8-9), 725-728. DOI:10.1016/S0141-0229(99)00106-4.
- Yan, Y.; Bornscheuer, U. T.; Stadler, G.; Lutz-Wahl, S.; Reuss, M.; Schmid, R. D. Production of sugar fatty acid esters by enzymatic esterification in a stirred-tank membrane reactor: Optimization of parameters by response surface methodology. *J. Amer. Oil Chem. Soc.* **2001**, *78* (2), 147-153. DOI:10.1007/s11746-001-0235-x.
- Yan, S. J.; Kim, M. H.; Kim, T. B.; Lee, Y. M.; Kim, S. B.; Park, S. W. Method of manufacturing d-galactose for use of the production of d-tagatose from whey permeate or oried whey permeate. US 2016/0152652A1, **2016**.
- Yang, S. T.; Silva, E. M. Novel products and new technologies for use of a familiar carbohydrate, milk lactose. *J. Dairy Sci.* **1995**, *78* (11), 2541-2562. DOI:10.3168/jds.S0022-0302(95)76884-9.
- Zaidan, U. H.; Abdul Rahman, M. B.; Othman, S. S.; Basri, M.; Abdulmalek, E.; Raja, N. Z. R. A. R.; Salleh, A. B. Biocatalytic production of lactose ester catalysed by mica-based immobilised lipase. *Food Chem.* **2012**, *131* (1), 199-205. DOI:10.1016/j.foodchem.2011.08.060.
- Zall, R. R. Trends in whey fractionation and utilization, a global perspective. *J. Dairy Sci.* **1984**, *67* (11), 2621-2629. DOI:10.3168/jds.S0022-0302(84)81623-9.

Zhang, X.; Song, F.; Taxipalati, M.; Wei, W.; Feng, F. Comparative Study of Surface-Active Properties and Antimicrobial Activities of Disaccharide Monoesters. *PLoS ONE* **2014**, *9* (12), e114845. DOI:10.1371/journal.pone.0114845.

Zhao, D.; Wan, Y. Chapter 8 - The Synthesis of Mesoporous Molecular Sieves. In *Studies in Surface Science and Catalysis*; Čejka, J.; van Bekkum, H.; Corma, A.; Schüth, F. Ed.; Elsevier, Volume 168, 2007, pp 241-300, I-III. DOI:10.1016/S0167-2991(07)80796-8.



# A | Appendix A

## A.1 Biocatalytic methods for the hydrolysed vegetable proteins from renewable resources

The rising concern amongst consumers about the potential side effects of many substances used in commodities, as well as the growing demand for natural and “healthy” products have induced manufacturers to increase both the use of natural ingredients in their formulations and of green and sustainable technologies for their production.

Hydrolysed vegetable proteins (HVPs) containing bioactive peptides represent the perfect answer to this market trend because they can be used as natural ingredients for nutraceutical applications, *i.e.*, health-promoting functional foods, dietary supplements and pharmaceutical products.

Bioactive peptides present in HVPs are in general short or medium sequences of amino acids that are inactive within the parent protein, which can display interesting biological functions once they are released after protein hydrolysis. These peptides hidden in the protein structure are frequently called cryptides. To date, several peptides and hydrolysates with a biological function, *i.e.*, angiotensin-converting enzyme (ACE) inhibition, mineral binding, antidiabetic, satiating, immunomodulating, opioid, antioxidant, antimicrobial activities, have been reported.

Enzymatic methods based on proteases are the most common way to produce bioactive peptides. The use of enzymes is preferred to other processes since reproducible molecular weight profiles and peptide composition are usually obtained.

Upgrading of agro-food residues by enzyme-mediated processes to obtain high-added value products is a clear example of “circular economy” where waste or by-products are managed sustainably by turning them into a resource, thus contributing to the development of new production pipelines and patterns.

However, several challenges must be faces to produce bioactive peptides, *i.e.*, the selection of inexpensive protein sources to be used as raw materials, the development of efficient bioprocesses for peptide production, the identification and

isolation of sequences, the elucidation of the mechanisms of action involved in their bioactivities.

The valorization of the residue derived from soybean seed oil production, namely soybean meal, which nowadays is only used as farm animal feed, represents the final goal of the research. This soybean by-product shows a high protein content, thus it can represent a valuable feedstock for the enzyme-aided production of HVPs and cryptides, fulfilling the “circular economy” requirements.

Within this study, enzymatic hydrolysis of a soy protein isolate by food-grade proteases was carried out. Enrichment of peptides contained in HVP mixtures was achieved by using membrane ultrafiltration procedures (in the range 10 to 1 kDa). The resulting HVP fractions were investigated for their ACE-inhibitory activity and the most active one was purified by semi-preparative RP-HPLC. Four putative sequences were identified by NMR analysis and Edman degradation as possible responsible for the bioactivity. Such peptides were prepared by solid-phase synthesis and submitted to ACE inhibition assays which led to the identification of a novel ACE-inhibitory peptide (NDRP) stable towards *in vitro* simulated gastrointestinal digestion, which acts as a non-competitive inhibitor of ACE.

This research was funded by Cariplo Foundation and Innovhub-SSI (Italy) “Integrated research on industrial bio-technologies and bioeconomy-joint Call 2017”, project BIOCOSM, ID 2017-0978). It was also funded by APC Central Fund - Università degli Studi di Milano and recently published on the MDPI open access journal *Foods* (*Foods* Editorial Office - MDPI, St. Alban-Anlage 66, 4052 Basel, Switzerland).



Article

# Preparation, Characterization and In Vitro Stability of a Novel ACE-Inhibitory Peptide from Soybean Protein

Sara Sangiorgio<sup>1</sup>, Nikolina Vidović<sup>1</sup>, Giovanna Boschin<sup>2</sup>, Gilda Aiello<sup>2,3</sup>, Patrizia Arcidiaco<sup>4</sup>, Anna Arnoldi<sup>2</sup>, Carlo F. Morelli<sup>1</sup>, Marco Rabuffetti<sup>1</sup>, Teresa Recca<sup>4</sup>, Letizia Scarabattoli<sup>1</sup>, Daniela Ubiali<sup>5</sup> and Giovanna Speranza<sup>1,\*</sup>

<sup>1</sup> Department of Chemistry, University of Milan, Golgi 19, 20133 Milan, Italy

<sup>2</sup> Department of Pharmaceutical Sciences, University of Milan, L. Mangiagalli 25, 20133 Milan, Italy

<sup>3</sup> Department of Human Science and Quality of Life Promotion, Telematic University San Raffaele, 00166 Rome, Italy

<sup>4</sup> Centro Grandi Strumenti, University of Pavia, Bassi 21, 27100 Pavia, Italy

<sup>5</sup> Department of Drug Sciences, University of Pavia, Viale Taramelli 12, 27100 Pavia, Italy

\* Correspondence: giovanna.speranza@unimi.it; Tel.: +(39)-02503-14097

**Abstract:** A soy protein isolate was hydrolyzed with Alcalase<sup>®</sup>, Flavourzyme<sup>®</sup> and their combination, and the resulting hydrolysates (A, F and A + F) were ultrafiltered and analyzed through SDS-PAGE. Fractions with MW < 1 kDa were investigated for their ACE-inhibitory activity, and the most active one (A < 1 kDa) was purified by semi-preparative RP-HPLC, affording three further subfractions. NMR analysis and Edman degradation of the most active subfraction (A1) enabled the identification of four putative sequences (ALKPDNR, VVPD, NDRP and NDTP), which were prepared by solid-phase synthesis. The comparison of their ACE-inhibitory activities suggested that the novel peptide NDRP might be the main agent responsible for A1 fraction ACE inhibition (ACE inhibition = 87.75 ± 0.61%; IC<sub>50</sub> = 148.28 ± 9.83 µg mL<sup>-1</sup>). NDRP acts as a non-competitive inhibitor and is stable towards gastrointestinal simulated digestion. The Multiple Reaction Monitoring (MRM) analysis confirmed the presence of NDRP in A < 1 kDa.

**Keywords:** soybean protein hydrolysate; ACE inhibitor; peptide synthesis; Lineweaver–Burk plot; simulated gastrointestinal digestion; functional food



**Citation:** Sangiorgio, S.; Vidović, N.; Boschin, G.; Aiello, G.; Arcidiaco, P.; Arnoldi, A.; Morelli, C.F.; Rabuffetti, M.; Recca, T.; Scarabattoli, L.; et al. Preparation, Characterization and In Vitro Stability of a Novel ACE-Inhibitory Peptide from Soybean Protein. *Foods* **2022**, *11*, 2667. <https://doi.org/10.3390/foods11172667>

Academic Editor: Bo Li

Received: 21 July 2022

Accepted: 29 August 2022

Published: 1 September 2022

**Publisher's Note:** MDPI stays neutral with regard to jurisdictional claims in published maps and institutional affiliations.



**Copyright:** © 2022 by the authors. Licensee MDPI, Basel, Switzerland. This article is an open access article distributed under the terms and conditions of the Creative Commons Attribution (CC BY) license (<https://creativecommons.org/licenses/by/4.0/>).

## 1. Introduction

Bioactive peptides, i.e., peptides that exert some health benefits beyond their nutritional value, may be already present in foods as natural components, but more frequently are in a latent state within the sequence of the parent protein, from which they can be released during digestion or food processing. These peptides encrypted in the protein sequence are referred to as cryptides [1]. In this regard, the nutritional and functional value of a protein depends on its amino acid content, but also on the presence of cryptides in its sequence.

Enzymatic hydrolysis based on the use of proteases is the most common procedure used to produce bioactive food peptides [2]. The use of proteolytic enzymes is preferred to chemical hydrolysis because reproducible molecular weight profiles and peptide composition are usually obtained. Moreover, enzymatic methods are safer and milder than the chemical ones [3]. To date, numerous food protein hydrolysates endowed with a biological function, such as angiotensin I-converting enzyme (ACE) inhibition and mineral binding, as well as antidiabetic, satiating, immunomodulating, antioxidant or antimicrobial activities, have been reported [4] and several cryptides responsible for these activities have been identified. Blood pressure reduction activity is one of the most frequently observed health benefits in food protein cryptides [3,5].

Hypertension, which is a major cause of premature death worldwide, is a condition in which the blood vessels have persistently elevated pressure [6]. Angiotensin I-converting enzyme (ACE, EC 3.4.15.1) is a zinc-dependent carboxypeptidase that strongly influences the regulation of blood pressure by playing a double physiological role: it catalyzes the conversion of the decapeptide angiotensin I into the octapeptide angiotensin II, a potent vasopressor, and it promotes the inactivation of the vasodilator bradykinin [7]. ACE inhibitors, e.g., lisinopril, benazepril, enalapril and captopril, are the gold standard for treating hypertension [8]. However, the prolonged use of ACE inhibitor drugs is associated with negative side effects, such as dry cough, skin rashes, taste alterations, headache, fatigue, nausea and even hyperkalemia [4]. Therefore, food-derived protein hydrolysates with ACE-inhibitory activity have attracted a growing interest as potential ingredients in functional foods [9] to complement antihypertensive drugs, with the advantage of having fewer adverse effects [10]. ACE-inhibitory activity of protein hydrolysates can be influenced by several factors, such as protein source, hydrolysis conditions, degree of hydrolysis, molecular weights of generated peptides and their amino acid sequences [11].

Soybeans are one of the world's most abundant sources of plant protein, with a rich and balanced amino acid profile. Moreover, it is well-recognized that soybean proteins are an important source of bioactive peptides (cryptides) [5] and that soy protein hydrolysates (SPH) represent an alternative to native proteins due to their superior functional properties [12]; in particular, increased solubility and nutritional characteristics. Specifically, SPH are reported to be suitable as food substitutes for the preparation of hospital diets, geriatric products, high-energy supplements and hypoallergenic infant formulas [3,12]. Soybean bioactive peptides are frequently endowed with antihypertensive activity [5], and although several ACE-inhibitory peptides with different chain lengths and amino acid compositions (e.g., NWGPLV, DLP, LSW, DG, GY, SY, etc.) have been identified in soybean protein hydrolysates, their mechanisms of action remain unclear [13,14]. Thus, further investigations are necessary, both to validate the antihypertensive potential of soybean hydrolysates and cryptides [15], and to overcome the challenges related to their production and purification processes in good yield [14,16].

The aim of this work is the development of an enzymatic process to achieve bioactive soybean hydrolysates as promising natural ingredients for nutraceutical applications. The use of the commercially available food-grade proteases Alcalase<sup>®</sup> and Flavourzyme<sup>®</sup> and their combination led to the preparation of soybean hydrolysates with a high degree of hydrolysis, good ACE-inhibitory activity and techno-functional properties suitable for scale-up. A novel ACE-inhibitory cryptide was identified, and its mechanism of action and stability in simulated gastrointestinal digestion were evaluated.

## 2. Materials and Methods

### 2.1. Materials

All solvents and reagents were purchased from Merck Life Science (Milano, Italy) and Fluorochem (Milano, Italy) and were used without further purification. Soy protein isolate (SPI) type 90 was kindly provided by ABS FOOD s.r.l. (Peraga di Vigonza, Italy). The chemical composition was  $\geq 90.0\%$  proteins,  $\leq 7.0\%$  moisture,  $\leq 1.0\%$  fat,  $\leq 6.0\%$  ash, and 1% total fiber (dry matter basis as reported by the producer). Proteolytic enzymes were kindly supplied by Novozymes<sup>®</sup> (Bagsværd, Denmark): the endopeptidase Alcalase<sup>®</sup> 2.4 L FG (enzyme activity:  $2.4 \text{ AU g}^{-1}$ ) derived from *Bacillus licheniformis* and the mixture of endopeptidase and exopeptidase Flavourzyme<sup>®</sup> (enzyme activity:  $1000 \text{ LAPU g}^{-1}$ ) derived from *Aspergillus oryzae*.

### 2.2. Hydrolysis of Soy Protein Isolate (SPI)

Soy protein isolate (SPI) was suspended in distilled H<sub>2</sub>O (10% w<sub>SPI</sub>/v<sub>H<sub>2</sub>O</sub>) and the resulting mixture was heated to 50 °C, then treated with proteolytic enzyme(s) under mechanical stirring. Reaction conditions were set up according to the optimal pH and temperature for each enzyme [17,18]. In the case of one-enzyme hydrolysis, Alcalase<sup>®</sup> was

added (1% w/w<sub>SPI</sub>) after adjusting pH to ca. 8.5 with 0.1 M NaOH, whereas Flavourzyme<sup>®</sup> was added (2% w/w<sub>SPI</sub>) after adjusting pH to ca. 6.5 with 0.1 M HCl, and the resulting mixtures were incubated for 24 h. In the two-enzyme experiment, proteins were initially hydrolyzed by Alcalase<sup>®</sup> (1% w/w<sub>SPI</sub>) at pH ca. 8.5 for 2 h. The pH was then adjusted to ca. 6.5 and the mixture was further hydrolyzed by Flavourzyme<sup>®</sup> (2% w/w<sub>SPI</sub>) for 22 h. The enzymes were inactivated by heat treatment at 85 °C for 15 min. Reaction mixtures were then centrifuged at 9000 rpm for 15 min, and supernatants (soy proteins hydrolysates, SPH) were collected, freeze-dried and stored at −20 °C. SPH yields for each enzymatic treatment (A, F, A + F) are reported in Table 1.

**Table 1.** Percentages of soy protein hydrolysates (SPH) after hydrolysis with Alcalase<sup>®</sup>, Flavourzyme<sup>®</sup> and Alcalase<sup>®</sup> + Flavourzyme<sup>®</sup> (A, F and A + F, respectively) and degree of hydrolysis (DH).

Enzymatic Protocol	SPH (%)	DH (%) *
A	43	17 ± 5.3 <sup>a</sup>
F	64	34 ± 5.5 <sup>b</sup>
A + F	77	36 ± 5.6 <sup>b</sup>

\* Values are reported as mean ± error% of three independent replicates. Different superscript lowercase letters represent values with a discrepancy greater than the calculated error.

### 2.3. Protein and Hydrolysate Profiles

#### 2.3.1. Degree of Hydrolysis (DH)

The degree of hydrolysis (DH) of the obtained SPH (A, F, A + F) was determined using the trinitrobenzenesulfonic acid (TNBS) method [19,20]. Each assay was performed in triplicate. L-Leucine (0–2 mM) was used to generate a standard curve. DH values were calculated using the following equation [21]:

$$\text{DH (\%)} = 100 \left( \frac{\text{AN}_2 - \text{AN}_1}{\text{N}_{\text{pb}}} \right)$$

where AN<sub>1</sub> is the amino nitrogen content of the protein substrate before hydrolysis (SPI, mg g<sup>−1</sup><sub>protein</sub>), AN<sub>2</sub> the amino nitrogen content of the protein substrate after hydrolysis (SPH, mg g<sup>−1</sup><sub>protein</sub>), and N<sub>pb</sub> the nitrogen content of the peptide bonds in the protein substrate (mg g<sup>−1</sup><sub>protein</sub>). The nitrogen contents of both SPI and SPH were determined by elemental analysis using the value of 6.25 as protein conversion factor. A N<sub>pb</sub> value of 88.01 mg g<sup>−1</sup><sub>protein</sub> was used for SPI. This value was obtained by assuming that all the nitrogen content in the starting material was related to proteins, and by multiplying the molecular mass of nitrogen by the moles sum of each amino acid present in the SPI, as reported in the amino acid profile provided by the supplier. Resulting DH% values are listed in Table 1.

#### 2.3.2. SDS-PAGE Analysis

The molecular weight distribution of SPI and of the three SPH (A, F, A + F) was determined by SDS PAGE analysis (Figure 1), using the NuPAGE<sup>®</sup> Electrophoresis System (Invitrogen, Thermo Fisher, Milano, Italy) with a 12% pre-cast NuPAGE<sup>®</sup> Novex<sup>®</sup> Bis-Tris Gel. Prior to analysis, 65 µL of each sample (SPI concentration: 1 mg mL<sup>−1</sup>; SPH concentration: 10 mg mL<sup>−1</sup>) was mixed with 25 µL of NuPAGE<sup>®</sup> LDS Sample Buffer (4×) and 10 µL of NuPAGE<sup>®</sup> Reducing Agent (10×). Samples were heated at 70 °C for 10 min for denaturing proteins. Then, 10 µL of each sample were loaded in each well, and Thermo Scientific<sup>™</sup> PageRuler<sup>™</sup> Prestained Protein Ladder (M) was added as a molecular weight marker. Electrophoresis was performed using the NuPAGE<sup>®</sup> MES SDS Running Buffer (pH 7.3), in an XCell Surelock<sup>™</sup> Mini-Cell, at constant voltage (200 V; 1 h). The gel was stained with 0.1% Coomassie R-250 in 40% ethanol and 10% acetic acid solution and destained in 10% ethanol and 7.5% acetic acid solution.

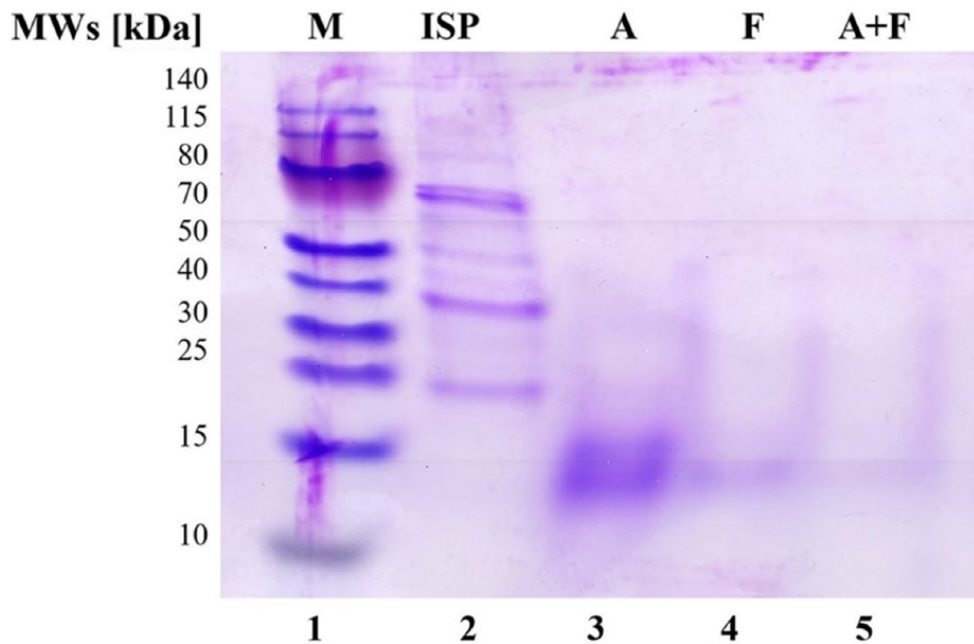


**Figure 1.** SDS-PAGE analysis of protein MWs by 12% precast Bis-Tris Invitrogen<sup>®</sup>: Thermo Scientific<sup>™</sup> PageRuler<sup>™</sup>. Lanes: prestained protein ladder (M, lane 1); soy protein isolate (SPI, lane 2); SPH obtained from the reaction with Alcalase<sup>®</sup> (A, lane 3), Flavourzyme<sup>®</sup> (F, lane 4) and Alcalase<sup>®</sup> + Flavourzyme<sup>®</sup> (A + F, lane 5).

2.4. Ultrafiltration

Each SPH was dissolved in milli-Q H<sub>2</sub>O, and the resulting solutions (*ca* 1% *w/v*) were ultrafiltered through 10, 5 and 1 kDa molecular weight cut-off membranes (MWCO) by using an Amicon<sup>®</sup> ultrafiltration cell (model 8400, 400 mL, Merck Millipore Corporation, Milano, Italy). Fractions ranging from 10 kDa to 1 kDa were recovered separately and freeze-dried. Ultrafiltration yields (*w/w*,%, referring to the weight of the starting dry hydrolysates) are reported in Figure 2.

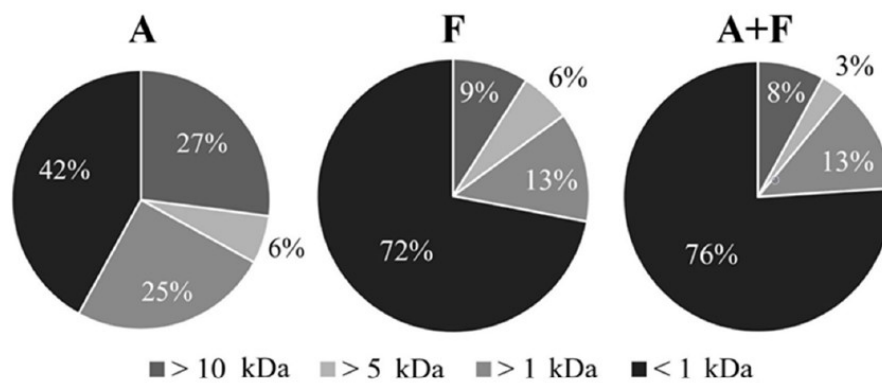


**Figure 2.** Yields (*w/w*,%) after sequential ultrafiltration of hydrolysates A, F, and A + F through MWCO membranes of 10, 5 and 1 kDa.

## 2.5. Characterization of SPH < 1 kDa Fraction

### 2.5.1. ACE Inhibition Assay

ACE-inhibitory activity was determined as previously reported [22], by evaluating hippuric acid (HA) formation from hippuryl-histidyl-leucine (HHL), a mimic substrate for angiotensin I, by HPLC analysis in the absence of and at increasing concentrations of the inhibitor (86.3, 172.5, 345.1, 690.1, 1035.2  $\mu\text{g mL}^{-1}$ ).  $\text{IC}_{50}$  is defined as the concentration of the inhibitor required to inhibit 50% of the ACE activity under the assay conditions.  $\text{IC}_{50}$  values are reported in Table 2 as mean value  $\pm$  standard deviation (SD) of three independent assays.

**Table 2.** Angiotensin-I-converting enzyme (ACE) inhibitory activity of three SPH < 1 kDa (A < 1 kDa; F < 1 kDa; A + F < 1 kDa), of three isolated RP-HPLC fractions from A < 1 kDa (A1; A2; A3) and of four peptides prepared by chemical synthesis.

Sample	Max ACE Inhibition (%) *	$\text{IC}_{50}$ ( $\mu\text{g mL}^{-1}$ ) *
A < 1 kDa	77.01 $\pm$ 0.57 <sup>g</sup>	296.57 $\pm$ 2.24 <sup>c</sup>
F < 1 kDa	54.42 $\pm$ 3.34 <sup>d</sup>	869.87 $\pm$ 15.46 <sup>f</sup>
A + F < 1 kDa	66.54 $\pm$ 0.59 <sup>e</sup>	558.35 $\pm$ 26.88 <sup>e</sup>
A1	92.2 $\pm$ 0.13 <sup>i</sup>	231.75 $\pm$ 2.43 <sup>b</sup>
A2	70.63 $\pm$ 0.32 <sup>f</sup>	361.66 $\pm$ 2.73 <sup>d</sup>
A3	75.72 $\pm$ 0.18 <sup>g</sup>	304.61 $\pm$ 4.81 <sup>c</sup>
ALKPDNR	25.72 $\pm$ 0.84 <sup>b</sup>	//
VVPD	13.23 $\pm$ 1.18 <sup>a</sup>	//
NDRP	87.76 $\pm$ 0.61 <sup>h</sup>	148.28 $\pm$ 9.83 <sup>a</sup>
NDTP	46.15 $\pm$ 1.72 <sup>c</sup>	//

\* Values are reported as mean value  $\pm$  standard deviation of three independent experiments; different superscript lowercase letters represent statistically significant differences between mean values at  $p < 0.05$  obtained by one-way ANOVA followed by a Fisher's Least Significant Difference procedure.

### 2.5.2. Determination of ACE Inhibition Pattern

The inhibition mode by the peptide showing the highest ACE-inhibitory activity (i.e., NDRP) was determined using Lineweaver–Burk plots (Figure 3) of  $1/\text{HA}$  production rate vs.  $1/\text{HHL}$  concentration ( $\text{mM}^{-1}$ ). ACE inhibition was measured by varying the concentration of the enzyme substrate HHL (2.32, 1.16, 0.58, 0.29 mM) in the absence of the inhibitor and using two different concentrations of the peptide (0.689, 0.172 mM). All experiments were performed in triplicate.

### 2.5.3. RP-HPLC

RP-HPLC experiments were performed on an AKTA Basic 100 instrument (Cytiva Europe GmbH, Buccinasco, Italy), equipped with a UV detector and monitored by the Unicorn™ Software (Cytiva Europe GmbH, Buccinasco, Italy). Analytical and semipreparative analyses were carried out on reverse phase Jupiter 10  $\mu\text{m}$  Proteo 90 Å columns (250 mm  $\times$  4.6 mm and 250 mm  $\times$  10 mm, respectively) (Phenomenex, Torrance, CA, USA), at room temperature and at a flow rate of 1  $\text{mL min}^{-1}$  and 5  $\text{mL min}^{-1}$ , respectively. Samples were dissolved in 0.1% formic acid in water.

Chromatographic conditions: 0.1% formic acid in water (solvent A) and 0.1% formic acid in water/acetonitrile, 2:8 (solvent B); from 0% to 30% B in 30 min, then to 100% B in 10 min; detection at  $\lambda$  226 nm. Semipreparative separation (see Supplementary data, Figure S5) of SPH with MW < 1 kDa obtained by hydrolysis with Alcalase® (A < 1 kDa) afforded three fractions (A1, A2 and A3) that, after removal of the organic solvent under reduced pressure, were freeze dried and stored at  $-20$  °C.

### 2.5.4. NMR Analysis

NMR experiments were performed at 298 K on 400 MHz Bruker NMR spectrometer (Bruker Corporation, Billerica, MA, USA) equipped with a z-gradient coil probe. Chemical shifts ( $\delta$ ) are given in parts per million (ppm) and were referenced to the solvent signal



(DMSO- $d_6$ ,  $\delta_H$  2.50 ppm and  $\delta_C$  39.52 ppm from TMS (tetramethylsilane), respectively). All 1D and 2D NMR spectra were collected using the standard pulse sequences available with Bruker Topspin 3.6. The 2D TOCSY and 2D NOESY analyses were recorded with short mixing times: 80 ms and 500 ms, respectively. Proton resonances were assigned using standard methods. See Supplementary data, Figures S6 and S7.

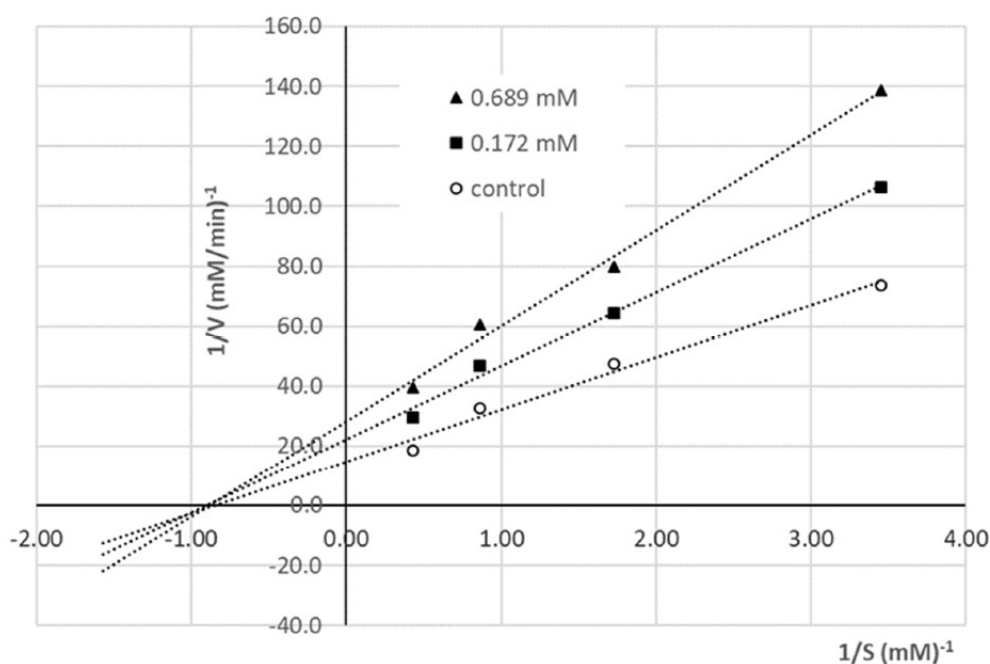


**Figure 3.** Lineweaver–Burk plots of ACE activity in the presence of NDRP at concentrations of 0.689 mM (▲) and 0.172 mM (■) and without the inhibitory peptide (○, control); HHL was used as the enzyme substrate. All experiments were conducted in triplicate.

#### 2.5.5. Determination of Amino Acid Sequence

For amino acid sequence determination, fraction A1 was submitted to automatic Edman degradation (Hewlett-Packard Protein Sequencer HP G1000A, Agilent Technologies Italia S.p.A., Cernusco sul Naviglio, Milano, Italy), using the manufacturer's phenylisothiocyanate (PTH)-4M HPLC method (Hewlett-Packard Technical note 95-1). In detail, the sample was loaded on a Hewlett-Packard adsorptive biphasic column, and the PTH-derivatized amino acids were identified by comparison with a reference mixture of phenylthiohydantoin amino acids. Analysis of the relative abundance of the PTH-amino acid peaks in the chromatograms obtained after each cycle of Edman degradation (see Supplementary data) led to the identification of putative sequences, which were used as queries for the screening of the soybean protein sequences in the Uniprot database [23].

The main components of the A1 fraction were found to be a heptapeptide, whose putative sequence was ALKPDNR, and three tetrapeptides, whose putative sequences were VVPD, NDRP and NDTP, respectively. All the peptide patterns were searched against the UniProt database [23] and were found to be present in soybean glycinins (G1, G2, G3).

#### 2.5.6. Mass Spectrometry of Synthetic Peptides

Electrospray ionization mass spectra (ESI-MS) were recorded on a Thermo Finnigan LCQ Advantage spectrometer (Hemel Hempstead, Hertfordshire, UK). Mass spectra acquisition was performed in positive and negative ion mode in a mass range of 50–2000  $m/z$ .

Source parameters: T, 200 °C; sheath gas flow rate, 20 arb; aux gas flow rate, 10 arb; spray voltage, 5.50 kV; capillary temperature, 275 °C; capillary voltage, 38.00 V; tube lens, 65.00 V.

Electrospray ionization high-resolution mass spectrometry (ESI-HR-MS) analyses were performed on a Synapt G2-Si QToF instrument (Waters, Milford, MA, USA) equipped with a Zspray™ ESI-probe for electrospray ionization (Waters, Milford, MA, USA). The sample was dissolved in water–0.1% formic acid in methanol and analyzed by direct infusion. The ion source and interface conditions were as follows: capillary voltage 1.3 kV, sampling cone 120 V, source temperature 120 °C, desolvation temperature 150 °C and desolvation gas flow rate 600 L h<sup>-1</sup>. Mass spectra were acquired over the *m/z* range 50–1000 in a positive ion Full Scan mode. Leucine enkephalin was used as a lock-mass compound. Data were processed with MassLynx™ V4.2 software (Waters Milford, MA, USA).

### 2.6. Peptides Synthesis

The peptides identified by the Edman degradation (ALKPDNR, VVPD, NDRP and NDTP) were synthesized by microwave-assisted solid phase automated synthesis using the Fmoc-protocol on a Biotage® Initiator<sup>+</sup> SP wave peptide synthesizer (Biotage, Uppsala, Sweden). All the syntheses were carried out on 200 mg of preloaded 2-chlorotrityl resin, corresponding to 0.18 mmol of Fmoc-Arg(Pbf)- used for ALKPDNR, 0.14 mmol of Fmoc-Asp(OtBu)- for VVPD and 0.13 mmol of Fmoc-Pro- for NDRP and NDTP, respectively. Fmoc deprotection was performed using 25% piperidine in DMF. Each coupling reaction was carried out at 50 °C in DMF using HOBt and HBTU (3-fold excess) as coupling agents and DIPEA (6-fold excess) as a base; reaction time was 15 min. The functional groups of the amino acid side chains were protected as follows: Asn(Trt), Asp(OtBu), Lys(Boc), Arg(Pbf) and Thr(*t*Bu). Each amino acid was used in 3-fold excess and dissolved along with coupling agents and DIPEA in DMF (3 mL) 15 min before reaction. For cleavage, a trifluoroacetic acid (TFA) (15.60 mL)/phenol (0.89 g)/H<sub>2</sub>O (0.88 mL)/triisopropylsilane (TIPS) (0.34 mL) solution was used; all resins were treated with the cleavage solution for 1–5 h, depending on the presence of the Trt protecting group at the *N*-terminus of the peptide, which takes longer to be cleaved. The solid supports were then removed by filtration and the resulting yellow oils were treated with Et<sub>2</sub>O at 0 °C. The white precipitates were centrifuged (4000 rpm, 10 min), decanted, dissolved in H<sub>2</sub>O and freeze-dried.

The identity and molecular weight of the obtained peptides (ALKPDNR, 19%; VVPD, 51%; NDRP, 45%; and NDTP, 31% yield, respectively) were confirmed by ESI-MS in positive ion mode analysis.

**ALKPDNR ESI-MS:** *m/z* calcd. for [C<sub>34</sub>H<sub>61</sub>N<sub>12</sub>O<sub>11</sub>]<sup>+</sup>: 813.45, found: 813.32 [M + H]<sup>+</sup>, 835.35 [M + Na]<sup>+</sup>.

**VVPD ESI-MS:** *m/z* calcd. for [C<sub>19</sub>H<sub>33</sub>N<sub>4</sub>O<sub>7</sub>]<sup>+</sup>: 429.23, found: 429.53 [M + H]<sup>+</sup>, 451.67 [M + Na]<sup>+</sup>, 857.05 [2M + H]<sup>+</sup>, 879.23 [2M + Na]<sup>+</sup>.

**NDRP ESI-MS:** *m/z* calcd. for [C<sub>19</sub>H<sub>33</sub>N<sub>8</sub>O<sub>8</sub>]<sup>+</sup>: 501.23, found: 501.56 [M + H]<sup>+</sup>, 523.50 [M + Na]<sup>+</sup>, 1001.47 [2M + H]<sup>+</sup>.

**NDTP ESI-MS:** *m/z* calcd. for [C<sub>17</sub>H<sub>28</sub>N<sub>5</sub>O<sub>9</sub>]<sup>+</sup>: 446.18, found: 446.32 [M + H]<sup>+</sup>, 468.46 [M + Na]<sup>+</sup>, 891.21 [2M + H]<sup>+</sup>, 913.18 [2M + Na]<sup>+</sup>.

Moreover, the peptide identified as the most active ACE inhibitor, namely NDRP, was further characterized by <sup>1</sup>H and <sup>13</sup>C NMR analysis and HR-MS.

**<sup>1</sup>H NMR (400 MHz, DMSO-*d*<sub>6</sub>) δ/ppm:** 8.71 (d, *J* = 7.4 Hz, 1H), 8.10 (d, *J* = 7.7 Hz, 1H), 7.79 (s, 1H), 7.70 (s, 1H), 7.23 (br s, 2H), 4.57 (m, 1H), 4.45 (m, 1H), 4.24 (dd, *J* = 8.6, 4.5 Hz, 1H), 4.05 (dd, *J* = 8.2, 4.5 Hz, 1H), 3.64 (m, 1H), 3.53 (m', 2H), 3.10 (br d, *J* = 5.1 Hz, 2H), 2.70 (ddd, *J* = 25.3, 16.8, 4.4 Hz, 2H), 2.57 (dd, *J* = 14.4, 5.7 Hz, 2H), 2.15 (m, 1H), 1.96–1.77 (m, 3H), 1.71 (br s, 1H), 1.56 (br s, 2H).

**<sup>13</sup>C NMR (100 MHz, DMSO-*d*<sub>6</sub>) δ/ppm:** 173.67, 171.99, 171.15, 170.55, 169.89, 168.94, 158.90, 158.59, 157.33, 59.03, 50.67, 50.03, 49.59, 46.86, 40.97, 36.61, 36.22, 29.07, 28.37, 25.01, 24.91.

**NDRP HR-MS:** *m/z* calcd. for [C<sub>19</sub>H<sub>33</sub>N<sub>8</sub>O<sub>8</sub>]<sup>+</sup>: calcd: 501.2421, found: 501.2413.

### 2.7. Detection of Peptide NDRP in the A < 1 kDa Fraction by Multiple Reaction Monitoring (MRM)

Pure NDRP obtained by chemical synthesis and the hydrolysate A < 1 kDa were analyzed on an SL IT mass spectrometer interfaced with a HPLC-Chip Cube source (Agilent Technologies, Palo Alto, CA, USA). Data were processed with MSD Trap control 4.2, and Data analysis 4.2 version (Agilent Technologies, Palo Alto, CA, USA). The samples (1  $\mu$ L), acidified with formic acid, were injected in infusion mode. Data acquisition occurred in positive ionization mode. Capillary voltage was  $-1900$  V, with endplate offset  $-500$  V. Mass spectra were acquired with an ICC target of 30,000 and a maximum accumulation time of 150 ms. LC/MS analysis was performed in multiple reaction monitoring (MRM) mode. Specifically, the detection of NDRP was carried out by monitoring the mono-charged precursor ion  $[M + H]^+$  ( $m/z$  501.2). The MS/MS fragment ions were then covered along the peptide sequence.

### 2.8. In Vitro Simulated Digestion of NDRP

The in vitro simulated digestion of NDRP was carried out according to the method reported by Xu [14], with slight modifications. Briefly, NDRP (49.9 mg) was dissolved in HPLC-grade  $H_2O$  ( $10 \text{ mg mL}^{-1}$ ) and the pH of the solution was adjusted to 2 with 0.1 M HCl. Pepsin (1 mg) was added, and the mixture was stirred at  $37^\circ\text{C}$  for 2 h. Then, the pH was adjusted to 6 with 0.9 M  $NaHCO_3$ , and afterwards to 7.5 with 1 M NaOH. Pancreatin (1 mg) was added, and the solution was incubated at  $37^\circ\text{C}$  for 4 h. After deactivation of the enzymes by heating in a boiling water bath for 10 min, the solution was cooled and freeze-dried, and the resulting in vitro-digested NDRP (55.6 mg, 10% of salts) was submitted to ESI-MS and ACE-inhibitory activity assay (ACE inhibition =  $82.47 \pm 1.07\%$ ).

**NDRP after in vitro simulated digestion ESI-MS:** ( $m/z$  calcd. for  $[C_{19}H_{33}N_8O_8]^+$ : 501.23 Da, found: 501.55 Da  $[M + H]^+$ , 523.51 Da  $[M + Na]^+$ ).

### 2.9. Data Treatment and Statistical Analysis

Degrees of hydrolysis (DH) was calculated by taking into account the propagation of the experimental error; the significance of the results is expressed through the evaluation of discrepancies. Statistical analyses of ACE-inhibitory activities were performed with StatGraphics Plus (version 2.1 for Windows). The data were evaluated using one-way analysis of variance followed by a Fisher's Least Significant Difference procedure; values with different letters are significantly different for  $p < 0.05$ .

## 3. Results and Discussion

### 3.1. Enzymatic Hydrolysis of Soy Proteins and Degree of Hydrolysis

Among the numerous proteases commonly employed to hydrolyze soybean protein [24], we selected Alcalase<sup>®</sup> and Flavourzyme<sup>®</sup>. Alcalase<sup>®</sup>, a mixture of endopeptidases, has been found to be one of the most efficient biocatalysts in releasing bioactive peptides from different protein sources [25]. Flavourzyme<sup>®</sup>, a mixture of endopeptidases and exopeptidases, is frequently used for debittering food protein hydrolysates [26]. In this work, these proteolytic enzymes were used individually and in combination.

A commercial soy protein isolate (SPI) was hydrolyzed by treatment with Alcalase<sup>®</sup> and Flavourzyme<sup>®</sup> separately and by sequential treatment with both Alcalase<sup>®</sup> and Flavourzyme<sup>®</sup>. Table 1 reports the rough weight percentages of the three different SPH (A, F and A + F) obtained after centrifugation and lyophilization of supernatants, with respect to the amount of starting SPI. The enzyme combination appeared to be more effective in promoting protein hydrolysis, considering that the amounts of hydrolysates (as dry weight%  $w/w$ ) recovered, i.e., A, F and A + F, were 43%, 64% and 77%, respectively (Table 1).

Moreover, Table 1 reports the degree of hydrolysis (DH) values of the three hydrolysates (A, F, A + F). DH is defined as the proportion of cleaved peptide bonds in a protein hydrolysate, and is routinely used to compare different proteolytic processes. The enzyme choice, according to its specificity and selectivity, represents a crucial pa-

parameter to tune the DH and the final properties of the hydrolysates [25,27]. The DH of the obtained SPH (A, F, A + F) was determined using the trinitrobenzenesulfonic acid (TNBS) method [19], which is independent from the type of enzyme activity used during hydrolysis, unlike other reported methods [21]. The sample hydrolyzed by Flavourzyme<sup>®</sup> and the sample hydrolyzed by a combination of Alcalase<sup>®</sup> and Flavourzyme<sup>®</sup> showed similar and not statistically different DH ( $34 \pm 5.5\%$  and  $36 \pm 5.6\%$ , respectively), while the hydrolysate prepared with Alcalase<sup>®</sup> alone had the lowest degree of hydrolysis ( $17 \pm 5.3\%$ ). Thus, the combination of A + F exhibited nearly the same DH as for F used individually, while allowing an increase in hydrolysate recovery by more than 10% (Table 1). This result could be attributable to the operative conditions (pH and reaction time) selected for the experiment carried out with the enzymes in combination [11]. In fact, when combining enzymes, optimum conditions for each of them may not be attained. In addition, the latter enzyme hydrolyzes the peptides cleaved by the former biocatalyst.

### 3.2. SDS-PAGE

All three hydrolysates, as well as untreated SPI, were submitted to SDS-PAGE in NuPAGE<sup>®</sup> MES SDS Running Buffer (pH 7.3), using a 12% pre-cast NuPAGE<sup>®</sup> Novex<sup>®</sup> Bis-Tris Gel, which was selected for resolving proteins/peptides in the range 1–200 kDa. The resulting profiles are shown in Figure 1. Lanes 2–5 represent SPI, A, F and A + F, respectively. SPI (lane 2) presents an electrophoretic pattern characteristic for soy proteins [26]: the highly intense bands at 72 kDa and about 67 kDa and the less intense one at 63 kDa are attributable to  $\alpha'$ ,  $\alpha$  and  $\beta$  subunits of  $\beta$ -conglycinin, respectively. Furthermore, the acidic chain A3 of the G1 subunit of glycinin is observed at about 33 kDa and the basic chain of subunit G2 at 22 kDa [28]. It is worth noting that the use of both Alcalase<sup>®</sup> and Flavourzyme<sup>®</sup>, as well as of their combination, led to the complete disappearance of the bands of the main proteins commonly found in soy. In particular, after hydrolysis with Alcalase<sup>®</sup> (lane 3), the greater part of the hydrolysate had a molecular weight between 12 and 20 kDa; by contrast, the only band slightly visible after reaction with Flavourzyme<sup>®</sup> (lane 4) is the one at about 14 kDa. In addition, hydrolysis by Alcalase<sup>®</sup> + Flavourzyme<sup>®</sup> resulted in undetectable peptides with molecular weight higher than 10 kDa, thus indicating that such a protease mixture produced very small peptides. This pattern was consistent with results obtained from DH and ultrafiltration (see Sections 3.1 and 3.3, respectively).

### 3.3. Ultrafiltration and Evaluation of ACE-Inhibitory Activity

Results of SDS-PAGE and DH analysis suggested that SPHs produced following the three hydrolytic protocols are extensively hydrolyzed and composed of very small peptides, having a molecular weight lower than 15 kDa. The three SPHs (A, F, A + F) were fractionated by ultrafiltration through decreasing molecular weight cut-off membranes (10, 5 and 1 kDa).

As shown in Figure 2, F and A + F mainly contained < 1 kDa peptides (72% and 76%, respectively). Conversely, in the reaction with Alcalase<sup>®</sup>, the peptide fraction < 1 kDa represented only 42%, whereas higher amounts of peptides with a MW in the range 1–5 kDa and with MW > 10 kDa were produced (25% and 27%, respectively). The peptide size distribution of the protein hydrolysates depended on the protease mixture selected to perform proteolysis, and our results are in good agreement with the well-known mechanism of action of the two enzyme preparations (Alcalase<sup>®</sup> and Flavourzyme<sup>®</sup>) [27]. Indeed, the action of exopeptidases is facilitated by a previous hydrolytic step carried out by endopeptidases: firstly, endopeptidases of Alcalase<sup>®</sup> and Flavourzyme<sup>®</sup> hydrolyze peptide bonds within soy proteins, producing relatively large peptides, then exopeptidases of Flavourzyme<sup>®</sup> (two aminopeptidases and two dipeptidyl peptidases) [29] systematically remove amino acids or very small peptides from either the N-terminus or the C-terminus position, thus resulting in an increased hydrolytic degradation.

Short chain peptides are known to be generally good candidates as ACE inhibitors [30]. Thus, the three fractions with MW less than 1 kDa that were prepared by sequential

ultrafiltration of A, F and A + F (A < 1 kDa, F < 1 kDa, A + F < 1 kDa) were investigated for their ACE-inhibitory activity. The results obtained are shown in Table 2. Fraction A < 1 kDa, obtained by Alcalase<sup>®</sup> treatment, exhibited the maximal ACE-inhibitory activity ( $77.01 \pm 0.57\%$ ) at the highest tested concentration of hydrolysate. The fraction arising from hydrolysis with Alcalase<sup>®</sup> and Flavourzyme<sup>®</sup> reached  $66.54 \pm 0.59\%$  inhibitory activity at the same concentration, whereas the activity of F < 1 kDa fraction dropped to  $54.42 \pm 3.34\%$ .

#### 3.4. Purification, Characterization and Synthesis of ACE-Inhibitory Peptides

The most active fraction, i.e., A < 1 kDa, was selected and separated by preparative RP-HPLC into three subfractions (A1, A2 and A3), which were in turn screened for their ACE-inhibitory activities (see Table 2 and Figure S7). The data in Table 2 indicate that the purification step obtained a peptide mixture with improved antihypertensive properties, considering that in the isolated fraction A1, the ACE inhibition activity increased from  $77.01 \pm 0.57\%$  to  $92.2 \pm 0.13\%$  with an  $IC_{50}$  value of  $231.75 \pm 2.43 \mu\text{g mL}^{-1}$ .

With the aim of determining the composition of the A1 fraction, NMR and MS analyses were carried out. <sup>1</sup>H NMR spectrum in DMSO-*d*<sub>6</sub> appeared to be very crowded, especially in the amide-NH region between 6.5 and 9.0 ppm, indicating that the sample was a mixture of many different peptides. In order to obtain more structural information, 2D spectra were collected. Complete sequence-specific assignment of resonances of some amino acids was achieved using a combination of COSY and TOCSY experiments [31]. In particular, the spin systems of alanine (A), valine (V), aspartic acid (D) and arginine (R) (see Supplementary data) were evidenced from the analysis of the NH- $\alpha$ H region and that of proline (P) from the analysis of the  $\alpha$ H- $\alpha$ H region of the TOCSY spectrum. Moreover, no near-neighbour connections were found in the NOESY and ROESY spectra, thus suggesting that these extremely short peptides are not able to adopt a folded structure for a significant fraction of the time [32].

As spectroscopic analysis did not allow the identification of peptides in the isolated A1 fraction, it was submitted to Edman degradation, an effective method for determining the sequence of unknown peptides with a free amino terminus. Four putative sequences were identified; in particular, one heptapeptide (ALKPDNR) and three tetrapeptides (VVPD, NDRP and NDTP). It should be pointed out that all these peptide patterns are present within the sequences of storage soybean proteins (glycinins G1, G2 and G3), according to the UniProt database [23].

In order to define which peptide/s is/are mainly responsible for the ACE-inhibitory properties exhibited by A1 fraction, all identified peptides were synthesized by solid phase automated peptide synthesis using the Fmoc protocol, and their ACE-inhibitory activities were evaluated (Table 2). Among them, only NDRP showed an ACE inhibition capacity comparable to that of the starting A1 fraction (maximal ACE-inhibitory activity =  $87.76\%$ ,  $IC_{50} = 148.28 \mu\text{g mL}^{-1}$ ) (Table 2). This finding suggested that this peptide might be the main agent responsible for the observed bioactivity.

#### 3.5. Determination of the ACE Inhibition Mechanism

To investigate the inhibition mechanism, Lineweaver–Burk plots of ACE activity in the presence and absence of NDRP were drawn (Figure 3). These plots, characterized by a coincident intercept on the  $1/S$  axis, revealed that the peptide acts as a non-competitive inhibitor [33].

Inhibition is described as non-competitive when the inhibitor molecule has the same affinity for both the enzyme and enzyme–substrate complex. Hence, the peptide NDRP does not bind to ACE catalytic site, but to other sites, resulting in a decreased efficacy of the enzyme, independently of substrate binding [20].

Although competitive ACE inhibitors have been the most frequently reported, numerous peptides showing remarkable non-competitive ACE-inhibitory activity have also been identified, from both plant and animal food proteins. Some of them are: IFL ( $IC_{50}$  of  $44.8 \mu\text{M}$ ) and WL ( $IC_{50}$  of  $29.9 \mu\text{M}$ ) from Tofuyo (fermented soybean food) [34]; DEN-

SKF (IC<sub>50</sub> of 100 µM) from fruits of *T. chebula* Retz. [33]; RYPSYG (IC<sub>50</sub> of 54 µg mL<sup>-1</sup>) and DERF (IC<sub>50</sub> of 21 µg mL<sup>-1</sup>) from bovine casein hydrolysate [35]; GDLGKTTTVS-NWSPPKYKDTP (IC<sub>50</sub> of 11.28 µM) from tuna frame protein hydrolysate [7]; RLPSEFDL-SAFRLA (IC<sub>50</sub> of 0.45 mg mL<sup>-1</sup>) and RLSGQTIEVTSEYLFRH (IC<sub>50</sub> of 1.10 mg mL<sup>-1</sup>) from *Pleurotus cornucopiae* mushroom [36]. To the best of our knowledge, no non-competitive ACE-inhibitory peptide has been identified in soybean protein isolates so far. As non-competitive ACE-inhibitory peptides bind to a different site from the substrate, their structure–activity relationships are not yet well established.

Usually, ACE-inhibitory peptides have a short chain bearing 2–12 residues, although active peptides with up to 21 amino acids have been identified [7,37]. Concerning amino acid composition and peptide sequence, the presence of a net negative charge induced by highly acidic amino acids (Asp and Glu) may reduce the catalytic rate of ACE by chelating zinc atom, which is vital for ACE activity [10]. Moreover, it has been reported that the presence of tyrosine, phenylalanine, tryptophan, proline, lysine, isoleucine, valine, leucine and arginine in peptides has a strong influence on ACE binding. In particular, most ACE-inhibitory peptides carry hydrophobic or branched amino acids at the N-terminus, while residues with cyclic or aromatic rings, such as tyrosine, phenylalanine, tryptophan and proline, are characteristic for the C-terminus [22,37]. The non-competitive ACE inhibitor peptide isolated during this study (NDRP) possesses a few features that are consistent with its ACE-inhibitory activity: it is short (it is composed of four amino acids), it bears an acidic amino acid (Asp) as a potential zinc-chelating site, and a Pro residue at the C-terminus.

### 3.6. Detection of Peptide NDRP in the A < 1 kDa Fraction Assessed by MRM Mass Spectrometry Analysis

To confirm the presence of NDRP in the A < 1 kDa fraction, the multiple reaction monitoring (MRM) technique was employed using an ion trap mass spectrometer by infusion. Specifically, NDRP was observed by monitoring the mono-charged precursor ion [M + H]<sup>+</sup> (*m/z* 501.2). The MS/MS fragment ions were then covered along the peptide sequence. Figure 4 shows the MS/MS spectrum of NDRP with the highlighted sequence coverage. The ions *y*<sub>3</sub> and *y*<sub>2</sub>, corresponding to DRP and RP, respectively, were the main detected ions, whereas the *b*<sub>2</sub> ion, corresponding to ND, was the most representative ion of the *b* series.

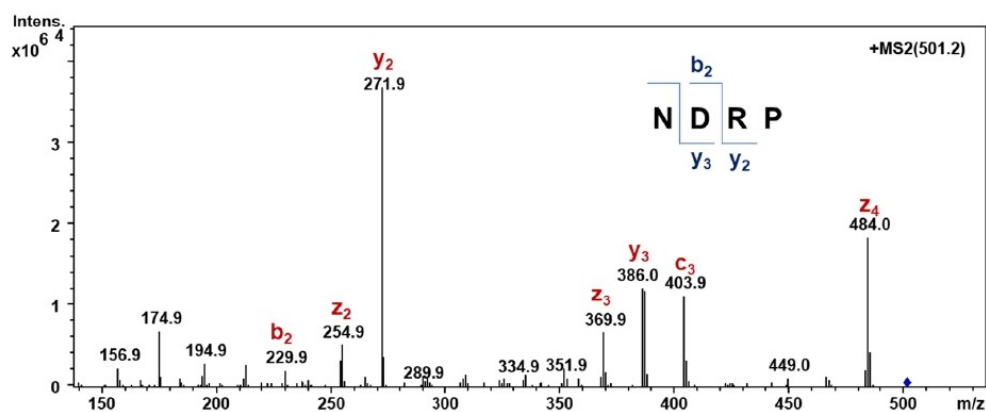


Figure 4. MS/MS spectrum of NDRP detected by infusion of A < 1 kDa by MRM.

### 3.7. Stability of NDRP toward In Vitro Simulated Digestion

To exert their health-promoting properties, bioactive peptides must survive gastrointestinal digestion and reach their target sites in an intact and active form. It is known that short-chain peptides, especially those with C-terminal proline, are generally less susceptible

to degradation by proteolytic enzymes [13,38]. Moreover, they are absorbed in the small intestine more rapidly than free amino acids and large oligopeptides [30].

To evaluate the resistance of NDRP to digestive enzymes, this peptide was subjected to a two-stage hydrolysis process that simulated *in vivo* conditions during physiological digestion, and the changes in its bioactivity were examined. After treatment with gastrointestinal proteases (pepsin and pancreatin), the maximal ACE inhibition of the NDRP digested sample was found to be  $82.47 \pm 1.07\%$ . This value roughly corresponds to about 94% of the ACE-inhibitory activity of pure NDRP, thus indicating that NDRP might be resistant to gastrointestinal digestion. In addition, the *in vitro*-digested NDRP was analyzed by ESI-MS in positive ion mode, and the presence in the spectrum of a peak corresponding to the molecular weight of the peptide ( $m/z$  calcd. for  $[C_{19}H_{33}N_8O_8]^+$ : 501.23 Da, found: 501.55 Da  $[M + H]^+$ , 523.51 Da  $[M + Na]^+$ ) was observed, further corroborating its stability in intestinal proteolysis.

It is worth noting that in a recent study conducted by Xu and co-workers [14], a number of different peptides were detected in a hydrolysate of soy protein prepared by Alcalase<sup>®</sup> in experimental conditions different from those used in this work (pH = 7.5, 55 °C, 8 h vs. pH = 8.5, 50 °C, 24 h). Differences in the hydrolytic conditions as well as in the starting material and separation techniques may affect the release and/or the identification of specific peptide sequences having different mechanisms of action. Indeed, all the peptides reported by Xu are competitive ACE inhibitors, and some of them were found to be unstable in *in vitro* simulated gastrointestinal digestion.

#### 4. Conclusions

This study provides a comparative analysis of three hydrolytic protocols applied on inexpensive soy protein isolate, exploiting cheap and commercially available proteolytic enzymes (Alcalase<sup>®</sup> and Flavourzyme<sup>®</sup>) used either individually or in combination. The resulting soy protein hydrolysates (A, F and A + F) consisted of small peptides with enhanced solubility in water, with respect to starting proteins.

Furthermore, the hydrolysate obtained through the process catalyzed by Alcalase<sup>®</sup> (A) was found to have the highest ACE-inhibitory activity. From this hydrolysate, upon a sequential ultrafiltration process, a novel peptide (NDRP) was identified and prepared by chemical synthesis. To the best of our knowledge, such a peptide has never been isolated from either soy and soybean-derived products or from other food proteins. Besides ACE-inhibitory activity, NDRP was found to be highly stable in *in vitro* simulated gastrointestinal digestion (residual activity of the digested sample was 94% of the ACE-inhibitory activity of the pure peptide).

Our data confirm the relevance of soy as a valuable and cheap source of bioactive peptides that may be exploited as components of functional foods for the prevention of chronic diseases.

**Supplementary Materials:** The following supporting information can be downloaded at: <https://www.mdpi.com/article/10.3390/foods11172667/s1>, Figure S1: ACE-inhibitory activity curves comparison of ultrafiltered hydrolysates A < 1 kDa, F < 1 kDa and A+F < 1 kDa; Figure S2: ACE-inhibitory activity curves comparison of ultrafiltered hydrolysates A < 1 kDa and fractions purified via semipreparative RP-HPLC from A < 1 kDa (A1, A2 and A3); Figure S3: ACE-inhibitory activity curves comparison of synthesized peptides (ALKPDNR, VVPD, NDRP and NDTP); Figure S4: ACE-inhibitory activity curves comparison of ultrafiltered hydrolysates A < 1 kDa, purified fraction A1, synthesized peptide NDRP and *in vitro* digested NDRP; Figure S5: RP-HPLC chromatogram on reverse phase Jupiter 10  $\mu$ m Proteo 90 Å column of active fraction A < 1 kDa; Figure S6: 1H NMR (400 MHz; DMSO-*d*<sub>6</sub>) spectrum of A1 sample; Figure S7: (a) NH- $\alpha$ H region and (b)  $\alpha$ H- $\alpha$ H region of the TOCSY spectrum of the A1 sample; dashed lines correspond to the patterns of alanine (red), valine (green), aspartic acid (blue), arginine (pink) and proline (black); Figure S8: HPLC chromatograms of (a) PTH-Std and (b), (c), (d), (e), (f), (g), (h), (i) 8 cycles of Edman degradation; Figure S9: Mass spectra of ALKPDNR carried out in positive ion mode; Figure S10: Mass spectra of VVPD carried out in positive ion mode; Figure S11: Mass spectra of NDRP carried out in positive ion mode; Figure S12:

Mass spectra of NDTP carried out in positive ion mode; Figure S13: Mass spectra of in vitro digested NDRP carried out in positive ion mode; Figure S14: <sup>1</sup>H NMR (400 MHz) spectra of NDRP recorded in DMSO-d<sub>6</sub>; Figure S15: <sup>13</sup>C NMR (101 MHz) spectra of NDRP recorded in DMSO-d<sub>6</sub>; Figure S16: High-resolution ESI mass spectra (positive ion mode) of NDRP; Figure S17: <sup>13</sup>C NMR (101 MHz) spectra of NDRP recorded in DMSO-d<sub>6</sub>; Figure S18: High-resolution ESI mass spectra (positive ion mode) of NDRP; Table S1: L-Leu samples analysis for calibration curve; Table S2: AN<sub>L-Leu</sub> calibration curve; Table S3: Amino acids profile of SPI and N<sub>pb</sub> calculation; Table S4: Starting isolate soy proteins (SPI) and hydrolysates samples (A; F; A+F) analysis; Table S5: AN calculation; Table S6: DH calculation; Table S7: Foaming capacity (FC) and foaming stability (FS) over time; Table S8: Amino acids profile of A1.

**Author Contributions:** Conceptualization, G.S., S.S. and N.V.; methodology, S.S., N.V. and G.A.; validation, C.F.M. and M.R.; formal analysis, C.F.M. and M.R.; investigation, S.S., N.V., G.B., G.A., P.A., T.R. and L.S.; resources, G.S.; writing—original draft preparation, G.S., S.S. and D.U.; writing—review and editing, A.A.; visualization, S.S., G.B. and G.A.; supervision, G.S.; project administration, G.S.; funding acquisition, G.S. and D.U. All authors have read and agreed to the published version of the manuscript.

**Funding:** This research was funded by Cariplo Foundation and Innovhub-SSI (Italy)—“Integrated research on industrial bio-technologies and bioeconomy-joint Call 2017”, project BIOCOSM, ID 2017-0978). This research is also part of the project “One Health Action Hub: University Task Force for the resilience of territorial ecosystems”, supported by Università degli Studi di Milano-PSR 2021-GSA-Linea 6. This research was also funded by APC Central Fund—Università degli Studi di Milano.

**Institutional Review Board Statement:** Not applicable.

**Informed Consent Statement:** Not applicable.

**Data Availability Statement:** Data is contained within the article or Supplementary Materials.

**Acknowledgments:** The authors acknowledge the support of the APC Central Fund of the University of Milan. A special acknowledgement is due to Cariplo Foundation for supporting young researchers in this project (S.S., N.V.). We thank Marina S. Robescu (University of Pavia) for the SDS-PAGE analysis. We also thank ABS FOOD and Novozymes for kindly providing us with soy protein isolate and proteolytic enzymes (Alcalase® and Flavourzyme®), respectively.

**Conflicts of Interest:** The authors declare no conflict of interest. The funders had no role in the design of the study; in the collection, analyses or interpretation of data; in the writing of the manuscript; or in the decision to publish the results.

## References

1. Iavarone, F.; Desiderio, C.; Vitali, A.; Messana, I.; Martelli, C.; Castagnola, M.; Cabras, T. Cryptides: Latent peptides everywhere. *Crit. Rev. Biochem. Mol. Biol.* **2018**, *53*, 246–263. [CrossRef] [PubMed]
2. Ulug, S.K.; Jahandideh, F.; Wu, J. Novel technologies for the production of bioactive peptides. *Trends Food Sci. Technol.* **2021**, *108*, 27–39. [CrossRef]
3. Sun, X.D. Enzymatic hydrolysis of soy proteins and the hydrolysates utilisation. *Int. J. Food Sci. Technol.* **2011**, *46*, 2447–2459. [CrossRef]
4. Xue, L.; Yin, R.; Howell, K.; Zhang, P. Activity and bioavailability of food protein-derived angiotensin-I-converting enzyme-inhibitory peptides. *Compr. Rev. Food. Sci. Food. Saf.* **2021**, *20*, 1150–1187. [CrossRef] [PubMed]
5. Coscueta, E.R.; Camposa, D.A.; Osório, H.; Nerli, B.B.; Pintado, M. Enzymatic soy protein hydrolysis: A tool for biofunctional food ingredient production. *Food Chem. X* **2019**, *1*, 100006. [CrossRef]
6. WHO (World Health Organization). Available online: [https://www.who.int/health-topics/hypertension#tab=tab\\_1](https://www.who.int/health-topics/hypertension#tab=tab_1) (accessed on 15 July 2022).
7. Lee, S.H.; Qian, Z.J.; Kim, S.K. A novel angiotensin I converting enzyme inhibitory peptide from tuna frame protein hydrolysate and its antihypertensive effect in spontaneously hypertensive rats. *Food Chem.* **2010**, *118*, 96–102. [CrossRef]
8. Sica, D.A. Angiotensin-converting enzyme inhibitors side effects—physiologic and non-physiologic considerations. *J. Clin. Hypertens.* **2004**, *6*, 410–416. [CrossRef]
9. Conde, J.M.; Patino, J.M.R. The effect of enzymatic treatment of a sunflower protein isolate on the rate of adsorption at the air–water interface. *J. Food Eng.* **2007**, *78*, 1001–1009. [CrossRef]



10. Aluko, R.E. Structure and function of plant protein-derived antihypertensive peptides. *Curr. Opin. Food Sci.* **2015**, *4*, 444–450. [[CrossRef](#)]
11. Ambigaipalan, P.; Al-Khalifa, A.S.; Shahidi, F. Antioxidant and angiotensin I converting enzyme (ACE) inhibitory activities of date seed protein hydrolysates prepared using Alcalase, Flavourzyme and Thermolysin. *J. Funct. Foods* **2015**, *18*, 1125–1137. [[CrossRef](#)]
12. Ashaolu, T.P. Applications of soy protein hydrolysates in the emerging functional foods: A review. *Int. J. Food Sci. Technol.* **2020**, *55*, 421–428. [[CrossRef](#)]
13. Shobako, N. Hypotensive peptides derived from plant proteins. *Peptides* **2021**, *142*, 170573. [[CrossRef](#)] [[PubMed](#)]
14. Xu, Z.; Wu, C.; Sun-Waterhouse, D.; Zhao, T.; Waterhouse, G.I.N.; Zhao, M.; Su, G. Identification of post-digestion angiotensin-I converting enzyme (ACE) inhibitory peptides from soybean protein Isolate: Their production conditions and in silico molecular docking with ACE. *Food Chem.* **2021**, *345*, 128855. [[CrossRef](#)] [[PubMed](#)]
15. Petersen, K.S. The Dilemma with the Soy Protein Health Claim. *J. Am. Heart Assoc.* **2019**, *8*, 13. [[CrossRef](#)]
16. Li-Chan, E.C.Y. Bioactive peptides and protein hydrolysates: Research trends and challenges for application as nutraceuticals and functional food ingredients. *Curr. Opin. Food Sci.* **2015**, *1*, 28–37. [[CrossRef](#)]
17. Ma, Y.; Wang, L.; Sun, X.; Zhang, J.; Wang, J.; Li, Y. Study on hydrolysis conditions of flavourzyme in soy polypeptide alcalase hydrolysate and soy polypeptide refining process. *Adv. J. Food Sci. Technol.* **2014**, *6*, 1027–1032. [[CrossRef](#)]
18. Rostammiry, L.; Reza Saeidi Asl, M.; Safar, R.; Javadian, R. Optimization of the Enzymatic Hydrolysis of Soy Protein Isolate by Alcalase and Trypsin. *Biosci. Biotechnol. Res. Asia* **2017**, *14*, 193–200. [[CrossRef](#)]
19. Adler-Nissen, J. Determination of the Degree of Hydrolysis of Food Protein Hydrolysates by Trinitrobenzenesulfonic Acid. *J. Agric. Food Chem.* **1979**, *27*, 1256–1262. [[CrossRef](#)]
20. Barbana, C.; Boye, J.I. Angiotensin I-converting enzyme inhibitory properties of lentil protein hydrolysates: Determination of the kinetics of inhibition. *Food Chem.* **2011**, *127*, 94–101. [[CrossRef](#)]
21. Spellman, D.; McEvoy, E.; O’Cuinn, G.; FitzGerald, R.J. Proteinase and exopeptidase hydrolysis of whey protein: Comparison of the TNBS, OPA and pH stat methods for quantification of degree of hydrolysis. *Int. Dairy J.* **2003**, *13*, 447–453. [[CrossRef](#)]
22. Orio, L.P.; Boschin, G.; Recca, T.; Morelli, C.F.; Ragona, L.; Francescato, P.; Arnoldi, A.; Speranza, G. New ACE-Inhibitory Peptides from Hemp Seed (*Cannabis sativa* L.) Proteins. *J. Agric. Food Chem.* **2017**, *65*, 10482–10488. [[CrossRef](#)] [[PubMed](#)]
23. UniProt. Available online: <https://www.uniprot.org/> (accessed on 15 July 2022).
24. Kaur, A.; Kehinde, B.A.; Sharma, P.; Sharma, D.; Kaur, S. Recently isolated food-derived antihypertensive hydrolysates and peptides: A review. *Food Chem.* **2021**, *346*, 128719. [[CrossRef](#)]
25. Tacias-Pascacio, V.G.; Morellon-Sterling, R.; Siar, E.H.; Tavano, O.; Berenguer-Murcia, A.; Fernandez-Lafuente, R. Use of Alcalase in the production of bioactive peptides: A review. *Int. J. Biol. Macromol.* **2020**, *165*, 2143–2196. [[CrossRef](#)] [[PubMed](#)]
26. Meinschmidt, P.; Sussmann, D.; Schweiggert-Weisz, U.; Eisner, P. Enzymatic treatment of soy protein isolates: Effects on the potential allergenicity, technofunctionality, and sensory properties. *Food Sci. Nutr.* **2016**, *4*, 11–23. [[CrossRef](#)] [[PubMed](#)]
27. Clemente, A. Enzymatic protein hydrolysates in human nutrition. *Trends Food Sci. Technol.* **2000**, *11*, 254–262. [[CrossRef](#)]
28. Amnuaycheewa, P.; Gonzalez de Mejia, E. Purification, characterisation, and quantification of the soy allergen profilin (Gly m 3) in soy products. *Food Chem.* **2010**, *119*, 1671–1680. [[CrossRef](#)]
29. Merz, M.; Eisele, T.; Berends, P.; Appel, D.; Rabe, S.; Blank, I.; Stressler, T.; Fischer, L. Flavourzyme, an Enzyme Preparation with Industrial Relevance: Automated Nine-Step Purification and Partial Characterization of Eight Enzymes. *J. Agric. Food Chem.* **2015**, *63*, 5682–5693. [[CrossRef](#)]
30. Zhao, T.; Zheng, L.; Zhang, Q.; Wang, S.; Zhao, Q.; Su, G.; Zhao, M. Stability towards the gastrointestinal simulated digestion and bioactivity of PAYCS and its digestive product PAY with cognitive improving properties. *Food Funct.* **2019**, *10*, 2439–2449. [[CrossRef](#)]
31. Bax, A.; Grzesiek, S. ROESY. In *Encyclopedia of Nuclear Magnetic Resonance*; John Wiley and Sons: Chichester, UK, 2007; Reo-Tim; Volume 7, pp. 4157–4166.
32. Wang, Y.; Shortle, D. Residual helical and turn structure in the denatured state of staphylococcal nuclease: Analysis of peptide fragments. *Fold Des.* **1997**, *2*, 93–100. [[CrossRef](#)]
33. Sornwatana, T.; Bangphoomi, K.; Roytrakul, S.; Wetprasit, N.; Choowongkamon, K.; Ratanapo, S. Chebulin: Terminalia chebula Retz. fruit-derived peptide with angiotensin-I-converting enzyme inhibitory activity. *Biotechnol. Appl. Biochem.* **2015**, *62*, 746–753. [[CrossRef](#)]
34. Kuba, M.; Tanaka, K.; Tawata, S.; Takeda, Y.; Yasuda, M. Angiotensin I-converting enzyme inhibitory peptides isolated from tofuyo fermented soybean food. *Biosci. Biotechnol. Biochem.* **2003**, *67*, 1278–1283. [[CrossRef](#)]
35. Jiang, Z.; Tian, B.; Brodcrob, A.; Huo, G. Production, analysis and in vivo evaluation of novel angiotensin-I-converting enzyme inhibitory peptides from bovine casein. *Food Chem.* **2010**, *123*, 779–786. [[CrossRef](#)]
36. Jang, J.H.; Jeong, S.C.; Kim, J.H.; Lee, Y.H.; Ju, Y.C.; Lee, J.S. Characterisation of a new antihypertensive angiotensin I-converting enzyme inhibitory peptide from *Pleurotus cornucopiae*. *Food Chem.* **2011**, *127*, 412–418. [[CrossRef](#)] [[PubMed](#)]
37. Daskaya-Dikmen, C.; Yucetepe, A.; Karbancioglu-Guler, F.; Daskaya, H.; Ozcelik, B. Angiotensin-I-Converting Enzyme (ACE)-Inhibitory Peptides from Plants. *Nutrients* **2017**, *9*, 316. [[CrossRef](#)]
38. Quirós, A.; del Mar Contreras, M.; Ramos, M.; Amigo, L.; Recio, I. Stability to gastrointestinal enzymes and structure–activity relationship of  $\beta$ -casein-peptides with antihypertensive properties. *Peptides* **2009**, *30*, 1848–1853. [[CrossRef](#)] [[PubMed](#)]

